Synthesis and Characterisation of Polymers Containing the Pyrrolidone Functional Group

ROSE EMILY SIMNETT

Synthesis and Characterisation of Polymers Containing the Pyrrolidone Functional Group

A thesis submitted for the degree of

Doctor of Philosophy by

Rose Emily Simnett, Ustinov College

March 2017

Abstract

The exceptional properties of polymers containing the pyrrolidone functional group (aqueous & organic solvent soluble, high complexation ability, non-toxic and FDA approved) allow for wide-ranging product application. The development of pyrrolidone containing polymers is therefore, a highly interesting area for academic and commercial research. The focus of this project is the synthesis and characterisation of a range of novel pyrrolidone containing homo- and co-polymers. The work uses two approaches: 1) a bottom up, with the synthesis of known and novel pyrrolidone containing monomers and, 2) a top down, by functionalisation of commercially available polymer precursors.

A range of molecules containing the pyrrolidone moiety and monomer functional groups (styrene, epoxide and acrylate), were prepared. The homo- and co-polymerisation of the known and novel monomers, 1-(2-(oxiran-2-ylmethoxy) ethyl) pyrrolidin-2-one) or glycidyl ethylpyrrolidone (GEP, **1**), 4-vinylbenzyloxy ethyl pyrrolidone (**2**) and 5-ethacryloxyethyl-12-ethylpyrrolidyl-N,N'hexane biscarbamate (**3**) were explored. The polymerisation methods were chosen to be synthetically simple, industrially viable and, were designed to produce pyrrolidone containing polymers with varying properties. The polymeric products were characterised by solution and solid state NMR, SEC, thermal analysis, mass spectrometry and, FTIR. GEP (**1**) was also successfully utilised in the post polymerisation modification of two commercial (poly(epichlorohydrin), poly(butadiene)) and one novel (poly(vinyl alcohol-*graft*-hyperbranched polyglycerol) (PVA-*g*-hPG)) polymer motifs.

The development, synthesis and characterisation of a range of novel pyrrolidone containing homo- and co-polymers is detailed herein. The success of the synthesis in an industrially viable manner provides a unique insight into the possibilities of pyrrolidone polymer progress.

Thesis Summary

Chapter 1 provides a general introduction to *N*-vinyl pyrrolidone and polymerisation techniques such as; atom transfer radical polymerisation (ATRP), reversible addition-fragmentation chain transfer (RAFT) and ring opening polymerisation (ROP). The introduction also covers polymer morphologies and a review of the literature for pyrrolidone containing polymers.

Chapter 2 discusses the synthesis, development and characterisation of novel and known monomers containing the pyrrolidone functionality. The pyrrolidone monomers 1-(2-(oxiran-2-ylmethoxy) ethyl) pyrrolidin-2-one) or glycidyl ethylpyrrolidone (GEP, **1**), 4-vinylbenzyloxy ethyl pyrrolidone (**2**) and 5-ethacryloxyethyl-12-ethylpyrrolidyl-N,N'hexane biscarbamate (**3**) were designed/chosen to incorporate a variety of functional groups capable on undergoing synthetically simple polymerisation reactions. The synthesis of 5-ethacryloxyethyl-12-ethylpyrrolidyl-N,N'hexane biscarbamate (**3**) also produced two side products, a di-acrylate (**4**) and a di-pyrrolidone (**5**). **4** was isolated and fully characterised, however, the di-pyrrolidone (**5**) was not isolated due to the high polarity of the product.

Chapter 3 explores the homopolymerisation reactions of the pyrrolidone monomers (**1**-**3**). The ring opening polymerisation (ROP) of monomer **1** (GEP) produced oligomers of poly(1-(2-(oxiran-2-ylmethoxy) ethyl) pyrrolidin-2-one), (**6**). MALDI mass analysis indicated a molecular weight range from 414.10 to 2797.54 $gmol^{-1}$. Poly(4-vinylbenzyloxy ethyl pyrrolidone) (**7**) produced by the homopolymerisation of monomer **2** under the reaction conditions reported in the literature was found to be an insoluble translucent gummy solid. The solid was analysed by solid state NMR (SSNMR), TGA, DSC and FTIR and it was concluded that chain transfer reactions formed a cross-linked polymer network. It is postulated that this polymer network entrapped the remaining unreacted monomer and limited the progress of the reaction. The novel peptide mimic poly(5-ethacryloxyethyl-12-ethylpyrrolidyl-N,N'hexane biscarbamate) (**8**) was synthesised *via* free-radical polymerisation and fully characterised.

In chapter 4, copolymerisation reactions of monomers **1**-**3** are described. The copolymerisation of **1** (GEP) and ethylene oxide (EO) with a benzyl alcohol/potassium naphthalenide initiating system to produce poly(1-(2-(oxiran-2-ylmethoxy) ethyl) pyrrolidin-2-one-*co*-ethylene oxide (**9**) was unsuccessful. The initiating system was found to produce poly(ethylene oxide) (PEO) or poly(ethylene glycol) (PEG) when GEP (**1**) was absent. The aluminium mediated ring opening copolymerisation (ROP) of GEP (**1**) and succinic anhydride (SA) produced the novel polyester poly(1-(2-(oxiran-2-ylmethoxy) ethyl) pyrrolidin-2-one-*co*-succinic anhydride) (**10**). Copolymer **10** was fully characterised and MALDI mass analysis indicated that the structure was alternating in nature. The copolymerisation of monomer **2** with styrene (St) (**11**), *N*-vinyl pyrrolidone (NVP) (**12**) and hydroxyethyl acrylate (HEA) (**13**) following the literature procedure produced insoluble solid. The solids were characterised by thermal analysis, FTIR and SSNMR. The thermal analysis and lack of solubility indicated that the samples are most likely cross-linked. Poly(5-ethacryloxyethyl-12-ethylpyrrolidyl-N,N'hexane biscarbamate-*co*-vinyl pyrrolidone (**14**) produced *via* the copolymerisation of novel monomer **3** and NVP was designed as a peptide mimic. Copolymer **14** exhibited a decreased T_g when compared to the homopolymer **8** (poly(5-ethacryloxyethyl-12-ethylpyrrolidyl-N,N'hexane biscarbamate).

Chapter 5 investigates the functionalisation of commercially available poly(epichlorohydrin) (PECH) and poly(butadiene) (PB) as well as the hyperbranched polymer, poly(vinyl alcohol-*graft*-hyperbranched polyglycerol) (PVA-*g*-hPG). The Finkelstein reaction of PECH and sodium iodide was found to produce a random copolymer of poly(epichlorohydrin-*co*-epiiodohydrin) (PECH-*co*-EIH) (**15**) and the conversion was calculated to be 59%. The subsequent pyrrolidonation produced poly(epichlorohydrin-*co*-epiiodohydrin-glycidyl ethylpyrrolidone) (PECH-*co*-EIH-GEP) (**16**) with 24% pyrrolidone functionality. The retention of the chloro- and iodo- functional groups limited the applicability of the polymer. The functionalisation of PB was conducted *via* two routes; hydroboration-oxidation and thiol-ene "click". The hydroboration-oxidation did not convert every pendant vinyl group within the polymer, producing polyhydroxylated polybutadiene (PHPB) (**17**) with an estimated composition of 28% 1,4-addition, 19%, 1,2-addition and 53% hydroxylated. Polypyrrolidonated polybutadiene (PPPB) (**18**) was estimated to have 100% OH conversion, however, some alkene retention in the final polymer is undesirable. The thiol-ene "click"

reaction was found to convert 100% of the alkene units to give thioether-polyhydroxylated polybutadiene (TPHPB) (**19**). Initial analysis of the thioether-polypyrrolidonated polybutadiene (TPPPB) (**20**) suggested that the pyrrolidone moiety was successfully reacted onto the polymer. The epoxide GEP (**1**) was ring opened onto PVA-*g*-hPG to produce poly(vinyl alcohol-*graft*-hyperbranched polyglycerol-glycidyl ethylpyrrolidone) (PVA-*g*-hPG-GEP) (**21**). The pyrrolidone functionality was found to react with primary hydroxyl groups of the PVA-*g*-hPG and an increase in the T_g, T_m and degradation was observed when compared to the PVA-*g*-hPG starting material.

Chapter 6 draws the main conclusions of the work discussed.

Finally, chapter 7 explores the future perspectives of the project.

Acknowledgements

Firstly, I would like to thank Dr Ezat Khosravi for giving me the opportunity to continue my studies at Durham University and travel extensively whilst presenting my research. I would like to extend my gratitude to Ashland Inc., specifically Dr Osama Musa for funding the PhD studentship. I would also like to thank all members of the NMR and Mass Spectrometry service staff who have answered all my questions, no matter how trivial. I am grateful to all the members of the Khosravi group for all the fun in the lab. Thanks to everyone from CG156, CG159 and MC106. I thank Dr Lian Hutchings for guidance and allowing me to conduct the ethylene oxide work in his research laboratory as well as his group, especially Dr Serena Agostini for her support and advice during that time.

Ustinov College and the friends I made there are synonymous with my time at Durham University. The numerous college events, academic discussion and nights working at the bar have been a highlight. Nowhere else would you find such a diverse group of wonderful people and I thank you all for the experience, I am saddened that Ustinov as we know it will be no more. To the organisation group, thank you for distracting me when I needed it, celebrating with me when there was cause to and most of all, for dealing with 'pleasant Rose'. To my longest friends, Natalie Depledge, Emma Payling and Dr Amy Roberts, thank you for believing that I could do this and for all the fun Christmas times. Thanks to Caitlin Mooney for teaching me to be able to say no to social events I never wanted to attend and keeping me sane in my final months. Dr Arron Briddick for a 'ladz' perspective and (transport to) climbing fun, even if the car was sometimes more embarrassment than it was worth. What can I say about my partner in crime and one half of 'Rocky', Dr Victoria Linthwaite, you have been there for the highs and the lows and I can't thank you enough.

I would like to thank my former work colleague Dr Alexander Stephen Hudson for his enduring support and love over the last 4 years of my life. Finally, my family have been invaluable to me throughout this process, thank you for the huge amounts of moral and emotional support and always talking to me when I'm walking home.

Memorandum

The work reported in this thesis was conducted in the Durham University Chemistry Department between October 2012 and June 2016. Unless acknowledged by references, the work presented is the original work of the author and has not been submitted for any other degree in Durham or elsewhere.

The work submitted in this thesis has been presented, in part, at:

- Durham University Postgraduate Symposium, 18th June 2014, Durham, England.
- Biopolymer Materials and Engineering conference, 15th-17th April 2015, Slovenj Gradec, Slovenia.
- Durham University Postgraduate Symposium, 24th June 2015, Durham, England.
- North East Polymer Association Young Persons' Lecture Competition, local heat, 24th February 2016, Durham, England.
- North East Polymer Association Young Persons' Lecture Competition, regional final, 17th March 2016, Middlesbrough, England.

In addition to the meetings stated above, the author has attended the following conferences:

- IUPAC 10th international conference on Advanced Polymers via Macromolecular Engineering, 18th-22nd August 2013, Durham, England.
- IUPAC World Polymer Congress, 6th-11th July 2014, Chiang Mai, Thaliand.

In addition, the author has contributed towards the following publication:

Xanthantes Designed for the Perparation of N-Vinyl Pyrrolidone-Based Linear and Star Architectures via RAFT polymerization, I. J. Johnson, E. Khosravi, O. M. Musa, R. E. Simnett and A. M. Eissa, *Journal of Polym. Sci. Part A: Polym. Chem.*, **2015**, 53, 775-786.

Statement of Copyright

Financial Support

The author gratefully acknowledges Ashland Inc. for their funding of this research.

Contents

Abbreviations

Expanded form	Abbreviation
Degree of pyrrolidonation	%D(Py)
Bis(triethylaminophosphine)inium salt	[PPN]X
9-Borabicyclo[3.3.1]nonane	9-BBN
Activated chain-end	ACE
Allylglycidyl ether	AGE
Activators generated by electron transfer	AGET
Azobisisobutyronitrile	AIBN
Aluminium isopropoxide	$Al(O^iPr)$
Activated monomer	AM
Activators regenerated by electron transfer	ARGET
Anionic ring opening polymerisation	AROP
Atom transfer radical addition	ATRA
Atom transfer radical polymerisation	ATRP
Boron triflouride diethyl etherate	$BF_3{\cdot}Et_2O$
Butylated hydroxytoluene	BHT
Deuterated chloroform	$CDCl_3$
α-Cyano-4-hydroxycinnamic acid	CHCA
Chloroform	$CHCl_3$
Correlation spectroscopy	COSY
Cationic ring opening polymerisation	CROP
Controlled radical polymerisation	CRP
Commonwealth Scientific and Industrial Research Organisation	CSIRO
Continuous spin fractionation	CSF
Chain transfer agent	CTA
Copper mediated azide-alkyne cycloaddition	CuAAC
Diels-Alder	DA
Dichloromethane	DCM
Trans-2-[3-(4-tert-Butylphenyl)-2-methyl-2-propenylidene]malononitrile	DCTB
Deuterated dimethylformamide	d_7-DMF
Deuterated dimethyl sulfoxide	d_6-DMSO
Distortion-less enhancement by polarisation transfer	DEPT
Density functional theory	DFT
2,5-Dihydroxybenzoic acid	DHB

Expanded form	Abbreviation
4-Dimethylaminopyridine	DMAP
Dimethylformamide	DMF
Dimethyl sulfoxide	DMSO
Refractive index increment	dn/dc
Deoxyribonucleic acid	DNA
Differential scanning calorimetry	DSC
Dispersity	Đ
Elemental analysis	EA
Electrochemical atom transfer radical polymerisation	eATRP
Epichlorohydrin	ECH
Ethylene oxide	EO
Electrospray	ES
Ethylene glycol vinyl ether	EVEGE
Electron withdrawing group	EWG
U.S. Food and Drug Administration	FDA
Free radical polymerisation	FRP
Fourier transform infrared	FTIR
Glycidyl ethylpyrrolidone	GEP
Hydrogen peroxide	H_2O_2
Hydrochloric acid	HCl
Hexamethylene diisocyanate	HDI
2-Hydroxyethyl acrylate	HEA
Hydroxyethyl acrylate	HEA
Hydroxyethyl pyrrolidone	HEP
Heteronuclear multiple-bond correlation	HMBC
Hyperbranched polyglycerol	hPG
Heteronuclear shift correlation spectroscopy	HSQC
Initiators for continuous activator regeneration	ICAR
Potassium carbonate	K_2CO_3
Potassium hydroxide	KOH
Lower critical solution temperature	LCST
Matrix-assisted laser desorption-ionization	MALDI
Methanol	MeOH
Potassium methoxide	MeOK
m-Hydroxystyrene	MHS
Number average molecular weight	M_n
Mass spectrometry	MS
Sodium hydride	NaH
Sodium iodide	NaI
Sodium hydroxide	NaOH

Expanded form	Abbreviation
n-Butyl lithium	*n*-BuLi
Triethylamine	NEt_3
n-methyl pyrrolidone	NMP
Nitroxide mediated polymerisation	NMP
Nuclear magnetic resonance	NMR
n-vinyl pyrrolidone	NVP
Outer-sphere single electron transfer	OSET
Poly(butadiene)	PB
Poly(epichlorohydrin)	PECH
Poly(epichlorohydrin-*co*-epiiodohydrin)	PECH-*co*-PEIH
Poly(ethylene glycol)	PEG
Poly(epiiodohydrin)	PEIH
Poly(ethylene oxide)	PEO
Poly(hydroxylated polybutadiene)	PHPB
Polymethyl methacrylate	PMMA
p-Methylstyrene	PMS
Polypyrrolidonated polybutadiene	PPPB
Poly(styrene)	PS
Pure shift yielded by chirp excitation	PSYCHE
Poly(vinyl alcohol)	PVA
Poly(vinyl alcohol-*graft*-hyperbranched polyglycerol)	PVA-*g*-hPG
Poly(vinyl alcohol-*graft*-hyperbranched polyglycerol-glycidyl-ethylpyrrolidone)	PVA-*g*-hPG-GEP
Poly(vinyl pyrrolidone)	PVP
Reversible addition-fragmentation chain transfer	RAFT
Retro-Diels-Alder	rDA
Reversible deactivation radical polymerisation	RDRP
Ring opening polymerisation	ROP
Succinic anhydride	SA
Size exclusion chromatography	SEC
Single electron transfer living radical polymerisation	SET-LRP
Small interfering ribonucleic acid	siRNA
Bimolecular nucleophilic substitution	S_N2
Solvent purification service	SPS
Simultaneous reverse and normal initiation	SR&NI
Solid state nuclear magnetic resonance	SSNMR
Styrene	St
Crystallisation temperature	T_c
2,2,6,6-tetramethylpiperidinyl-1-oxy	TEMPO
Glass transition	T_g

Expanded form	Abbreviation
Thermogravimetric analysis	TGA
Tetrahydrofuran	THF
Melting temperature	T_m
Total correlation spectroscopy	TOCSY
Thioether-polyhydroxylated polybutadiene	TPHPB
Thioether-polypyrrolidonated polybutadiene	TPPPB
Ultraviolet	UV
Vinyl acetate	VAc
Variable temperature	VT
ε-Caprolactone	εCl

List of Figures

List of Schemes

List of Tables

Chapter 1

Introduction

The pyrrolidone unit is a versatile functional group. Small molecules containing the pyrrolidone unit such as, *N*-vinyl pyrrolidone (NVP) (Figure 1.1) and *N*-methyl pyrrolidone (NMP) are widely used as monomers[1] and solvents,[2,3] respectively. Macromolecules containing the pyrrolidone functionality such as poly(vinyl pyrrolidone) (PVP) and its derivatives have an extensive range of applications[4–8] due to excellent solvation and complexation properties in addition to being non-toxic and FDA approved.[9] The unique properties of the pyrrolidone moiety and wide-ranging industrial application present an area for research and development which could lead to a large scientific impact.

1.1 *N*-Vinyl Pyrrolidone

NVP was first polymerised *via* free-radical polymerisation (FRP) in the 1940's by Fikentscher *et. al.*[10] Today, PVP has been synthesised by a variety of radical polymerisation processes including reversible addition-fragmentation chain transfer (RAFT) polymerisation and atom transfer radical polymerisation (ATRP).[11–14] The difference in polarity from the highly polar carbonyl to the non-polar (CH_2) polymer backbone allows PVP and its derivatives to be soluble in organic and aqueous solvents.

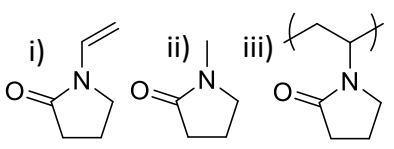

Figure 1.1 – Structure of i) NVP ii) NMP and iii) PVP

PVP is a versatile substance with multiple uses spanning a wide range of industries and products: adhesives,[15] ceramics,[16] electrical,[17] textiles,[18] household & industrial cleaning products,[19] lithography, metallurgy,[20] oil/gas,[21] and paper.[22] PVP also has excellent complexation properties and has been shown to complex DNA and demonstrate drug binding ability.[23] The scope of industrial application for PVP makes it a very attractive area of research.

Currently PVP is industrially synthesised *via* FRP in ethanol or isopropanol solvent, producing homopolymer or random copolymer with vinyl acetate (VAc). In polymer chemistry, being able to target the synthesis of the polymer to the application is extremely important. There are many ways in which this can be done, for example: controlled polymerisation to obtain specific molecular weights, copolymerisation to produce random and block morphologies or polymer modifications to introduce new properties and functionality.

NVP is a less activated monomer due to the lack of intermediate stabilisation during polymerisation. This introduces some challenges when controlled polymerisation routes are pursued and extensive optimisation is often required. It has also been shown that the nitrogen present in the monomer can lead to difficulties with metal complexation, this is especially relevant for ATRP which often employs copper to initiate the reaction.[24]

1.2 Free Radical Polymerisation

FRP is a versatile and ubiquitous polymerisation technique that is employed to produce vast quantities of polymer worldwide. FRP is an example of chain growth polymerisation, developed in the 1920's by Staudinger *et. al.*[25] It is now an important industrial process employed to produce 100 million tons of plastic material and 4.6 million tons of synthetic rubber annually.[26] The reaction proceeds *via* initiation, propagation and termination steps (Scheme 1.1).

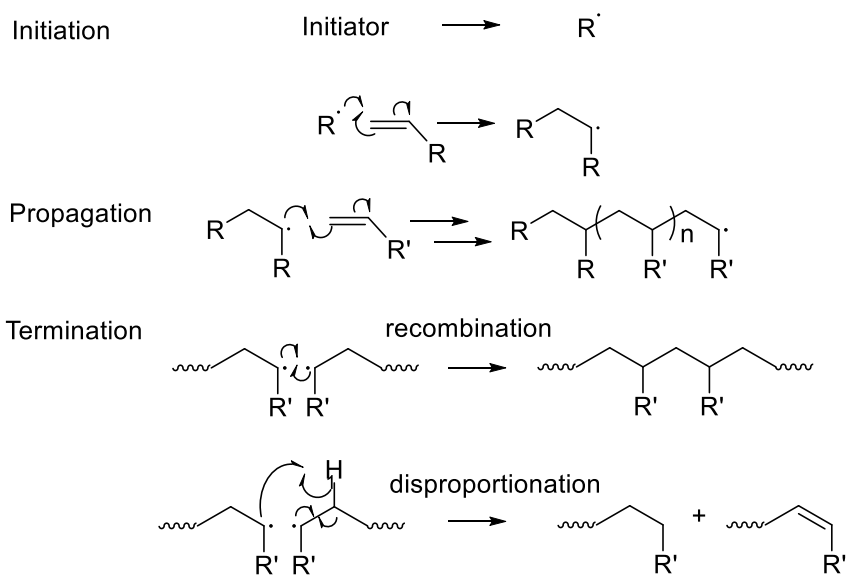

Scheme 1.1 – Mechanism of a typical free radical polymerisation

1.2.1 Kinetics

Initiation usually consists of a two-step process, first homolysis of the initiator to form a radical species, initiators such as AIBN are common. The second step involves the reaction of the initiator and monomer unit to create an active centre. Dissociation of the initiator molecule is the rate determining step and the subsequent reaction to form the active centre is fast. The rate of initiation is described by Equation 1.1.

$$\boldsymbol{r_{init} = k_i\,[I]}$$

Equation 1.1

Where k_i is the rate constant for initiation and [I] the concentration of initiator.

Propagation of the polymer chain occurs with the reaction of an active radical with a monomer unit. The rate constant of propagation (k_p) is independent of chain length and the rate of propagation is given by Equation 1.2.

$$\boldsymbol{r_{prop} = k_p[M][M\cdot]}$$

Equation 1.2

Where k_p is th rate constant for propagation, [M] is the concentration of monomer and [M·] the concentration of active radical.

Termination can occur by recombination and disproportionation pathways, both of which are bimolecular reactions. The rate constant for termination *via* recombination (k_{tc}) and disproportionation (k_{td}) are often combined into one term for simplicity (k_t) (Equation 1.3). As the reactions are bimolecular with respect to the concentration of active radical ([M·]), termination is more greatly affected by changes [M·] than initiation of propagation.

$$\boldsymbol{r_{term} = 2k_t\,[M\cdot]^2}$$

Equation 1.3

Where k_t is the rate constant for termination and [M·] the concentration of active radical.

The overall rate of free radical polymerisation initiated *via* thermolysis under steady state conditions is given in Equation 1.4.

$$\boldsymbol{r_{pol} = k_p\left[\frac{fk_d\,[I]}{k_t}\right]^{\frac{1}{2}}\,[M]}$$

Equation 1.4

Where k_p, k_d and k_t are the rate constants of propagation, dissociation (of initiator) and termination, respectively. f is the initiator efficiency [I] is the concentration of initiator and [M] is the concentration of monomer.

This equation (Equation 1.4) is first order with respect to monomer concentration, therefore as the reaction progresses and the concentration of monomer decreases, the rate of reaction will also decrease. It is possible to calculate the number average degree of polymerisation (DP_n) for FRP initiated by thermolysis using Equation 1.5.

$$\boldsymbol{DP_n = \frac{k_p\,[M]}{(1+q)(fk_dk_t)^{\frac{1}{2}}[I]^{\frac{1}{2}}}}$$

Equation 1.5

Where k_p, k_d and k_t are the rate constants of propagation, dissociation (of initiator) and termination, respectively. q is the fraction of termination reactions that proceed by disproportionation ($q = k_{td}/k_t$). When termination occurs solely *via* disproportionation, q = 1

and when termination occurs *via* recombination only q = 0. f is the initiator efficiency [I] is the concentration of initiator and [M] is the concentration of monomer.

From Equation 1.4 and Equation 1.5, it can be deduced that the degree of polymerisation and the rate of polymerisation can be increased by increasing [M], as both equations are directly proportional to [M]. If the [I] is altered, the affect will not be the same for DP_n and r_{pol}, as r_{pol} is directly proportional and DP_n inversely proportional to [I].

When [M] is high however, autoacceleration is often observed. As the reaction proceeds (and [M] decreases) the viscosity of the reaction will increase as the concentration of polymer increases. The increase in viscosity affects termination more than initiation or propagation as the small monomer molecules retain relatively high mobility when compared to the entangled polymer active chain end. All polymerisation reactions are exothermic and as the viscosity increases, it is increasingly difficult to dissipate the released energy and therefore autoacceleration occurs. To reduce the risk of autoacceleration, reactions can be terminated at low conversion or solvent could be added to decrease the effect of the increase in viscosity.

Unwanted chain transfer reactions can also occur between radicals and other substances in the reaction mixture such as monomer, polymer and solvent (if present). This produces a dead chain end and a new radical. If the new radical reacts quickly with a monomer unit to begin a new polymer chain, the overall rate of polymerisation is little affected, however, the original propagating chain is terminated early and a new chain is formed, therefore the DP_n is decreased. Chain transfer to initiator, monomer and solvent all reduce the DP_n of the polymer produced. Chain transfer to polymer does not affect DP_n but does affect polymer architecture by producing branching points (Scheme 1.2).

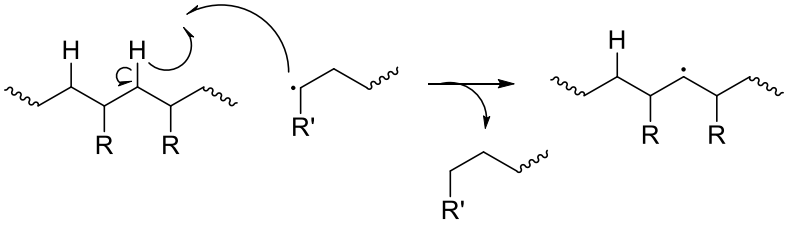

Scheme 1.2 – Mechanism of chain transfer to polymer

Chain transfer constants can be derived for different species and must be taken into account when selecting a monomer:initiator:solvent system. High chain transfer constants indicate that chain transfer occurs readily. These substances are considered as chain transfer agents (CTA). The CTA works by forming a dead chain end and a new radical containing the CTA when the propagating radical abstracts a hydrogen from the CTA (Scheme 1.3). The new CTA radical then reacts with a monomer unit to produce a new propagating radical.[27] CTAs reduce the molecular weight of the polymers produced by the reaction and reduce the Đ, allowing the production of polymers with decreased molecular weights; thiols are commonly used as CTAs in free radical polymerisation due to the weak S-H bond and high reactivity of the S· radical.[28]

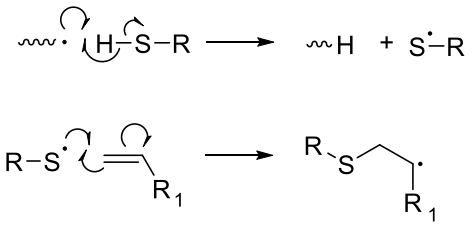

Scheme 1.3 – Mechanism of chain transfer between polymer and tiol-chain transfer agent

FRP is a widely utilised technique in the multi-billion dollar polymer industry.[26] However, the reaction lacks control over molecular weight and architecture which can limit the application prospects of the polymers produced *via* this method.

Calculation of the molar mass of the polymer is possible but requires complex derivation due to the number of possibilities during the reaction; propagation, termination and chain transfer (to monomer, polymer and solvent).

1.2.2 Polymerisation Reaction Methods

There are predominantly utilised methods for FRP: bulk, solution, suspension and emulsion polymerisation

Bulk polymerisation eliminates the challenges that solvent can introduce to the polymerisation, such as chain transfer to solvent. However, autoacceleration can be a problem as the reaction mixture will become viscous as the polymerisation progresses. To avoid this, reactions are usually terminated at low conversions. Industrially, this introduces difficulties with recovery of the unreacted monomer, however, high molecular weight polymers with high levels of purity can be produced *via* this method.

The addition of solvent introduces the possibility of addition chain transfer reactions but also decreases the probability of autoacceleration. A solvent with a low chain transfer constant can be chosen to ensure the polymer produced is minimally affected. The decrease in monomer concentration, will lead to a proportionate decrease in the r_{pol} and DP_n *vide supra* and the recovery of the resulting polymers requires the additional step of solvent reduction/removal.

Suspension polymerisation combines the advantages of bulk and solution polymerisation methods. The polymerisation is conducted in a non-solvent, in which the monomer, initiator and polymer are non-soluble (Figure 1.2). The polymerisation mixture is added to the non-solvent and is agitated to form a suspension of 'bulk' polymerisation droplets. The droplets are often stabilised by surfactants and have a high surface area to disperse the exothermic energy produced during the reaction. This system is able to produce high molecular weight, high purity polymers with a reduced risk of autoacceleration and without limiting conversion. However, additional purification techniques are required, the product shape is predetermined (bead shaped) and autoacceleration can still occur.

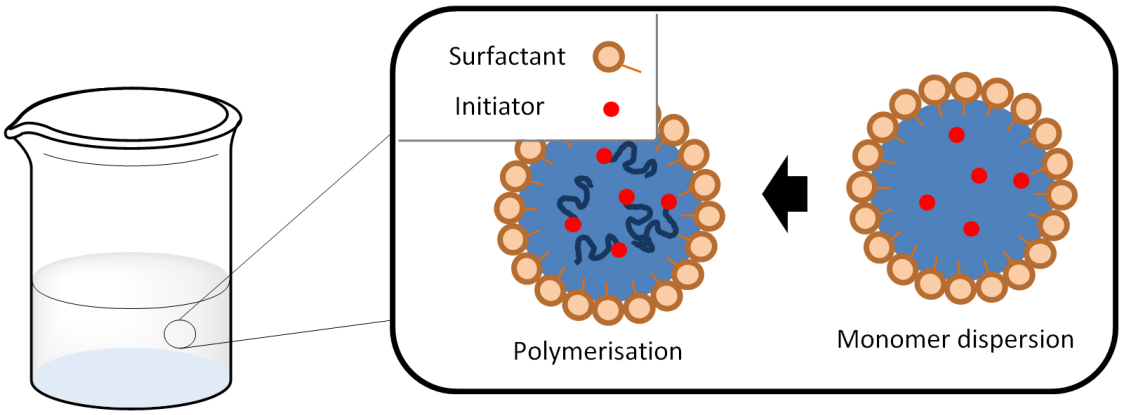

Figure 1.2 – Schematic of suspension polymerisation

Emulsion Polymerisation is similar to suspension polymerisation however, the initiator is not soluble in the monomer and is soluble in the dispersion media. The monomer is added to a dispersion media of (often anionic) surfactants at a concentration above the critical micelle concentration (CMC) and a 3 main phases are formed (Figure 1.3). The dispersion media contains a very small quantity of monomer, some small monomer-micelles are formed and there are also large droplets of monomer stabilised by the anionic surfactants. The polymerisation is initiated in the aqueous phase and as the reaction proceeds in the small micelles, the concentration of monomer decreases. This establishes a concentration gradient where the monomer diffuses to the growing polymer chain from the large droplets. The radical species are not able to penetrate the large droplets due to the concentration of (anionic) surfactant at the interface. This system also reduces termination as one radical initiates one growing chain and that chain is stabilised by (anionic) surfactants and will rarely come into contact with another active radical.

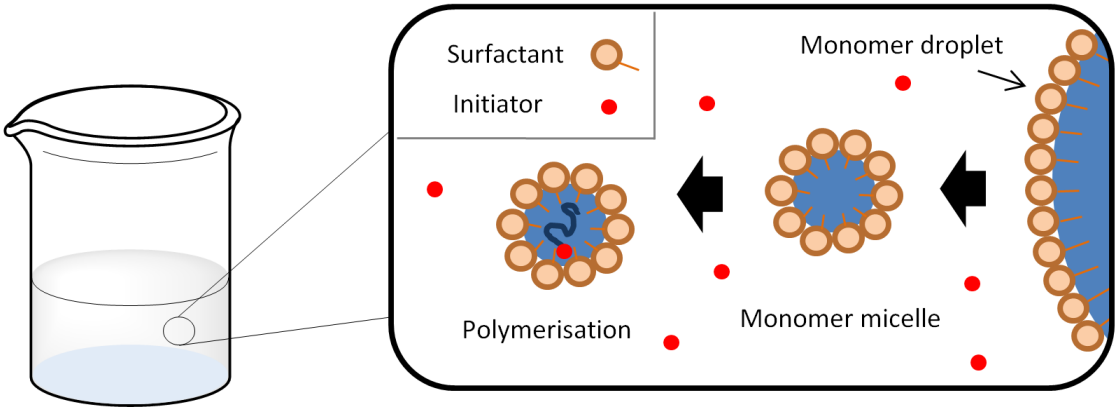

Figure 1.3 – Schematic of emulsion polymerisation

Once again, autoacceleration is reduced as the dispersion media allows rapid heat transfer from the growing polymer micelle. This method produces high molecular weight, high purity polymers however, surfactants can be extremely difficult to remove from the product and chain transfer to polymer is increased when compared to other methods.

1.3 Reversible-Deactivation Radical Polymerisation

In an ideal living polymerisation, initiation is fast and there is no termination,[29] this was first achieved by Szwarc *et. al.* for living anionic polymerisation.[30] Following those principles, reversible-deactivation radical polymerisation (RDRP) has developed. RDRP allows polymers with predetermined molecular weights to be easily synthesised, hence increasing the academic and commercial interest in the field.

RDRP's have been the subject of much interest and research, due to the versatility and industrial relevance of the techniques and polymers formed. The reactions employ reversible-deactivation pathways to impart control over the reaction and the molecular weight of the polymers produced. RDRP techniques supress the rate of termination due to the formation of the equilibrium established between a dormant and an active species (Scheme 1.4). The equilibrium lies to the dormant side therefore decreasing the concentration of active species and in turn reducing the chance of the active chains terminating by either recombination or disproportionation. Termination however, does still occur therefore these systems are not thought of as truly living polymerisations.

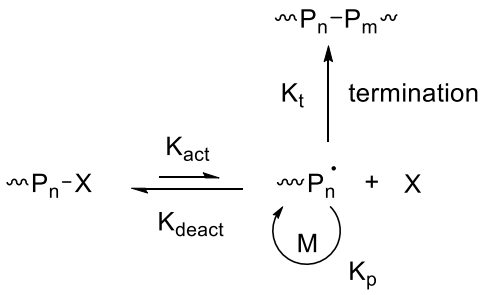

Scheme 1.4 – General scheme for reversible-deactivation radical polymerisation

The equilibrium established in RDRP is established in one of three ways; reversible deactivation of propagating radicals to form a dormant species (catalysed or spontaneous), such as in ATRP and nitroxide mediated polymerisation (NMP) or by degenerative transfer from the propagating radical to the dormant species as in RAFT.

1.3.1 Nitroxide Mediated Polymerisation

NMP employs nitroxides or alkoxyamines, such as 2,2,6,6-tetramethylpiperidinyl-1-oxy (TEMPO, Figure 1.4), and obeys the persistent radical effect. It was patented by the Commonwealth Scientific and Industrial Research Organisation (CSIRO).[31] The kinetics of the reaction are a combination of the persistent radical effect and the equilibrium established during the reaction. The concentration of initiator therefore greatly affects the kinetics of the reaction and so it is very important to control the ratio of [monomer]:[initiator].

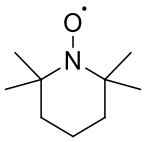

Figure 1.4 – Structure of 2,2,6,6-tetramethylpiperidinyl-1-oxy (TEMPO)

1.3.2 Atom Transfer Radical Polymerisation

Typically, an ATRP reaction consists of a monomer, initiator, catalyst and ligand. The initiator must contain a (pseudo)halogen which is transferred to the transition metal catalyst during the reaction. Nitrogen donor ligands are typically used to solubilise the transition metal catalysts and a number of transition metals: Ti,[32] Co,[33] Ni,[34] Mo,[35] Ru,[36] Rh,[37] Pd,[38] Re,[39] Os,[40] Fe,[41,42] and Cu,[43,44] have been investigated. ATRP follows a typical chain growth polymerisation mechanism with the usual initiation, propagation and termination steps. ATRP is tolerant to a range of monomers, has a simple experimental set-up and gives good control over molecular weight, Đ, architecture and, chain end functionality of the polymers produced. High chain end functionality allows the product of reaction to be used as a macroinitiator in subsequent reactions.

Disadvantages include; often high catalyst loading, high residual levels of catalysts, reactions highly sensitive to oxygen and other contaminants. To alleviate these problems variations of the ATRP reaction were developed: reverse ATRP, simultaneous reverse and normal initiation (SR&NI), activators generated by electron transfer (AGET), activators regenerated

by electron transfer (ARGET), initiators for continuous activator regeneration (ICAR) and electrochemical ATRP (eATRP). These variations incorporate a variety of methods to decrease the concentration of activated species therefore decreasing the quantity of catalyst required and (re)generate the activator species throughout the reaction.

1.3.3 Reverse Addition-Fragmentation Chain-Transfer Polymerisation

RAFT polymerisation utilises an addition-fragmentation pathway to produce polymers with predetermined molecular weights, low Đ and designed architecture. The addition-fragmentation process was first reported in the 1970's[47,48] and was later developed into the RAFT polymerisation procedure by CSIRO in the 1990's.[49] RAFT involves degenerative chain transfer mediated by a CTA, such as a thiocarbonyl-thio compound (Scheme 1.5, where X = A = S).

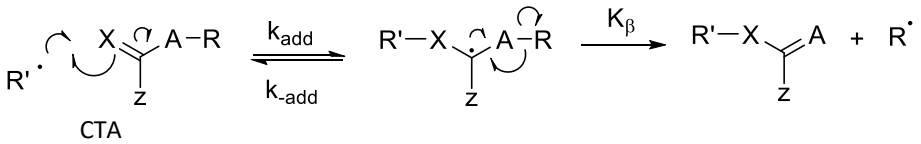

Scheme 1.5 – Addition-fragmentation mechanism of RAFT agent

The majority of the polymers formed contain the transfer agent end group and achieve lower molecular weights than when no RAFT agent is added. This allows subsequent reactions at the active chain-end producing polymers with well-defined tertiary structures. RAFT has been conducted in aqueous media,[50,51] this is advantageous as organic solvents are costly and have a negative environmental impact. Previous work within our group and others has shown that RAFT polymerisation has also been utilised to polymerise less activated monomers such as NVP[52,53,54] and *N*-vinylcaprolactam,[55,56] amongst others.

1.4 Ring Opening Polymerisations of Epoxides

Ring opening polymerisation (ROP) was first reported by Leuchs in 1906[57] and has since developed into a wide-ranging and valuable technique for polymer chemists.[58–60] The driving force of ROP is often the release of ring strain and can be conducted under a variety of conditions. There are three main methods of ROP; anionic, cationic and coordination-insertion. The ROP of epoxides is usually achieved under anionic or cationic conditions.[61]

1.4.1 Cationic Ring Opening Polymerisation of Epoxides

There are two propagation pathways, activated monomer (AM) and activated chain-end (ACE) mechanism. The ACE pathway proceeds *via* an S_N1 mechanism and the AM *via* and S_N2 (Scheme 1.6). For some systems it has been shown that both pathways proceed simultaneously.[62]

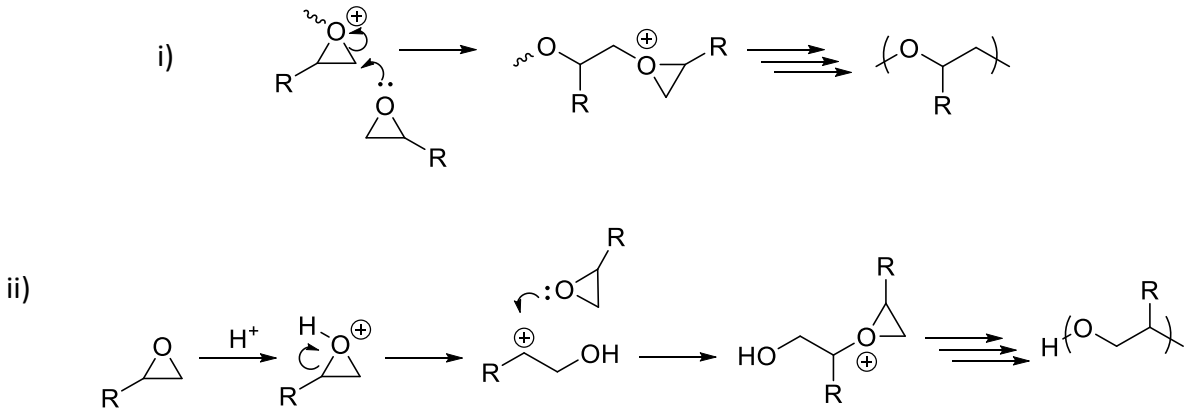

Scheme 1.6 – Mechanism or propagation *via* i) activated monomer and ii) activated chain end

The ACE method is the most common mechanism of cationic ring opening polymerisation (CROP) for oxygen containing heterocycle monomers. Back-biting and ring elimination occur in CROP limiting the molecular weight of the polymers produced.[63] Therefore, this project utilised anionic ring opening polymerisation (AROP) for the polymerisation of epoxide monomers.

1.4.2 Anionic Ring Opening Polymerisation of Epoxides

AROP has been utilised to synthesise polyethylene glycol (PEG) and functional derivatives producing water-soluble polymers for a variety of applications.[64] The polymers produced have narrow Đ and well-defined macrostructure.[65] Ethylene oxide (EO) was the first epoxide to be polymerised in the 1940's by Flory et. al.[66] A limitation of polyethylene oxide (PEO), or PEG, is the lack of functionality. To introduce functionality, substituted epoxides can be polymerised *via* AROP. When substituted epoxides are polymerised, the nucleophile (often an alkoxide) attacks at the least hindered side (Scheme 1.7).

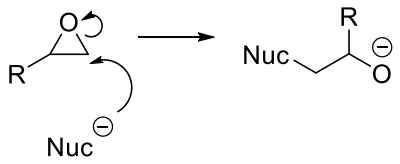

Scheme 1.7 – Nucleophilic attack of substituted epoxides

Frey et al. have reported many linear copolymers of EO and substituted epoxides[65,67–69] as well as investigating hyperbranched epoxide based polymers.[70–72] AROP has proven a successful "living" polymerisation technique for substituted epoxides. Ion pairs and aggregates can affect the polymerisation progress, therefore, complexing agents (crown ethers/cryptands) or coordinative solvents, such as DMF or DMSO, are employed to dissociate the active species. AROP with and alkoxide initiator was employed in the polymerisation investigations of the pyrrolidone functionalised epoxide monomer 1-(2-(oxiran-2-ylmethoxy) ethyl) pyrrolidin-2-one or glycidyl ethylpyrrolidone (GEP), discussed in Ch. 2, 2.3.1.

1.4.3 Coordination-Insertion Ring Opening Polymerisation

The most widely utilised and explored ROP method is the pseudo-anionic coordination-insertions ROP, where a metal centre is employed to impart control over the reaction.

Coordination-insertion ROP is commonly employed in the copolymerisation of epoxides and anhydrides. A wide variety of systems have been developed with a range of metal catalysts (including Al, Cr, Co, Zn, Sn, Mg, Ca and Fe[58,73,74]) with a co-catalyst such as 4-dimethylaminopyridine (DMAP) or bis(triethylaminophosphine)inium salts ([PPN]X). Progress in the catalyst systems led to the development of complex catalyst macrostructures such as porphyrins and *N,N'*-Bis(salicylidene)cyclohexane diamine catalysts (Figure 1.5).[58]

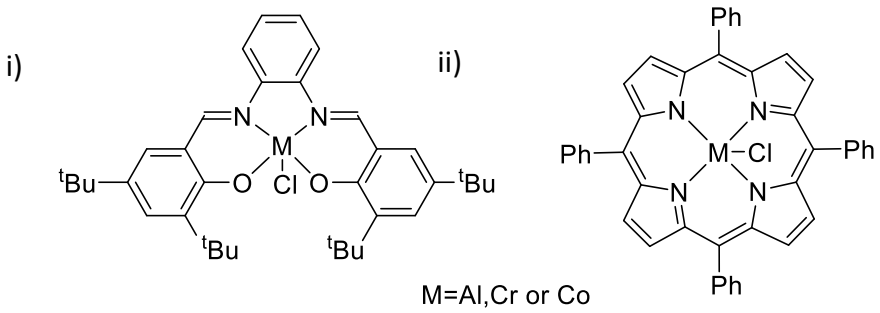

Figure 1.5 – Structure of i) porphyrin and ii) *N,N'*-Bis(salicylidene)cyclohexane diamine catalysts

The advantage of coordination-insertion ROP is the ability to control the structure of the polymer.[74] The catalyst systems can be very complex which introduces high cost and reduces industrial viability. Aluminium isopropoxide (Al(O^iPr)) is an inexpensive and readily available aluminium species which has been highly investigated.[75,76,77] The advantages of employing a commercially available initiator are ease of industrial scale-up without excessive cost. The aluminium isopropoxide initiating system has been shown to produce alternating copolymers of (functionalised) epoxides and anhydrides.[78–80] Feng *et. al*. reported the synthesis of degradable thermoresponsive polyesters utilising an Al(O^iPr) initiator.[78,79] The alternating nature of the polymerisation leads to the formation of hydrolysable ester groups along the polymer backbone, therefore, providing routes for degradation. This method was employed in the synthesis of pyrrolidone functionalised epoxide with succinic anhydride (Ch. 4, 4.3.2).

1.5 Post-polymerisation Functionalisation

Post-polymerisation functionalisation is a highly utilised method to introduce functionality into the polymer chain. The necessity for post-polymerisation functionalisation comes from the reduced functional group tolerance of polymerisation techniques. It is possible to introduce groups that would inhibit or interfere with the polymerisation mechanism or are unstable under polymerisation conditions. With the increasing need for well-defined polymers to target properties for applications, the ability to modify polymers with precise molecular weights and architecture is attractive. RDRP techniques such as ATRP and RAFT (*vide supra*) are suited to be utilised to produce well-defined polymers to undergo further modification.

With post-polymerisation functionalisation, achieving complete conversion of functional groups is desirable but often challenging. Side reactions are common and, where co-monomers are employed, differences in reactivity can introduce complications. Research has explored high conversion functionalisation *via* "click" reactions as well as increasing the scope of functional polymers with the introduction of novel functional groups.

1.5.1 End Functionalisation

End functionalisation can be achieved through the polymerisation process as is the case in RAFT polymerisation, where the polymer retains the chain-end functionality of the CTA. It is also possible to modify reactive polymer end groups, such as hydroxyl terminated polymers. End-functionalised polymers are used to produce (multi)block copolymers and allow the formation of more complex macrostructure (Figure 1.6).

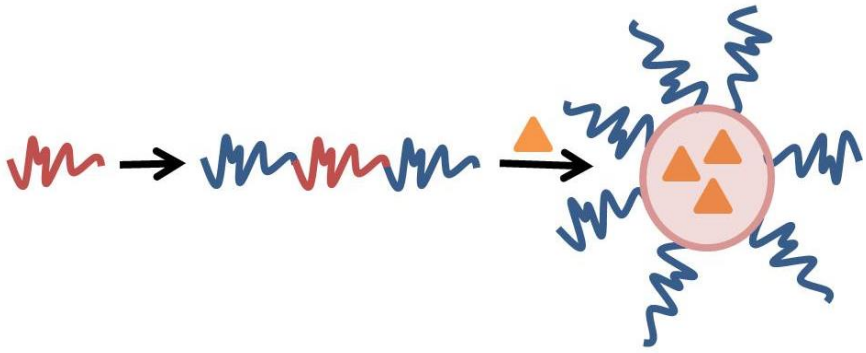

Figure 1.6 – Schematic of progress of end functionalised polymers leading to complex macrostructure

Often, protecting groups which are impervious to the polymerisation conditions are introduced in the monomer and removed after polymerisation leaving a functional group capable of further reactions. The end groups can be functionalised with ATRP initiators,[81,82] proteins[83,84] or macrostructures capable of host-guest chemistry.[85,86]

Whilst end functionalisation is a useful technique alone, it is also advantageous to introduce functionality along the polymer backbone. This can be achieved by the implementation of "click" chemistry due to the properties that underpin "click" reactions: high yielding, wide in scope, stereospecific, benign or easily removed solvent and, by-products which are removable without chromatography.[87]

1.5.2 "Click" Reactions

"Click" reactions are idea for post-polymerisation functionalisation due to the mild reaction conditions and high yield meaning high conversion. The benchmark "click" reaction is the copper mediated azide-alkyne cycloaddition (CuAAC) (Scheme 1.8).[87]

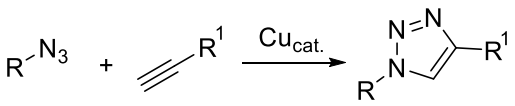

Scheme 1.8 – Copper catalysed azide-alkyne "click" reaction

CuAAC utilises Cu(I) to impart control over the reaction and produce a 1,4-disubstituted triazole ring. The first reported reactions were conducted in the absence of copper at high temperatures. The products of the non-catalysed reaction were a mixture of 1,4- and 1,5-disubstituted 1,2,3-triazole rings.[87] CuAAC does not need elevated temperatures and can be conducted in many solvents, including water and, the triazole produced is highly stable to subsequent reactions.[88] As Cu(I) is highly reactive, often it is produced *in situ* by the addition of a Cu(II) species and a reducing agent.[89] Large quantities of Cu(II) can lead to the formation of by-products, however, Rostovtsev *et. al*. discovered that the mild reducing agent ascorbic acid with a Cu(II) salt, produced the desired product with high yield, purity and in water, negating the need for oxygen-free conditions as was required for many Cu(I) protocols.[90]

The Diels-Alder (DA) [4+2] cycloaddition (and retro-Diels-Alder, rDA) are also considered to be "click" reactions as they adhere to the strict reaction criteria (Scheme 1.9). The reversible reaction has been employed in thermoresponsive polymers,[91] drug-delivery systems,[92] recyclable networks[93] and self-healing materials.[94]

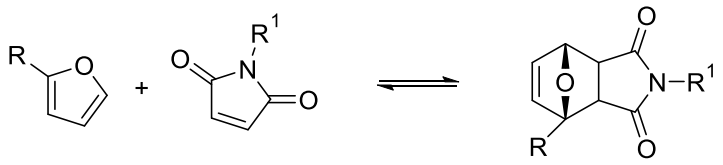

Scheme 1.9 – Reversible Diels-Alder "click" reaction

The advantage of the DA cycloaddition is the lack of catalyst needed during the reaction as well as the reversible nature of the reaction. However, the reversibility of the reaction could also be perceived as a drawback to this technique for some uses.

The thiol-ene "click" reaction proceeds under mild conditions with either a radical initiator or UV light/heat.[95] The reaction conditions are chosen to limit any side-reactions as the thiol moiety is reactive towards other functional groups.[88] The thiol-ene reaction has become a well utilised technique which can achieve the best of both the CuAAC and DA "click" reactions; no metal catalyst, non-reversible.[96]

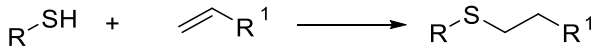

Scheme 1.10 – Thiol-ene "click" reaction

An extensive review of externally stimulated "click", including DA and thiol-ene has recently been published by Tasdelen *et. al*.[97] Other examples of "click" reactions include nucleophilic ring opening reactions as well as the reactions of non-aldol carbonyls for example, imine, hydrazine and oximine formation.[97,98] This (re-)emerging area is likely to impact the synthetic organic community in a similar way to how CuAAC, DA and thiol-ene "click" already have.

1.6 Polymer Architecture

1.6.1 Linear Polymers

Linear polymers synthesised by free radical or RDRP methods are widely used in synthetic polymer chemistry as macroinitiators, cross-linkable chains and in additives for formulations (Figure 1.7). Linear polymers with reactive end groups can be modified for further polymerisation to produce interesting architecture such as polymer brushes and stars as well as block copolymers. PVP is an excellent additive as it is soluble in organic and aqueous solvents, and has a high complexation ability, therefore acting as a stabiliser in many formulations. Linear PVP is often used as an additive in formulations for a wide variety of applications: hydrogels, printing inks, tablet formation, adhesives, and personal products. The addition of linear PVP homopolymer into hydrogels has also been shown to increase the mechanical strength.[99]

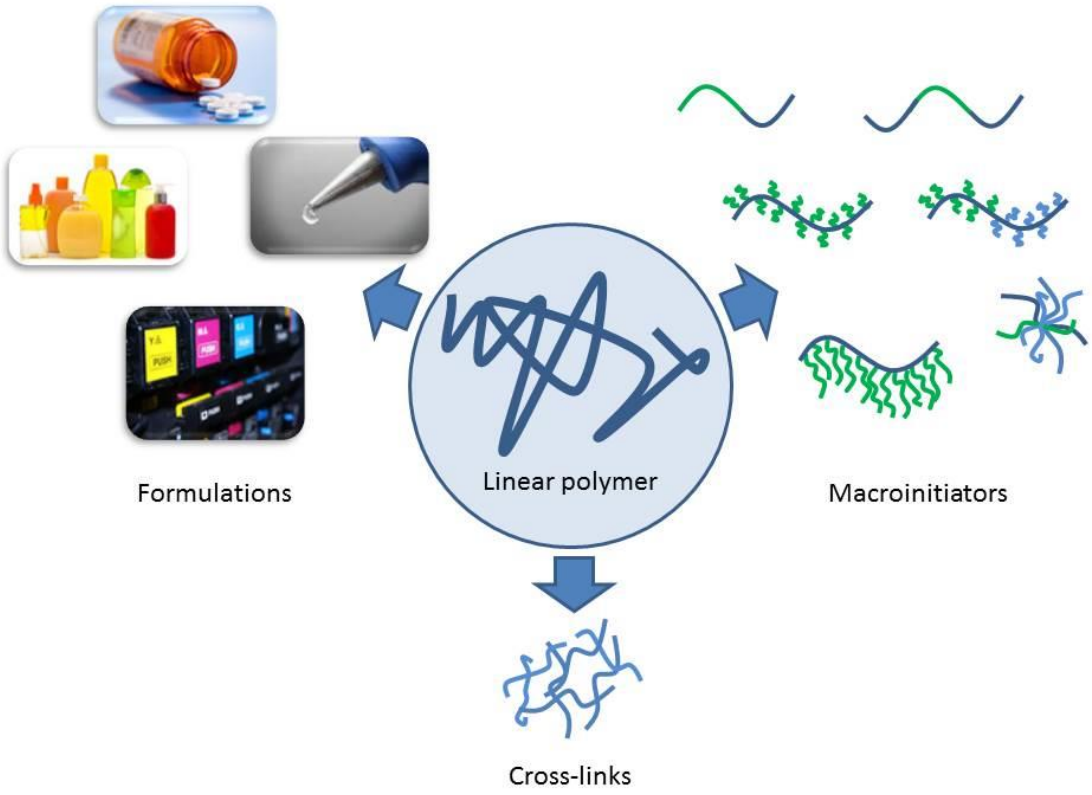

Figure 1.7 – Uses of linear polymers

1.6.2 Copolymers

Linear copolymers can be random, graduated, alternating, or block in structure. Random, graduated and alternating linear copolymers are produced in a one pot synthesis, whereas block copolymers often require a two-step process. The distribution of monomer units within a copolymer can be described using the Mayo-Lewis equation.[100] By calculating the reactivity ratios from experimental concentration values, it is possible to determine the copolymer composition. Block copolymers are synthesised in two steps and this can be achieved by RDRP techniques such as ATRP, AROP and RAFT, where an active chain end is retained after the polymerisation of the first block.[101] Block copolymers are often synthesised with hydrophilic and hydrophobic sections, allowing micelle formation under certain conditions.[102]

1.6.3 Cross-linked Polymer Networks

Cross-linked polymer networks are employed both industrially and in academic research. Car tyres are produced by the cross-linking of rubbers *via* the vulcanisation process. Cross-linked PVP (or crospovidone[103]) is utilised in tablet formulations and as a clarification agent in beverages.[104] Recent research on cross-linked polymers has focused on stimuli responsive reversible cross-linking,[105,106] hydrogel formation[107,108] and controlled drug delivery systems.[109,110]

1.6.4 Hyperbranched Polymers

Hyperbranched polymers have complex architectures with a high degree of functionality. The ability to produce polymers with extremely high complexation ability or that are highly charged is commercially attractive.[111] However, the synthesis and characterisation of hyper-branched materials is difficult due to the complex 3D-structure.

1.7 Pyrrolidone Functionalised Polymers

Industrially, as previously mentioned, PVP, P(VP-*co*-VAc) and cross-linked PVP (crospovidone) are synthesised by FRP and have a wide range of applications due to the excellent solubility, complexation and biocompatibility of the polymers. PVP based polymers have also found much success in more specialised applications which are discussed below.

As PVP is non-toxic, biocompatible and FDA approved, it is used in many biomedical applications. PVP hydrogels have received much attention[112–114] and have been shown to exhibit pH sensitive drug release properties when bound to chitosan.[112] Rimmer *et. al.* identified that the poly(vinyl pyrrolidone-*co*-diethylene glycol bisallylcarbonate) (PVP-*co*-DEGBAG) could be used in the development of wound dressings.[114] The same group showed that glucomannan-PVP hydrogels, specifically poly(vinyl pyrrolidone-*co*-poly(ethyleneglycol)diacrylate) (P(VP-*co*-PEGDA)) cross-linked with konjac glucomannan (KGM), were cytocompatible and stimulated fibroblast metabolic activity as well as fibroblast

and keratinocyte migration.[113] This demonstrates the advantageous properties of PVP hydrogels.

PVP based polymers have shown stimuli-responsive behaviours,[115,116] displaying another beneficial property that can be exploited for many uses. Dongxiang *et. al.* (2007) demonstrated that metal nanoparticles coated with PVP exhibited pH responsive behaviour,[117] this and other work by Pastoriza-Santos[118] amongst others have led to the prevalent use in nanoparticle stabilisation and functionalisation.[119–121]

Many of the pyrrolidone based polymers documented are based on NVP; copolymers, homo/copolymers of modified NVP or blends. This approach retains the problems associated with NVP polymerisation as NVP is a less activated monomer and leaves a gap for monomers modified with the pyrrolidone unit. By modifying more activated monomers with the pyrrolidone moiety, one is able to access a new range of pyrrolidone functionalised polymers. Utilising functional groups capable of undergoing polymerisation under simple reaction conditions will increase the scope of the applications for these polymers even further.

1.8 References

1 Mixtures of polymeric N-vinyl Pyrrolidone and Halogens, US Pat. 2739922, **1956**.

2 Process For Forming Film Of Hydrolysed Ethylene-vinyl Acetate Copolymer, UK Pat. 2150934, **1984**.

3 Method For Producing Anti-pollution Modified Polyvinylidene Flouride Hollow Fiber Membranes, US Pat. 10488458, **2015**.

4 Recording Ink Containing Pigment Particles And Polyvinyl Pyrrolidone, US Pat. 5847026, **1998**.

5 Cosmetic Eyeliner Formulation, US Pat. 5013543, **1991**.

6 Glossy Miltilayered Casing For Food Products, Permeable To Water And Smoke, WO 104946A1, **2014**.

7 Water-Soluble Film, US Pat. 4544693, **1985**.

8 Flexible Contact Lense, US Pat. 4062627, **1977**.

9 A. Tiwari, M. Ramalingam, H. Kobayashi and A. P. F. Turner, *Biomedical Materials and Diagnostic Devices*, Scrivener Publishing LLC. and John Wiley & Sons, Inc., **2012**.

10 H. Fikentscher and K. Herrle, *Mod. Plast.*, **1945**, 23, 157–163.

11 A. Guinaudeau, S. Mazières, D. J. Wilson and M. Destarac, *Polym. Chem.*, **2012**, 3, 81–84.

12 X. Lu, S. Gong, L. Meng, C. Li, S. Yang and L. Zhang, *Polymer (Guildf).*, **2007**, 48, 2835–2842.

13 I. J. Johnson, E. Khosravi, O. M. Musa, R. E. Simnett and A. M. Eissa, *J. Polym. Sci. Part A Polym. Chem.*, **2015**, 53, 775–786.

14 W. N. A. Bergius, L. R. Hutchings, N. M. Sarih, R. L. Thompson, M. Jeschke and R. Fisher, *Polym. Chem.*, **2013**, 4, 2815–2827.

15 Production of Lubricious Coating on Adhesive Hydrogels, US 6,846,291 B2, **2005**.

16 Microcrystalline Alumina-Based Ceramic Articles, CA Pat. 1317978, **1987**.

17 Electrically Conductive Metal Oxide Coatings, 4,904,526, **1990**.

18 K. Nishida, Y. Ando and S. Toriumi, *J. Soc. Dye. Colour.*, **1988**, 104, 96–99.

19 Reductive Cleaner Used for Polyester Fabrics, CN102816656 (A), **2012**.

20 Method of Heat Treating Metal Using A Washable Synthetic Quenchant, 4,738,731, **1997**.

21 Preventing Aqs Scale Deposits - byadding PVP esp in Petroleum Industry, DE Pat. 2151564, **1972**.

22 Laser and Thermally Writable Surface Coating for Materials, WO 2010130352, **2010**.

23 L. Zhang, Y. Liang, L. Meng and C. Wang, *Polym. Adv. Technol.*, **2009**, 20, 410–415.

24 X. Pan, M. A. Tasdelen, J. Laun, T. Junkers, Y. Yagci and K. Matyjaszewski, *Prog. Polym. Sci.*, **2016**, 62, 73–125.

25 H. Staudinger, *Berichte Der Dtsch. Chem. Gesellschaft*, **1920**, 53, 1073–1085.

26 D. Braun, *Int. J. Polym. Sci.*, **2009**, 1–10.

27 T. Furuncuolu, D. Ugur and V. Aviyente, *Macromolecules*, **2010**, 43, 1823–1835.

28 K. Matyjaszewski, *Handbook of Radical Polymerisation*, John Wiley and Sons Inc., **2012**.

29 M. Szwarc, *J. Polym. Sci. Part A Polym. Chem.*, **1998**, 36, ix–xv.

30 M. Szwarc, *Nature*, **1956**, 178, 1168–1169.

31 Polymerization Process and Polymers Produced Thereby, US Pat. 4581429, **1986**.

32 Y. A. Kabachii, S. Y. Kochev, L. M. Bronstein, I. B. Blagodatskikh and P. M. Valetsky, *Polym. Bull.*, **2003**, 50, 271–278.

33 Z. H. Li, Y. M. Zhang, M. Z. Xue, L. Zhou and Y. G. Liu, *J. Polym. Sci. Part A Polym. Chem.*, **2005**, 43, 5207–5216.

34 E. Duquesne, J. Habimana, P. Degée and P. Dubois, *Macromolecules*, **2005**, 38, 9999–10006.

35 J. A. M. Brandts, de G. P. van, F. E. E. van, J. Boersma and K. G. Van, *J. Organomet. Chem.*, **1999**, 584, 246–253.

36 F. Simal, A. Demonceau and A. F. Noels, *Tetrahedron Lett.*, **1999**, 40, 5689–5693.

37 V. Percec, B. Barboiu and A. Neumann, *Macromolecules*, **1996**, 29, 3665–3668.

38 P. Lecomte, I. Drapier, P. Dubois, P. Teyssié and R. Jérôme, *Macromolecules*, **1997**, 30, 7631–7633.

39 Y. Kotani, M. Kamigaito and M. Sawamoto, *Macromolecules*, **2000**, 33, 6746–6751.

40 W. A. Braunecker, Y. Itami and K. Matyjaszewski, *Macromolecules*, **2005**, 38, 9402–9404.

41 J. Louie and R. H. Grubbs, *Chem. Commun.*, **2000**, 1363, 1479–1480.

42 Y. Wang, Y. Zhang, B. Parker and K. Matyjaszewski, *Macromolecules*, **2011**, 44, 4022–4025.

43 J. S. Wang and K. Matyjaszewski, *J. Am. Chem. Soc.*, **1995**, 117, 5614–5615.

44 J.-S. Wang and K. Matyjaszewski, *Macromolecules*, **1995**, 28, 7901–7910.

45 B. M. Rosen and V. Percec, *Chem. Rev.*, **2009**, 109, 5069–5119.

46 D. Konkolewicz, Y. Wang, P. Krys, M. Zhong, A. A. Isse, A. Gennaro and K. Matyjaszewski, *Polym. Chem.*, **2014**, 5, 43960–4417.

47 A. L. J. Beckwith, *Angew. Chemie*, **1987**, 99, 824–825.

48 W. B. Motherwell, D. Crich, A. R. Katritzky, O. Meth-Cohn and C. S. Rees, *Free Radical Chain Reactions in Organic Synthesis*, Elsevier Ltd., **1992**.

49 J. Chiefari, Y. K. B. Chong, F. Ercole, J. Krstina, J. Jeffery, T. P. T. Le, R. T. A. Mayadunne, G. F. Meijs, C. L. Moad, G. Moad, E. Rizzardo, S. H. Thang and C. South, *Macromolecules*, **1998**, 31, 5559–5562.

50 J. Rieger, *Macromol. Rapid Commun.*, **2015**, 36, 1458–1471.

51 C. L. McCormick and A. B. Lowe, *Acc. Chem. Res.*, **2004**, 37, 312–325.

52 I. J. Johnson, E. Khosravi, O. M. Musa, R. E. Simnett and A. M. Eissa, *J. Polym. Sci. Part A Polym. Chem.*, **2015**, 53, 775–786.

53 J. Zhou and B. Hu, *J. Appl. Polym. Sci.*, **2015**, 132, 42649–42656.

54 Y. Xiang, H. Cong, L. Li and S. Zheng, *J. Polym. Sci. Part A Polym. Chem.*, **2016**, 54, 1852–1863.

55 L. Etchenausia, A. M. Rodrigues, S. Harrisson, E. Deniau Lejeune and M. Save, *Macromolecules*, **2016**, 49, 6799–6809.

56 H. Peng, K. Rübsam, X. Huang, F. Jakob, M. Karperien, U. Schwaneberg and A. Pich, *Macromolecules*, **2016**, 49, 7141–7154.

57 H. Leuchs, *Berichte Der Dtsch. Chem. Gesellschaft*, **1906**, 39, 857–861.

58 J. M. Longo, M. J. Sanford and G. W. Coates, *Chem. Rev.*, **2016**, 116, 15167–15197.

59 Y. Sarazin and J. F. Carpentier, *Chem. Rev.*, **2015**, 115, 3564–3614.

60 T. Öztürk, M. N. Atalar, M. Göktaş and B. Hazer, *J. Polym. Sci. Part A Polym. Chem.*, **2013**, 51, 2651–2659.

61 O. Nuyken and S. D. Pask, *Polymers (Basel).*, **2013**, 5, 361–403.

62 M. Bednarek, P. Kubisa and S. Penczek, *Macromolecules*, **1999**, 32, 5257–5263.

63 J. Jagur-Grodzinski, *Living and Controlled Polymerization Synthesis, Characterization*

and Properties of the Respective Polymers and Copolymers, Nova Science Publishes Inc., **2005**.

64 V. S. Reuss, M. Werre and H. Frey, *Macromol. Rapid Commun.*, **2012**, 33, 1556–1561.

65 C. Mangold, B. Obermeier, F. Wurm and H. Frey, *Macromol. Rapid Commun.*, **2011**, 32, 1930–1934.

66 J. Flory, *J. Am. Chem. Soc.*, **1940**, 62, 1561–1565.

67 A. Thomas, S. S. Müller and H. Frey, *Biomacromolecules*, **2014**, 15, 1935–1954.

68 C. Moers, R. Wrazidlo, A. Natalello, I. Netz, M. Mondeshki and H. Frey, *Macromol. Rapid Commun.*, **2014**, 35, 1075–1080.

69 J. Geschwind and H. Frey, *Macromol. Rapid Commun.*, **2013**, 34, 150–155.

70 M. Schömer, J. Seiwert and H. Frey, *ACS Macro Lett.*, **2012**, 1, 888–891.

71 A. M. Fischer, C. Schüll and H. Frey, *Polym. (United Kingdom)*, **2015**, 72, 436–446.

72 J. Seiwert, J. Herzberger, D. Leibig and H. Frey, *Macromol. Rapid Commun.*, **2016**, 38, 1–7.

73 N. Ajellal, J.-F. Carpentier, C. Guillaume, S. M. Guillaume, M. Helou, V. Poirier, Y. Sarazin and A. Trifonov, *Dalton Trans.*, **2010**, 39, 8363–8376.

74 S. Paul, Y. Zhu, C. Romain, R. Brooks, P. K. Saini and C. K. Williams, *Chem. Commun.*, **2015**, 51, 6459–6479.

75 A. L. Brocas, C. Mantzaridis, D. Tunc and S. Carlotti, *Prog. Polym. Sci.*, **2013**, 38, 845–873.

76 A. Duda and S. Penczek, *Macromolecules*, **1998**, 31, 2114–2122.

77 A. Duda and S. Penczek, *Macromolecules*, **1995**, 28, 5981–5992.

78 L. Feng, J. Hao, C. Xiong and X. Deng, *Chem. Commun.*, **2009**, 4411–4413.

79 L. Feng, Y. Liu, J. Hao, X. Li, C. Xiong and X. Deng, *Macromol. Chem. Phys.*, **2011**, 212,

2626–2632.

80 L. Feng, Z. Yang, Y. Liu, J. Hao, C. Xiong and X. Deng, *Iran. Polym. J. (English Ed.*, **2014**, 23, 217–226.

81 N. C. Ataman and H.-A. Klok, *Macromolecules*, **2016**, 49, 9035–9047.

82 L. Wu, U. Glebe and A. Böker, *Macromolecules*, **2016**, 49, 9586–9596.

83 S. A. Isarov, P. W. Lee and J. K. Pokorski, *Biomacromolecules*, **2016**, 17, 641–648.

84 M. Seyfollahi, R. Yegani, H. Etemadi and M. Rabiee, *Sep. Purif. Technol.*, **2016**, 177, 350–362.

85 X. Song, J. Zhu, Y. Wen, F. Zhao, Z.-X. Zhang and J. Li, *J. Colloid Interface Sci.*, **2017**, 490, 372–379.

86 S. Dong, B. Zheng, F. Wang and F. Huang, *Acc. Chem. Res.*, **2014**, 47, 1982–1994.

87 H. C. Kolb, M. G. Finn and K. B. Sharpless, *Angew. Chemie - Int. Ed.*, **2001**, 40, 2004–2021.

88 G. K. Such, A. P. R. Johnston, K. Liang and F. Caruso, *Prog. Polym. Sci.*, **2012**, 37, 985–1003.

89 J. E. Hein and V. V Fokin, *Chem Soc Rev*, **2010**, 39, 1302–1315.

90 V. V. Rostovtsev, L. G. Green, V. V. Fokin and K. B. Sharpless, *Angew. Chemie - Int. Ed.*, **2002**, 41, 2596–2599.

91 E. Dolci, V. Froidevaux, G. Michaud, F. Simon, R. Auvergne, S. Fouquay and S. Caillol, *J. Appl. Polym. Sci.*, **2017**, 134, 1–11.

92 H. Li, J. Li, W. Ke and Z. Ge, *Macromol. Rapid Commun.*, **2015**, 36, 1841–1849.

93 S. Motoki, T. Nakano, Y. Tokiwa, K. Saruwatari, I. Tomita and T. Iwamura, *Polym. (United Kingdom)*, **2016**, 101, 98–106.

94 Y.-L. Liu and T.-W. Chuo, *Polym. Chem.*, **2013**, 4, 2194–2205.

95 C. E. Hoyle and C. N. Bowman, *Angew. Chemie - Int. Ed.*, **2010**, 49, 1540–1573.

96 T. O. Machado, C. Sayer and P. H. H. Araujo, *Eur. Polym. J.*, **2015**, 86, 200–215.

97 M. A. Tasdelen, B. Kiskan and Y. Yagci, *Prog. Polym. Sci.*, **2016**, 52, 19–78.

98 J. Collins, Z. Xiao, M. Müllner and L. A. Connal, *Polym. Chem.*, **2016**, 7, 3812–3826.

99 S. V. Risbud, M.V.; Bhat, *J. Mater. Sci.*, **2001**, 12, 75–79.

100 F. R. Mayo and F. M. Lewis, *J. Am. Chem. Soc.*, **1944**, 66, 1594–1601.

101 D. J. Keddie, *Chem. Soc. Rev.*, **2014**, 43, 496–505.

102 J.-F. Gohy, *Block Copolymer Micelles*, Springer Berlin Heidelberg, **2005**.

103 A. Inc., *http://www.ashland.com/industries/personal-and-home-care/oral-care/polyplasdone-polymers*, accessed **27 March 2017**.

104 F. Haaf, A. Sanner and F. Straub, *Polym. J.*, **1985**, 17, 143–152.

105 Y. Liu, B. Xu, S. Sun, J. Wei, L. Wu and Y. Yu, *Adv. Mater.*, **2017**, 29, 1–7.

106 L. Dong, C. Shi, L. Guo, T. Yang, Y. Sun and X. Cui, *Ultrason. Sonochem.*, **2017**, 36, 437–445.

107 M. Hamidi, A. Azadi and P. Rafiei, *Adv. Drug Deliv. Rev.*, **2008**, 60, 1638–1649.

108 M. Rassu, V. Alzari, D. Nuvoli, L. Nuvoli, D. Sanna, V. Sanna, G. Malucelli and A. Mariani, *J. Polym. Sci. Part A Polym. Chem.*, **2017**, 55, 1268–1274.

109 S. Rehmani, M. Ahmad, M. U. Minhas, H. Anwar, M. I. ud din Zangi and M. Sohail, *Polym. Bull.*, **2016**, 74, 1–25.

110 D. Felicia, A. Loghin, G. Biliuta, S. Coseri and E. S. Dragan, *Int. J. Biol. Macromol.*, **2017**, 96, 589–599.

111 A. Lederer and W. Burchard, *Hyperbranched Polymers*, The Royal Society of Chemistry, **2015**.

112 M. V. Risbud, A. A. Hardikar, S. V. Bhat and R. R. Bhonde, *J. Control. Release*, **2000**, 68,

23–30.

113 M. Shahbuddin, A. J. Bullock, S. MacNeil and S. Rimmer, *J. Mater. Chem. B*, **2014**, 2, 727–738.

114 L. E. Smith, S. Rimmer and S. MacNeil, *Biomaterials*, **2006**, 27, 2806–2812.

115 W. Wang, Q. Wang and A. Wang, *Macromol. Res.*, **2011**, 19, 57–65.

116 N. Yan, J. Zhang, Y. Yuan, G.-T. Chen, P. J. Dyson, Z.-C. Li and Y. Kou, *Chem. Commun. (Camb).*, **2010**, 46, 1631–1633.

117 D. Li, Q. He, Y. Cui and J. Li, *Chem. Mater.*, **2007**, 19, 412–417.

118 I. Pastoriza-Santos and L. M. Liz-Marzán, *Langmuir*, **2002**, 18, 2888–2894.

119 T. Silva, L. R. Pokhrel, B. Dubey, T. M. Tolaymat, K. J. Maier and X. Liu, *Sci. Total Environ.*, **2014**, 468–469, 968–976.

120 S. Siankevich, G. Savoglidis, Z. Fei, G. Laurenczy, D. T. L. Alexander, N. Yan and P. J. Dyson, *J. Catal.*, **2014**, 315, 67–74.

121 K. M. Koczkur, S. Mourdikoudis, L. Polavarapu and S. E. Skrabalak, *Dalt. Trans.*, **2015**, 44, 17883–17905.

Chapter 2

Synthesis of Pyrrolidone Containing Monomers

This chapter describes the synthesis, development and characterisation of monomers containing the pyrrolidone functionality. 1,2-epoxy-3-oxyethyl pyrrolidone (**1**), 4-vinylbenzyloxy ethyl pyrrolidone (**2**) and 5-Ethacryloxyethyl-12-ethylpyrrolidyl-N,N'hexane biscarbamate (**3**) were designed (**3**) or chosen (**1**, **2**) for subsequent use in the development of novel homo and co-polymers. The highly reactive functional groups within monomers **1**-**3**, provide an efficient route to high molecular weight polymers *via* free radical or ring opening polymerisation. The monomers were analysed using 1D and 2D NMR spectroscopy, mass spectrometry and FTIR spectroscopy.

2.1 Introduction

The pyrrolidone group is prevalent in drugs accounting for 14.7% of drugs the contain five-membered N-heterocycles in 2014.[1] PVP is utilised in a large variety of applications: printing inks,[2] makeup products,[3] food packaging,[4] agrochemical storage[5] and contact lenses[6] amongst others. The versatility of pyrrolidone containing materials is evident by the diversity of the products that contain the polymer.

NVP is predominantly used as a monomer to produce PVP homo- and co-polymers. PVP has a large variety of applications due to the chemical and physical properties of the polymer. It is possible, by altering the molecular weight, to change the physical properties of the polymer and therefore tune the product for a specific use. High molecular weight polymers have increased mechanical strength, increased viscosity and are harder to process than lower molecular weight polymers. Low molecular weight polymers can be employed as thin/flexible films as they are less viscous and easier to process.

Ashland Inc. is a major global supplier of NMP, NVP, and PVP. The PVP K-series is a PVP homopolymer available to purchase at different molecular weights based on viscosity of the sample. Ashland Inc. also produces co-polymers of PVP with vinyl acetate (VAc) with a PVP content from 30 to 70%. PVP is used in food production and packaging, medications, printing inks, home care and personal care products due to its unique solubilising[7] and film forming[8] properties. The number of patents containing 'pyrrolidone polymer' has more than doubled in the last ten years from 365 in 2005 to 768 in 2015.[9] This increase demonstrates the current and ongoing importance of pyrrolidone and pyrrolidone containing polymers. Pyrrolidone-containing polymers have exhibited stimuli responsive behaviour.[10] Thermo- and pH-responsive pyrrolidone polymers have been employed in the oral delivery of therapeutic proteins[11] and in the site specific delivery of siRNA to combat inflammatory bowel disease.[12] Therefore, with a desire to increase the scope of compatibility and versatility within this range of polymers, a variety of pyrrolidone containing monomers were produced. There are examples of pyrrolidone containing monomers in the literature which contain a variety of functional groups, in this chapter we focus on acrylates, epoxide and styrene.

Acrylates (Figure 2.1i) and related functional groups (methacrylates, acrylamides and methacrylamides) are widely used in adhesives, inks and coatings due to the speed at which they react and the adhesive properties of the polymers produced. Often, the polymerisation occurs on contact with air and with no additional increase in temperature, pressure or UV light. This efficacy of polymerisation and the ability to produce polymers with high molecular weights are among the reasons for producing pyrrolidone containing polymers with acrylate functional groups.

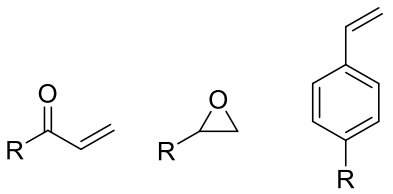

i) ii) iii)

Figure 2.1 – Structure of i) Acrylate ii) Epoxide and iii) Styrene functional groups

Epoxides (Figure 2.1ii) are common resins for coatings and as a sealant as well as for detergents and surfactants. The strained three-membered ring is easily opened to produce polymers and oligomers with hydroxyl end groups. Water soluble, non-toxic and biocompatible polymers that can aid the solubilisation of insoluble or partially soluble additives are of great interest to the pharmaceutical, cosmetic and personal product industries.

Styrene (Figure 2.1iii, R=H) was first polymerised in 1839 by Eduard Simon in Berlin and now accounts for 7.1% of plastic products in Europe.[13] The ease of polymerisation, extrusion and moulding allows polystyrene (PS) to be utilised in a wide variety of applications. Typically PS is used for foam packing or containers. The introduction of the highly polar pyrrolidone group was thought to introduce some interesting solubility, with the aim to make the styrene-based polymer that is soluble in a wider range of solvents compared with PS.

2.2 Experimental

2.2.1 Materials

Hydroxyethyl Pyrrolidone (HEP) was obtained from Ashland Inc. and used as supplied. Acryloyl chloride (≥97%, contains ~400 ppm phenothiazine as stabiliser) was distilled prior to use. 2-Hydroxyethyl acrylate (HEA, 96%, 200-650 ppm monomethylether hydroquinone) and 4-Vinylbenzyl chloride (90%), purchased from Sigma-Aldrich, was washed with 5% $NaOH_{aq}$ to remove inhibitors. Butylated hydroxytoluene (BHT, ≥99%), epichlorohydrin (ECH, ≥99%), hexamethylene diisocyanate (HDI, ≥99%), potassium hydroxide (KOH, ≥90%), sodium hydroxide (NaOH, ≥98%), triethylamine (NEt_3 ≥99%), were purchased from Sigma-Aldrich and used as supplied. Acetone, DCM, ethyl acetate and hexane analytical grade solvents were purchased from Fisher Scientific and used as received. Dry DMF, THF and toluene were obtained from the Durham University Chemistry Department solvent purification service (SPS). Silica gel (40-60 micron) was purchased from Fluorochem and used as supplied.

2.2.2 Instrumentation

^{1}H and ^{13}C Nuclear Magnetic Resonance (NMR) spectra were recorded on a Bruker Avance 400 operating at 400 MHz or a Varian VNMRS 700 spectrometer operating at 700 MHz (^{1}H) and 176 MHz (^{13}C) with *J* values given in Hz. $CDCl_3$ was used as the deuterated solvent for ^{1}H and ^{13}C NMR analysis and the spectra were referenced to the solvent at 7.26ppm and 77.16 ppm, respectively. The following abbreviations are used in describing NMR spectra: s = singlet, d = doublet, t = triplet, dd = doublet of doublets, m = multiplet and b = broad. 2D NMR experiments were also used to fully assign the proton and carbon environments in the products. ^{1}H-^{1}H Correlation Spectroscopy (COSY) demonstrated proton-proton correlations over two or three bonds. ^{1}H-^{13}C Heteronuclear Shift Correlation Spectroscopy (HSQC) showed the correlation between directly bonded proton and carbon atoms. ^{1}H-^{13}C

Heteronuclear Multiple-bond Correlation (HMBC) NMR demonstrated the correlation between proton and carbon atoms through several bonds.

Accurate mass data was obtained using a *QtoF Premier* mass spectrometer and an Acquity UPLC (Waters Ltd, UK) with an electrospray (ES) ion source for positive ionisation. The samples solution (1 $mgmL^{-1}$) was injected (~10$\mu Lmin^{-1}$) into a flow (0.2 $mLmin^{-1}$) of acetonitrile.

Fourier transform infra-red (FTIR) spectroscopy was conducted using a Perkin Elmer 1600 series spectrometer.

Elemental Analysis was conducted using an Exeter CE-440 Elemental Analyser.

2.2.3 Synthesis of 1-(2-(oxiran-2-ylmethoxy) ethyl) pyrrolidin-2-one, (1)

To a solution of HEP (5 g, 38.7 mmol) and NaOH (1.54 g, 38.7 mmol) stirred at 0°C, epichlorohydrin (7.16 g, 77.4 mmol) was added slowly and the mixture stirred until homogeneous. The reaction was heated to 50 °C and stirred for 12 h. The solid was removed by filtration and excess solvent was removed under reduced pressure to give a pale yellow liquid. The product (**1**) was purified by column chromatography (SiO_2, gradient 100% Ethyl acetate to 100% Acetone) (71%). ^{1}H NMR (400 MHz, $CDCl_3$) δ = 3.78 (m, 2H, OC**H**$_2$CHOCH$_2$), 3.68-3.58 (m, 2H, NCH$_2$C**H**$_2$O), 3.52-3.45 (m, 4H, NC**H**$_2$CH$_2$CH$_2$CO, NC**H**$_2$CH$_2$O), 3.37 (m, 2H, OC**H**$_2$CHOCH$_2$), 3.11-3.15 (m, 1H, C**H**OCH$_2$), 2.80 (m, 1H, CHOC**H**$_2$), 2.61 (m, 1H, CHOC**H**$_2$), 2.39 (t, 2H, 8 Hz, NCH$_2$CH$_2$C**H**$_2$CO), 1.98-2.05 (m, 2H, NCH$_2$C**H**$_2$CH$_2$CO) ppm. ^{13}C NMR (176 MHz, $CDCl_3$) δ = 175.1(NCH$_2$CH$_2$CH$_2$**C**O), 71.4 (O**C**H$_2$CHOCH$_2$), 69.4 (NCH$_2$**C**H$_2$O), 50.7 (OCH$_2$**C**HOCH$_2$), 48.4 (N**C**H$_2$CH$_2$CH$_2$CO), 44.0 (CHO**C**H$_2$), 42.4 (N**C**H$_2$CH$_2$O), 30.8 (NCH$_2$CH$_2$**C**H$_2$CO), 18.0 (NCH$_2$**C**H$_2$CH$_2$CO) ppm. MS: *m/z* ES$^+$, [M + H] $^+$ = 186.11, [M + Na] $^+$ = 208.10. FTIR ν (cm^{-1}) = 2866 (CH$_2$), 1670 (C=O). Anal. Calc. for $C_9H_{15}NO_3$; C, 59.66; H, 6.12, N, 7.73%. Found: C, 55.39; H, 8.37; N, 6.40%.

2.2.4 Synthesis of 4-vinylbenzyloxy ethyl pyrrolidone, (2)

HEP (5 g, 38.7 mmol) in dry DMF (50 mL) was stirred at 0 °C. KOH (2.17 g, 38.7 mmol) was added, the mixture was stirred until homogeneous. 4-Vinylbenzyl chloride (5.9 g, 38.7 mmol) was added slowly and the reaction warmed to room temperature and stirred for 18 h. DCM (30 mL) was added and the precipitate was removed by filtration. The excess solvent was removed under reduced pressure to afford a concentrated solution of product (**2**) in DMF (NMR yield >99%). ^{1}H NMR (400 MHz, $CDCl_3$) δ = 7.36 (m, 2H, Hz, m-C**H**) , 7.24 (m, 2H, *o*-C**H**), 6.68 (dd, 1H, J = 17.6, 10.9 Hz, C**H**), 5.71 (d, 1H, J = 17.6 Hz, C**H**$_2$), 5.21 (d, 1H, J = 10.8 Hz, C**H**$_2$), 4.46 (s, 2H, CC**H**$_2$O), 3.59-3.56 (m, 2H, OC**H**$_2$CH$_2$N), 3.49-3.44 (m, 4H, OCH$_2$C**H**$_2$N, NC**H**$_2$CH$_2$CH$_2$CO), 2.34 (m, 2H, NCH$_2$CH$_2$C**H**$_2$CO), 2.00-1.93 (m, 2H, NCH$_2$C**H**$_2$CH$_2$CO) ppm. ^{13}C NMR (176 MHz, $CDCl_3$) δ = 175.2 (**C**=O), 137.6 (OCH$_2$**C**), 137.0 (CH$_2$CH**C**), 136.4 (CH$_2$**C**H) 127.8 (*Ar*-CH) 126.2 (*Ar*-CH), 113.8 (**C**H$_2$CH), 72.6 (O**C**H$_2$Ar), 68.3 (CH$_2$CH**C**), 48.5 (N**C**H$_2$CH$_2$CH$_2$CO), 42.5 (OCH$_2$**C**H$_2$N), 30.9 (NCH$_2$**C**H$_2$CH$_2$CO), 18.1 (NCH$_2$CH$_2$**C**H$_2$CO) ppm. MS: *m/z* ES$^+$, [M + H]$^+$ = 246.15, [M + Na]$^+$ =268.13. FTIR ν (cm^{-1}) = 2941 (CH$_2$), 2878 (CH$_2$), 1660 (C=O), 1414 (CH$_2$ bend). Anal. Calc. for $C_{15}H_{19}NO_2$; C, 73.44; H, 7.81, N, 5.71%. Found: C, 71.03; H, 7.75; N, 5.06%.

2.2.5 Synthesis of 5-ethacryloxyethyl-12-ethylpyrrolidyl-N,N'hexane biscarbamate, (3)

HEP (5 g, 38.7 mmol) was added to HEA (4.5 g, 38.7 mmol) before the mixture was degassed by three freeze-pump-thaw cycles. Toluene (100 mL) was added and the mixture was degassed with one further freeze-pump-thaw cycle. HDI (6.25 mL, 38.7 mmol) was added to the stirring mixture slowly while the mixture was cold. The reaction was allowed to warm to room temperature then slowly heated to 50 °C and stirred for 18 h. The progress of reaction was followed by FTIR, noting the disappearance of the distinctive NCO band at 2300 cm^{-1}. Excess solvent was removed under reduced pressure and the resulting product was purified by column chromatography (gradient, 100% Hexane to 100% Ethyl Acetate) to afford a white crystalline solid (**3**) (55%). ^{1}H NMR (600 MHz, $CDCl_3$) δ = 6.42 (d, 1H, *J* = 17.3 Hz, CHC**H**$_2$), 6.13 (dd, 1H, *J* = 17.3, 10.5 Hz, C**H**CH$_2$), 5.85 (d, 1H, *J* = 10.4 Hz, CHC**H**$_2$), 4.88-4.59 (m, 2H, N**H**), 4.33 (s, 2H, CH$_2$CHCOOC**H**$_2$), 4.29 (s, 2H, CH$_2$CHCOOCH$_2$C**H**$_2$O), 4.17 (s, 2H, OC**H**$_2$CH$_2$N),

3.50 (s, 2H, $OCH_2C\mathbf{H}_2N$), 3.44 (t, 2H, J = 4.6 Hz, $NC\mathbf{H}_2CH_2CH_2CO$), 3.06-3.20 (m, 4H, $NHC\mathbf{H}_2CH_2CH_2CH_2C\mathbf{H}_2NH$), 2.36 (t, 2H, J = 5.4 Hz, $NCH_2CH_2C\mathbf{H}_2CO$), 2.03-1.98 (m, 2H, $NCH_2C\mathbf{H}_2CH_2CO$), 1.42-1.54 (m, 4H, $NHCH_2C\mathbf{H}_2CH_2CH_2C\mathbf{H}_2CH_2NH$-), 1.27-1.37 (m, $NHCH_2CH_2C\mathbf{H}_2C\mathbf{H}_2CH_2CH_2NH$) ppm. ^{13}C NMR (176 MHz, $CDCl_3$) δ = 175.4 ($NCH_2CH_2CH_2\mathbf{C}O$), 165.9 ($CH_2CH\mathbf{C}O$), 156.2 ($NH\mathbf{C}OOCH_2CH_2N$), 156.1 ($NH\mathbf{C}OOCH_2CH_2O$), 131.2 ($\mathbf{C}H_2CH$), 128.0 ($CH_2\mathbf{C}H$), 62.8 ($CH_2CHCOO\mathbf{C}H_2CH_2O$), 62.4 ($CH_2CHCOOCH_2\mathbf{C}H_2O$), 61.7 ($O\mathbf{C}H_2CH_2N$), 47.6 ($NCH_2CH_2\mathbf{C}H_2CO$), 42.1 ($OCH_2\mathbf{C}H_2N$), 40.8 ($NH\mathbf{C}H_2CH_2CH_2CH_2CH_2\mathbf{C}H_2NH$), 30.8 ($N\mathbf{C}H_2CH_2CH_2CO$), 29.7 ($NHCH_2\mathbf{C}H_2CH_2CH_2\mathbf{C}H_2CH_2NH$), 26.2 ($NHCH_2CH_2\mathbf{C}H_2\mathbf{C}H_2CH_2CH_2NH$), 18.0 ($NCH_2\mathbf{C}H_2CH_2CO$) ppm. MS: *m/z* ES^+, $[M + H]^+ = 414.22$, $[M + Na]^+ = 436.21$. FTIR ν (cm^{-1}) = 3333 (NH), 2939-2859 (CH_2), 1719 (C=O ester), 1680 (C=O lactam), 1675 (C=O urethane). Anal. Calc. for $C_{19}H_{31}N_3O_7$; C, 55.28; H, 7.53, N, 10.09%. Found: C, 55.19; H, 7.56; N, 10.16%.

2.3 Results & Discussion

2.3.1 1-(2-(oxiran-2-ylmethoxy) ethyl) pyrrolidin-2-one, (1)

Monomer **1**, glycidyl ethylpyrrolidone (GEP) (Scheme 2.1) combines the pyrrolidone group with an epoxide. This known monomer is able to undergo ring opening polymerisation with an aim to produce polymers with a polar (polyethylene glycol, PEG) backbone as well as a polar pendant group (pyrrolidone). Highly polar polymers are expected to be water soluble, this could lead to uses in personal products and medicines. The synthesis of monomer **1** is acknowledged in patents[14,15,16] however, the synthesis and characterisation has not been fully explored, therefore it is described here.

To a stirring mixture of hydroxyethyl pyrrolidone, sodium hydroxide was added to deprotonate the hydroxyl group. Epichlorohydrin was added dropwise at 0 °C to ensure anionic polymerisation of the epoxide did not occur. The monomer was obtained as a yellow oil (**1**) (71%). The results of this synthesis were analysed with the use of ^{1}H NMR, ^{13}C NMR, accurate mass spectrometry, FTIR spectroscopy and 2D NMR spectroscopy such as COSY, ^{1}H-^{13}C HSQC and HMBC NMR.

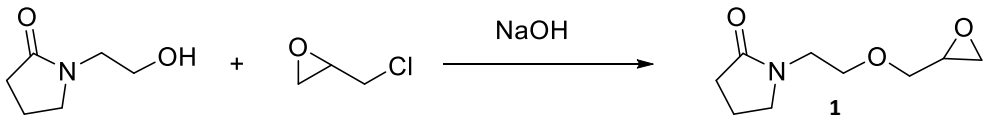

Scheme 2.1 – Synthesis of monomer 1

Under basic conditions epoxide reactions proceed *via* an S_N2 mechanism (Scheme 2.2)[17]. The anion generated from the HEP, attacks the least hindered side of the epoxide which opens the 3-membered ring. The anion formed in this step then regenerates the epoxide

with the chlorine as the leaving group. The excess sodium in the system then forms sodium chloride which is removed by filtration.

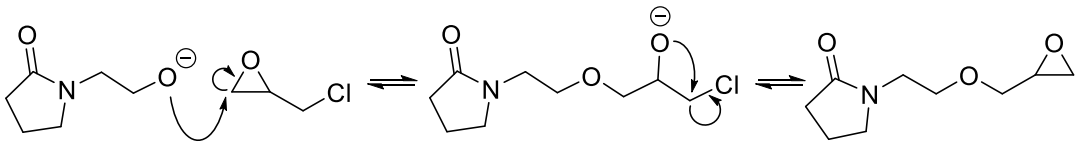

Scheme 2.2 – S_N2 mechanism of reaction of HEP and ECH under basic conditions

Method development was conducted to improve the reaction. Epichlorohydrin equivalents of 2, 1.5 and 1 gave yields of 52, 63 and 71%, respectively. The optimum conditions were determined to be 1:1 ratio of epichlorohydrin to sodium hydroxide as expected for the reaction. The reaction temperature was varied at 50 and 100 °C (reflux) (Figure 2.2) and also at room temperature (20 °C, not shown), the reaction progress was followed by NMR spectroscopy.

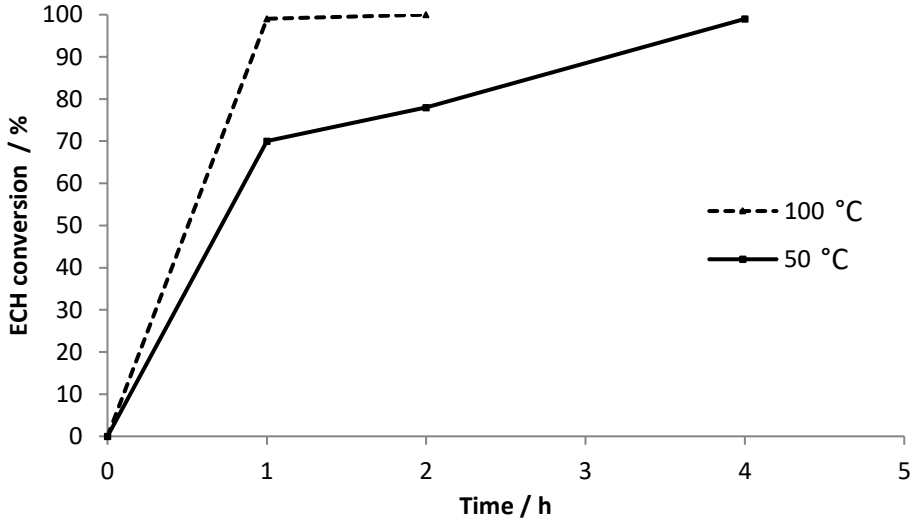

Figure 2.2 – Showing equivalents of epichlorohydrin vs yield of reaction

At room temperature, the reaction reached 99% conversion of epichlorohydrin after 48 h compared to 4 h at 50 °C and 1 h at 100 °C. The yield of the reaction was not affected greatly with the change in reaction temperature, remaining within 61-71%. There is only a minimal decrease in the purity of the crude product with increasing the temperature.

Increasing the temperature of a reaction on an industrial scale increases costs, therefore the reaction was conducted routinely at 50 °C to markedly reduce reaction time and maintain lower costs.

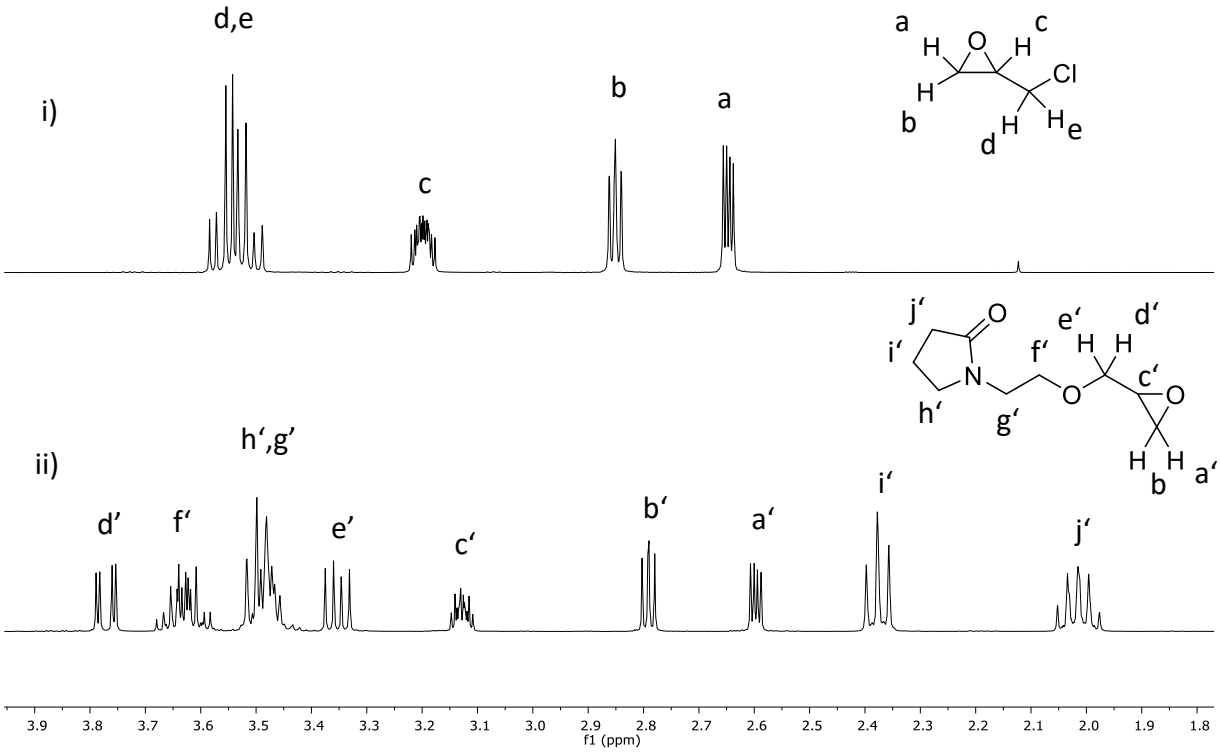

Figure 2.3 – ^{1}H NMR spectrum of i) Epichlorohydrin and ii) Monomer 1

The reactions were followed by ^{1}H NMR spectroscopy. It was clear to see the formation of the epoxide as the characteristic resonances attributed to the three-membered ring were shifted downfield as shown in Figure 2.3 (**a** to **a'**, **b** to **b'** and **c** to **c'**). The ^{13}C NMR spectrum contains 9 resonances (Figure 2.4) which correlate directly to the ^{1}H NMR spectrum in the ^{1}H-^{13}C HSQC. Proton **j'** correlates to carbon **H**, **i'** to **G**, **f'** to **D**, **e'** and **d'** to **C**, **c'** to **B**, and, **b'** and **a'** to **A**. It is not possible to assign carbons **E** and **F** from the HSQC spectrum. The HMBC allows the assignment of carbon **E** at δ = 42.4 ppm and **F** at δ = 48.5 ppm.

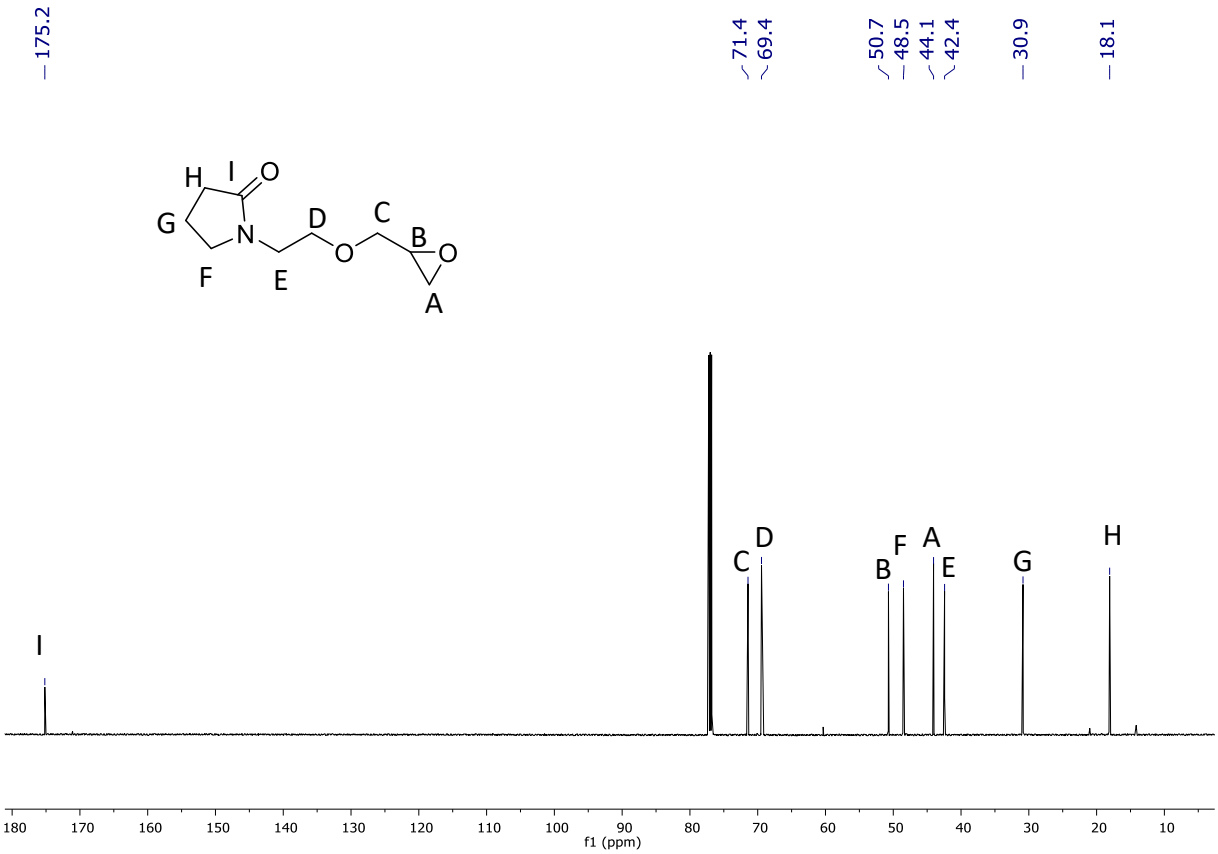

Figure 2.4 – ^{13}C NMR spectrum of monomer 1

The FTIR spectrum shows the disappearance of the broad OH resonance present in the HEP starting material at 3366 cm^{-1}. The accumulated analysis, including the accurate mass of m/z $[M + H]^+$ = 186.11 and $[M + Na]^+$ = 208.10 and elemental analysis support the formation of the desired product.

The epoxide monomer (**1**) was synthesised, characterised and the reaction conditions were optimised. The equivalents of epichlorohydrin as well as reaction time and temperature were varied to obtain the optimal conditions of 1 equiv., 50 °C and a reaction time of 4 h. The simple reaction process, availability of starting materials and yield of reaction all contribute to the industrial viability of this monomer.

2.3.2 4-Vinylbenzyloxy ethyl pyrrolidone, (2)

Monomer **2** (Figure 2.5) incorporates the highly reactive styrene functional moiety with the polar pyrrolidone group. The known monomer (**2**) was produced with the aim to generate styrene based copolymers with greater solubility when compared to standard PS. The synthesis of 4-(oxo-1-pyrrolidinyl) methyl styrene and monomer **2** (Figure 2.5) using sodium hydride has been previously reported.[18] This approach was adopted as a starting point for the development of the synthesis.

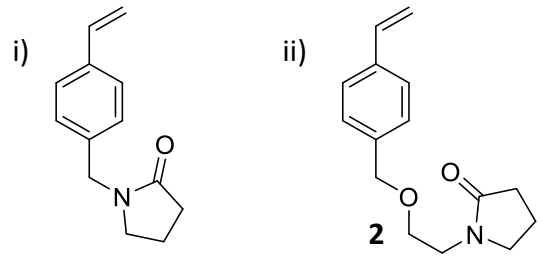

Figure 2.5 – Structure of i) 4-(oxo-1-pyrrolidinyl) methyl styrene and ii) Monomer 2

The reaction (Scheme 2.3) was first conducted as reported in the literature[18] in a two-step process: using a dispersion of sodium hydride (NaH) in DMF to deprotonate the HEP for 5 h before adding the 4-vinyl benzyl chloride and stirring for an additional 5 h. Excess DMF was removed before the product was extracted, dried and purified by column chromatography, giving a yield of 54%. The literature reports the yield to be 45%[18] therefore, method development was conducted to improve the reaction yield. Addition of saturated ammonium chloride solution to the work up, as carried out in similar reactions[19], increased the yield to 72%. To optimise the reaction various bases were used.

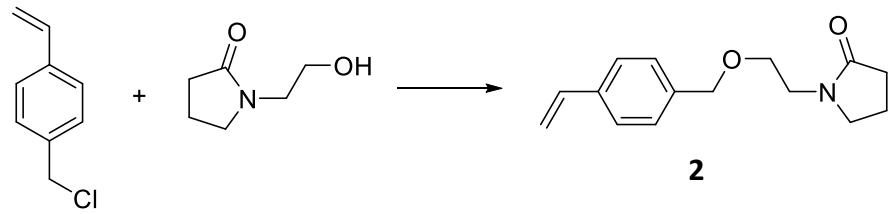

Scheme 2.3 – Synthesis of monomer 2

n-Butyl lithium (*n*-BuLi) in THF at −78 °C gave a 10% yield after 2 h. The reaction time was limited to 2 h due to the difficulty of maintaining the reaction at −78 °C. Potassium hydroxide was employed as a replacement for NaH to investigate if a less hazardous base could be employed in this reaction.[20] Additionally, NaH is more than four times the cost of KOH, making the adapted procedure more cost effective and therefore more industrially viable.

Potassium hydroxide was used to deprotonate the hydroxyethyl pyrrolidone in DMF which then reacted with the 4-vinyl benzyl chloride. The mixture was stirred for 18 h at room temperature to allow the reaction to reach completion. Attempts were made to remove the DMF fully, however, the monomer spontaneously polymerised into an insoluble translucent solid at room temperature. Therefore, the monomer was kept as a solution in DMF. The results of this synthesis were analysed with the use of ^{1}H NMR, ^{13}C NMR, accurate mass spectrometry, FTIR spectroscopy and 2D NMR spectroscopy such as COSY, ^{1}H-^{13}C HSQC and HMBC NMR.

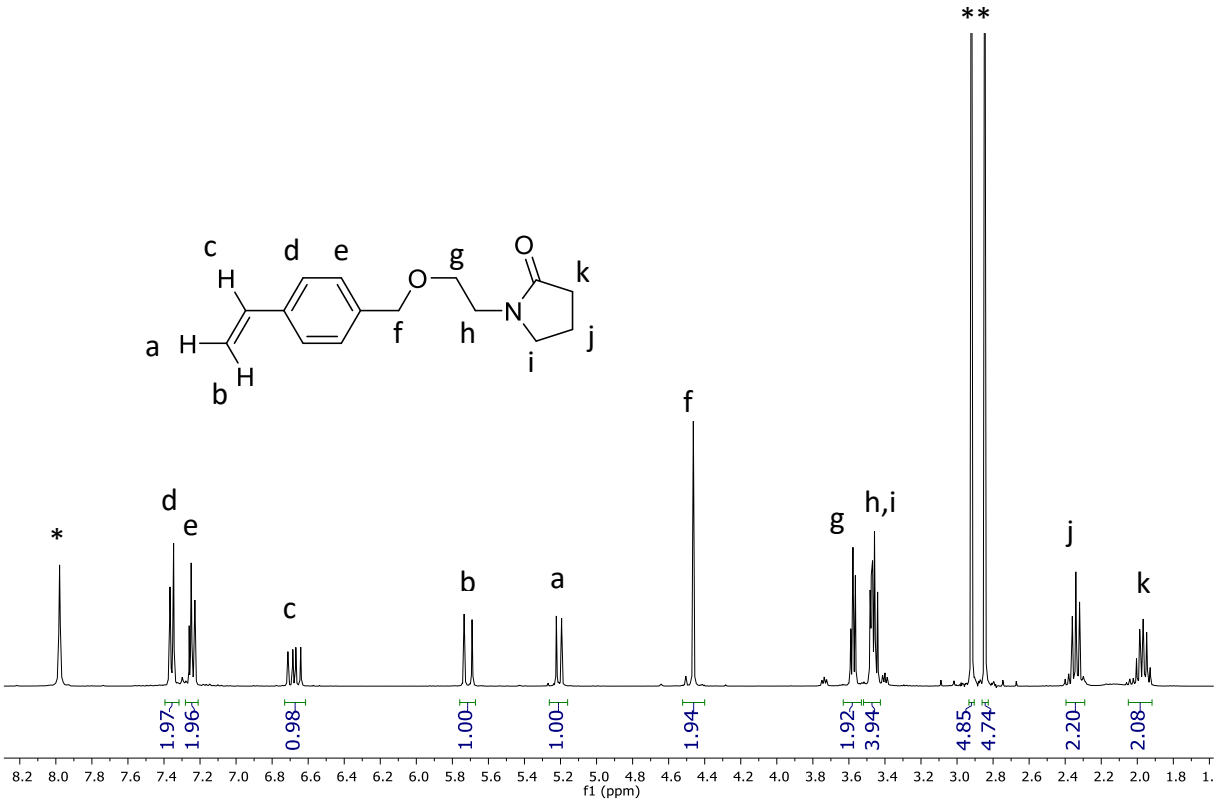

Figure 2.6 – ^{1}H NMR spectrum of monomer 2

The ^{1}H NMR spectrum (Figure 2.6) shows the aromatic CH's, **d** and **e**, at δ = 7.36 and 7.24 ppm, respectively. The methine proton **c** is at δ = 6.67 ppm and the methylene protons **a** and **b** are at δ = 5.22 and 5.77, respectively. The coupling constants of 11.7 Hz for **a** and 16.8 Hz for **b** indicate that **b** is *trans* to proton **c**. The pyrrolidone group shows the characteristic profile with **i** at δ = 3.46 ppm, more downfield than **j** and **k** at δ = 2.34 and 1.96 ppm, respectively. In this spectrum, protons **j** and **i** are overlapping at δ = 3.46 ppm. In the ^{1}H-^{1}H COSY spectrum, the resonance at δ = 3.46 ppm also couples to the resonance at δ = 3.57 ppm, this resonance corresponds to proton **g**.

The ^{13}C spectrum has 13 resonances that correspond to the 13 carbon environments in the molecule (Figure 2.7). The ^{13}C Spectrum is easily assigned from the ^{1}H-^{13}C HSQC spectrum. Protons **a** and **b** correlate to carbon **A**, **c** to **B**, **d** to **D**, **e** to **E**, **f** to **G**, **g** to **H**, **j** to **K**, and **k** to **L**. It is not possible to assign protons **h** and **i** from the HSQC spectrum as the resonances are overlapping. The carbons at δ = 175.2, 137.6 and 137.0 show no correlation in the HSQC spectrum, indicating the resonances are attributed to quaternary carbons.

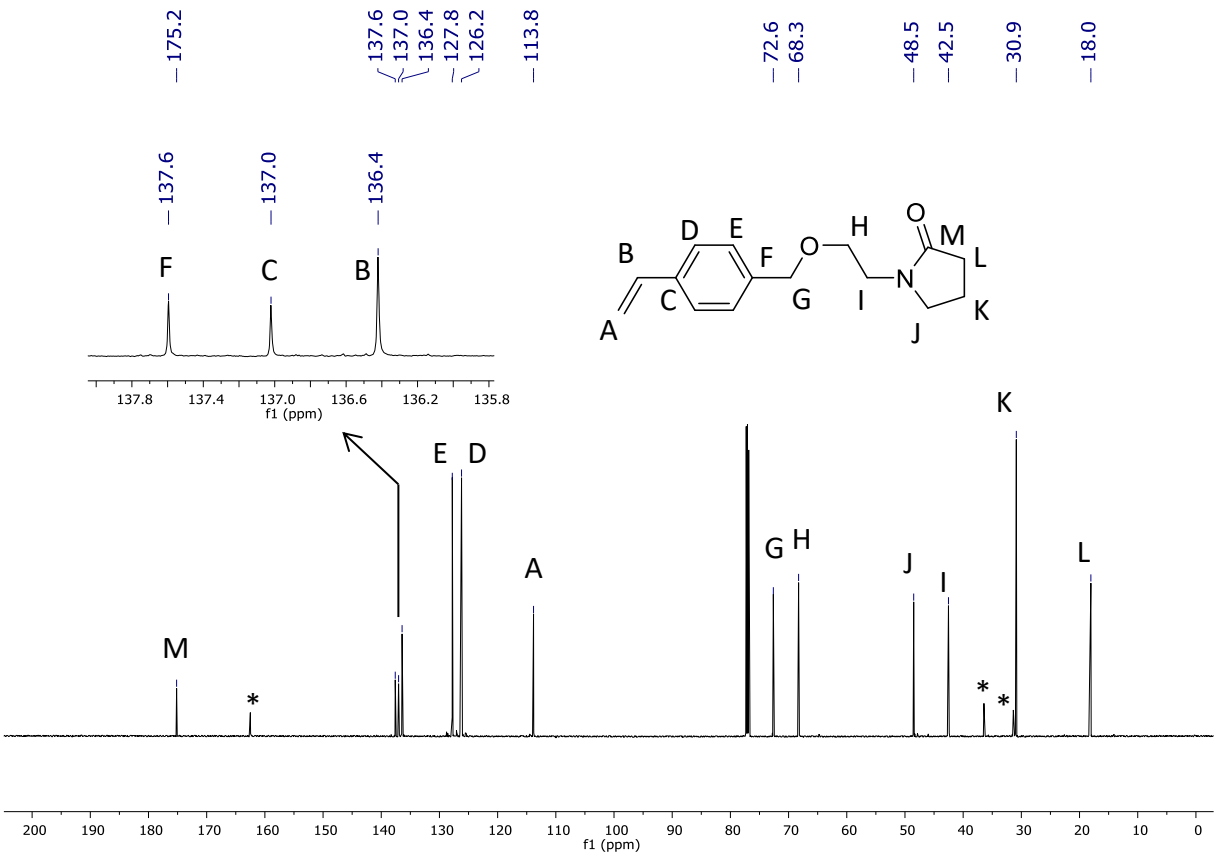

Figure 2.7 – ^{13}C NMR spectrum of monomer 2

The ^{1}H-^{13}C HMBC spectrum allows characterisation of the remaining carbon resonances. The proton resonance for **h** and **i** are overlapping but unsymmetrical. This asymmetry is more obvious in the HMBC but is visible in the ^{1}H-^{1}H COSY and shows that the proton resonance that is more upfield correlates to protons **j** and **k**, therefore is attributed to proton **i**. This upfield ^{1}H resonance (**i**) correlates to carbon **J** at δ = 48.5 ppm and the downfield ^{1}H resonance (**h**) correlates to carbon **I** at δ = 42.5 ppm. The carbonyl is attributed to the resonance at δ = 175.2 ppm due to the shift. The HMBC also allows assignment of the remaining quaternary carbons **C** and **F**. The carbon at δ = 137.0 ppm correlates to proton **e**, therefore this is carbon **C** and the resonance at δ = 137.6 is due to **F**.

Analysis of the FTIR spectrum shows the loss of the broad OH resonance in the HEP starting material (at 3366 cm^{-1}) as well as the retention of the carbonyl stretching at 1660 cm^{-1}. The additional analysis (EA and 2D-NMR) along with the accurate mass of m/z $[M + Na]^{+}$ = 246.15 endorse the formation of the desired product.

Monomer **2** was synthesised to a high yield and the product was fully characterised. It was not possible to fully remove the residual DMF due to the high reactivity of the monomer. Potassium hydroxide was substituted for sodium hydride to reduce cost and hazards associated with the experiment, making the reaction more industrially viable.

2.3.3 5-Ethacryloxyethyl-12-ethylpyrrolidyl-N,N'hexane biscarbamate, (3)

As discussed previously, acrylates and related functional groups are key components of many inks, adhesives and coatings. The monomers *N*-(2-acryloyloxyethyl)-pyrrolidone and *N*-(2-methacryloyloxyethyl)-pyrrolidone (Figure 2.8) are known monomers and are well documented.[21–27] The success of these monomers demonstrated by the scope of application from personal products and biocompatible hydrogels to synthetic nano-object formation inspired the development of an analogous but novel counterpart.

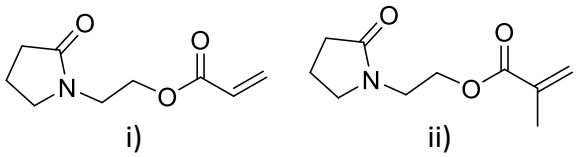

Figure 2.8 – Structure of i) 1-(2-acryloyloxyethyl)-pyrrolidone and ii) *N*-(2-methacryloyloxyethyl)-pyrrolidone

Initially the reaction of 2-chloroethyl acrylate with HEP was investigated as a route to a novel monomer *N*-[2-(2-acryloyloxyethoxy)-ethyl]-pyrrolidone), however, the reaction produced only the known monomer 1-(2-acryloyloxyethyl)-pyrrolidone. It is believed that the alkoxide formed with the deprotonation of HEP attack the carbonyl of the 2-chloroethyl acrylate preferentially over the chlorine leaving group, resulting in the loss of ethyl chloride. Therefore a more complex monomer structure was developed which contained the acrylate group, a pyrrolidone group, and urethane linkages.

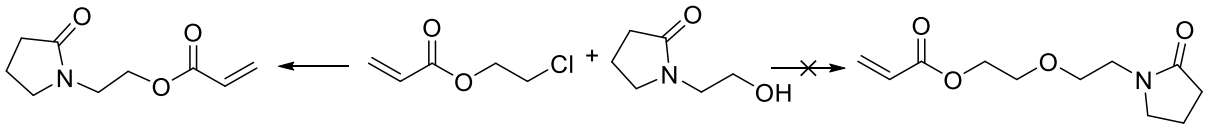

Scheme 2.4 – Reaction of 2-chloroethyl acrylate with HEP

To produce a variety of polymeric materials and with the aim to increase the product scope, monomer **3** (Figure 2.9) was synthesised. The highly polar groups within the molecule are countered by the hydrocarbon chain which would make up the backbone of the homopolymer. In addition, the high polarity of the carbonyl and pyrrolidone functional groups should lead to solubility in water and other polar solvents. There is also the advantage that hydrolysis of the urethane linkage will aid degradation of the polymers produced.

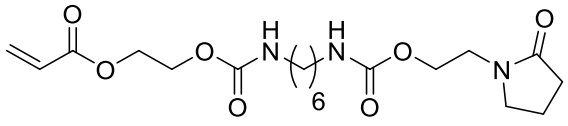

3

Figure 2.9 – Structure of monomer 3

Monomer **3** was prepared by reacting hydroxyethyl pyrrolidone, hydroxyethyl acrylate and hexamethyl diisocyanate in toluene. The progress of the reaction was followed by the decrease and eventual disappearance of the NCO band in the FTIR spectrum. The crude mixture was purified by column chromatography to separate the desired product (**3**), 55% yield, from the di-acrylate side product (Figure 2.10, **4**), 21%. The MS for the crude compound (Figure 2.11) shows peaks for m/z $[M + H]^+$ = 427.2 and $[M + Na]^+$ = 449.2 which corresponds to the di-pyrrolidone side product. This suggests that the remaining 24% is the di-pyrrolidone (Figure 2.10**, 5**).

i)

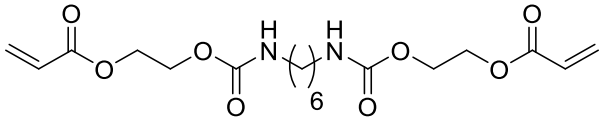

4

ii)

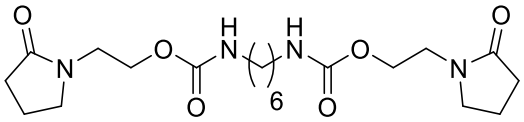

5

Figure 2.10 – Structure of i) di-acrylate (4) and ii) di-pyrrolidone (5) side products

The results of this synthesis were analysed with the use of ^{1}H NMR, ^{13}C NMR, accurate mass spectrometry, FTIR spectroscopy and 2D NMR spectroscopy such as COSY, ^{1}H-^{13}C HSQC and HMBC NMR.

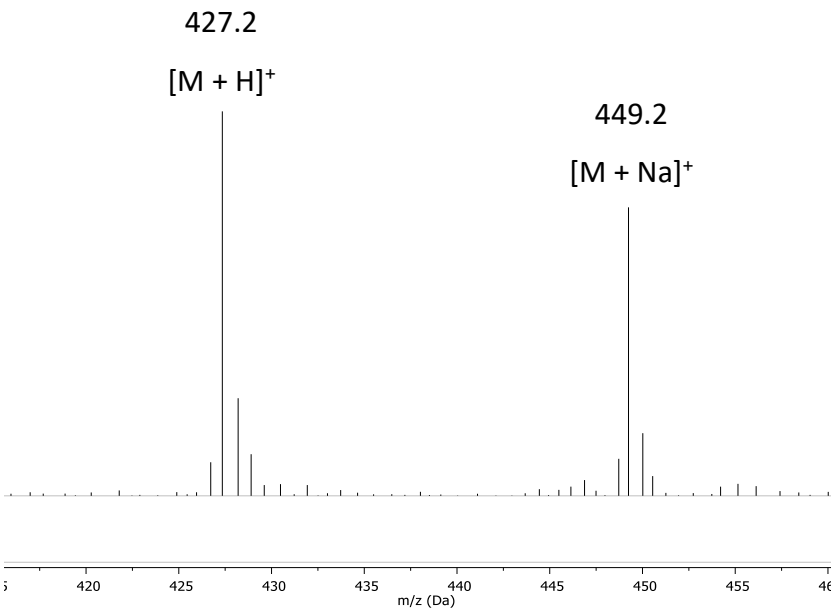

Figure 2.11 – Mass spectrum of crude mixture

The ^{1}H NMR spectrum (Figure 2.12) clearly shows the methylene acrylate protons **a** and **b** at δ = 6.41 and 5.84 ppm, respectively. The J coupling values of 17.3 and 10.5 Hz for **a** and **b** indicates that **a** is *trans* and **b** *cis* to methane proton **c** at δ = 6.14 ppm.

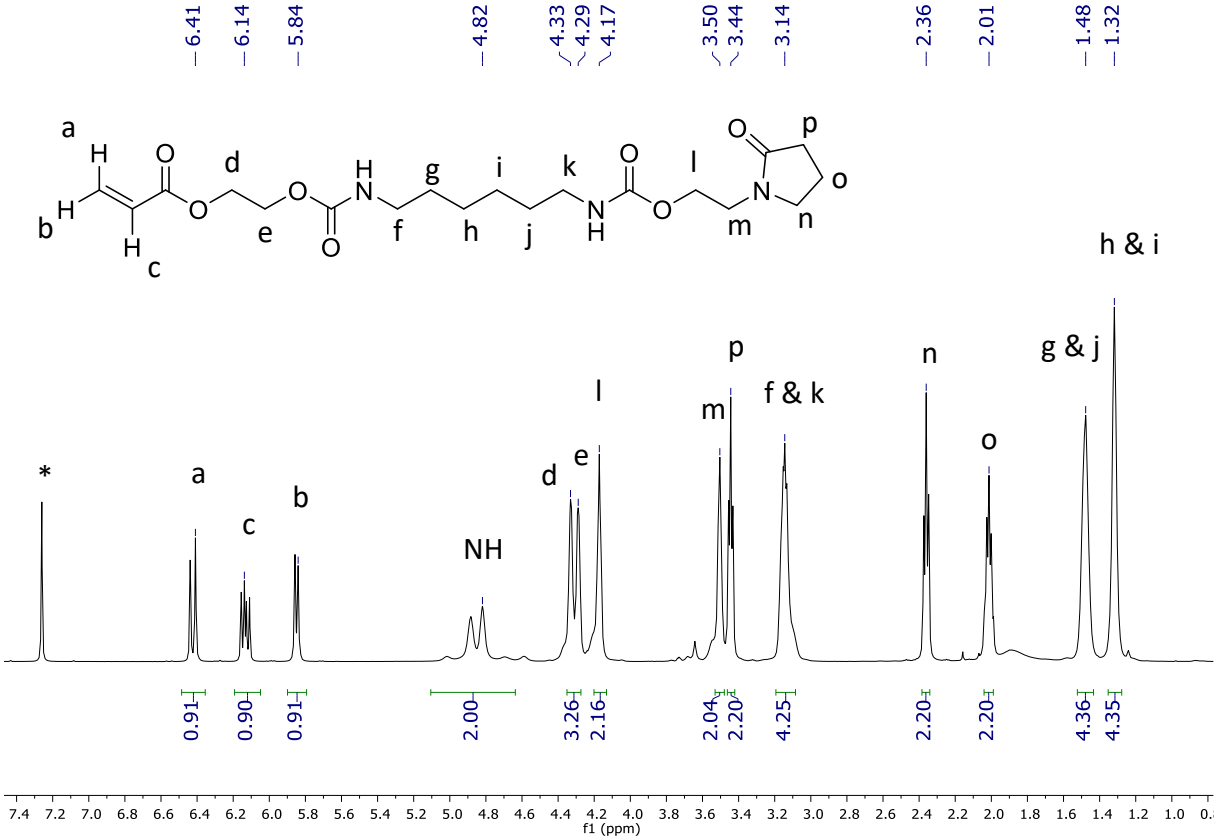

Figure 2.12 – ^{1}H NMR spectrum of monomer 3

The ^{1}H-^{1}H COSY spectrum (Figure 2.13) shows that the urethane protons around δ = 4.82 ppm correlate to the resonance at δ = 3.14 ppm which has an integral of 4 protons, therefore is assigned to **f** and **k**. Proton **d** is correlated to proton **e**, similarly **l** is correlated with **m**. It is only possible to fully characterize protons **d** and **e** by looking at the HMBC spectrum. It is possible, however, to distinguish between **l** and **m** due to the difference in shift (shielding of the proton between O and N). As the central part of the molecule is symmetric, the protons are in chemically similar environments. Therefore, the resonance for protons **f** & **k** (δ = 3.14 ppm) are overlying as are the resonances for **g** & **j** (δ = 1.48 ppm), and **h** & **i** (δ = 1.32 ppm).

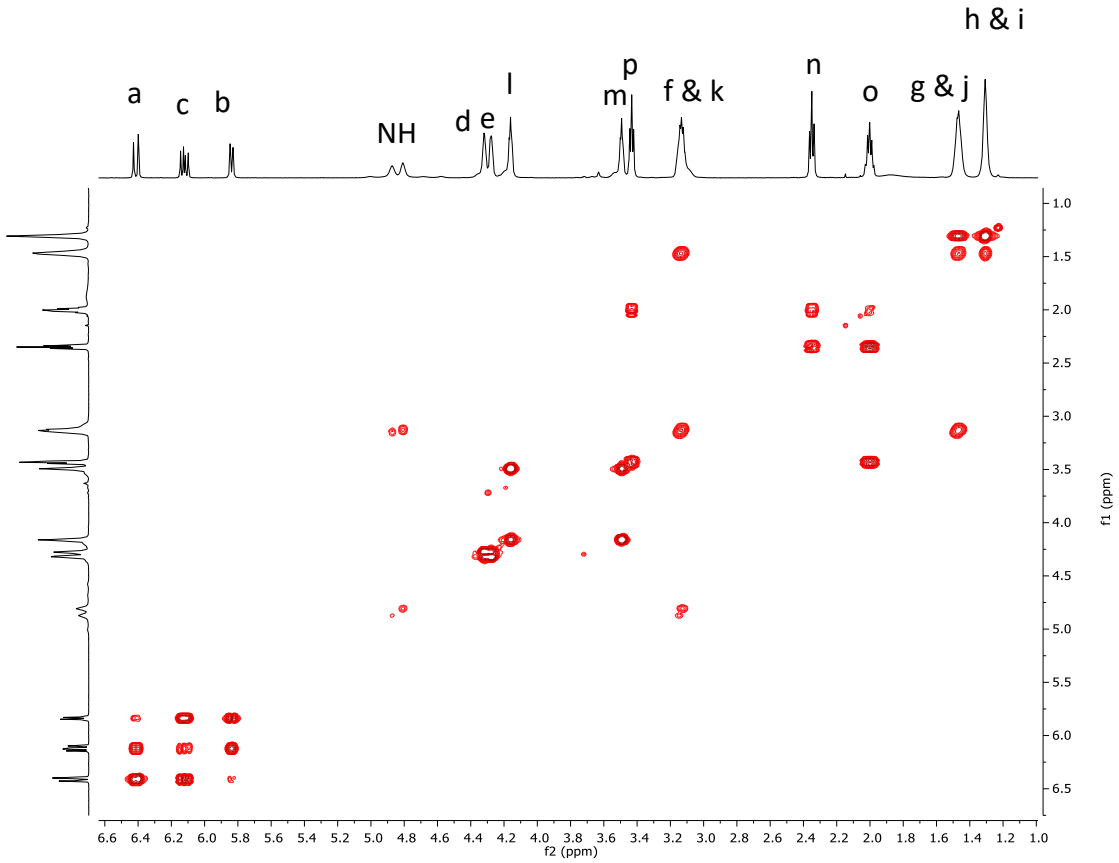

Figure 2.13 – ^{1}H-^{1}H COSY NMR spectrum of monomer 3

In the pyrrolidone moiety, **s** at δ = 2.36 ppm is correlated to **o** at δ = 2.01 ppm and, **o** is correlated to **p** at δ = 3.44 ppm. This is indicative of the pyrrolidone system and this pattern of splitting can be seen in the other pyrrolidone containing monomers.

The room temperature ^{1}H NMR spectrum (Figure 2.12) shows the NH of the urethane linkage as a multiplet resonance over a broad range, 4.61 - 5.12 ppm. In light of this, variable temperature NMR studies in chloroform were undertaken to help determine if the resonances were due to rotamers or diastereomers (Figure 2.14).

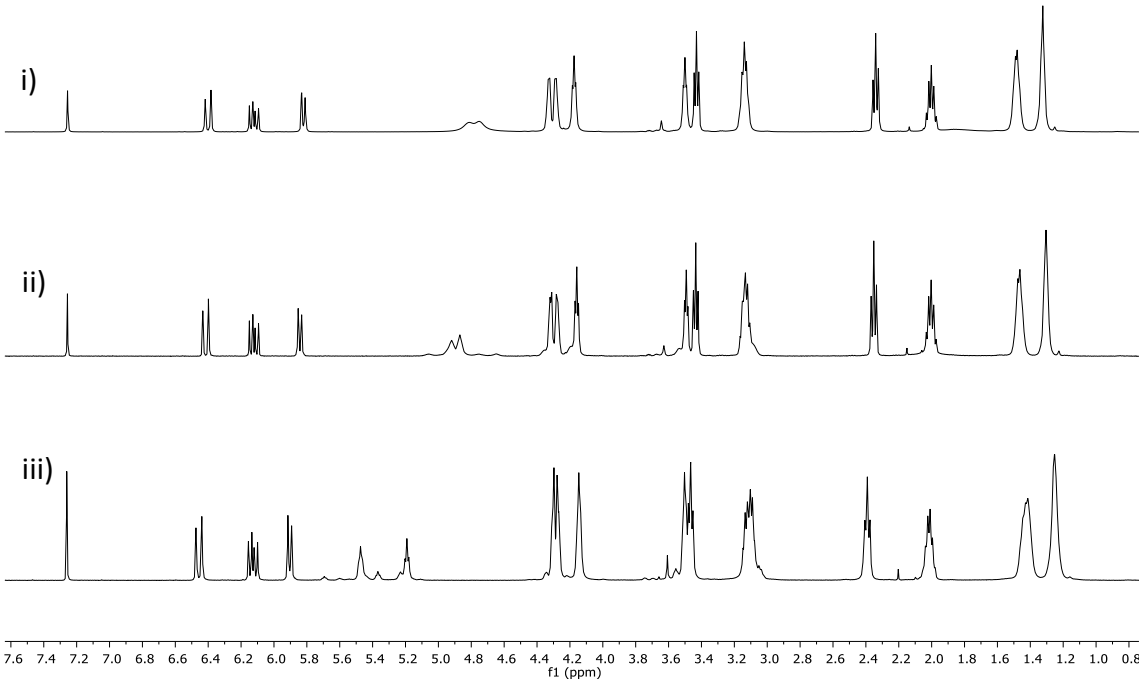

Figure 2.14 – VT ^{1}H NMR spectra of monomer 3 at i) 55 °C ii) 20 °C and iii) -60 °C

The temperature range analysed was -60 °C to +55 °C due to solvent limits (Figure 2.14). At the upper solvent limit, 55 °C, the peaks coalesce into one broad resonance with two peaks at $\delta = 4.82$ and 4.76 ppm (Figure 2.14i). At -60 °C the resonances separate into 8 visible resonances (Figure 2.15).

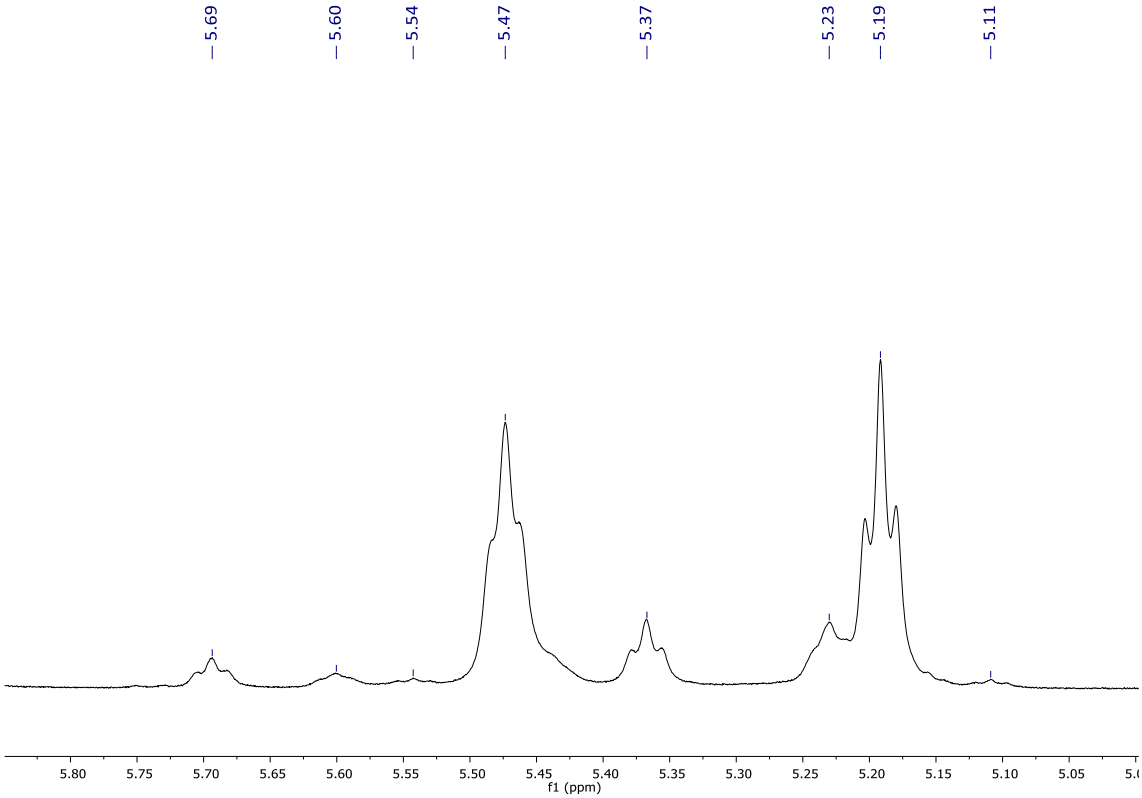

Figure 2.15 – ^{1}H NMR spectrum of monomer 3, expansion

A urethane bond has restricted rotation around the N-C bond due to the resonance forms (Scheme 2.5). The lone pair from the nitrogen can delocalise into the carbonyl to form a partial double bond. This removes electron density from the N-H bond therefore deshielding the hydrogen. At low temperatures the energy barrier for rotation is harder to overcome, resulting in distinct peaks in the ^{1}H NMR spectrum. At higher temperatures the bond can more freely rotate, therefore the peaks coalesce as an average is observed.

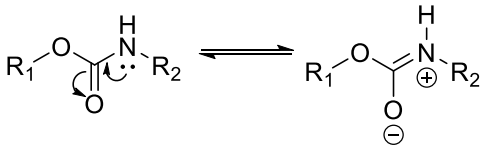

Scheme 2.5 – Resonance forms of a urethane bone

The ^{13}C NMR spectrum (Figure 2.16) shows 19 resonances which corresponds to the number of carbon environments in the molecule. As the central part of the molecule is symmetrical, the environments are chemically similar. This is why we see carbons **F** and **M**, **G** and **L**, **H** and

K, and **I** and **J** as overlying resonances, it is not possible to differentiate between the coinciding resonance pairs. There are 4 carbonyl carbons in the structure; **C**, **F**, **M** and **S**. The pyrrolidone carbonyl **S** characteristically appears at δ = 175.4 ppm and the two urethane carbonyls **F** and **M** are at δ = 156.2 and 156.1 ppm. Therefore the remaining resonance at δ = 165.9 ppm is due to **C**.

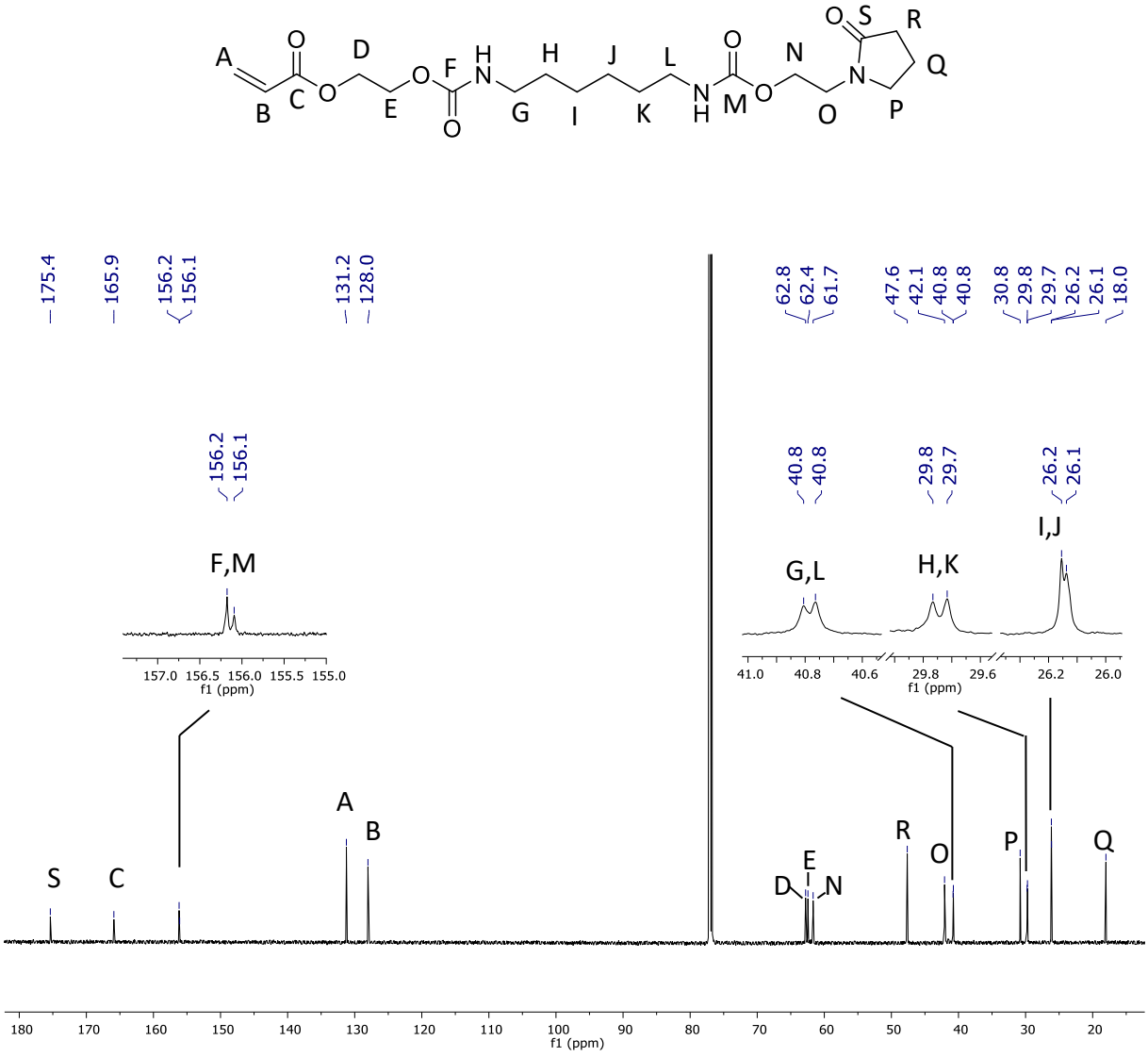

Figure 2.16 – ^{13}C NMR spectrum of monomer 3

From the ^{1}H-^{13}C HSQC spectrum (Figure 2.17) the ^{13}C resonances are easily corroborated and further resolved. The colour of the cross-peak for carbon **B** and proton **c** authenticates that

this is indeed the only CH in the molecule. It is also obvious that the methylene protons **a** and **b** are attached to carbon **A**.

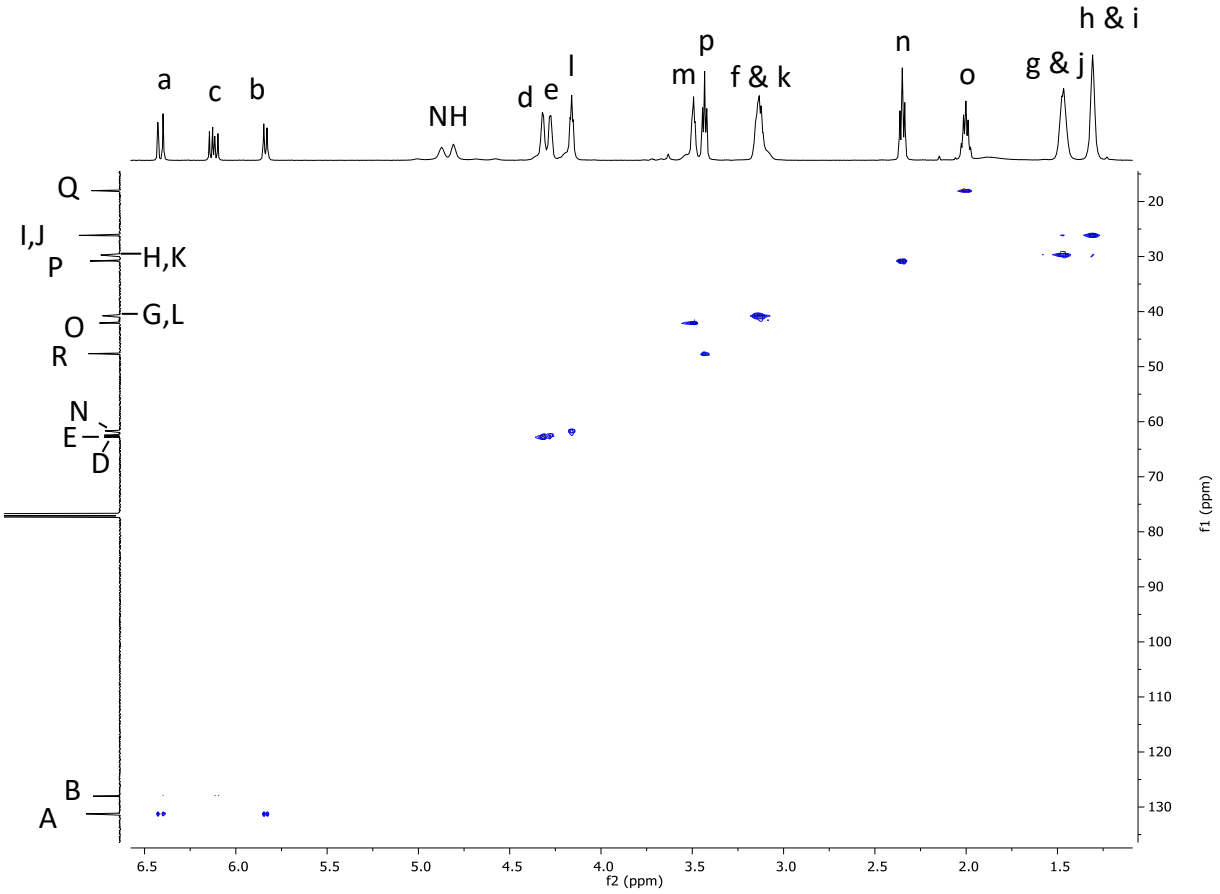

Figure 2.17 – ^{1}H-^{13}C HSQC NMR spectrum of monomer 3

The cross peaks for **d** and **e** (Figure 2.18), show that the more downfield ^{1}H peak at δ = 4.33 ppm correlates to the ^{13}C peak at δ = 62.8 ppm and the ^{1}H peak at δ = 4.29 ppm with the ^{13}C resonance at δ = 62.4 ppm. However, it is still not possible to differentiate which can be attributed to **d** and which is due to **e**.

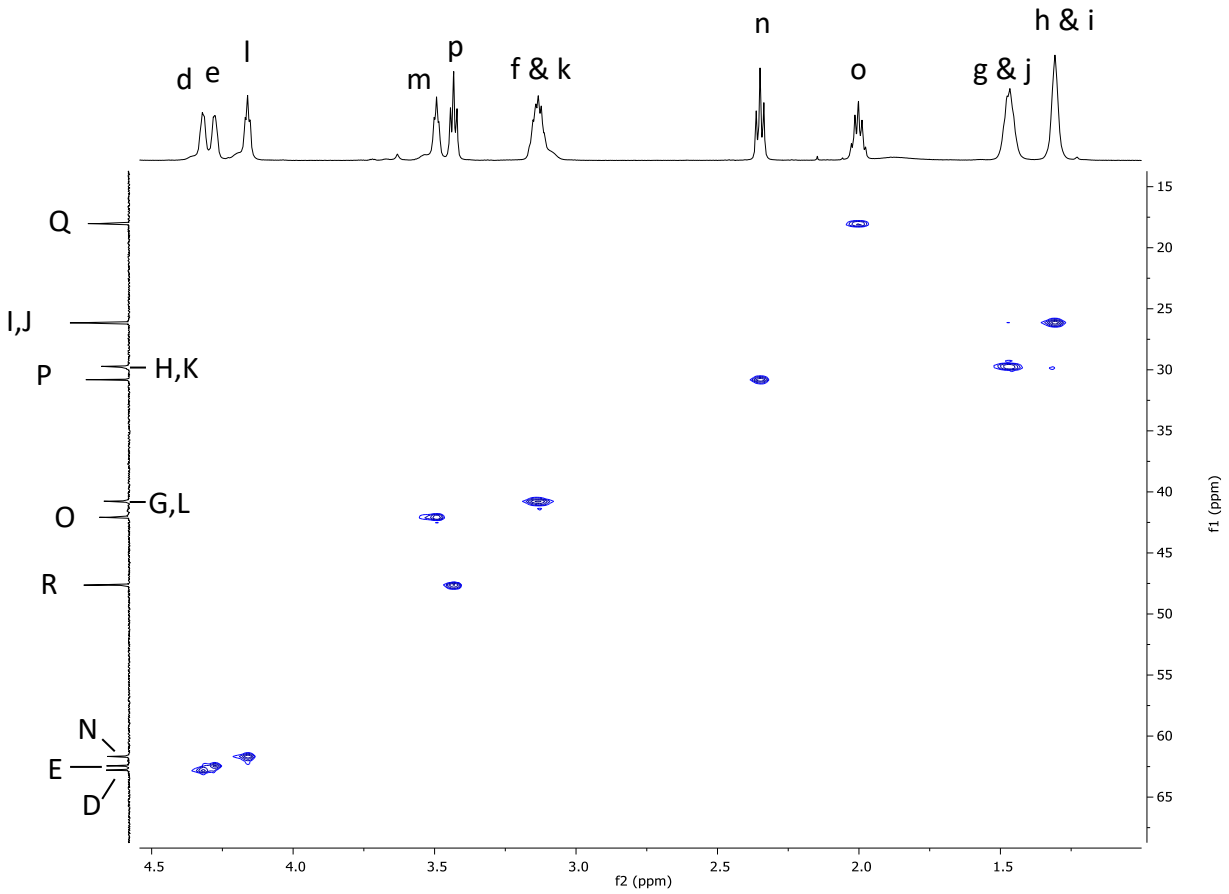

Figure 2.18 – ^{1}H-^{13}C HSQC spectrum of monomer 3, expansion

To completely assign protons **d** and **e** the HMBC spectrum (Figure 2.19) must be analysed. It can be seen that **d** is close to **C** and that **e** is close to **F, M**. Similarly, there is a cross-peak between **m** and the **S** and, **l** and **F, M**. Once again the spectrum clearly shows that the pyrrolidone protons **n**, **o** and **p** are in the ring. The resonance at δ = 3.14 ppm shows correlation with the urethane carbon resonances **F** and **M** supporting the assignment of protons **f** & **k**. The resonance at δ = 1.48 ppm correlates to the carbons **I**, **J**, **H** and **K** which verifies that this resonance is due to protons **g** and **j**. As the resonance for **g** and **j** is coupled to the resonance at δ = 1.32 ppm in the ^{1}H-^{1}H COSY NMR spectrum (Figure 2.13), this peak is attributed to protons **h** and **i**.

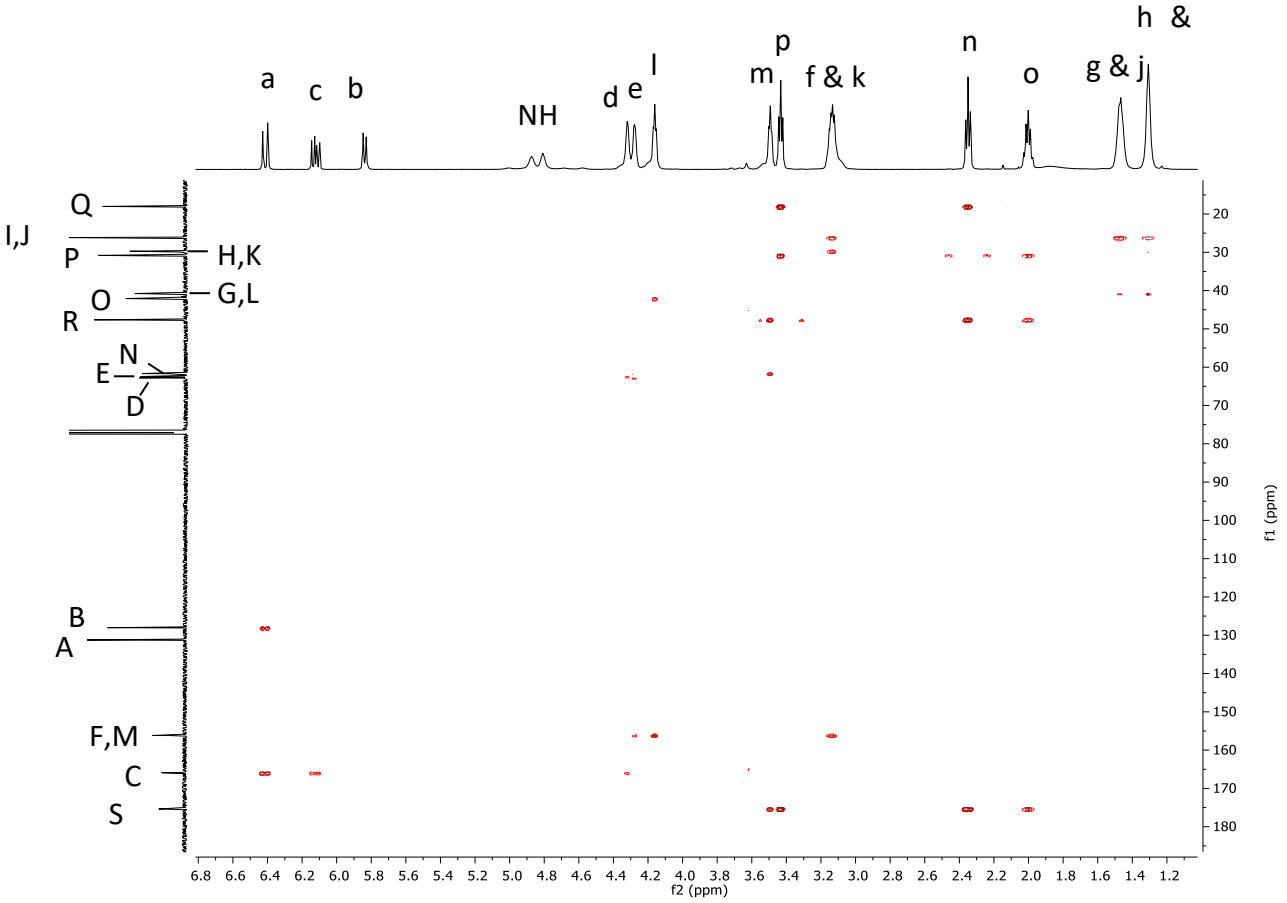

Figure 2.19 – ^{1}H-^{13}C HMBC NMR spectrum of monomer 3

Analysis of the FTIR spectrum of novel monomer **3** shows the formation of the urethane bond NH and C=O at 3333 cm^{-1} and 1675 cm^{-1}, respectively, along with the disappearance of the broad –OH band at 3366 cm^{-1} which is present in the HEP starting material. The accurate mass of m/z $[M + H]^{+}$ = 414.22 and $[M + Na]^{+}$ = 436.21 in addition to the other spectroscopic analysis verify the synthesis of the desired product. The EA results indicate that the monomer was pure and free of solvent.

In addition to the desired product **3**, a novel di-acrylate side product (**4**) was also isolated and fully characterised. There are 10 resonances in the ^{1}H NMR spectrum (Figure 2.20) as the molecule is symmetrical. The acrylate protons **a**, **b** and **c** are split in the characteristic manor with splitting of 17.3 Hz (**a**) and 10.5 Hz (**b**) indicating that **a** is *trans* to proton **c**. As with monomer **3**, the rotameric nature of the NH resonance is split. Protons **d** and **e** are very close in chemical shift and a correlation can be seen in the ^{1}H-^{1}H COSY NMR spectrum. The

protons at the centre of the molecule have similar chemical shifts when compared to the corresponding protons in monomer **3**.

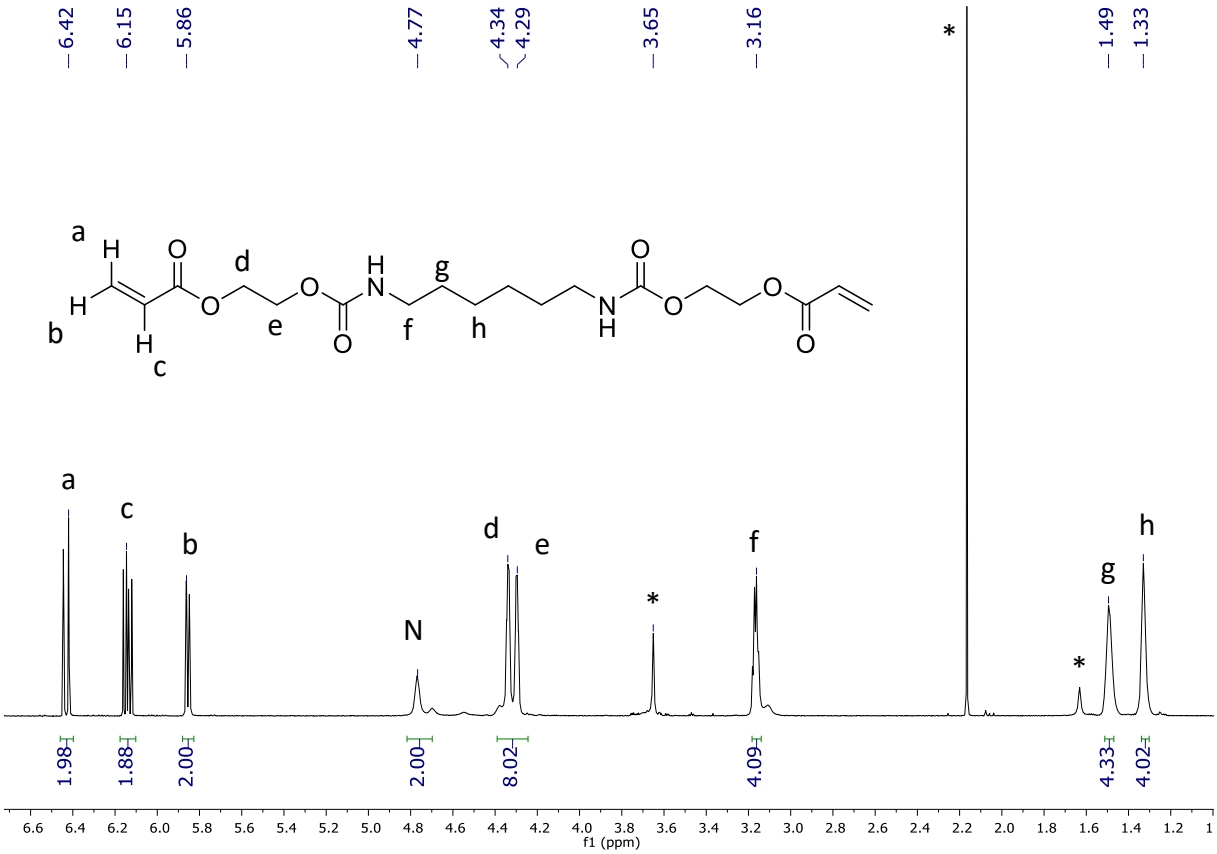

Figure 2.20 – ^{1}H NMR spectrum of di-acrylate side product 4

Again, due to the symmetry of the molecule, the ^{13}C NMR spectrum (Figure 2.21) contains 9 resonances. The carbonyl resonances of the acrylate and urethane at δ = 165.9 (**C**) and 156.1 (**F**) ppm are easily assigned. The resonances at δ = 131.2 and 128.0 ppm correspond to carbons **A** and **B** as in monomer **3**. Carbons **D**, **E**, **G**, **H** and **I** are attributed to the resonances at δ = 62.8, 62.5, 40.8, 29.8 and 26.2 ppm, respectively, the resonances are congruous to the corresponding resonances in the ^{1}H NMR spectrum of monomer **3**.

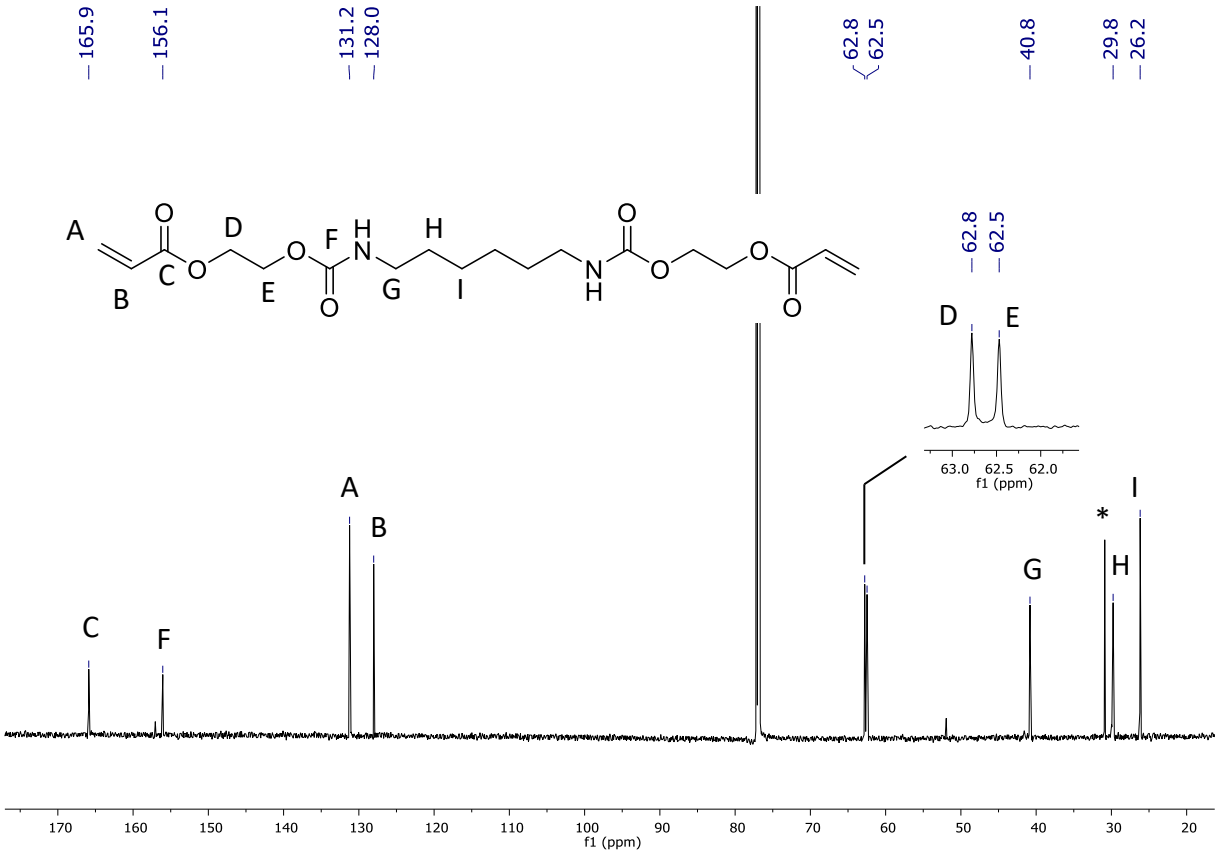

Figure 2.21 – ^{13}C NMR spectrum of di-acrylate monomer 4

The di-acrylate side product (**4**) was isolated by column chromatography and eluted with ethyl acetate:acetone (80:20). The desired product (**3**) did not move with the solvent system previously described and was eluted with 100% acetone. The mass spectrum of the reaction mixture showed the $[M + H]^+$ and the $[M + Na]^+$ ion for the di-pyrrolidone **5**. Despite attempts to recover **5** with increasing concentrations of methanol, none was isolated. It was concluded that the di-pyrrolidone **5** was too polar to elute from silica with these solvents. Therefore, no ^{1}H or ^{13}C NMR characterisation was obtained.

The synthesis and characterisation of monomer **3** has been described. The monomer was produced in a reasonable yield and purification was straightforward. The reaction gave two side products in di-acrylate **4** and di-pyrrolidone **5**. The di-acrylate **4** was isolated and fully characterised. The di-pyrrolidone was not isolated. The novel monomer can be utilised to produce novel homo- and co-polymers.

2.4 Conclusions

This chapter describes the synthesis and method development of monomers containing the pyrrolidone moiety and a functional group capable of undergoing polymerisation. Novel monomer **3** was synthesised and developed along with selected monomers (**1** - **3**). The synthetic procedures for monomers **1**-**3** were highly optimised to reduce cost and allow the reactions to be industrially viable.

The synthesis of monomer **1** was optimised from a literature procedure and the optimum conditions were found to be 50 °C for 4 h with 1 equivalent of epichlorohydrin.

The novel methodology for monomer **2** was developed and the yield of reaction was found to increase greatly when sodium hydride was replaced by potassium hydroxide. The replacement of NaH with KOH also reduced reaction costs and associated hazards.

Novel monomer **3** was synthesised and fully characterised. The monomer was designed to be water soluble and have degradable linkages. Additionally, the di-acrylate side product (**4**) was isolated and fully characterised, however, the di-pyrrolidone side product (**5**) could not be isolated due to the high polarity. The formation of di-pyrrolidone (**5**) is suggested by the presence of the peaks for m/z $[M + H]^+$ = 427.2 and $[M + Na]^+$ = 446.2 in the MS of the product.

2.5 References

1 N. González, C. Elvira and J. San Román, *J. Polym. Sci. Part A Polym. Chem.*, **2003**, 41, 395–407.

2 Recording Ink Containing Pigment Particles And Polyvinyl Pyrrolidone, US Pat. 5847026, **1998**.

3 Cosmetic Eyeliner Fromulation, US Pat. 5013543, **1991**.

4 Glossy Miltilayered Casing For Food Products, Permeable To Water And Smoke, WO 104946A1, **2014**.

5 Water-Soluble Film, US Pat. 4544693, **1985**.

6 Flexible Contact Lense, US Pat. 4062627, **1977**.

7 T. Loftsson, H. Fririksdóttir and T. K. Gumundsdóttir, *Int. J. Pharm.*, **1996**, 127, 293–296.

8 R. Reisfeld, V. Levchenko, A. Lazarowska, S. Mahlik and M. Grinberg, *Opt. Mater. (Amst).*, **2016**, 59, 3–7.

9 European Patent Office, *http://www.epo.org/searching-for-patents/technical/espacenet.html#tab1*, accessed **9 May 2016**.

10 P. Liu, L. Xiang, Q. Tan, H. Tang and H. Zhang, *Polym. Chem.*, **2013**, 4, 1068–1076.

11 M. C. Koetting, J. F. Guido, M. Gupta, A. Zhang and N. A. Peppas, *J. Control. Release*, **2016**, 221, 18–25.

12 J. M. Knipe, L. E. Strong and N. A. Peppas, *Biomacromolecules*, **2016**, 17, 788–797.

13 PlasticsEurope,

http://www.plasticseurope.org/documents/document/20150227150049-final_plastics_the_facts_2014_2015_260215.pdf, accessed **27 October 2016**.

14 F. P. Sidel'kovskaya, N. A. Raspevina, A. V Ignatenko and V. A. Ponomarenko, *Bull. Acad. Sci. USSR, Div. Chem. Sci.*, **1985**, 35, 850–852.

15 Epoxy Pyrrolidone Based Non-Ionic Surfactants, US Pat. 4801400, **1989**.

16 F. P. Sidel'kovskaya, V. A. Ponomarenko, M. G. Zelenskaya, A. V Ignatenko, O. D. Trifonova, É. A. Abdula-Zade, A. G. Kechina and L. A. Sinitsyna, *Bull. Acad. Sci. USSR, Div. Chem. Sci.*, **1975**, 25, 587–593.

17 J. Clayden, N. Greeves, S. Warren and P. Worthers, in *Organic Chemistry*, Oxford University Press, **2001**.

18 T. Takata, I. Atobe and T. Endo, *J. Polym. Sci. Part A Polym. Chem.*, **1992**, 30, 1495–1498.

19 H. Miyamura, T. Yasukawa and S. Kobayashi, *Green Chem.*, **2010**, 12, 776–778.

20 L. Stavitskaya, J. Shim, J. R. Healy, R. R. Matsumoto, A. D. MacKerell and A. Coop, *Bioorganic Med. Chem.*, **2012**, 20, 4556–4563.

21 Compositions Comprising Styling Polymer, WO Pat. 087596, **2016**.

22 Personal Care Compositions Comprising Copolymers of Cationic Monomers and Acryloyl Lactam Based Monomers, Process for the Same and Method of Use, WO Pat. 087924, **2017**.

23 Polymerizable Hydrophobic Ultraviolet Light Absorbing Monomers, US Pat. 6036891, **2000**.

24 Catalytic Process for Preparing (Meth)Acrylic Esters of N-Hydroxyalkylated Lactams, US Pat. 0010236, **2010**.

25 V. J. Cunningham, Y. Ning, S. P. Armes and O. M. Musa, *Polym. (United Kingdom)*, **2016**, 106, 189–199.

26 M. Szwarc, *Nature*, **2016**, 536, 276–277.

27 J. L. O'Brien and F. Gornick, *J. Am. Chem. Soc.*, **1955**, 77, 4757–4763.

Chapter 3

Homopolymerisation Investigations of Pyrrolidone Monomers

This chapter will focus on the homopolymerisation of known monomer **1** (Figure 3.1, Ch. 2, 2.3.1) as well as the homopolymerisation of monomer **3** (Figure 3.1, Ch. 2, 2.3.3) and the attempted homopolymerisation of monomer **2** (Figure 3.1, Ch. 2, 2.3.2). The homopolymerisation of the known monomers (**1** and **2**) and the novel monomer (**3**) were carried out in a synthetically simple manner to provide an easy route to industrial application. The homopolymers were fully characterised by a range of analytical techniques including 1D and 2D NMR, SSNMR, SEC, TGA, DSC and FTIR.

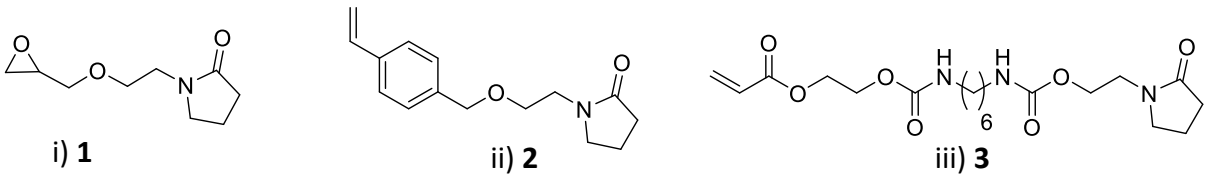

Figure 3.1 – Structure of i) 1-(2-(oxiran-2-ylmethoxy) ethyl) pyrrolidin-2-one, 1 ii) 4-vinylbenzyloxy ethyl pyrrolidone, 2 and iii) 5-Ethacryloxyethyl-12-ethylpyrrolidyl-N,N'hexane biscarbamate, 3

3.1 Introduction

The synthesis of monomer **1** (GEP) (Figure 3.1) was first published in 1975[1] followed by the first reported copolymerisation in 1987[2]. To the best of our knowledge, no homopolymerisation reactions have been reported in the literature. Functional polyethylene glycol (PEG) polymers and oligomers (Figure 3.2) are widely used in the biomedical and pharmaceutical industries. The unique chemical and physical properties of PEG[3] along with the availability and ease of synthesis have led to the polymer becoming one

of the most widely used in biomedical applications.[4] Uses include injectable hydrogels for drug delivery,[5] water treatment[6], linkers in macromolecules[7], stimuli-responsive polymers[8,9] and, self-assembly and nanoparticle formation[10,11] amongst others. As PEG dominates the area, investigations have revealed negative effects such as complement activation,[12] rapid blood clearance with repeated dosage[13] and adverse effects on tissue and cells replication, signalling and lifespan.[14–16] The range of possible applications plus the drawbacks with current PEG pharma-products, makes modified PEG alternatives highly interesting from a research perspective.

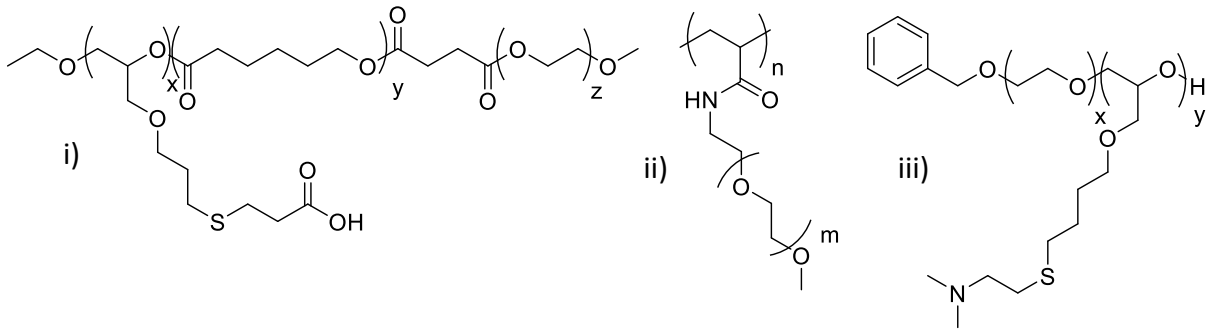

Figure 3.2 – Structure of modified PEG i) poly(allyl glycidyl ether)/cyctein-*b*-poly(ε-caprolactone-*b*-polyethylene glycol[10] ii) poly oligo(ethylene glycol methyl ether) acrylamide[8] and iii) polyethylene oxide-co-polyallyl glycidylether modified with *N,N*-dimethylaminoethanethiol[9]

Polystyrene is a common polymer for packaging and disposable products. Recent research focus has centred on nano-formulations,[17–19] some of which have exhibited thermoresponsive behaviour.[20,21] Functionalised polystyrene is often used as resins for chromatography[22] and polystyrenes with amine functionality have been shown to efficiently purify glycosides.[23]

Acrylate based polymers have a variety of uses from curable coatings[24,25] to biomaterials.[26,27] Research has shown that modified polyacrylates have been proven to support embryonic stem cell self-renewal.[28] This breadth of application demonstrates the versatility of acrylate based polymers. Many acrylate based systems are designed for drug delivery.[29,30] It can be advantageous when designing systems for drug delivery that the polymer is degradable and therefore able to be reabsorbed by the body instead of physical removal.[31] Peptide mimics have been implemented as drug carriers due to the low bioavailability and poor metabolic

stability of peptides.[32] The positives of a modified acrylate are ease of polymerisation and wide scope of applications.

3.2 Experimental

3.2.1 Materials

MeOK (25% in MeOH w/v solution) was used as supplied from Sigma-Aldrich. DCM and MeOH were purchased from Fisher Scientific and used as supplied. Dry Toluene and DMF were obtained from the Durham University Chemistry Department solvent purification service (SPS). Azobisisobutyronitrile (AIBN, 98%) was purchased from Sigma Aldrich and recrystallised from MeOH prior to use. 1,2-epoxy-3-oxyethyl pyrrolidone or glycidyl ethylpyrrolidone (GEP) (**1**), 4-vinylbenzyloxy ethyl pyrrolidone (**2**) and 5-ethacryloxyethyl-12-ethylpyrrolidyl-N,N'hexane biscarbamate (**3**) were synthesised as described in chapter 2.

3.2.2 Instrumentation

^{1}H and ^{13}C Nuclear Magnetic Resonance (NMR) spectra were recorded on a Bruker Avance 400 operating at 400 MHz or a Varian VNMRS 700 spectrometer operating at 700 MHz (^{1}H) and 176 MHz (^{13}C) with *J* values given in Hz. $CDCl_3$ was used as the deuterated solvent for ^{1}H and ^{13}C NMR analysis and the spectra were referenced to the solvent at 7.26ppm and 77.16 ppm, respectively. The following abbreviations are used in describing NMR spectra: s = singlet, d = doublet, t = triplet, m = multiplet and b = broad. 2D NMR experiments were also used to fully assign the proton and carbon environments in the products. ^{1}H-^{1}H Correlation Spectroscopy (COSY) demonstrated proton-proton correlations over two or three bonds. ^{1}H-^{13}C Heteronuclear Shift Correlation Spectroscopy (HSQC) showed the correlation between directly bonded proton and carbon atoms. ^{1}H-^{13}C Heteronuclear Multiple-bond Correlation (HMBC) NMR demonstrated the correlation between proton and carbon atoms through several bonds.

Solid State ^{13}C Nuclear Magnetic Resonance (SSNMR) spectra were recorded at 100.56 MHz using a Varian VNMRS spectrometer and a 4 mm (rotor o.d.) magic-angle spinning probe. They were obtained using cross-polarisation with a 1 s recycle delay, 1 ms contact time, at ambient probe temperature (~25 °C) and at a sample spin-rate of 8 kHz. 1200 repetitions were accumulated. Spectral referencing was with respect to an external sample of neat tetramethylsilane (carried out by setting the high-frequency signal from adamantane to 38.5 ppm). The direct excitation spectra were recorded at 100.56 MHz using a Varian VNMRS spectrometer and a 4 mm (rotor o.d.) magic-angle spinning probe with a relaxation time of 1 s. 1100 repetitions were accumulated.

SEC analysis was conducted using a Viskotek TDA 302 with 2 x 300 mL PLgel 5µm mixed C columns with THF or DMF eluent with a flow rate of 1 ml mg^{-1} at 35°C and 1 ml mg^{-1} at 70°C, respectively. The detectors were calibrated using narrow molecular weight distribution linear polystyrene or polyethylene oxide as standard. A conventional calculation was used to determine molecular weight.

Fourier transform infra-red (FTIR) spectroscopy was conducted using a Perkin Elmer 1600 series spectrometer. MALDI results were collected on the Autoflex II ToF/ToF mass spectrometer (Bruker Daltonik GmBH) with reflection enhanced mass resolution.

Differential scanning calorimetry (DSC) was carried out using a TA instrument Q1000 DSC, in N_2 gas, with a flow rate of 30 mL min^{-1} and heating rate of 10 °C min^{-1}. The second heating run was analysed. Thermogravimetric analysis (TGA) was carried out using a Perkin Elmer Pyris 1 TGA connected to a HIDEN HPR20 MS, in N_2 gas, with a heating rate of 10 °C min^{-1}.

3.2.3 Synthesis of Poly(1-(2-(oxiran-2-ylmethoxy) ethyl) pyrrolidin-2-one), (6)

108:1 Monomer:initiator, target molecular weight of 20,000 $gmol^{-1}$

MeOK (1 mL in 25% MeOH w/v solution, 0.1 mmol) was added to a round bottomed flask and excess MeOH was removed under reduced pressure to leave white solid MeOK. The reaction flask was backfilled with N_2 before addition of 1,2-epoxy-3-oxyethyl pyrrolidone (**1**)

(2 g, 107.5 mmol) in toluene (2 mL). The reaction was stirred at 100 °C for 2 h and then allowed to cool to room temperature. The excess solvent was removed under reduced pressure and the polymer was dried under reduced pressure at room temperature for 12 h, to give **6** (1.93 g, mass yield 97%). ^{1}H NMR (400 MHz, $CDCl_3$) δ = 3.70 – 3.18 (m, 11H, C**H$_2$**O, C**H** polymer backbone, CHC**H$_2$** polymer backbone, OC**H$_2$**CH_2, NC**H$_2$**CH_2CH_2CO, OCH_2C**H$_2$**), 2.19 (NCH_2CH_2C**H$_2$**CO), 1.90 (NCH_2C**H$_2$**CH_2CO) ppm. ^{13}C (176 MHz, $CDCl_3$) δ = 174.3 ($NCH_2CH_2CH_2$**C**O), 68.8 (O**C**H_2CH_2), 47.6 (N**C**$H_2CH_2CH_2CO$), 42.0 (OCH_2**C**H_2), 30.8 (NCH_2CH_2**C**H_2CO), 18.0 (NCH_2**C**H_2CH_2CO) ppm. SEC (DMF), M_n = 335 gmol^{-1}, Đ = 1.5. T_g = −40.05 °C. FTIR ν (cm^{-1}) = 2930 (br, CH_2, CH, polymer backbone), 1664 (C=O lactam), 1152 (C-O-C).

3.2.4 Synthesis of Poly(4-vinylbenzyloxy ethyl pyrrolidone), (7)

AIBN (2 mg, 0.01 mmol) was charged to a schlenk reaction flask and the flask was degassed and backfilled with N_2 three times. 4-vinylbenzyloxy ethyl pyrrolidone (**2**) (0.21 g, 0.82 mmol) was added and the reaction was heated to 60 °C and stirred for 1 h, after which the reaction has ceased stirring due to the formation of solid. The reaction was cooled to below 0 °C and exposed to air to terminate the reaction. The reaction was warmed to room temperature, the solid recovered was translucent and yellow in colour (0.18 g, mass yield 92%). The translucent gummy solid was extracted in DCM at 40 °C for 4 h and 0.072 g (31%) of insoluble solid (**7**) was recovered along with 0.182 g of monomer **2** (61%). ^{13}C SSNMR cross polarisation δ = 175.3 ($NCH_2CH_2CH_2$**C**O), 137.4 (aromatic **C**H), 128.6 (aromatic **C**H), 127.0 (aromatic **C**H), 114.4 (aromatic **C**H), 72.8 (Ph**C**H_2O), 68.9 (O**C**H_2CH_2), 48.6 (N**C**$H_2CH_2CH_2CO$), 42.9 (OCH_2**C**H_2), 31.5 (NCH_2CH_2**C**H_2CO), 18.7 (NCH_2**C**H_2CH_2CO) ppm. ^{13}C SSNMR direct excitation δ = 175.1 ($NCH_2CH_2CH_2$**C**O), 128.5 (aromatic **C**H), 72.0 (Ph**C**H_2O), 68.4 (O**C**H_2CH_2), 48.4 (N**C**$H_2CH_2CH_2CO$), 42.8 (OCH_2**C**H_2), 31.4 (NCH_2CH_2**C**H_2CO), 18.8 (NCH_2**C**H_2CH_2CO) ppm. FTIR ν (cm^{-1}) = 2920, 2918, 2860 (br, aromatic CH, CH_2), 1675 (C=O lactam). TGA, Onset X_1 = 385.16 °C, Onset X_2 = 460.72 °C, ΔY_1 = 89.910%, ΔY_2 = 23.262%.

The reaction was also conducted at 70 °C for 15 min, the mass yield afforded was 83%

3.2.5 Synthesis of Poly(5-ethacryloxyethyl-12-ethylpyrrolidyl -N,N'hexane biscarbamate), (8)

In a glove box, 5-ethacryloxyethyl-12-ethylpyrrolidyl-N,N'hexane biscarbamate (**3**) (0.501 g, 1.22 mmol) was added to a reaction flask containing AIBN (1.3 mg, 0.01 mmol) and DMF (1.5 mL). The reaction vessel was removed from the glove box, heated to 70 °C and stirred for 12 h. The reaction was cooled to below 0 °C and exposed to air to terminate the reaction. The mixture was allowed to warm to room temperature before the polymer was precipitated into hexane and dried under reduced pressure at 40 °C for 12 h to give **8** (mass yield 95%). ^{1}H NMR (400 MHz, $CDCl_3$) δ = 7.09 – 6.34 (br, m, 2H, N**H**), 4.25 (br, 4H, OC**H$_2$**C**H$_2$**O), 4.11 (br, 2H, OC**H$_2$**CH_2N), 3.46 (br, 4H, OCH_2C**H$_2$**N, NCH_2CH_2C**H$_2$**CO), 3.08 (br, 4H, NHC**H$_2$**$CH_2CH_2CH_2CH_2$C**H$_2$**NH), 2.24 (br, 2H, NC**H$_2$**CH_2CH_2CO), 1.97 (br, 2H, NCH_2C**H$_2$**CH_2CO), 1.48 (br, 4H, NHC**H$_2$**$CH_2CH_2CH_2$C**H$_2$**CH_2NH) and 1.32 (br, 4H, $NHCH_2CH_2$C**H$_2$**C**H$_2$**CH-$_2CH_2$NH) ppm. ^{13}C (176 MHz, $CDCl_3$) δ = 174.2 ($NCH_2CH_2CH_2$**C**O), 156.4 (NH**C**OOCH_2CH_2N), 63.0 and 62.0 (O**C**H_2**C**H_2O), 61.4 (O**C**H_2CH_2N), 47.3 (N**C**$H_2CH_2CH_2CO$), 41.8 (OCH_2**C**H_2N), 40.6 (NH**C**$H_2CH_2CH_2CH_2CH_2$**C**H_2NH), 30.4 (NCH_2CH_2**C**H_2CO), 29.5 ($NHCH_2$**C**$H_2CH_2CH_2$**C**H-$_2CH_2$NH, overlapping with solvent), 26.3 ($NHCH_2CH_2$**C**H_2**C**$H_2CH_2CH_2$NH), 17.9 (NCH_2**C**H_2CH_2CO) ppm. SEC (DMF), M_n = 963 gmol^{-1}, Đ = 16.8. FTIR ν (cm^{-1}) = 3318 (br, COONH) 2935 (CH_2), 1701 (br, C=O), 1668 (br, C=O).

3.3 Results & Discussion

3.3.1 Poly(1-(2-(oxiran-2-ylmethoxy) ethyl) pyrrolidin-2-one), (6)

Many amino functionalised polyethylene glycol (PEG) based polymers are synthesised from protected amine which are then deprotected *via* post-polymerisation modification.[33–35] In general post-polymerisation modification can impart problems as 100% conversion is not guaranteed. Polyethers containing tertiary amine groups have produced polymers with defined architectures,[36] functionalised nanoparticles[37] and have exhibited thermoresponsive behaviour.[38] Producing a polymer from a functionalised monomer will lead to a greater homogeneity in the final product when compared to post-polymerisation modification.

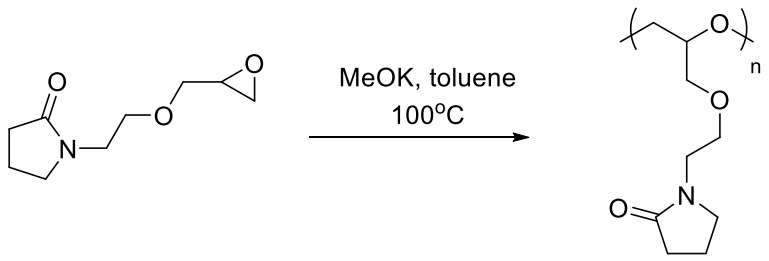

6

Scheme 3.1 – Synthesis of polymer 6

An anionic ring opening polymerisation procedure was used as the starting point for this investigation (as employed in the literature[39]). Potassium methoxide was chosen as the alkoxide initiator due to availability. Reactions were carried out at 100 °C in toluene with a monomer to initiator ration of 54:1 and 108:1 (Scheme 3.1). The potassium methoxide was supplied in a MeOH solution 25% w/v, the MeOH was removed under reduced pressure to give the solid potassium methoxide used to initiate the reaction.

The reactions were followed by ^{1}H NMR analysis, where it was possible to see the progress *via* the reduction and then disappearance of the characteristic epoxide peaks at δ = 3.16, 2.80 and 2.61 ppm of the CH and CH_2 of the three-membered ring. After 2 h, there were no epoxide peaks visible in the crude ^{1}H NMR spectrum. Upon recovery, the product was a gloopy yellow translucent liquid. The polymer produced was water soluble. The assigned ^{1}H NMR spectrum for proton environments **a** – **h** is shown below (Figure 3.3).

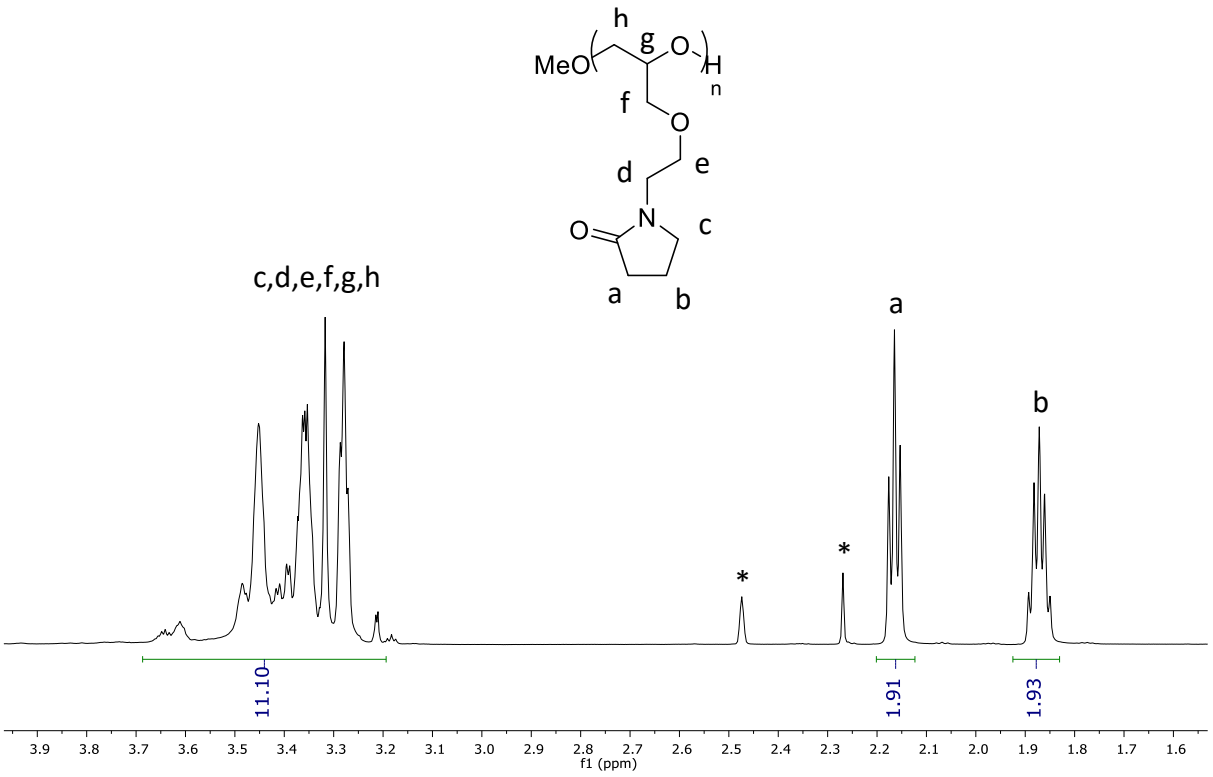

Figure 3.3 – ^{1}H NMR spectrum of 54:1 monomer:initiator ratio

Figure 3.3 shows a broad multiplet between δ = 2.93 – 3.92 ppm and two distinct signals at δ = 1.96 and 2.20 ppm. The two signals at δ = 1.96 and 2.20 ppm both integrate to 2H and the broad multiplet integrates to 11H. The integrations and chemical shift suggest that the peaks at δ = 1.96 and 2.20 ppm are due to the CH_2 groups in the pyrrolidone ring (**a** and **b**). The ^{1}H-^{1}H COSY correlation spectrum (Figure 3.4) shows the characteristic pattern of the pyrrolidone group, with protons **b** (δ = 2.19 ppm) and **a** (δ = 1.90 ppm) signals appearing upfield of proton **c**. It is possible to determine from the COSY that the signal for proton **c** is

observed at δ = 3.38 ppm. The correlation between the signals at δ = 3.30 and 3.48 ppm is also clearly visible. These signals correspond to protons **d** and **e** respectively. Due to the overlapping signals it is not possible to determine the exact shift for protons **f**, **g** or **h**.

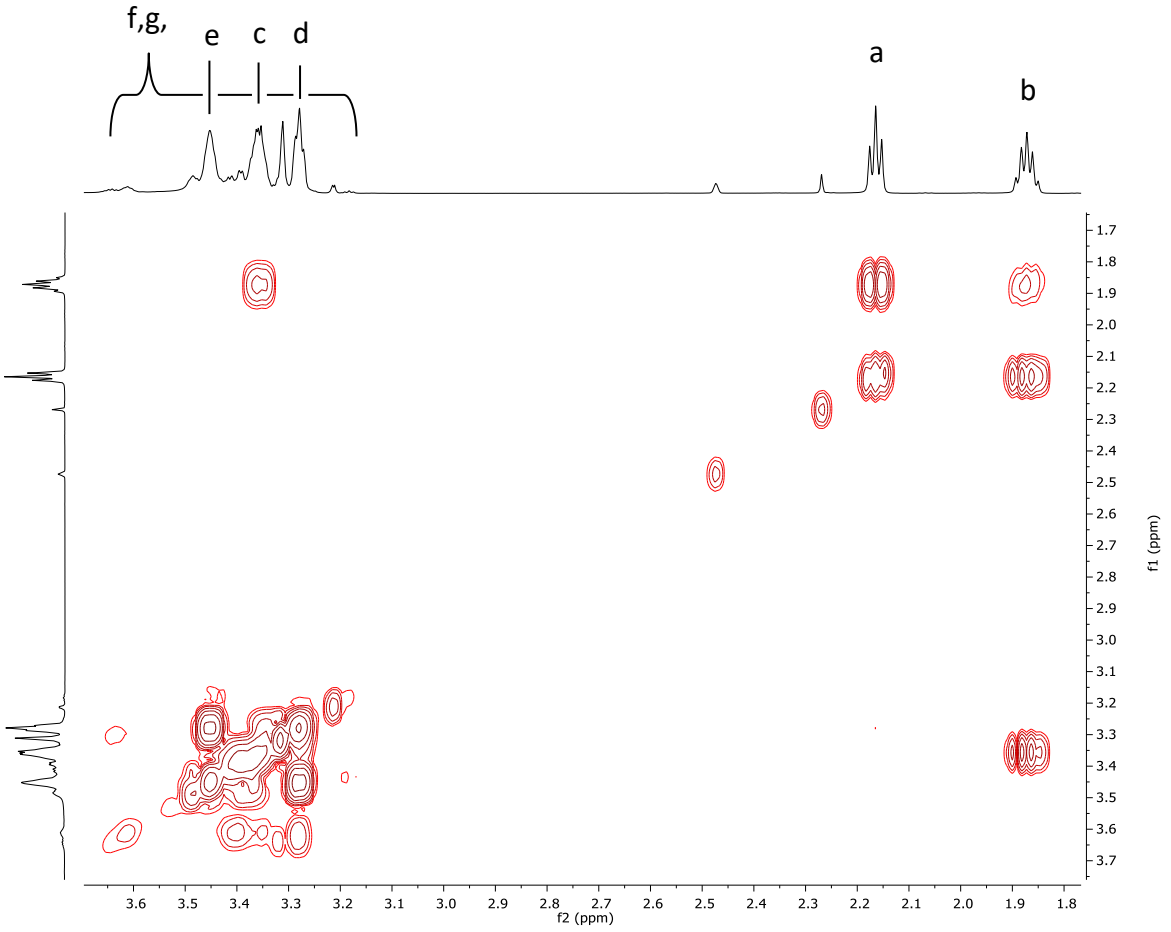

Figure 3.4 – ^{1}H-^{1}H COSY NMR spectrum of polymer 6

The ^{13}C NMR spectrum (Figure 3.5) show 6 major peaks and many other minor signals. The signals are broad multiplets. Broad carbon signals suggests that there are multiple carbon environments which are chemically similar, indicating that a polymer has been formed.[40] In order to identify each resonance the ^{1}H-^{13}C HMBC NMR spectrum must be analysed (Figure 3.6).

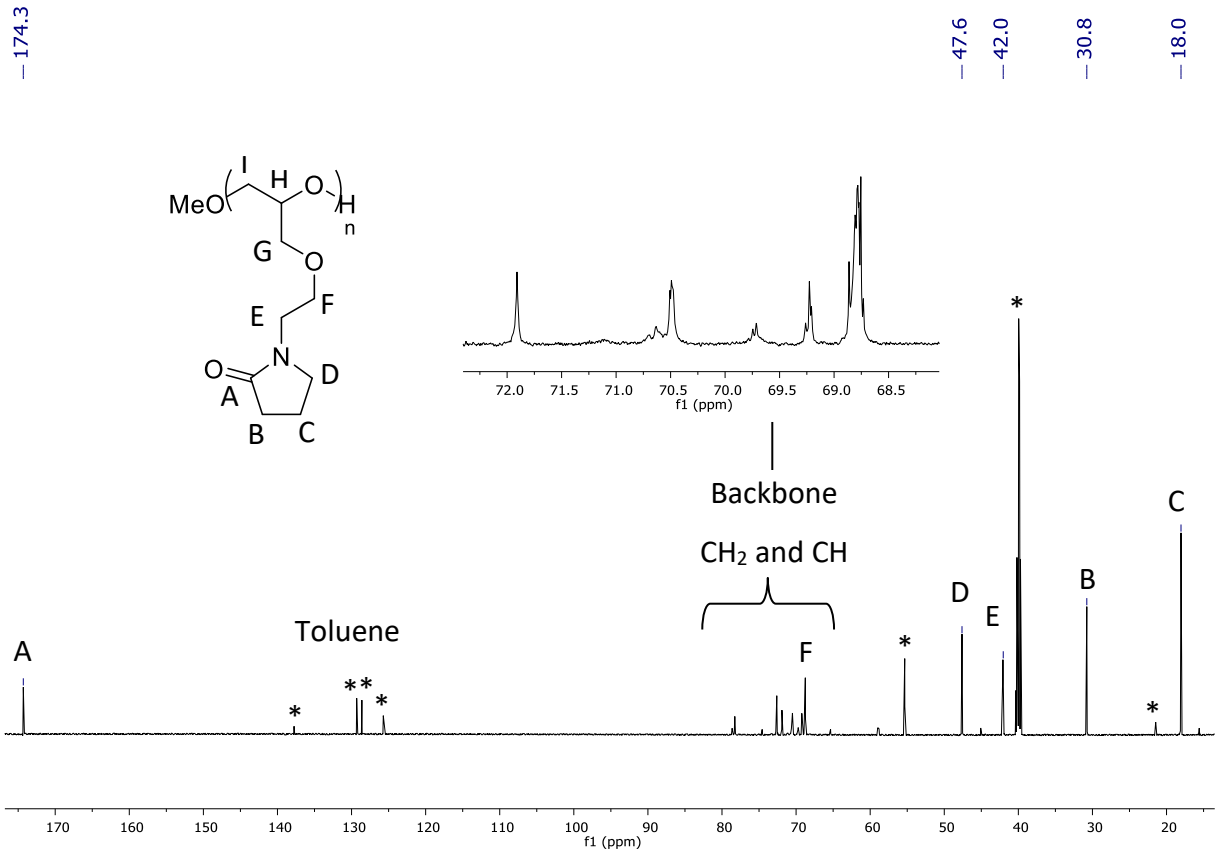

Figure 3.5 – ^{13}C NMR spectrum of polymer 6

The ^{13}C NMR spectrum expansion shows the region from δ = 68.0 to 72.5 ppm. This region contains the signals relating to the backbone chain. The signal at δ = 174.3 ppm is attributed to the carbonyl carbon **A**. The signals for residual toluene and DCM are also visible, marked with an asterisk (*). The ^{1}H-^{13}C HMBC NMR spectrum (Figure 3.6) allows characterisation of the majority of the carbon signals in the ^{13}C NMR spectrum. Proton **b** correlates to the carbon signal at δ = 18.1 ppm, carbon **C**. Proton **a** shows a correlation to δ = 30.8 ppm, carbon **B**. It is also possible to see correlations for carbons **E**, **D** and **F** at δ = 42.0, 47.6 and 68.8 ppm. As the proton signals are overlapping, it is not possible to fully assign the backbone signals of the polymer. The HMBC shows at least 5 signals (in red) which are out of phase with respect to the other carbon signals (in blue). This suggests that these signals (in red) are due to CH or CH_3 groups. The FTIR contains bands at ν = 2930, 1664 and 1152 cm^{-1} which correspond to CH_2/CH (polymer backbone), C=O and, C-O-C (polymer backbone and pendant unit), respectively.

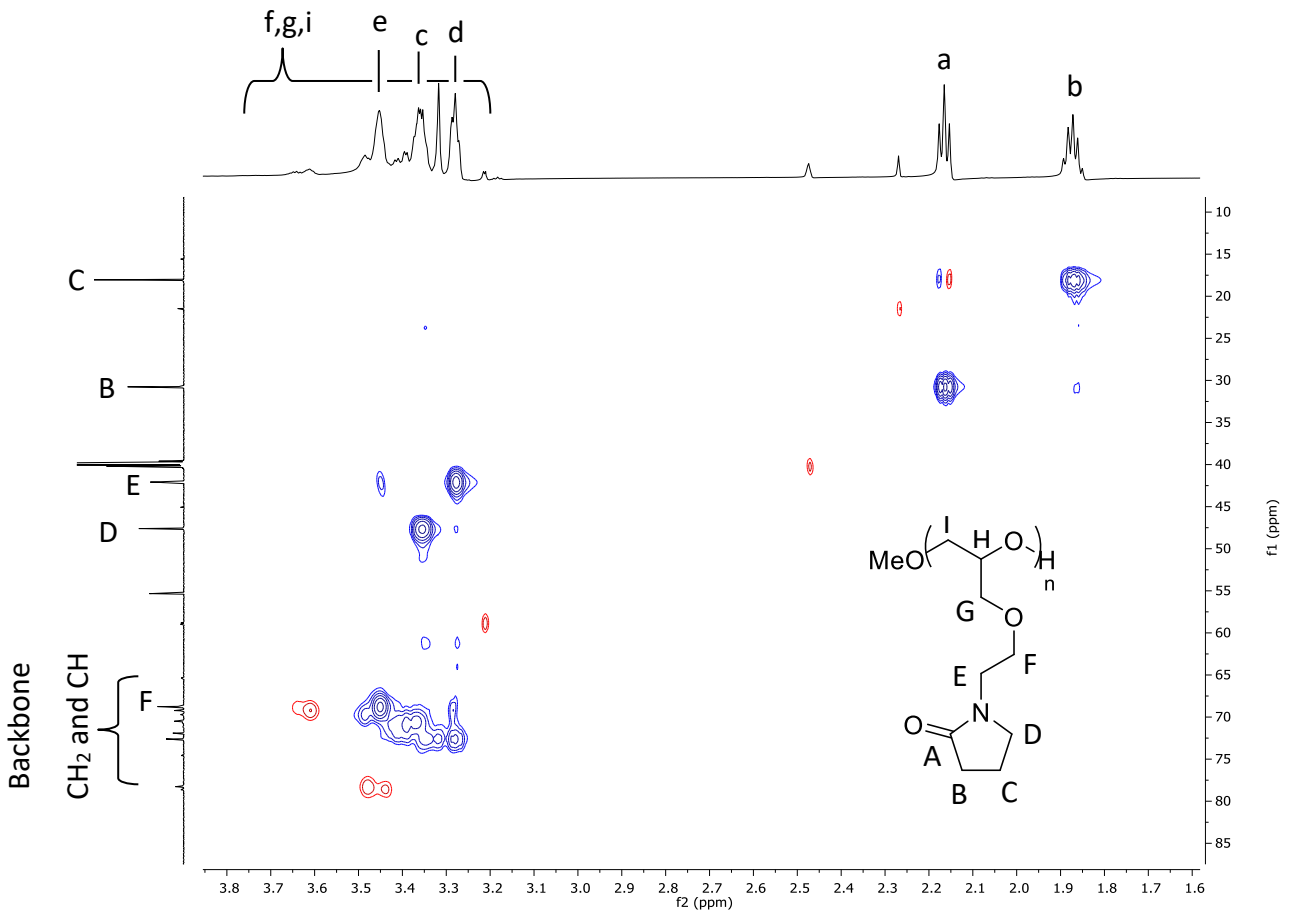

Figure 3.6 – ^{1}H-^{13}C HMBC NMR spectrum of polymer 6

The polymer was analysed by SEC in THF solvent using a conventional calibration as no light scattering was observed (Figure 3.7). The number average molecular weight (M_n) was found to be 335 $gmol^{-1}$ with Đ of 1.5 and the target molecular weight based on initiator to monomer ratio was 20,000 $gmol^{-1}$. The molecular weight of the monomer is 185.22 $gmol^{-1}$, the SEC data suggests that only small oligomers were formed in the reaction. The conventional calibration is based on polymethyl methacrylate (PMMA) standards, the difference in molecular structure and functional group composition between the calibration standard and polymer 6 will decrease the quantitative accuracy of the results. The SEC chromatogram (Figure 3.7) shows the peak observed to be extremely close to the solvent, this could affect the results of the conventional calculation due to the difficulty in setting baseline limits. The low molecular weight observed by SEC analysis is not surprising given the relatively sharp nature of the ^{1}H NMR resonances.

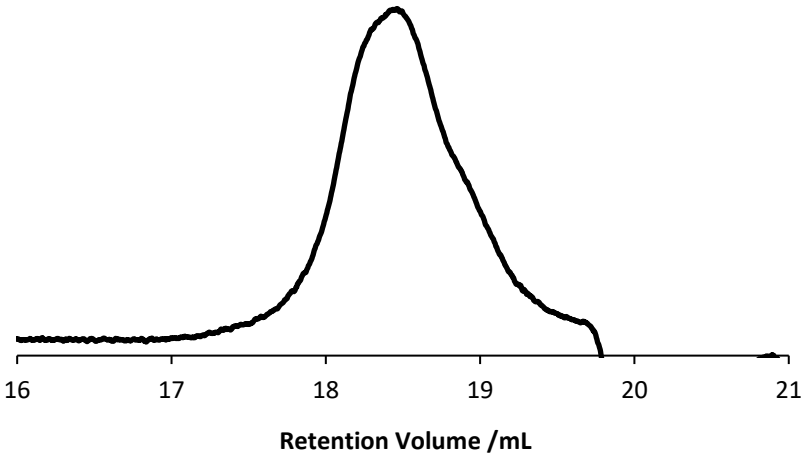

Figure 3.7 – SEC chromatogram of polymer 6

DSC analysis (Figure 3.8) was also conducted and the amorphous polymer shows a glass transition temperature (T_g) of −40.35 °C with a notable enthalpy of relaxation of 3.821 Jg^{-1}. The cooling curve (dotted line) shows that the melt solidifies amorphously. The enthalpy of relaxation was calculated by subtracting the second heating run from the first heating run.[41] PVP homopolymer is known to exhibit an enthalpy of relaxation[42] the incorporation of the pyrrolidone functionality in the PEG oligomer leads to a more amorphous macrostructure due to the flexible side chains capable of hydrogen bonding.

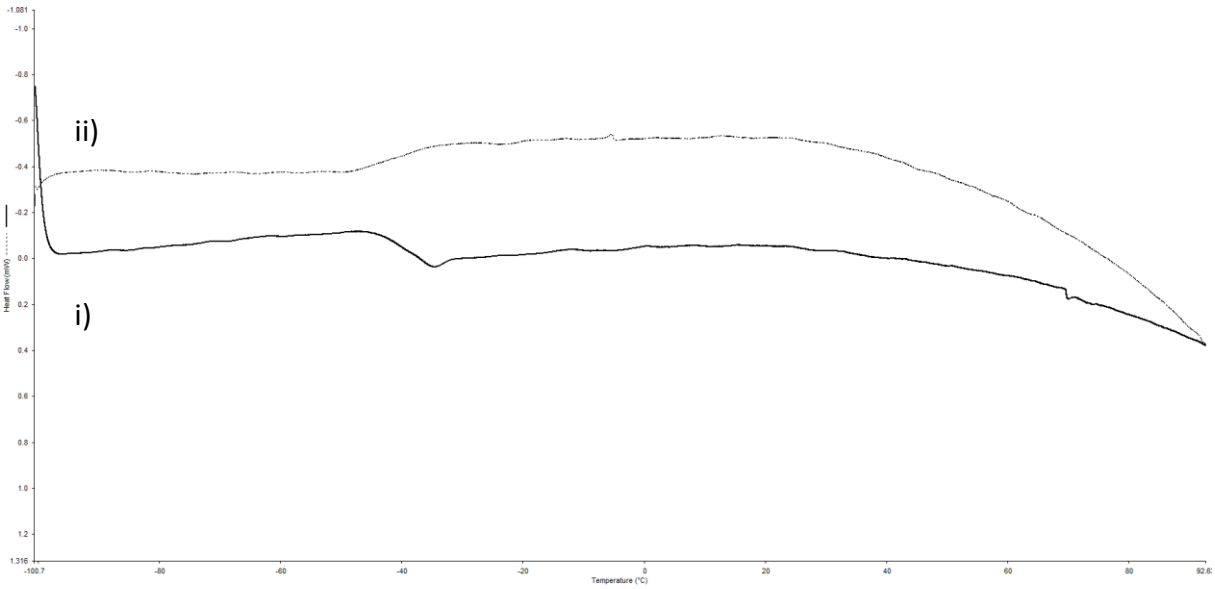

Figure 3.8 – DSC curve of polymer 6, i) second scan = black line, ii) cooling = dotted line

The product of the reaction was analysed by MALDI MS (Figure 3.9). The spectrum shows five distinct data sets, each identified by a coloured *. In each data set, the peaks are separated by 185 $gmol^{-1}$, the molecular weight of one monomer unit. This suggests that the polymer is made up of the ring opened epoxide monomer repeat units. The proposed reasoning for the different data sets is the inefficient initiation of the reaction by MeOK and high levels of chain transfer leading to a range of end groups in the final product.

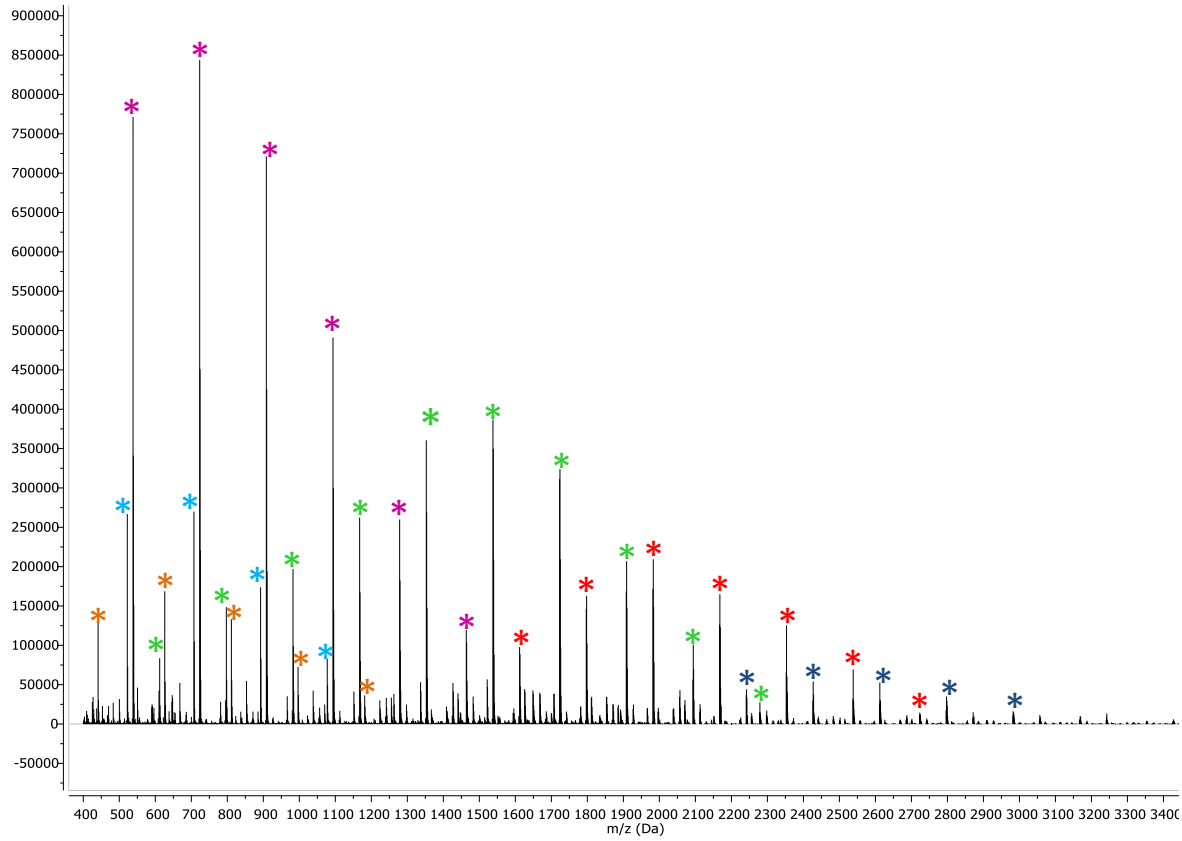

Figure 3.9 – MALDI MS of polymer 6

If the reaction proceeds *via* the activated chain end (ACE) mechanism, the polymerisation will be propagated by the anionic chain end (Scheme 3.2). This leads to the formation of a polymer with OMe and H end group, these peaks are visible in the MALDI as the orange set (Table 3.1). The orange peaks correspond to the K^+ counter-ion of the target polymer, the peaks are partnered by a smaller set of peaks (not marked) which are m/z 16 $gmol^{-1}$ less, these correspond to the Na^+ counter-ion. The number of monomer repeat units is between 2 and 5, this is in accordance with the SEC data.

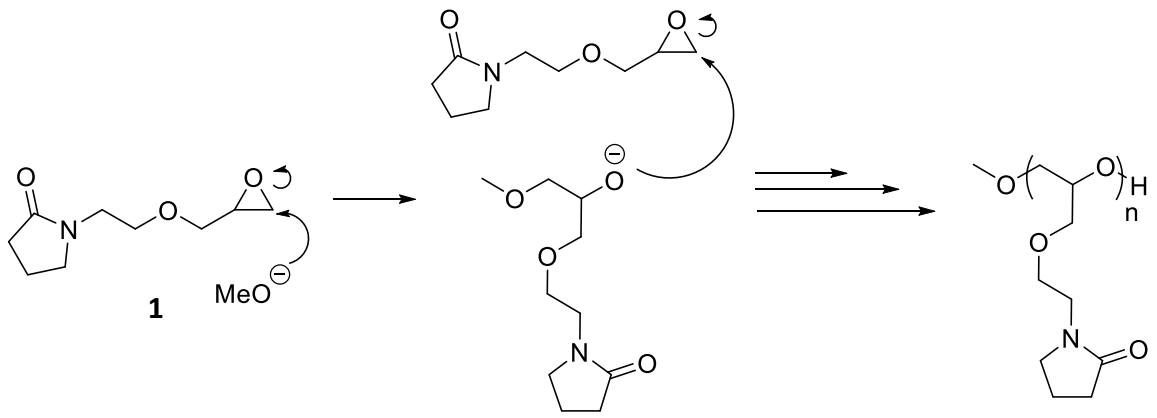

Scheme 3.2 – ACE mechanism of propagation for anionic ring opening polymerisation of monomer 1

The SEC and MALDI data show that the molecular weight of the polymer is much lower than expected. This occurs when high levels of chain transfer and termination events occur during the polymerisation. Chain transfer to initiator, monomer and solvent will reduce the molecular weight of the polymers produced. Chain transfer to polymer only results in a change in polymer architecture, with the introduction of branching points and would not affect the overall molecular weight. The dark blue data set (Table 3.1) could correspond to the end group produced from the chain transfer to monomer initiating the polymerisation (Scheme 3.3) and H.[43] The number of monomer repeat units would range from 10 to 14.

Table 3.1 – MALDI mass spectrometry hits of polymer 6

m/z	n	End Groups	Counterion
441.101	2	MeO, H	K
626.188	3		
811.299	4		
1181.554	5		
2057.092	10	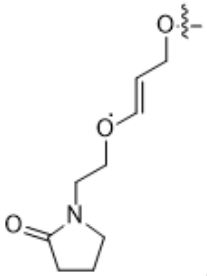 , H	Na
2242.086	11		
2427.193	12		
2612.310	13		
2797.536	14		

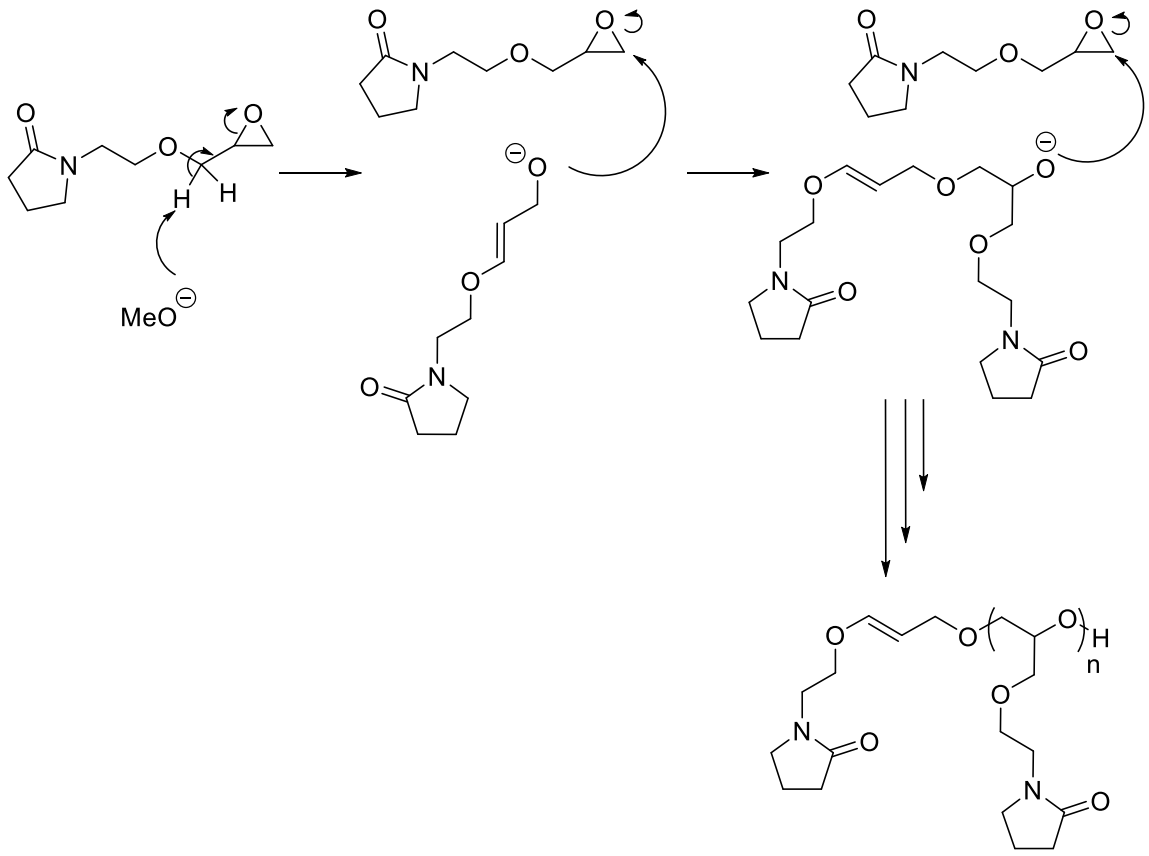

Scheme 3.3 – Chain transfer to initiate polymerisation of monomer 1

Additional evidence to support the theory of chain transfer to monomer is the presence of resonances in the alkene region of the ^{1}H NMR (Figure 3.10). Resonances associated with toluene are also visible in the expanded ^{1}H NMR spectrum, this could indicate that chain transfer to solvent has also occurred.

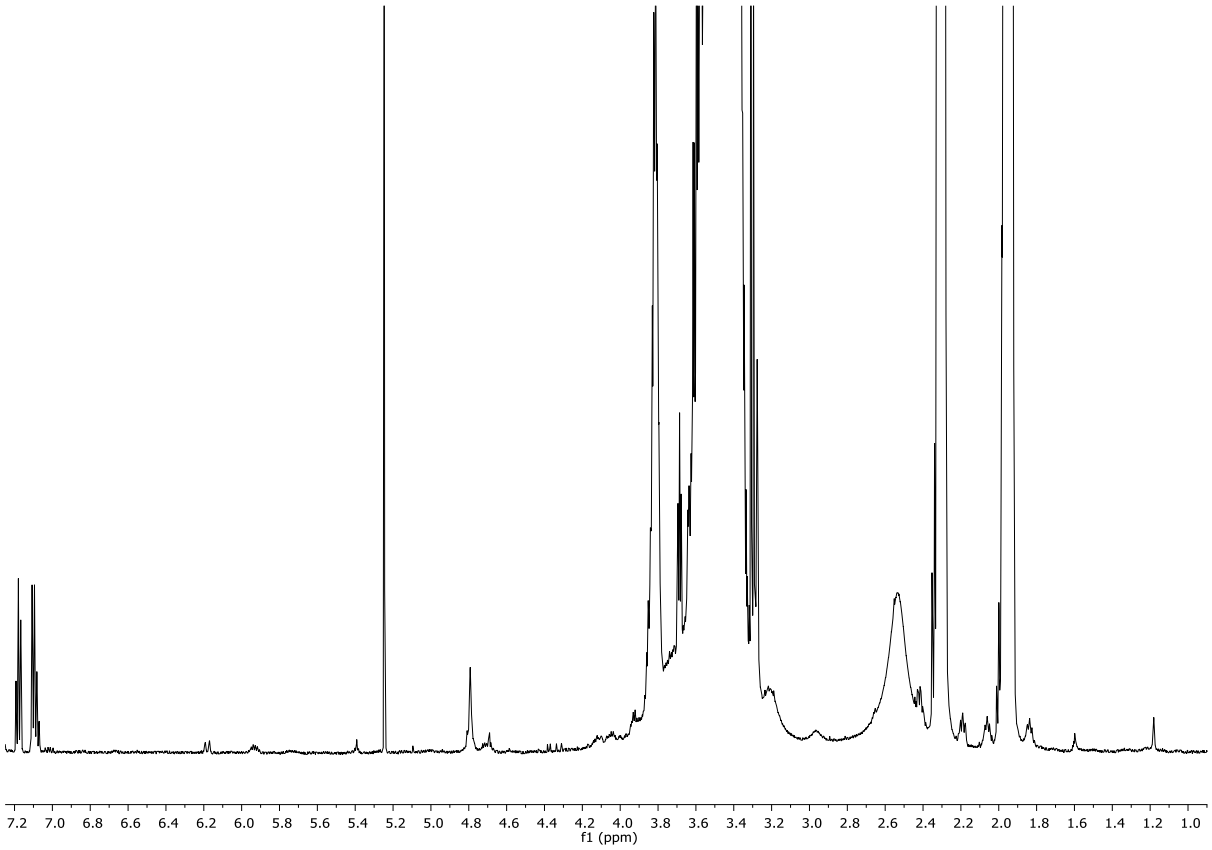

Figure 3.10 - ^{1}H NMR spectrum of polymer 6, expansion

The difference in molecular weight between the pink and the blue peaks is 16 gmol^{-1}, this suggests that they correspond to Na^+ and K^+ ions of the polymer with the same end groups. The end groups have a combined molecular weight of 130 gmol^{-1}. The green and red peaks are also partnered by a smaller set of peaks at 16 gmol^{-1} less, indicating that they correspond to a K^+ counter-ion. The end groups for the green and red peaks have a combined molecular weight of 19 gmol^{-1} and 56 gmol^{-1}, respectively. The multitude of data sets with a variety of end groups demonstrates the uncontrolled nature of the polymerisation.

The patent states that the number of epoxy pyrrolidone repeat units covered in the invention is between 2 and 50.[39] However, the example products demonstrate that a maximum of 6 repeat units was achieved in the synthesis of the surfactants using this method.[39] The results of this investigation have found that the polymerisation is uncontrolled with high levels of chain transfer. The maximum number of repeat units produced ranged from 2 – 14 across all the data sets observed by MALDI analysis.

To investigate the limitations of this procedure, two trial reactions were performed. The first in the absence of MeOK, the second with the addition of crown ether, 18-c-6. The addition of complexing agents has been often employed to increase the proportion of free propagating ions by reducing the aggregation around the ionic centres.[44] The trial reaction with MeOH in the absence of MeOK showed no polymerisation had occurred. It was determined that MeOH could not initiate the polymerisation, however, residual MeOH may still effect the initiated reaction. The trial reaction with the addition of crown ether, 18-c-6 also resulted with no polymerisation of monomer **1**. The crown ether was unable to control the polymerisation as exhibited by the number of end groups observed in the MALDI mass spectroscopy analysis (Figure 3.9). The lack of control could be due to residual MeOH in the reaction despite attempts to fully remove the solvent. To eliminate this issue, anhydrous potassium hydroxide (KOH) could be employed as the initiator for this system.[45] Additionally, a more polar solvent such as THF or DMSO could be employed to promote charge/aggregate dissociation and therefore propagation.

In summary, homopolymerisation attempts for 1,2-epoxy-3-oxyethyl pyrrolidone or glycidyl ethylpyrrolidone (GEP) (**1**) produced oligomers of the desired product. The oligomers were synthesised and characterised by 1D and 2D NMR, SEC, DSC, FTIR and MALDI MS. From the MALDI analysis, a range of data sets were observed with the number of monomer repeat units ranging from $2-14$. The polymers produced had a variety of end groups as the reaction had high levels of chain transfer. The water soluble product could be employed in nano-formulations as the incorporation of the pyrrolidone moiety will aid drug binding and retain biocompatibility.

The monomer (**1**) was taken forward to synthesise novel copolymers in chapter 4 and to modify polymers with terminal OH groups in chapter 5 to produce novel polymers.

3.3.2 Poly(4-vinylbenzyloxy ethyl pyrrolidone), (7)

Traditionally, polystyrene (PSt) is a widely used thermoplastic resin which can be easily processed and manipulated to meet the manufacturing needs. Recent research in this area has focused on the formulation and stabilisation of nanoparticles.[46,47] The stability of the

nanoparticles is dependent on the surfactant used. To remove the need for additional surfactants, some systems have been developed that include the styrene moiety and an aqueous soluble group.[17] The combination of hydrophilic and hydrophobic functional groups is the idea behind the polymerisation of monomer **2** (Scheme 3.4).

To the best of our knowledge the synthesis and (co)polymerisation of monomer **3** has only been published by one research group, Endo *et. al.*[48,49]

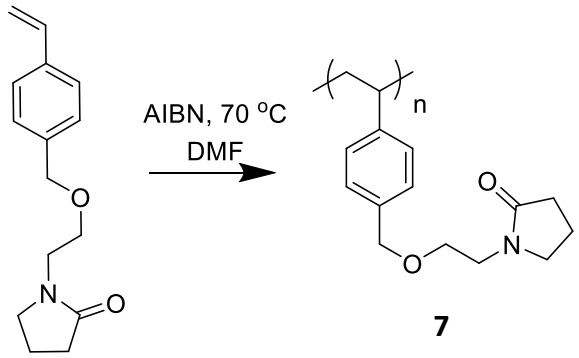

7

Scheme 3.4 – Synthesis of polymer 7

Endo *et. al.* report bulk polymerisation conditions to produce homo- and co-polymers of monomer **2**. The aim of the research was to investigate the nature of the polymerisation and how the pyrrolidone group may interact with the phenol functional groups *via* hydrogen bonding and interruption of π- π stacking. Homopolymerisation reactions were conducted with 1 mol% AIBN initiator at 60°C for 24h in a sealed tube in bulk or benzene at various monomer concentrations. The papers conclude that homopolymerisation of 4-(oxo-1-pyrrolidinyl) methyl styrene (first entry, Table 3.2) resulted in the formation of gelled polymer but that homopolymerisation of monomer **2** produced soluble polymer. The Đ of 3.05 to 3.61 are as expected for FRP and the M_n (as estimated by SEC analysis) shows the molecular weight of the polymer produced from monomer **2** to be lower than that for 4-(oxo-1-pyrrolidinyl) methyl styrene. This could be attributed to the implementation of a conventional calibration based on polystyrene (PSt) standards for M_n calculations.

Table 3.2 – Results published by Endo et. al.[49]

Monomer	Solvent	Yield %		M_n /gmol^{-1}	Đ
		insoluble	soluble		
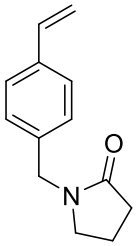	none	29[a]	65[a]	2x10^5	3.05
2	none	0	100[b]	9.1x10^4	3.61

[a] Soxhlet extraction in $CHCl_3$ followed by precipitation in hexane. [b] Precipitation in hexane. M_n and Đ estimated by SEC analysis based of PSt standard.

Following their literature procedure, the polymerisation of monomer **2** was attempted using AIBN at 60 °C in bulk.[48,49] After 1 h stirring the reaction had ceased stirring due to the formation of solid (0.184 g, mass yield 92%), indicating that polymerisation had occurred. The resulting yellow translucent gummy solid was insoluble in acetone, $CHCl_3$, DMSO and DMF amongst other solvents, thus limiting the analytical techniques available to characterise the polymer. Therefore, the reaction product was analysed by solid state NMR (SSNMR) with both cross-polarisation (Figure 3.11) and direct excitation (Figure 3.12) methods. To determine if the translucent gummy solid contained any trapped starting material, the solid was extracted with DCM at 40 °C for 4h. 0.112 g of liquid monomer (61% of 0.182 g) was isolated from the insoluble solid (0.072 g, 39% of 0.182 g). The 'insoluble solid' did swell in $CHCl_3$, DMSO and DMF solvent, suggesting that this was a cross-linked material.

The cross-polarisation method allows the rigid sections of the polymer to be observed whereas the direct excitation has a short relaxation time which permits only the more flexible parts of the polymer to be detected. The resonance at δ = 175.0 ppm (Figure 3.11) is due to the lactam carbonyl of the pyrrolidone group. The three resonances from δ = 128.2 to 146.3 ppm are attributed to the aromatic **C**H's of the phenyl ring. The resonances at δ = 18.5, 30.9 and 47.1 ppm correspond to the three **C**H_2 environments in the pyrrolidone ring, **C**, **B** and **D**, respectively. Carbons **E**, **F** and **G** are observed at δ = 40.3, 68.3 ppm

and 72.7 ppm, respectively. The assignments are based on the general trend of chemical shifts for polymers containing the ethyl pyrrolidone moiety,[50,51] as well as work presented in this thesis.

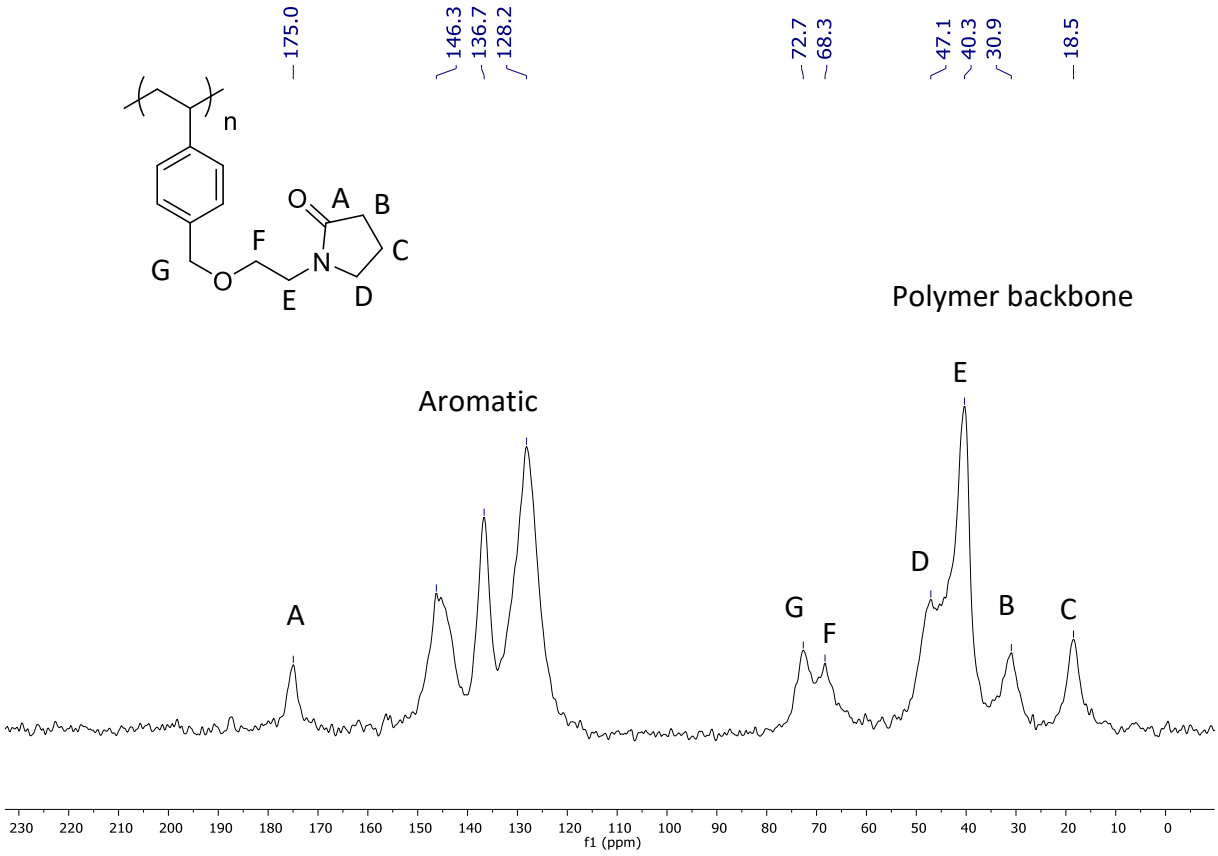

Figure 3.11 – Cross polarisation ^{13}C SSNMR spectrum of polymer 7

Dictating a short relaxation time for the direct excitation SSNMR experiment means that only the carbon environments with fast relaxation times, i.e. more mobile environments, are detected. Using this method along with the cross polarisation technique allows a more complete picture of the polymer material to be obtained. The direct excitation spectrum (Figure 3.12) shows larger peaks for the pyrrolidone when compared to the cross polarisation spectrum (Figure 3.11). The strength of the resonances between δ = 128.2 and 146.3 ppm has decreased in Figure 3.12 resulting in the loss of distinct resonances when compared to the direct excitation spectrum (Figure 3.11). This result is expected as the cross polarisation has a long relaxation time, allowing the more rigid/structurally confined

environments to be observed. It is expected that the carbon environments within and close to the polymer backbone are the most structurally confined i.e. polymer backbone CH and CH_2, and the aromatic styrene environments. Therefore, these are present in the cross polarisation spectrum (Figure 3.11). The pyrrolidone pendant group is expected to have more flexibility and therefore is observed in the direct excitation experiment (Figure 3.12).

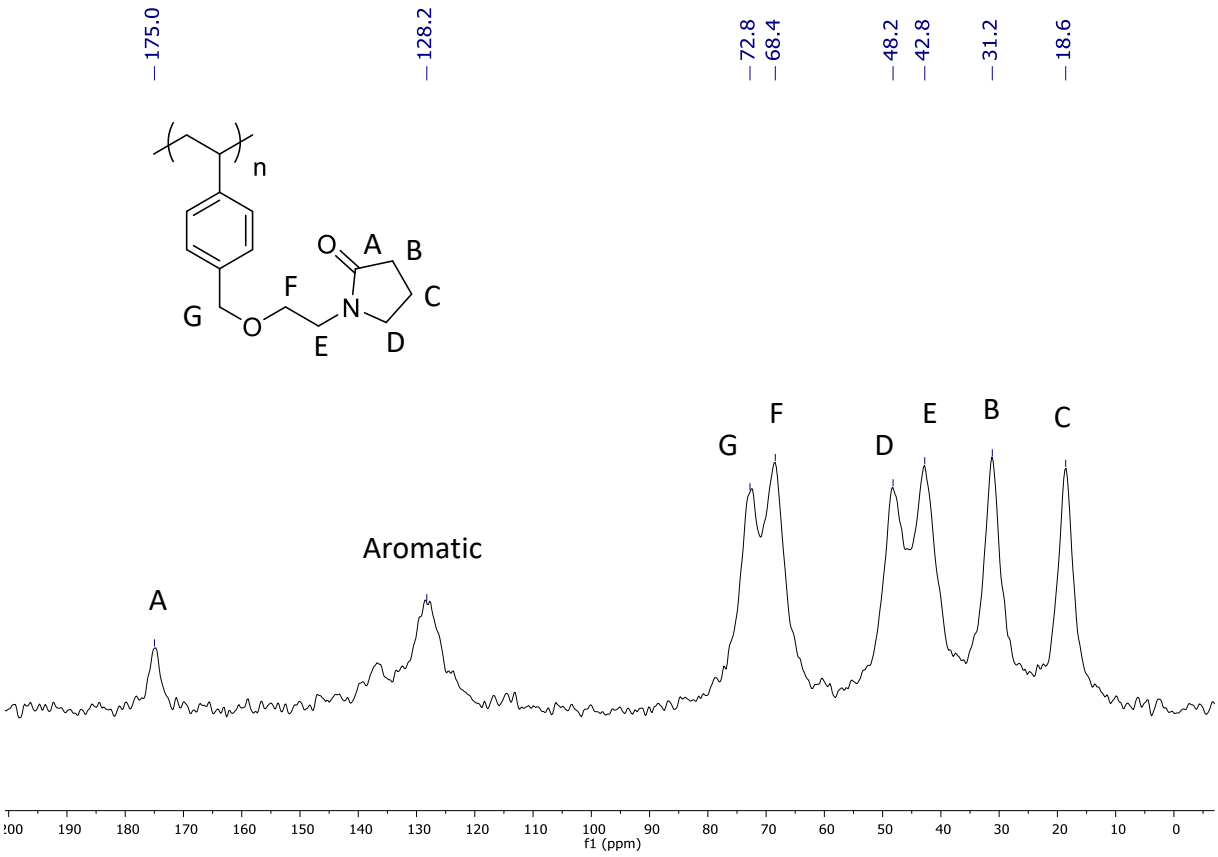

Figure 3.12 – Direct excitation ^{13}C SSNMR spectrum of polymer 7

The reaction was repeated in order to follow the reactions progress by NMR, however, after just 15 min the reaction vessel had ceased stirring due to the formation of solid. The mass yield of polymer recovered was 83%. The formation of an insoluble solid in less than 15 min could be due to the side reactions inherent in an uncontrolled free radical polymerisation. Chain transfer is known to occur to solvent, monomer, initiator and polymer in free radical polymerisations. Chain transfer to polymer creates branching points where cross-linking could occur (Scheme 3.5).[52]

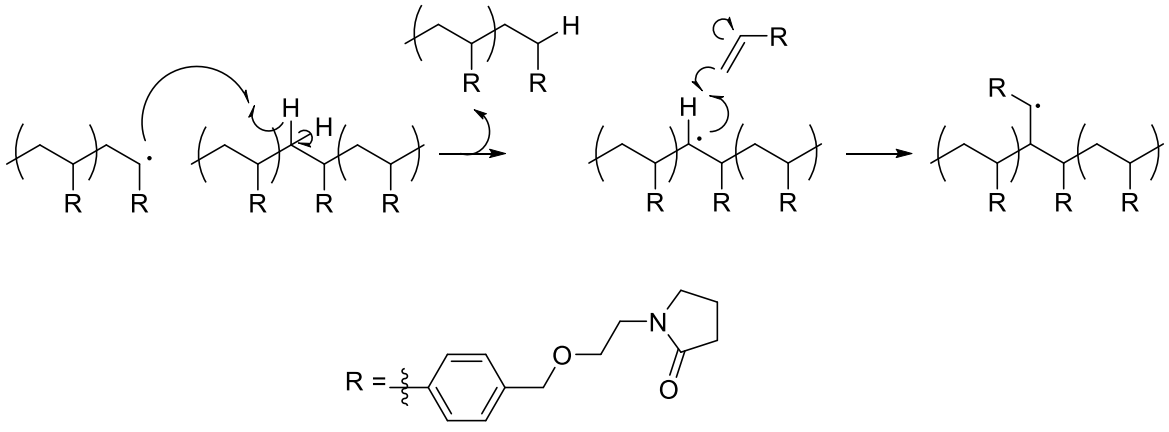

Scheme 3.5 – Mechanism of chain transfer to polymer for monomer 2

To further investigate the polymer, the thermal degradation properties were investigated (Figure 3.13). The first derivative clearly shows that two thermal events occur indicating a two-step thermal decomposition. One explanation for this could be the decomposition of the cross-linked polymer degrading at a higher temperature to the linear polymer chains. PSt is known to have a thermal degradation that begins at 250 °C and ends at 500 °C,[53] the two thermal degradation events of polymer **7** are within this range.

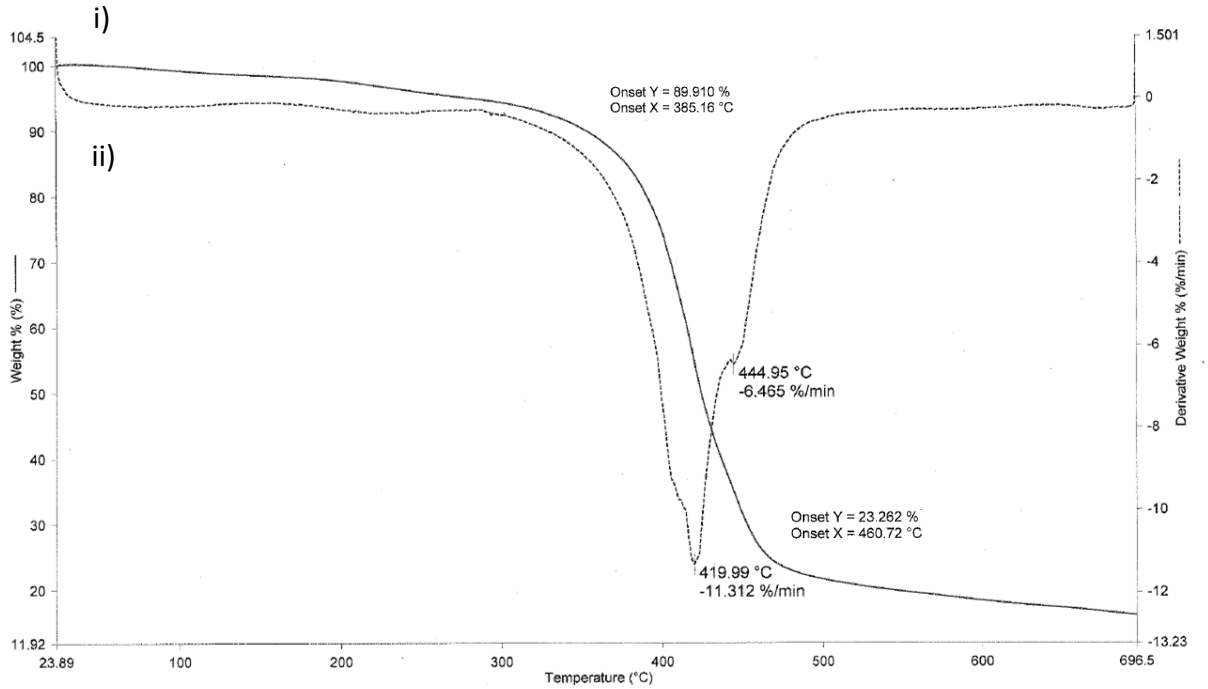

Figure 3.13 – TGA of polymer 7 i) solid line and ii) first derivative, dotted line

FTIR analysis of the insoluble solid showed a band with multiple peaks at ν = 2920, 2918, 2860 cm^{-1} corresponding to the aromatic CH and non-aromatic CH_2 environments. A carbonyl stretch at m/z = 1675 cm^{-1} was also observed, indicating that the pyrrolidone functional group is present in the insoluble solid.

The same reaction conditions were employed to successfully produce polystyrene (PSt), confirmed by NMR, FTIR and SEC analysis, indicating that the problem comes with the presence of the ethyl pyrrolidone moiety. It is postulated that cross-linking occurred during the reaction, leading to the formation of an insoluble cross-linked polymer network which swelled in solvent. This insoluble network could have entrapped the unreacted monomer and limited the progression of the reaction.

The publication by Endo *et. al.* describes how the polymerisation of monomer **2** can be conducted at 60 °C with AIBN as the initiator.[48,49] It was reported that the polymer was recovered by precipitation into hexane and no gelled polymer was obtained in the homopolymerisation of monomer **2**, even when the reaction was conducted in the absence of solvent. However, the publication does describe the polymer as a gummy solid. The molecular weight of the homopolymer produced was reportedly determined to be 9.1 x 10^4 and 8.6 x 10^4 for reactions in bulk and in dry benzene solvent with dispersity (Đ) values of 3.61 and 3.12, respectively. Moreover, the SEC calculations were based on PSt standards and no NMR characterisation is detailed in the publication. The uncontrolled free radical polymerisation leads to large Đ values when compared to living/controlled methods where the Đ would be closer to 1.0. The structural differences between PSt and **7** could reduce the reliability of the measurement and therefore, only relative information can be relied upon in this case. It was reported that the SEC was run in DMF solvent, however, as the solid recovered from the attempted polymerisation of monomer **2** was not soluble in DMF, *vide supra*, we were unable to analyse the polymer in the same manner. To reduce the difficulties associated with bulk polymerisation, the reaction could be conducted at a reduced temperature or in an adequate solvent such as cyclohexane or benzene. Comparable reactions in solvent were not conducted as work focused on more promising areas. Endo *et. al.* also synthesise copolymers of monomer **2** and styrene derivatives St, *p*-

methoxy styrene (PMS) and *m*-hydroxystyrene (MHS) in the same manner to produce polymers with some alternating character.[49]

SSNMR analysis along with the extraction data and FTIR analysis suggests that the polymer undergoes chain transfer to form a cross-linked polymer. The cross-linked polymer retains the pyrrolidone functionality. It is possible that during the reaction, the cross-linked polymer entraps the remaining monomer and limits the progress of the desired reaction.

Monomer **2** was further investigated for copolymerisation with a range of monomers which is discussed in chapter 4.

3.3.3 Poly(5-ethacryloxyethyl-12-ethylpyrrolidyl-N,N'hexane biscarbamate), (8)

The peptide-like mimic is designed to combine: 1) an acrylate group capable of undergoing polymerisation, 2) urethane bonds and 3) pyrrolidone functionality. Incorporation of the pyrrolidone moiety is intended to boost the binding efficiency of drug molecules. Additionally, the urethane bonds will contribute to hydrogen bonding and form the peptide mimic backbone. The acrylate functionality will freely undergo polymerisation, this polymerisation could be controlled to produce polymers with tuneable molecular weight and low Đ. The novel homopolymer **8** was synthesised and fully characterised, the polymer consists of a acrylate backbone and a long peptide-type chain capped with a pyrrolidone moiety.

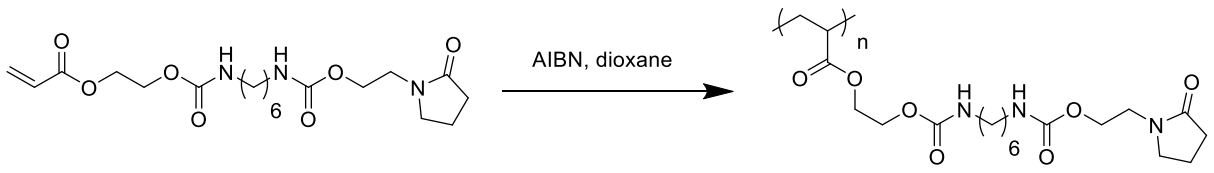

3 **8**

Scheme 3.6 – Synthesis of polymer 8

The free radical polymerisation of novel monomer **3** was undertaken utilising AIBN as the initiator (Scheme 3.6). The polymer was synthesised to a high yield, 95% and was characterised by 1D and 2D NMR techniques as well as FTIR, SEC, TGA and DSC analysis.

There is a clear reduction in the vinyl resonances associated with the monomer in the ^{1}H NMR spectrum (Figure 3.14) and from this the conversion to polymer can be estimated. The estimated conversion is 90% based on the integrals for the NH resonances in the polymer and the vinyl protons of the monomer (Appendix B). There are multiple broad NH resonances, as observed in the monomer (Ch. 2, Figure 2.14). A shift is observed from around δ = 4.85 ppm in the monomer to δ = 7.05 ppm in the polymer due to a change in solvent from $CDCl_3$-*d* to DMF-d_7. Integration of the peaks is unreliable due to the overlapping resonances of the acrylate backbone protons from δ = 1.50 to 2.50 ppm. The ^{1}H-^{1}H COSY NMR spectrum (Figure 3.15) allows for further confirmation of the proton resonances. Two environments for the methyl protons of DMF are observed due to the presence of deuterated and non-deuterated solvent in the sample, marked with an asterisk (*).

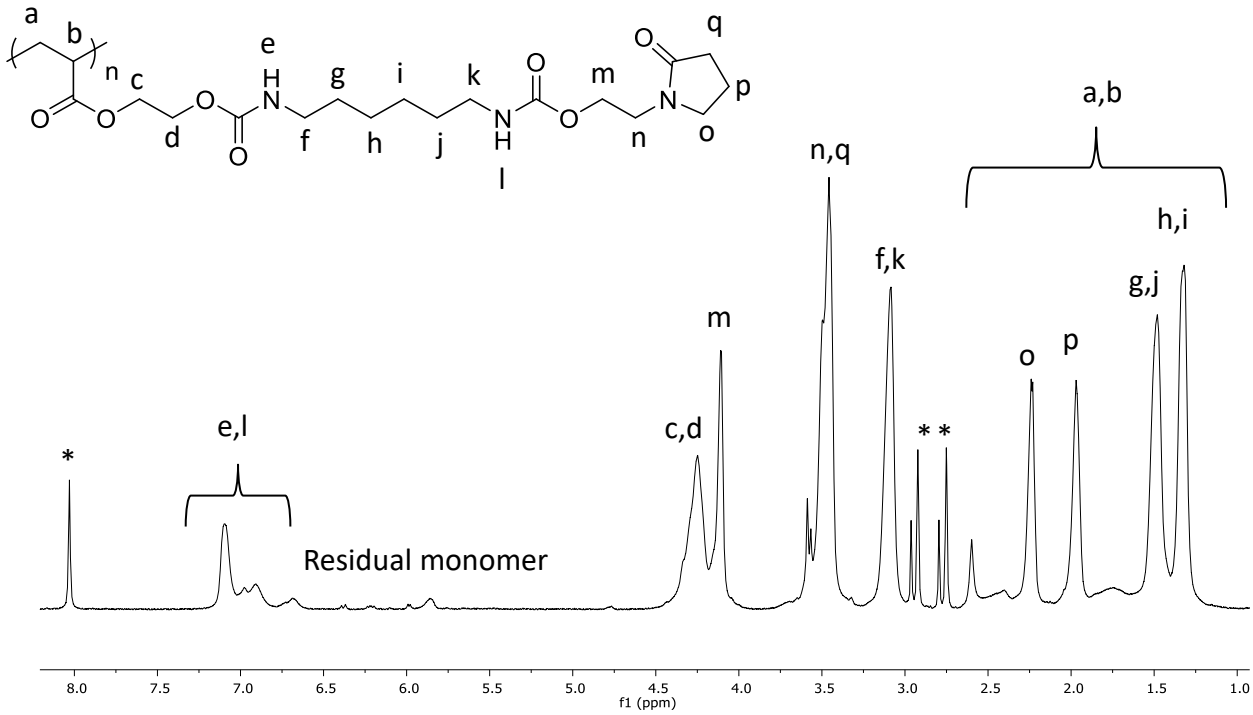

Figure 3.14 – ^{1}H NMR spectrum of polymer 8

From the ^{1}H-^{1}H COSY NMR spectrum (Figure 3.15) it is simple to determine the resonances associated with the CH_2 protons of the pyrrolidone moiety. Proton **p** correlates to proton **o** and **q**, whereas protons **o** and **p** do not couple to each other. Similarly, the resonance observed at δ = 1.48 ppm correlates to the resonances at δ = 1.32 ppm and 3.08 ppm and those resonances do not correlate to each other. This as well as the breadth of the resonance suggests that the resonances are due to the central hexyl linker; δ = 1.32 ppm, protons **h** and **j**, δ = 1.48 ppm, protons **g** and **i**, and δ = 3.08 ppm, protons **f** and **k**. Protons **f** and **k** also correlate to the main NH resonance at δ = 7.09 ppm. The correlation between the resonance at δ = 3.36 and 4.11 ppm (protons **n** and **m**) is also observed. The correlation between protons **c** and **d** is distinguished where the broad proton resonances are overlapping.

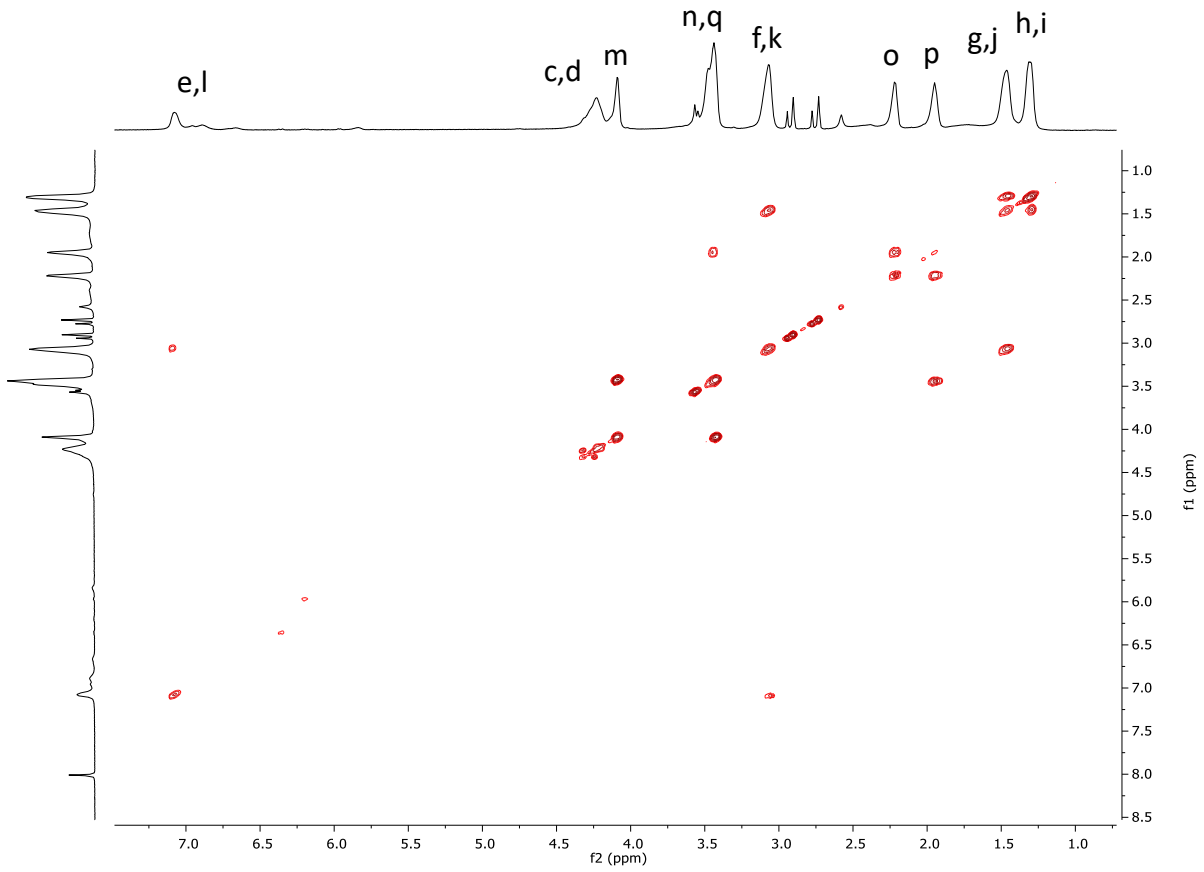

Figure 3.15 – ^{1}H-^{1}H COSY NMR spectrum of polymer 8

The ^{13}C NMR spectrum (Figure 3.16) allows for further characterisation of the polymer. The signals for the pendant group are much stronger the further from the polymer backbone. For example, the resonance for carbons **D**/**E** at δ = 62.0 ppm adjacent to the resonance for carbon **N** at δ = 61.4 ppm. Resonances for the acrylate backbone carbons **A** and **B** are not clearly visible due to the large number of chemically similar environments along the atactic backbone chain causing a broad signal as well as the lack of rigidity inherent in the long pendant chain when compared to the polymer backbone.

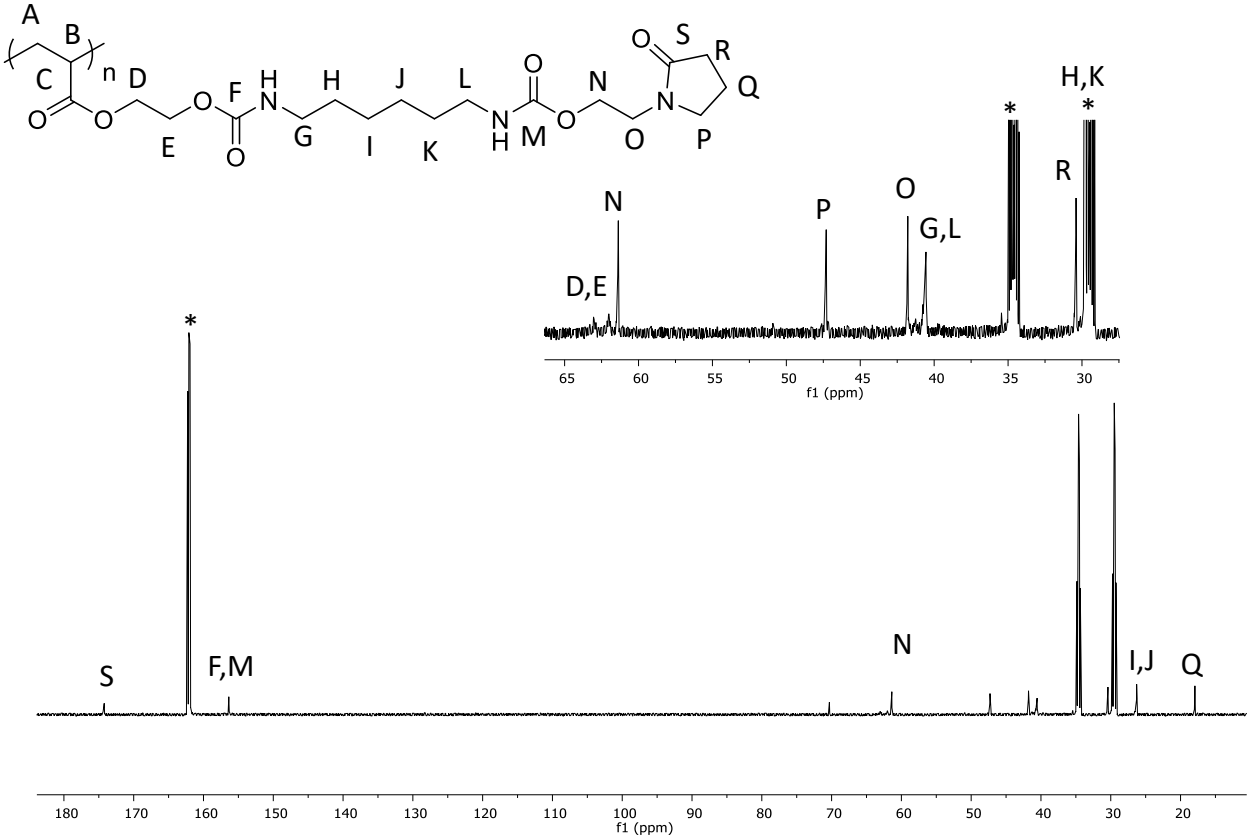

Figure 3.16 – ^{13}C NMR spectrum of polymer 8

The ^{1}H-^{13}C HSQC NMR spectrum (Figure 3.17) confirms the correlation between the ^{1}H and ^{13}C resonances in polymer **8**. All the signals are in the same phase, indicating that the observable correlations are due to CH_2 carbon environments. Protons **h** and **I** correlate to the carbons **I** and **J** at δ = 26.3 ppm. Protons **g** and **i** show a correlation to a carbon resonance which is overlapping with the solvent peak at δ = 29.8 ppm. A correlation is observed between carbons **G** and **L** at δ = 40.6 ppm with the proton resonance at δ = 3.08 ppm, attributed to protons **f** and **k**. Additionally, protons **o** and **p** of the pyrrolidone moiety couple to the carbon resonances at δ = 17.9 (**Q**) and 30.4 ppm (**R**), respectively.

The overlapping proton resonances of **n** and **q** correlate to two carbon environments, one at δ = 41.8 ppm and the other at δ = 47.3 ppm. It is only possible to fully characterise these resonance, by ^{1}H-^{13}C HMBC NMR analysis.

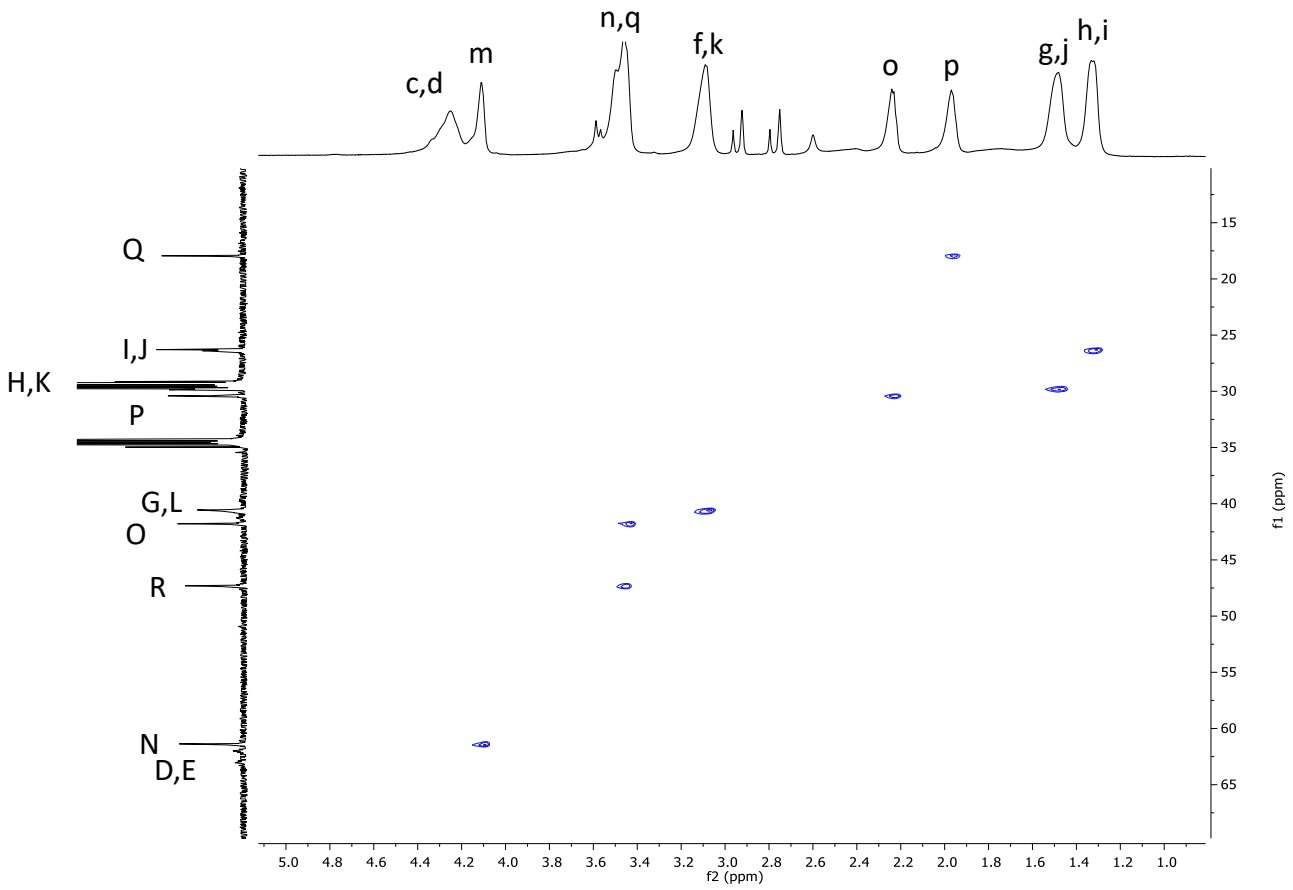

Figure 3.17 – ^{1}H-^{13}C HSQC NMR spectrum of polymer 8

The ^{1}H-^{13}C HMBC NMR spectrum (Figure 3.18) confirms the assignment of the carbonyl carbon environments **S**, **F** and **M**. The correlations between the carbonyl at δ = 174.2 ppm and the protons **o**, **p**, and the overlapping **n** and **q** are observed. Therefore this resonance is attributed to carbon **C**. The assignment of the two carbon environments **O** and **P** is also elucidated. There is a clear correlation between protons **o** and **p** with the carbon resonance at δ = 47.3 ppm, therefore this is attributed to carbon **P** in the pyrrolidone group. The carbon at δ = 41.8 ppm show a multiple bond coupling with proton **m**, therefore the carbon resonance is attributed to carbon **O**.

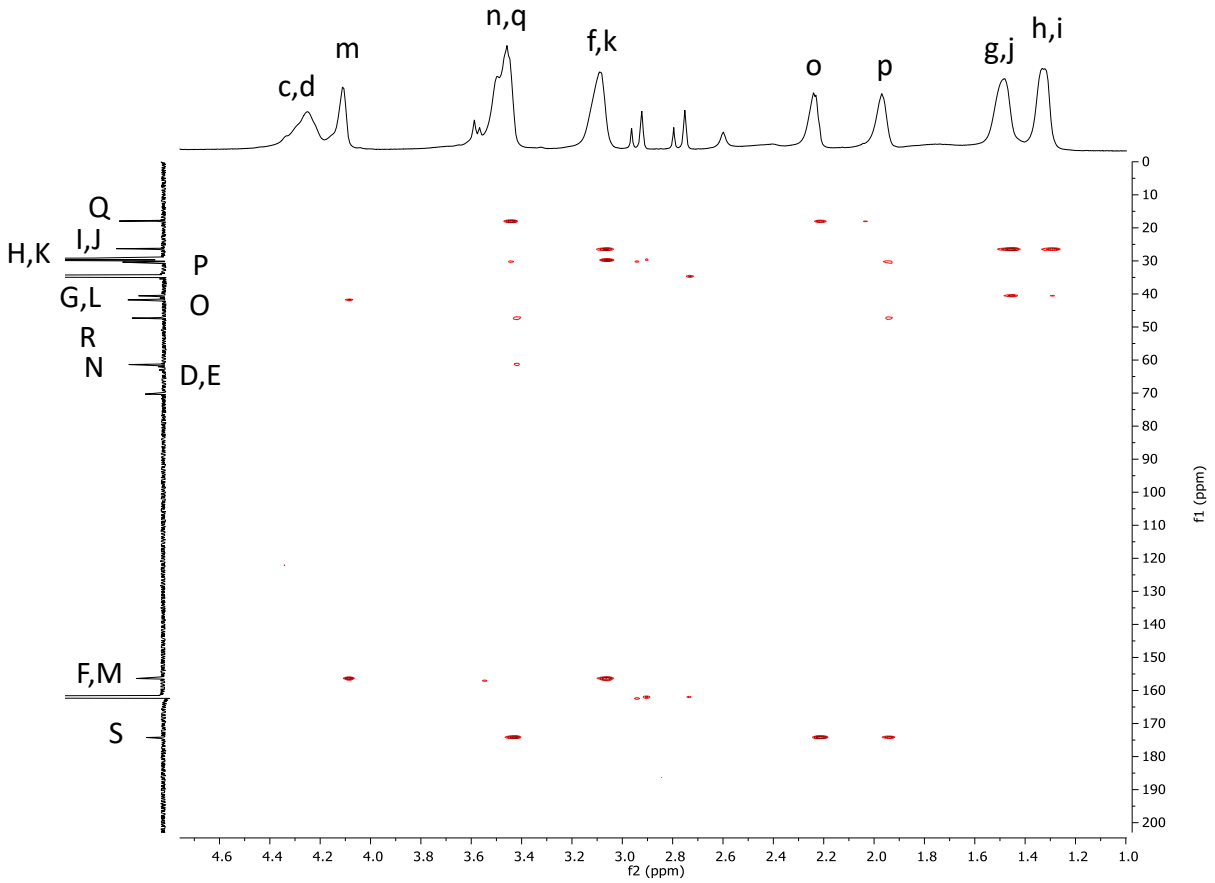

Figure 3.18 – ^{1}H-^{13}C HMBC NMR spectrum of polymer 8

The SEC trace (Figure 3.19) shows a multimodal distribution with a low M_n of 963 gmol^{-1} and large Đ of 16.8. The SEC was conducted in DMF solvent. The chromatogram shows a narrow low molecular weight peak and a broad distribution with a minimum of 3 overlapping peaks. The M_p for the low molecular weight peak is found to be 250 gmol^{-1} and the broad high molecular weight peak is 4 x 10^4 gmol^{-1}. The low molecular weight peak could be due to the residual monomer (413.22 gmol^{-1}) which can be seen in the ^{1}H NMR spectrum (Figure 3.14). Complex fractionation methods such as mixed solvent systems or continuous spin fractionation (CSF), could be employed in this instance to remove the monomer species and elucidate the multimodal SEC chromatogram further, however, due to time constraints, this was not undertaken. The broad tri-modal peak in the SEC chromatogram, could be a combination of 3 polymer species with varying molecular weights, indicated by the blue, red

and green shaded areas (Figure 3.19, ii)). However, without detailed fractionation the isolation and identification of these species is not possible.

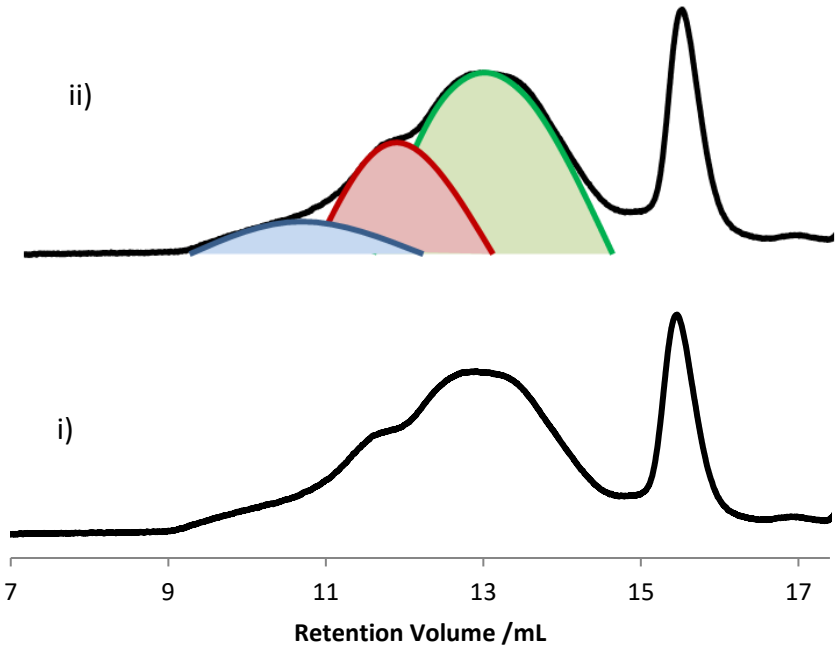

Figure 3.19 – SEC trace of i) polymer 8 and ii) with shaded sections

The molecular weight calculations are based on a conventional calibration constructed from polyethylene oxide (PEO) standard. The difference in polymer structure when compared to the PEO standard, will result in inaccurate values. No light scattering was observed, therefore triple detection analysis was not possible and conventional calibration was used to calculate the polymer molecular weight. The calculated molecular weight for the broad multimodal peak shows that polymer is produced under the reaction conditions, however, a broad molecular weight range is observed which is anticipated with a free radical reaction.

TGA analysis shows a three step thermal decomposition process (Figure 3.20). There is moderate water loss observed in the thermogram with a maximum observed in the first derivative at 94.64 °C, which is calculated to be 11.537% of the polymer composition. The first thermal event which the polymer will undergo is cleavage of the weak urethane bonds to produce small molecules leaving the acrylate polymer backbone (Figure 3.20).[55] The two

step thermal decomposition of polymer **8** begins with an onset of X^1 = 260.20 °C and maximum in the first derivative at 287.91 °C, it is believed that this is due to the pyrolysis (**Error! Reference source not found.**).

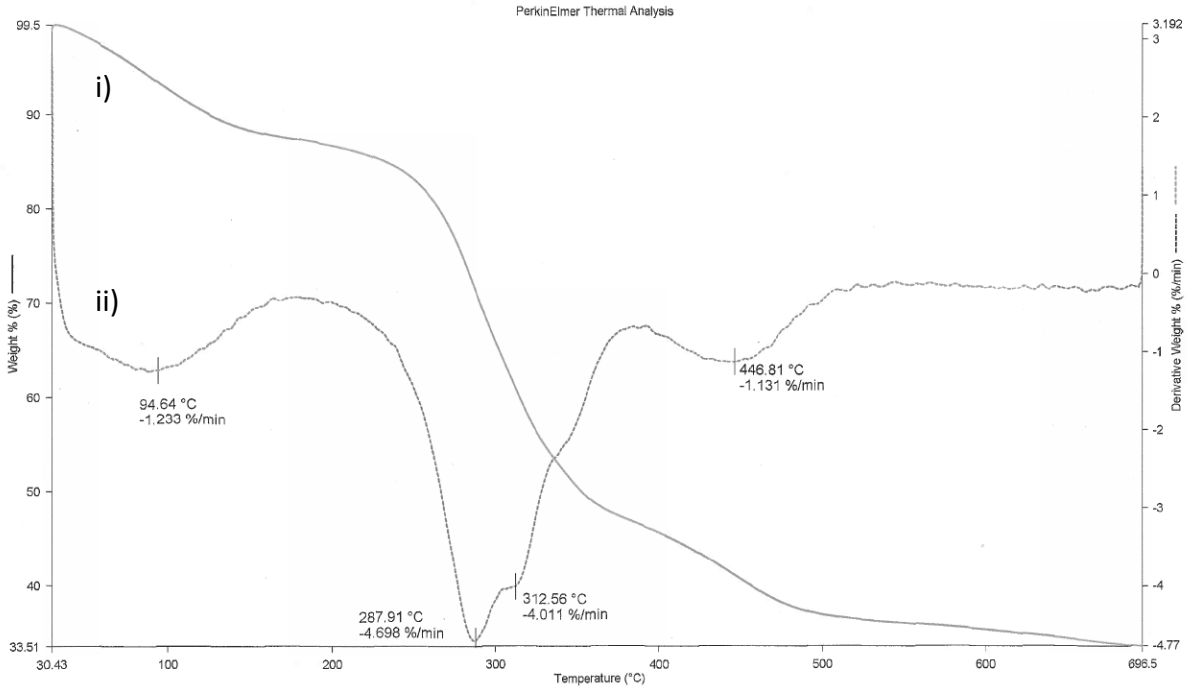

Figure 3.20 –TGA of polymer 8 i) solid line and ii) first derivative, dotted line

The polyacrylate decomposition differs to that of polymeth acrylates due to the presence of the methyl group in polymethacrylate polymers which inhibits intramolecular hydrogen bonding. Therefore the decomposition process of polyacrylates such as monomer **3** occurs *via* intra- and inter-molecular hydrogen transfer.[56] The second thermal degradation has an onset of X^2 = 341 °C with a maximum in the first derivative at 313 °C, it is postulated that this is due to the decomposition of the acrylate polymer backbone *via* scission. DSC analysis showed on the second heating run, a T_g of 22 °C. For comparison, PMA homopolymer has a T_g of 14 °C[57] and TGA of 325 °C.[58] The increase in T_g can be attributed to the large pendant group restricting the flexibility of the polymer. The final degradation observed with an onset of X^3 = 472 °C and maximum in the first derivative at 447 °C is believed to be due to the production of highly cross-linked and cyclised material.[56]

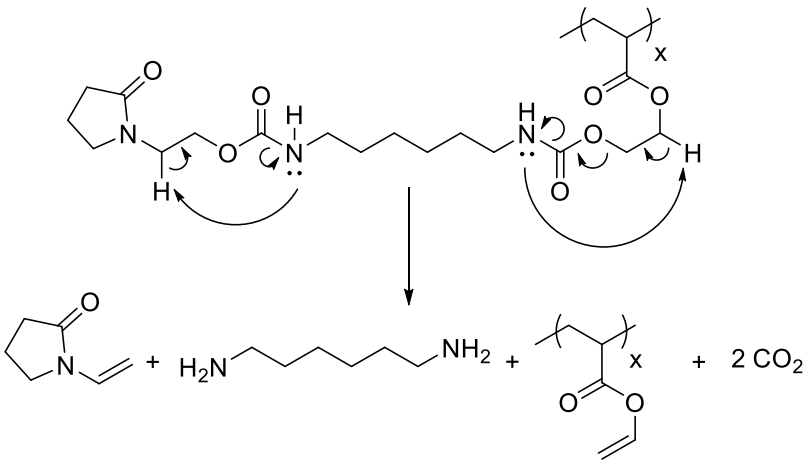

Scheme 3.7 – Thermal degradation mechanism *via* pyrolysis

The FTIR spectrum contains a broad band at ν = 3318 cm^{-1} which corresponds to the urethane bond vibration. The CH_2 stretch is also observed with a broad band at 2935 cm^{-1}. Two peaks can be seen in the broad carbonyl stretch at 1701 and 1668 cm^{-1}.

In summary, the novel homopolymer **8** was successfully synthesised *via* a free radical polymerisation with AIBN initiator. The simple synthetic procedure founded on widely used industrial polymerisation methods will aid a cost effective and straightforward industrial plant application. The polymer produced was synthesised and characterised by 1D, 2D NMR, SEC, FTIR, DSC and TGA analysis.

Copolymerisation reactions with novel monomer **3** are discussed in chapter 4.

3.4 Conclusions

The alkoxide initiated ring opening of monomer **1** resulted in the formation of oligomer **6**. MALDI analysis showed, the number of repeat units ranged from 2 – 14 with a molecular weight range from 414.10 to 2797.54 $gmol^{-1}$. The addition of macromolecular complexing agent crown ether 18-c-6 did not impart control, possibly due to the presence of residual MeOH in the reaction. The oligomer was water soluble and combined the PEG and pyrrolidone functionality which could be beneficial for drug binding.

The translucent gummy solid produced by the free radical polymerisation of monomer **2** was found to be insoluble in common organic solvents. Therefore, it was not possible to characterised the polymer by conventional techniques such as solution state NMR and SEC. The solid was extracted in DCM for 4 h at 40 °C, 0.072 g of insoluble solid (39% of 0.182 g) was isolated as well as 0.112 g of liquid monomer (61% of 0.182 g). The insoluble solid was analysed by SSNMR, TGA and FTIR. It is possible that chain transfer reactions occurred during the free-radical polymerisation which formed a cross-linked polymer network. It is postulated that this polymer network entrapped the remaining unreacted monomer and limited the progress of the reaction.

Free radical polymerisation was successfully employed to synthesise the novel peptide mimic **8** in a good yield (95%), and fully characterised by 1D, 2D NMR, SEC, DSC, TGA and FTIR. The polymer was found to be soluble in aqueous and organic media.

3.5 References

1 F. P. Sidel'kovskaya, V. A. Ponomarenko, M. G. Zelenskaya, A. V Ignatenko, O. D. Trifonova, É. A. Abdula-Zade, A. G. Kechina and L. A. Sinitsyna, *Bull. Acad. Sci. USSR, Div. Chem. Sci.*, **1975**, 25, 587–593.

2 Lactam Copolymers, US Pat. 4698412, **1987**.

3 K. Knop, R. Hoogenboom, D. Fischer and U. S. Schubert, *Angew. Chemie - Int. Ed.*, **2010**, 49, 6288–6308.

4 M. Barz, R. Luxenhofer, R. Zentel and M. J. Vicent, *Polym. Chem.*, **2011**, 2, 1900–1918.

5 J. Zhang, B. Muirhead, M. Dodd, L. Liu, F. Xu, N. Mangiacotte, T. Hoare and H. Sheardown, *Biomacromolecules*, **2016**, 17, 3648–3658.

6 I. C. Escobar and B. Van Der Bruggen, *J. Appl. Polym. Sci.*, **2015**, 132, 41661–41672.

7 K. Wei, J. Li, G. Chen and M. Jiang, *ACS Macro Lett.*, **2013**, 2, 278–283.

8 G. B. H. Chua, P. J. Roth, H. T. T. Duong, T. P. Davis and A. B. Lowe, *Macromolecules*, **2012**, 45, 1362–1374.

9 J. Lee, A. J. McGrath, C. J. Hawker and B.-S. Kim, *ACS Macro Lett.*, **2016**, 5, 1391–1396.

10 X. Shang, X. Fan, S. Yang, Z. Xie, Y. Guo and Z. Hu, *RSC Adv.*, **2015**, 5, 96181–96188.

11 Y. Zhang, E. Mintzer and K. E. Uhrich, *J. Colloid Interface Sci.*, **2016**, 482, 19–26.

12 I. Hamad, A. C. Hunter, J. Szebeni and S. M. Moghimi, *Mol. Immunol.*, **2008**, 46, 225–232.

13 T. Ishida and H. Kiwada, *Int. J. Pharm.*, **2008**, 354, 56–62.

14 H.-J. Sung, A. Luk, N. S. Murthy, E. Liu, M. Jois, A. Joy, J. Bushman, P. V. Moghe and J. Kohn, *Soft Matter*, **2010**, 6, 5196–5205.

15 H. J. Sung, P. Chandra, M. D. Treiser, E. Liu, C. P. Iovine, P. V. Moghe and J. Kohn, *J. Cell. Physiol.*, **2009**, 218, 549–557.

16 R. Lebovic, N. Pearce, L. Lacey, J. Xenakis, C. B. Faircloth and P. Thompson, *Pediatr. Blood Cancer*, **2017**, 1–5.

17 S. Pargen, C. Willems, H. Keul, A. Pich and M. Möller, *Macromolecules*, **2012**, 45, 1230–1240.

18 Y. Zang, M. Ye, A. Han and Y. Ding, *J. Appl. Polym. Sci.*, **2017**, 134, 1–9.

19 I. Asano, S. So and T. P. Lodge, *J. Am. Chem. Soc.*, **2016**, 138, 4714–4717.

20 W. Wang, C. Gao, Y. Qu, Z. Song and W. Zhang, *Macromolecules*, **2016**, 2772–2781.

21 N. P. Truong, J. F. Quinn, A. Anastasaki, D. M. Haddleton, M. R. Whittaker and T. P. Davis, *Chem. Commun.*, **2016**, 52, 4497–4500.

22 P. R. Haddad, P. N. Nesterenko and W. Buchberger, *J. Chromatogr. A*, **2008**, 1184, 456–473.

23 F. Ye, R. Yang, X. Hua and G. Zhao, *Food Chem.*, **2014**, 159, 38–46.

24 F. Bauer and R. Mehnert, *J. Polym. Res.*, **2005**, 12, 483–491.

25 D. J. Kang, G. U. Park, H. G. Im, H. Y. Park and J. Jin, *Polym. (United Kingdom)*, **2016**, 105, 19–24.

26 H. Rashidi, J. Yang and K. M. Shakesheff, *Biomater. Sci.*, **2014**, 2, 1318–1331.

27 J. Radhakrishnan, A. Subramanian, U. M. Krishnan and S. Sethuraman, *Biomacromolecules*, **2017**, 18, 1–26.

28 Y. Mei, K. Saha, S. R. Bogatyrev, J. Yang, A. L. Hook, Z. I. Kalcioglu, S. W. Cho, M. Mitalipova, N. Pyzocha, F. Rojas, K. J. Van Vliet, M. C. Davies, M. R. Alexander, R. Langer, R. Jaenisch and D. G. Anderson, *Nat. Mater.*, **2010**, 9, 768–778.

29 R. E. Richard, M. Schwarz, S. Ranade, A. K. Chan, K. Matyjaszewski and B. Sumerlin, *Controlled/Living Radiacl Polymerization*, Americal Chemical Society, **2006**.

30 A. Arun and B. S. R. Reddy, *J. Biomed. Mater. Res. - Part B Appl. Biomater.*, **2005**, 73, 291–300.

31 L. B. Peppas, *Int. J. Pharm.*, **1995**, 116, 1–9.

32 H. Li, R. Aneja and I. Chaiken, *Molecules*, **2013**, 18, 9797–9817.

33 B. Obermeier, F. Wurm and H. Frey, *Macromolecules*, **2010**, 43, 2244–2251.

34 J. Meyer, H. Keul and M. Möller, *Macromolecules*, **2011**, 44, 4082–4091.

35 Y. Koyama, M. Umehara, a Mizuno, M. Itaba, T. Yasukouchi, K. Natsume and a Suginaka, *Bioconjug. Chem.*, **1996**, 7, 298–301.

36 V. S. Reuss, B. Obermeier, C. Dingels and H. Frey, *Macromolecules*, **2012**, 45, 4581–4589.

37 V. S. Wilms, H. Bauer, C. Tonhauser, A. M. Schilmann, M. C. Millller, W. Tremel and H. Frey, *Biomacromolecules*, **2013**, 14, 193–199.

38 V. S. Reuss, M. Werre and H. Frey, *Macromol. Rapid Commun.*, **2012**, 33, 1556–1561.

39 Epoxy Pyrrolidone Based Non-Ionic Surfactants, US Pat. 4801400, **1989**.

40 D. Williams and I. Fleming, *Spectroscopic Methods in Organic Chemistry*, McGraw-Hill Education Ltd., 6th edn., **2008**.

41 M. Wagner, *Thermal Analysis in Practice*, Mettler-Toledo, **2009**.

42 B. C. Hancock and G. Zografi, *J. Pharm. Sci.*, **1997**, 86, 1–12.

43 J. Herzberger, K. Niederer, H. Pohlit, J. Seiwert, M. Worm, F. R. Wurm and H. Frey, *Chem. Rev.*, **2016**, 116, 2170–2243.

44 Z. Grobelny, M. Matlengiewicz, J. Jurek, M. Michalak, D. Kwapulińska, A. Swinarew and E. Schab-Balcerzak, *Eur. Polym. J.*, **2013**, 49, 3277–3288.

45 B. F. Lee, M. Wolffs, K. T. Delaney, J. K. Sprafke, F. A. Leibfarth, C. J. Hawker and N. A. Lynd, *Macromolecules*, **2012**, 45, 3722–3731.

46 M. Zhang, C. Zhang, Z. Du, H. Li and W. Zou, *Compos. Sci. Technol.*, **2017**, 138, 1–7.

47 S. Jaimuang, T. Vatanatham, S. Limtrakul and P. Prapainainar, *Polymer (Guildf).*, **2015**, 67, 249–257.

48 T. Takata, I. Atobe and T. Endo, *J. Polym. Sci. Part A Polym. Chem.*, **1992**, 30, 1495–1498.

49 I. Atobe, T. Takata and T. Endo, **1993**, 8, 3004–3008.

50 J. Sun, Y. Peng, Y. Chen, Y. Liu, J. Deng, L. Lu and Y. Cai, *Macromolecules*, **2010**, 43, 4041–4049.

51 J. Deng, Y. Shi, W. Jiang, Y. Peng, L. Lu and Y. Cai, *Macromolecules*, **2008**, 41, 3007–3014.

52 R. J. Young and P. A. Lovell, *Introduction to Polymers*, Chapman & Hall, London, Second., **1999**.

53 J. D. Peterson, S. Vyazovkin and C. A. Wight, *Macromol. Chem. Phys.*, **2001**, 202, 775–784.

54 S. Podzimek, *Light Scattering, Size Exclusion Chromatography and Asymmetric Flor Field Flow Fractionation*, A John Wiler & Sons, Inc., **2010**.

55 A. Ballistreri, A. Foti, P. Maravigna, G. Montaudo and E. Scamporrino, *J. Polym. Sci. Polym. Chem. Ed.*, **1980**, 18, 1923–1931.

56 C. L. Beyler and M. M. Hirschler, *SFPE Handbook of Fire Protection Engineering*, Springer-Verlag New York, Second., **2002**.

57 W. Chen and B. Qu, *Polym. Degrad. Stab.*, **2005**, 90, 162–166.

58 C. Wu, T. Xu and W. Yang, *Eur. Polym. J.*, **2005**, 41, 1901–1908.

Chapter 4

Copolymerisation Investigations of Pyrrolidone Monomers

The focus of this chapter is the copolymerisation of the known and novel monomers (**1** to **3**, Figure 3.1, Ch.3), following on from the homopolymerisation experiments described on chapter 3. The incomplete homopolymerisation of the known monomer 1-(2-(oxiran-2-ylmethoxy) ethyl) pyrrolidin-2-one or glycidyl ethylpyrrolidone (GEP) (**1**) with a simple alkoxide initiating system produced oligomers (Ch. 3, 3.3.1) therefore, copolymerisation reactions were explored. The copolymerisation of the known monomer **3** with styrene (St) (**11**), *N*-vinyl pyrrolidone (NVP) (**12**) and hydroxyethyl acrylate (HEA) (**13**) following the method outlined by Endo *et. al*[1] is described. The synthesis of novel copolymer poly(5-ethacryloxyethyl-12-ethylpyrrolidyl-N,N'hexane biscarbamate-*co*-vinyl pyrrolidone **14** was conducted in a method analogous to that of the novel homopolymer, poly(5-ethacryloxyethyl-12-ethylpyrrolidyl-N,N'hexane biscarbamate) (**8**), discussed in chapter 3.

4.1 Introduction

Copolymers of polyvinyl pyrrolidone (PVP) have a wide variety of uses and applications, such as tablet formulation[2] and optical fibre coatings.[3] As previously outlined, PVP has excellent complexation properties and PVP copolymers have exhibited complexation with DNA.[4] The wide variety of applications is due to the diverse choice of co-monomer available for copolymerisation with NVP. The versatility has shown PVP copolymers to be an important class of functionalised polymer.

Polyethylene oxide (PEO), known as polyethylene glycol (PEG), and its derivatives are widely used polyethers in pharmaceutical and biological applications due to the desirable properties of; solubility in water and organic solvents,[5] no immunogenicity, toxicity or antigenisity,[6] high flexibility,[7] and, FDA approval.[8] One drawback of PEG homopolymer is the lack of functionality, there have been many strategies employed to introduce functionality to this class of polymers. End-group functionalisation is widely used,[9] however, this method limits the functionality to the ends of the polymer chain. To attain functionality throughout the polymer chain, it is necessary to synthesise copolymers of ethylene oxide (EO) and substituted epoxides [as previously discussed PVP is FDA approved[8], soluble in water and organic solvents[10], and forms flexible films[11]]. The addition of a pyrrolidone containing epoxide monomer introduces excellent complexation potential without compromising the central properties of PEG units.

As pyrrolidone containing polymers are so versatile and used in a wide variety of products, the synthesis of a degradable pyrrolidone containing polymer could lead to an increase in their applicability. Currently pyrrolidone polymers are used in food production and packaging industry,[12–14] having the degradable functionality within the backbone of the polymer would be advantageous in applications such as these. Often, polymers described as 'biodegradable' contain cleavable pendant groups or spacers within the polymer and are not truly biodegradable. Having the degradable functionality throughout the backbone chain allows for a more complete degradation.

Many different aluminium species have been employed in the polymerisation and copolymerisation of epoxides.[15] Aluminium isopropoxide ($Al(O^iPr)_3$) is an inexpensive and readily available aluminium species that exists in a trimeric or tetrameric form[16] where the tetrameric form is more stable. To ensure the majority of the aluminium aggregates are the active trimers for polymerisation, the $Al(O^iPr)_3$ is distilled immediately prior to polymerisation. It has been reported that for the polymerisation of ε-caprolactone (εCl) with freshly distilled $Al(O^iPr)_3$, there are three propagating chains for every Al centre (see 4.3.2).[17] The advantages of employing a commercially available initiator are ease of industrial scale-up without excessive cost.

The advantages of combining a hydrophilic and hydrophobic functional groups are evident in the self-assembly of nano-structures. Many PSt-PVP copolymers focus on micellar formulations[18] due to the difference in polarity and therefore hydrophobicity of the monomers.

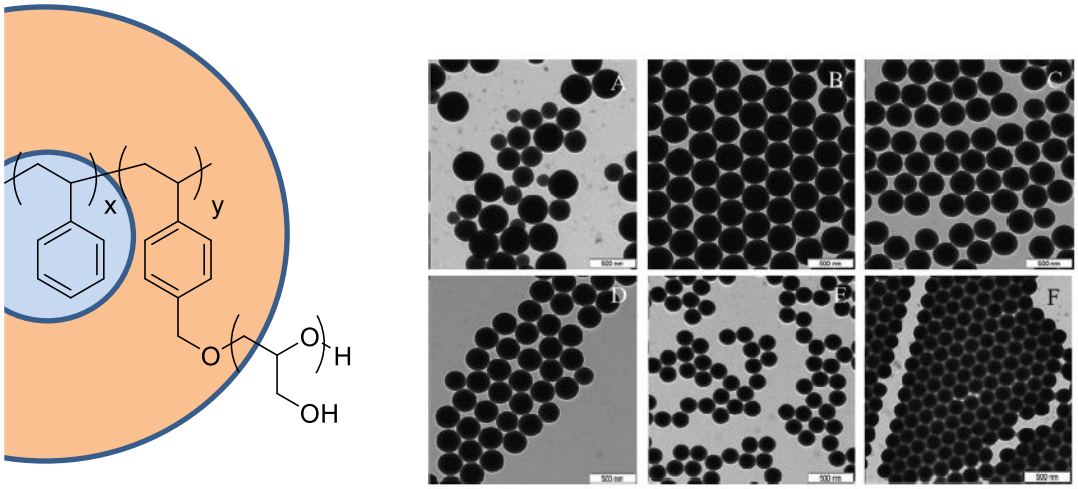

Figure 4.1 – Structure of modified styrene (left) and TEM images of the nanoparticles synthesised with varying concentrations of modified styrene monomer A: 0.1%, B: 0.3%, C: 0.5%, D: 1%, E: 3%, F: 5%, scale bar = 500 nm[19]

Polyamides and peptide mimics are a highly interesting area of research which include polymer materials which undergo transitions in response to a variety of stimuli.[20] Recent advances have led to clinical trials and even to commercial output.[21] The addition of the pyrrolidone moiety should increase the binding efficiency and allow a greater breadth of application for drug delivery systems.

The aim of this work is to synthesise a range of novel PVP copolymers with a variety of properties utilising readily available chemicals and practiced synthetic procedures. The target pyrrolidone copolymers include a functionalised polyether, degradable polyester, polyamide peptide mimic and polystyrene based copolymers.

4.2 Experimental

4.2.1 Materials

Dry DMF, THF and Toluene were obtained from the Durham University Chemistry Department solvent purification service (SPS). Potassium napthalenide solution in THF was prepared according to literature.[22] Ethylene oxide (EO) was distilled over CaH_2 prior to use. MeOH, DCM, $CHCl_3$ and hexane were purchased from Fisher Scientific and used without prior purification. Aluminium isopropoxide (≥98%), Hydroxyethyl acrylate (HEA, 96%) and Styrene (St, ≥99%) were purchased from Sigma Aldrich and distilled prior to use. Succinic anhydride (SA, 97%) was purchased from Sigma Aldrich and recrystallised from $CHCl_3$ prior to use. Azobisisobutyronitrile (AIBN, 98%) was purchased from Sigma Aldrich and recrystallised from MeOH prior to use. *N*-vinyl pyrrolidone (NVP) was provided by Ashland Inc. and distilled prior to use. Benzyl alcohol (anhydrous, 99.8%) was purchased from Sigma Aldrich and used without prior purification. Monomers **1**, **2** and **3** were synthesised according to the procedures outlined in chapter 2.

4.2.2 Instrumentation

^{1}H and ^{13}C Nuclear Magnetic Resonance (NMR) spectra were recorded on a Bruker Avance 400 operating at 400 MHz or a Varian VNMRS 700 spectrometer operating at 700 MHz (^{1}H) and 176 MHz (^{13}C) with *J* values given in Hz. $CDCl_3$ was used as the deuterated solvent for ^{1}H and ^{13}C NMR analysis and the spectra were referenced to the solvent at 7.26ppm and 77.16 ppm, respectively. The following abbreviations are used in describing NMR spectra: s = singlet, d = doublet, t = triplet, m = multiplet and b = broad, bm = broad multiplet. 2D NMR experiments were also used to fully assign the proton and carbon environments in the products. ^{1}H-^{1}H Correlation Spectroscopy (COSY) demonstrated proton-proton correlations

over two or three bonds. ^{1}H-^{13}C Heteronuclear Shift Correlation Spectroscopy (HSQC) showed the correlation between directly bonded proton and carbon atoms. ^{1}H-^{13}C Heteronuclear Multiple-bond Correlation (HMBC) NMR demonstrated the correlation between proton and carbon atoms through several bonds.

Solid state ^{13}C Nuclear Magnetic Resonance (SSNMR) spectra were recorded at 100.56 MHz using a Varian VNMRS spectrometer and a 4 mm (rotor o.d.) magic-angle spinning probe. They were obtained using cross-polarisation with a 1 s recycle delay, 1 ms contact time, at ambient probe temperature (~25 °C) and at a sample spin-rate of 8 kHz. 1200 repetitions were accumulated. Spectral referencing was with respect to an external sample of neat tetramethylsilane (carried out by setting the high-frequency signal from adamantane to 38.5 ppm). The direct excitation spectra were recorded at 100.56 MHz using a Varian VNMRS spectrometer and a 4 mm (rotor o.d.) magic-angle spinning probe with a relaxation time of 1 s. 1100 repetitions were accumulated.

SEC analysis was conducted using a Viskotek TDA 302 with 2 x 300 mL PLgel 5µm mixed C columns with THF or DMF eluent with a flow rate of 1 ml mg^{-1} at 35°C and 1 ml mg^{-1} at 70°C, respectively. The detectors were calibrated using narrow molecular weight distribution linear polystyrene or polyethylene oxide as standard. A conventional calculation was used to determine molecular weight.

Fourier Transform-infra-red (FTIR) spectroscopy was conducted using a Perkin Elmer 1600 series spectrometer. MALDI results were collected on the Autoflex II ToF/ToF mass spectrometer (Brucker Daltonik GmBH) with reflection enhanced mass resolution.

Differential scanning calorimetry (DSC) was carried out using a TA instrument Q1000 DSC, in N_2 gas, with a flow rate of 30 mL min^{-1} and heating rate of 10 °C min^{-1}. The second heating run was analysed. Thermogravimetric analysis (TGA) was carried out using a Perkin Elmer Pyris 1 TGA connected to a HIDEN HPR20 MS, in N_2 gas, with a heating rate of 10 °C min^{-1}.

4.2.3 Synthesis of Poly(1-(2-(oxiran-2-ylmethoxy) ethyl) pyrrolidin-2-one-*co*-ethylene oxide), (9)

Benzyl alcohol (0.03 mL) was washed aezotropically with benzene twice before THF (15 mL) was added and the solution was dried by three freeze-pump-thaw cycles. Potassium naphthalenide was titrated in until green colour persisted (1.5 mL). Ethylene oxide (0.26 g, 5.40 mmol) was dried over CaH_2 and distilled into the reaction flask. 1-(2-(oxiran-2-ylmethoxy) ethyl) pyrrolidone (monomer **1**) (1 g, 5.40 mmol) was dried aezotropically with benzene then added *via* gastight syringe to the reaction flask. The reaction was stirred at 45 °C for 24 h before it was terminated with methanol (1 mL). The mixture was added dropwise into hexane in order to recover the polymer, however, no precipitate was formed.

4.2.3.1 Synthesis of Poly(ethylene oxide)

Benzyl alcohol (0.06 mL, 0.51 mmol) was washed aezotropically with benzene twice before THF (15 mL) was added and the solution was dried by three freeze-pump-thaw cycles. Potassium naphthalenide was titrated in until green colour persisted (2.65 mL). EO (5.20 g, 0.12 mmol) was dried over CaH_2 and distilled into the reaction flask. The reaction was stirred at 45 °C for 24 h before it was terminated with methanol (1 mL). The mixture was precipitated into hexane and the polymer precipitate was isolated by filtration (2.24g, 43 wt%). ^{1}H NMR (400 MHz, $CDCl_3$) δ = 3.63 (s,C**H$_2$** polymer backbone), 4.56 (2H,C**H$_2$** benzyl), 7.26 (2H, **Ph**, overlapping with $CDCl_3$ solvent resonance), 7.33 (3H, **Ph**) ppm. ^{13}C (176 MHz, $CDCl_3$) δ = 70.5 (**C**H$_2$ polymer backbone), 73.2 (**C**H$_2$ benzyl), 127.6 (**C**H, Ph), 127.7 (**C**H, Ph), 128.3 (**C**H, Ph) ppm. FTIR ν (cm^{-1}) = 2890, 2871 (CH_2 stretching), 1096 (C-O stretching). DSC, T_m = 56 °C, T_c = 36 °C. TGA Onset X = 391 °C SEC = M_n = 3.5x10^3 gmol^{-1}, Đ = 1.1. Molecular weight calculated by NMR analysis = 2.4x10^3 gmol^{-1}.

4.2.4 Synthesis of Poly(1-(2-(oxiran-2-ylmethoxy) ethyl) pyrrolidin-2-one-*co*-succinic anhydride), (10)

Al(O^{i}Pr) (0.09 g, 0.44 mmol) was distilled into the solvent flask which was then charged with toluene (45 mL) to make a stock solution of 2 mgmL^{-1}. The reaction flask was evacuated and backfilled three times prior to the reaction. Succinic anhydride (0.144 g, 1.35 mmol) and monomer **1** (0.253 g, 1.35 mmol) were charged to the reaction flask before the Al(O^{i}Pr) stock

solution (0.5 mL, 1 mg, 0.005 mmol) was added. The reaction was stirred at 120 °C for 12 h. After 1 h, a colour change from yellow/orange to dark brown was noted. After 12 h the reaction had ceased stirring due to increased viscosity. The product was diluted with chloroform and precipitated into hexane twice. The resulting solid, **10**, was dried under vacuum (0.363 g, 91 % mass yield). ^{1}H NMR (400 MHz, $CDCl_3$) δ = 1.90 (bm, 2H, $NCH_2C\mathbf{H_2}CH_2CO$), 2.27 ($NCH_2CH_2C\mathbf{H_2}CO$), 2.51 (bm, 4H, $COC\mathbf{H_2}C\mathbf{H_2}CO$, polymer backbone), 3.35 (bm, 4H, $NCH_2C\mathbf{H_2}CH_2CO$, $C\mathbf{H_2}CH_2O$), 3.46 (bm, 4H, $CH_2C\mathbf{H_2}O$, $OC\mathbf{H_2}CH$ pendant group), 4.05 (bm, 1H, $COOC\mathbf{H_2}CH$), 4.16 (bm, 1H, $COOC\mathbf{H_2}CH$) 5.04 (bm, 1H, $COOCH_2C\mathbf{H}$). ^{13}C (176 MHz, $CDCl_3$) δ = 18.2 ($NCH_2\mathbf{C}H_2CH_2CO$), 29.1 ($CO\mathbf{C}H_2\mathbf{C}H_2CO$, polymer backbone), 31.0 ($NCH_2CH_2\mathbf{C}H_2CO$), 42.5 ($\mathbf{C}H_2\mathbf{C}H_2O$), 48.8 ($N\mathbf{C}H_2CH_2CH_2CO$), 63.0 ($COO\mathbf{C}H_2CH$), 69.0 ($O\mathbf{C}H_2CH$ pendant group), 70.6 ($COOCH_2\mathbf{C}H$), 172.0 (C=O polymer backbone), 175.8 (C=O lactam). FTIR ν (cm^{-1}) = 2850 to 2981 (CH_2 stretching), 1732 (backbone), 1678 cm^{-1} (lactam). DSC, T_g = −35.56 °C. TGA Onset = 350.98 °C. SEC, total M_n = 570 $gmol^{-1}$, Đ = 1.21, M_p (lower peak) = 172 $gmol^{-1}$, M_p (higher peak) = 650 $gmol^{-1}$. MALDI DHB matrix $[M + H]^+$ = 874.5, 974.5, 1159.7, 1259.7, 1444.8, 1544.9, 1730.0, 1830.0, 2016.1, 2116.1, 2301.0, 2400.8 $gmol^{-1}$. MALDI CHCA matrix $[M + Na]^+$ = 797.6, 896.5, 996.5, 1081.6, 1181.6, 1281.6, 1466.7, 1566.7, 1751.8, 1851.8, 2037.9, 2138.0, 2323.2, 2423.2, 2609.2, 2709.2, 2893.9, 2993.9 $gmol^{-1}$.

4.2.5 Synthesis of Poly(4-vinylbenzyloxy ethyl pyrrolidone-*co*-styrene), (11)

AIBN (2 mg, 0.01 mmol) was charged to a schlenk reaction flask and the flask was degassed and backfilled with N_2 three times. 4-vinylbenzyloxy ethyl pyrrolidone (**2**) (0.302 g, 1.22 mmol) and styrene (0.129 g, 1.22 mmol) were added simultaneously and the reaction was heated to 70 °C and stirred for 1 h, after which the reaction has ceased stirring due to the formation of solid. The reaction was cooled to below 0 °C and exposed to air to terminate the reaction. The reaction was warmed to room temperature, the solid recovered was translucent and yellow in colour (0.362 g, mass yield 84%). The translucent gummy solid was extracted in DCM at 40 °C for 4 h and 0.085 g (24%) of insoluble solid (**11**) was recovered along with 0.227 g of liquid monomers (76%). ^{13}C SSNMR cross polarisation δ = 174.6 ($NCH_2CH_2CH_2\mathbf{C}O$), 145.3 (aromatic **C**H), 136.6 (aromatic **C**H), 128.1 (aromatic **C**H), 72.5

(Ph**C**H_2O), 68.7 (O**C**H_2CH_2), 47.2 (N**C**$H_2CH_2CH_2CO$), 40.3 (OCH_2**C**H_2), 31.0 (NCH_2CH_2**C**H_2CO), 18.6 (NCH_2**C**H_2CH_2CO) ppm. ^{13}C SSNMR direct excitation δ = 174.4 ($NCH_2CH_2CH_2$**C**O), 127.4 (aromatic **C**H), 72.7 (Ph**C**H_2O), 67.9 (O**C**H_2CH_2), 48.1 (N**C**$H_2CH_2CH_2CO$), 42.7 (OCH_2**C**H_2), 31.3 (NCH_2H_2**C**H_2CO), 18.7 (NCH_2**C**H_2CH_2CO). FTIR ν (cm^{-1}) = 2928, 2857 (br, aromatic CH, CH_2), 1679 (C=O lactam). TGA, Onset X_1 = 438.24 °C, Onset X_2 = 559.87 °C, ΔY_1 = 93.325%, ΔY_2 = 22.319%.

4.2.6 Synthesis of Poly(4-vinylbenzyloxy ethyl pyrrolidone-*co*-vinyl pyrrolidone), (12)

AIBN (2 mg, 0.01 mmol) was charged to a schlenk reaction flask and the flask was degassed and backfilled with N_2 three times. 4-vinylbenzyloxy ethyl pyrrolidone (**2**) (0.299 g, 1.22 mmol) and N-vinyl pyrrolidone (0.136 g, 1.22 mmol) were added simultaneously and the reaction was heated to 70 °C and stirred for 1 h, after which the reaction has ceased stirring due to the formation of solid. The reaction was cooled to below 0 °C and exposed to air to terminate the reaction. The reaction was warmed to room temperature, the solid recovered was translucent and yellow in colour (0.413 g, mass yield 95%). The translucent gummy solid was extracted in DCM at 40 °C for 4 h and 0.091 g (22%) of insoluble solid (**12**) was recovered along with 0.322 g of liquid monomers (78%). ^{13}C SSNMR cross polarisation δ = 175.1 ($NCH_2CH_2CH_2$**C**O), 145.4 (aromatic **C**H), 136.8 (aromatic **C**H), 128.2 (aromatic **C**H), 72.5 (Ph**C**H_2O), 68.2 (O**C**H_2CH_2), 47.9 to 40.4 (br, N**C**$H_2CH_2CH_2CO$, OCH_2**C**H_2), 31.6 (NCH_2CH_2**C**H_2CO), 18.7 (NCH_2**C**H_2CH_2CO) ppm. ^{13}C SSNMR direct excitation δ = 175.6 ($NCH_2CH_2CH_2$**C**O), 129.0 (aromatic **C**H), 73.0 (Ph**C**H_2O), 68.7 (O**C**H_2CH_2), 48.3 (N**C**$H_2CH_2CH_2CO$), 42.9 (OCH_2**C**H_2), 31.5 (NCH_2H_2**C**H_2CO), 18.7 (NCH_2**C**H_2CH_2CO). FTIR ν (cm^{-1}) = 2921, 2853 (br, aromatic CH, CH_2), 1672 (C=O lactam). TGA, Onset X_1 = 432.48 °C, Onset X_2 = 519.64 °C, ΔY_1 = 92.211%, ΔY_2 = 16.249%.

4.2.7 Synthesis of Poly(4-vinylbenzyloxy ethyl pyrrolidone-*co*-hydroxyethly acxrylate), (13)

AIBN (2 mg, 0.01 mmol) was charged to a schlenk reaction flask and the flask was degassed and backfilled with N_2 three times. 4-vinylbenzyloxy ethyl pyrrolidone (**2**) (0.303 g, 1.22 mmol) and hydroxyethly acxrylate (0.142 g, 1.22 mmol) were added simultaneously and the reaction was heated to 70 °C and stirred for 1 h, after which the reaction has ceased stirring due to the formation of solid. The reaction was cooled to below 0 °C and exposed to air to terminate the reaction. The reaction was warmed to room temperature, the solid recovered was translucent and yellow in colour (0.413 g, mass yield 93%). The translucent gummy solid was extracted in DCM at 40 °C for 4 h and 0.332 g (75%) of insoluble solid (**13**) was recovered along with 0.113 g of liquid monomers (25%). ^{13}C SSNMR cross polarisation δ = 176.3 ($NCH_2CH_2CH_2\mathbf{C}O$, $\mathbf{C}OO$), 144.5 (aromatic **C**H), 137.0 (aromatic **C**H), 128.8 (aromatic **C**H), 72.7 ($Ph\mathbf{C}H_2O$), 66.6 ($O\mathbf{C}H_2CH_2$, $\mathbf{C}H_2CH_2OH$), 60.5 ($CH_2\mathbf{C}H_2OH$), 47.9 ($N\mathbf{C}H_2CH_2CH_2CO$), 41.5 ($OCH_2\mathbf{C}H_2$), 32.3 ($NCH_2CH_2\mathbf{C}H_2CO$), 18.8 ($NCH_2\mathbf{C}H_2CH_2CO$) ppm. ^{13}C SSNMR direct excitation δ = 177.0 ($NCH_2CH_2CH_2\mathbf{C}O$, $\mathbf{C}OO$), 129.7 (aromatic **C**H), 73.0 ($Ph\mathbf{C}H_2O$), 66.8 ($O\mathbf{C}H_2CH_2$, $\mathbf{C}H_2CH_2OH$), 60.5 ($CH_2\mathbf{C}H_2OH$), 48.8 ($N\mathbf{C}H_2CH_2CH_2CO$), 43.1 ($OCH_2\mathbf{C}H_2$), 31.4 ($NCH_2CH_2\mathbf{C}H_2CO$), 18.6 ($NCH_2\mathbf{C}H_2CH_2CO$) ppm. FTIR ν (cm^{-1}) = 3390 (br OH), 2925, 2865 (br, aromatic CH, CH_2), 1725 (C=O), 1661 (C=O lactam). TGA, Onset X_1 = 397.52 °C, Onset X_2 = 474.67 °C, ΔY_1 = 89.881%, ΔY_2 = 26.852%.

4.2.8 Synthesis of Poly(5-ethacryloxyethyl-12-ethylpyrrolidyl -N,N'hexane biscarbamate-*co*-vinyl pyrrolidone (14)

A mixture of 5-ethacryloxyethyl-12-ethylpyrrolidyl-N,N'hexane biscarbamate (**3**) (0.510 g, 1.22 mmol) and *N*-vinyl pyrrolidone (0.142 g, 1.22 mmol) was degassed by three freeze-pump-thaw cycles. A solution of AIBN (2.4 mg, 0.01 mmol) in DMF (1 mL) was degassed by three freeze-pump-thaw cycles before the initiating solution was added to the reaction flask. The reaction was stirred for 4 h at 70 °C. The reaction was cooled to room temperature, the polymer isolated by precipitation into ether and dried under reduced pressure to afford an off-white brittle solid (**14**) (0.472, mass yield 72%). ^{1}H NMR (400 MHz, *d*-DMF) δ = 7.12 (br, N**H**), 4.24 (br, $OC\mathbf{H_2}C\mathbf{H_2}O$), 4.13 (br, $OC\mathbf{H_2}CH_2N$), 3.47 (br, $OCH_2C\mathbf{H_2}N$, $NCH_2CH_2C\mathbf{H_2}CO$), 3.29

(br, NC**H$_2$**CH$_2$CH$_2$CO), 3.11 (br, NHC**H$_2$**CH$_2$CH$_2$CH$_2$CH$_2$C**H$_2$**NH), 2.26 (br, NC**H$_2$**CH$_2$CH$_2$CO), 1.99 (br, NCH$_2$C**H$_2$**CH$_2$CO), 1.50 (br, NHC**H$_2$**CH$_2$CH$_2$CH$_2$C**H$_2$**CH$_2$NH), 1.35 (br, NHC**H$_2$**CH$_2$CH$_2$CH$_2$C**H$_2$**CH$_2$NH). ^{13}C (176 MHz, *d*-DMF) δ = 176.1 (br, NCH$_2$CH$_2$CH$_2$**C**O), 175.3 (NCH$_2$CH$_2$CH$_2$**C**O), 157.4 (NH**C**OOCH$_2$CH$_2$N), 63.8 and 62.9 (br, O**C**H$_2$**C**H$_2$O), 62.5 (O**C**H$_2$CH$_2$N), 48.4 (N**C**H$_2$CH$_2$CH$_2$CO), 42.9 (OCH$_2$**C**H$_2$N), 41.7 (NH**C**H$_2$CH$_2$CH$_2$CH$_2$CH$_2$**C**H$_2$NH), 32.2 (br, NCH$_2$CH$_2$**C**H$_2$CO), 31.5 (NCH$_2$CH$_2$**C**H$_2$CO), 30.6 (NHCH$_2$**C**H$_2$CH$_2$CH$_2$**C**H$_2$CH$_2$NH, overlapping with solvent), 27.4 (NHCH$_2$CH$_2$**C**H$_2$**C**H$_2$CH$_2$CH$_2$NH), 19.3 (br, NCH$_2$**C**H$_2$CH$_2$CO), 19.0 (NCH$_2$**C**H$_2$CH$_2$CO). DSC, T_g = 8.54 °C. TGA, Onset X_1 = 260 °C, Onset X_2 = 342 °C, X_3 = 428 °C, Onset, ΔY_1 = 30%, ΔY_2 = 7%, ΔY_3 = 34%. SEC (DMF), M_n = 4.2x10^5 gmol^{-1}, Đ = 3.54. FTIR ν (cm^{-1}) = 3319 (br, COONH) 2937 and 2864 (CH$_2$), 1717 (C=O), 1666 (br, C=O).

4.3 Results & Discussion

4.3.1 Poly(1-(2-(oxiran-2-ylmethoxy) ethyl) pyrrolidin-2-one-*co*-ethylene oxide), (9)

C. Hawker *et. al.* (2012) synthesised a range of copolymers based on ethylene oxide (EO) and substituted epoxide monomers.[23] They utilised an alkoxide initiating system of benzyl alcohol and potassium naphthalenide to produce random copolymers of ethylene oxide with allylglycidyl ether (AGE) or ethylene glycol vinyl ether (EVEGE) (Figure 4.2). Their method produced copolymers with low Đ and with a reasonable degree of polymerisation.[1] The initiating system and experimental procedure described in the publication was employed here in the copolymerisation of EO and 1-(2-(oxiran-2-ylmethoxy) ethyl) pyrrolidin-2-one or glycidyl ethylpyrrolidone (GEP) (**1**) with the aim of producing a novel PEG based copolymer.

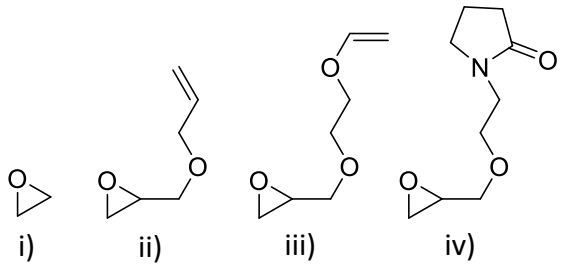

Figure 4.2 – Structure of i) ethylene oxide ii) allyl glycidyl ether iii) ethylene glycol vinyl glycidyl ether and iv) monomer 1

A benzyl alcohol/potassium naphthalenide initiating system was employed to copolymerise GEP (**2**) with EO (Scheme 4.1). The initiating system generated an alkoxide in situ which would then react with the monomers to produce a copolymer. All reactants were aezatropically dried prior to use to ensure dry reaction conditions. After the reaction was stirred at 45 °C for 24 h, the mixture was precipitated into hexane in order to recover the polymer, however, no precipitate was formed. The excess solvent was removed and the resulting viscous yellow liquid (0.96 g, 77% mass yield) was analysed by ^{1}H and ^{13}C NMR.

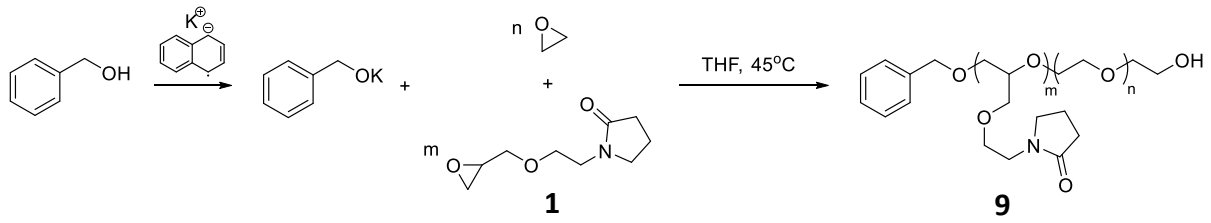

Scheme 4.1 – Synthesis of polymer 9

The benzyl alcohol/potassium naphthalenide initiating system did not produce copolymer **9**. ^{1}H NMR analysis showed that only GEP (**2**) was recovered from the reaction (0.96g recovered = 96% molar yield of GEP (**2**), ethylene oxide was not recovered as it is a gas at room temperature. It is interesting to note that the epoxide functional group is still intact and unreacted. A reason for the lack of reaction could be the potassium naphthalenide solution. The green colouring observed upon titration of the potassium naphthalenide disappeared after 2 h. A hypothesis for this is a deactivation of the initiating system due to the presence of residual oxygen or other impurities which were not removed during the azeotropic drying of GEP (**2**).

A homopolymerisation of EO was conducted to determine if the potassium naphthalenide was the cause of the failed reaction. The homopolymerisation of EO produced polyethylene glycol (PEG) in a 43 weight% yield. The polymer was confirmed by ^{1}H and ^{13}C NMR, SEC, TGA, DSC, MALDI and FTIR. The ^{1}H NMR spectrum (Figure 4.3) shows the large polymer backbone signals at δ = 3.63 ppm with end group peaks at δ = 4.56, 7.26 and 7.33 ppm for the CH_2 and two environments for the CH (Ph).

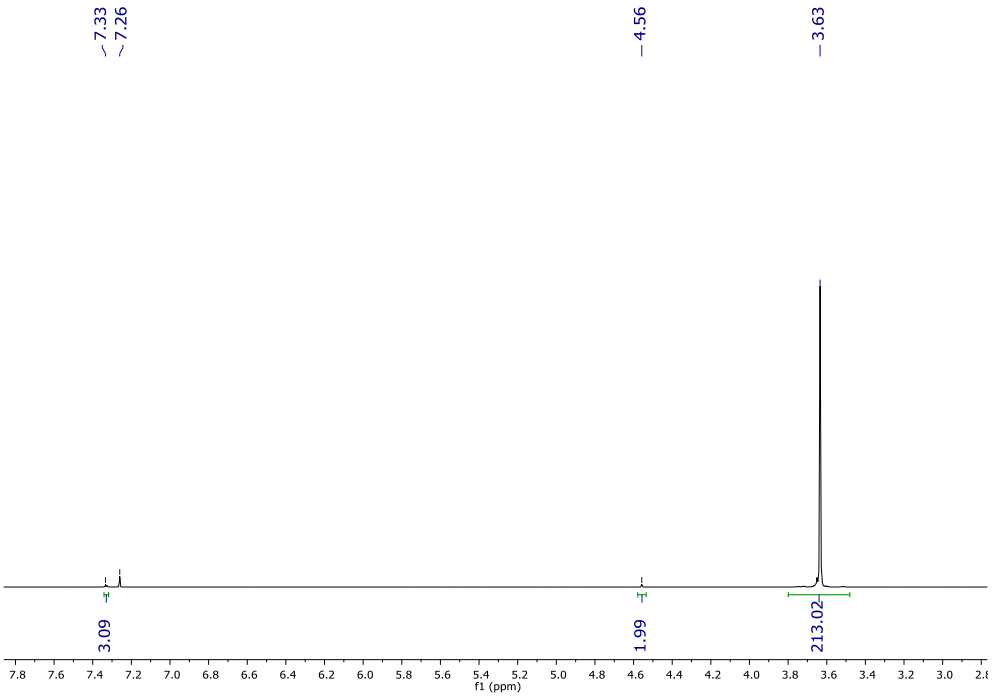

Figure 4.3 – ^{1}H NMR spectrum of PEG

The SEC (Figure 4.4 i)) shows a monomodal distribution with a M_n = 3.5x10^3 gmol^{-1} and Đ = 1.08. The DSC showed a T_m = 56 °C and a T_c = 36 °C and, the TGA (Figure 4.4 ii)) showed an onset of 391 °C, this is consistent with the literature.[24] End group analysis allows an estimation of molecular weight based on integrals corresponding to environments in the backbone and end-groups, obtained from the ^{1}H NMR spectrum. The average value for one proton in the PEG backbone (213.02 ÷ 4 = 53.255) was divided by the average integration for one proton of the end group ((3.09 + 1.99) ÷ 5 = 1.016) to give the number of repeat units (53.255 ÷ 1.016 = 52.416), 52. The molecular weight for a polymer containing 52 repeat units and the benzyl end group was determined to be 2.4x10^3 gmol^{-1}. FTIR analysis confirms the presence of CH_2 with a bands observed at 2890 and 2871 cm^{-1} as well as C-O groups at 1096 cm^{-1}.

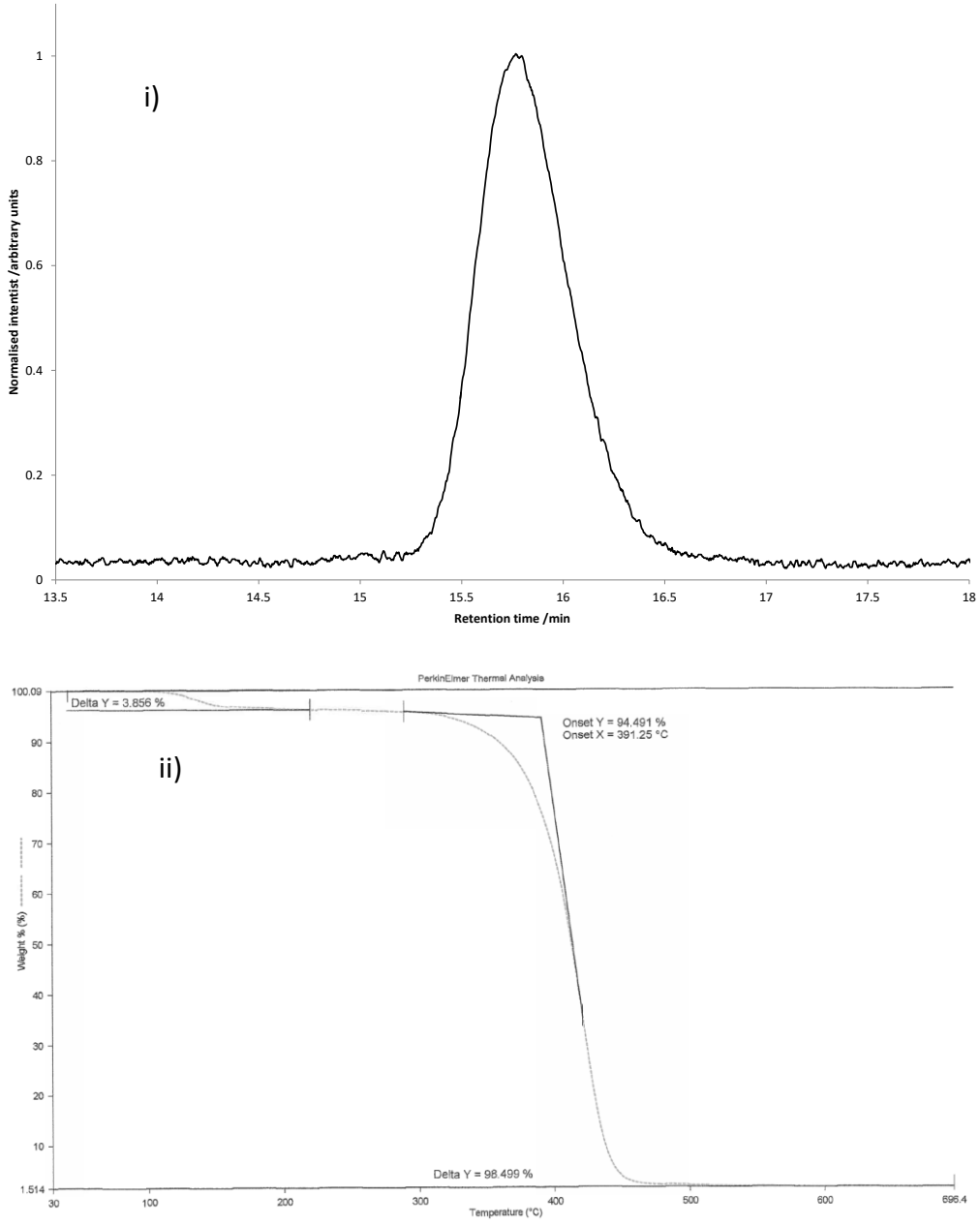

Figure 4.4 – Characterisation of polyethylene glycol i) SEC chromatogram and ii) TGA thermogram

The initiating system was successful in the production of PEG. The monomodal distribution and low dispersity indicates a controlled polymerisation with low levels of termination or chain transfer. This suggests that the problem is with the addition of GEP (**1**). It is interesting to note that the presence of GEP (**2**) also inhibited the homopolymerisation of EO. Hawker *et. al.*[23] conducted density functional theory (DFT) analysis and showed the transition state barrier to be lower for an AGE and EGVGE than for EO for the first monomer addition [and second monomer for AGE]. The reasoning for this observation is the increased

electron donation of the epoxide ring due to the electron rich allyl ether moiety and increasing coordination from the additional heteroatom(s) within the system (the chemical structures of AGE, EVEGE and GEP (**1**) are shown in Figure 4.2). Following the trend, with an increasing number of heteroatoms present (EO<AGE<EVEGE<GEP (**1**)) it could be expected that GEP (**1**) would have a lower transition state energy barrier than EO, AGE and EVEGE, and therefore would be easily synthesised. However, the additional nitrogen does not overcome the reduction in the electron donation of the substituent group. Due to the resonance associated with amide bonds (Ch. 2, Scheme 2.5), the pyrrolidone group is not electron donating like the allyl ether moiety. This is one explanation for the lack of reactivity of GEP (**1**) under these reaction conditions.

In summary, the copolymerisation of GEP (**1**) and EO with benzyl alcohol/potassium naphthalenide initiating system was unsuccessful. No polymer product was isolated however, the initiating system was successful for the homopolymerisation of EO. Due to the inherent difficulty working with EO and time constraints, further investigations into the unsuccessful reaction were minimal. Further work regarding GEP (**1**) focused on the post-polymerisation functionalisation of various polymers *via* end capping is discussed in Chapter 5.

4.3.2 Poly(1-(2-(oxiran-2-ylmethoxy) ethyl) pyrrolidin-2-one-*co*-succinic anhydride), (10)

Feng *et. al.* (2009, 2011 and 2014) reported the alternating copolymerisation of succinic anhydride (SA) with a functionalised epoxide.[25–27] Polymers of modest molecular weight (M_w up to $5x10^3$ $gmol^{-1}$) were produced, with reasonable dispersity (Đ) (<1.6) values. The polymers were shown to exhibit thermoresponsive behaviour with lower critical solution temperature (LCST) values ranging from 17.8 to 73.3 °C depending on the length of the ethylene glycol pendant chain. The polyester chains were shown to be biodegradable in a range of phosphate buffer solutions with varying pH values (5.9, 7.4 and 8.4). The greatest decrease in molecular weight was observed at pH=8.4. The postulation for this effect was that the basic buffer could facilitate the acidic degradation of the ester bonds by

neutralisation. The aim of this synthesis was to produce a novel pyrrolidone based polyester that would be capable of degradation.

The aluminium isopropoxide initiating system has been shown to produce alternating copolymers of SA and (functionalised) epoxides.[25–27] The mechanism proceeds *via* the addition-insertion pathway that begins with the coordination of the SA monomer (Scheme 4.2).[27] The alternating nature should facilitate degradation as the ester bonds will be spaced along the polymer backbone, leading to more complete degradation than with block copolymers.

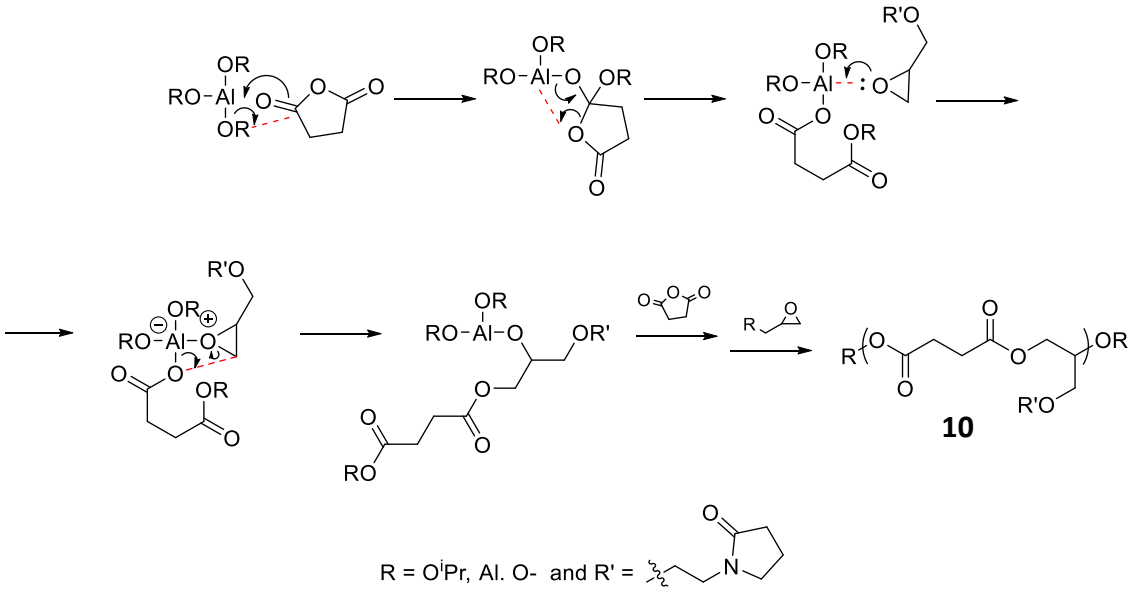

Scheme 4.2 – Addition-insertion mechanism of aluminium for synthesis of polymer 10

The aluminium isopropoxide was stirred to allow the formation of active species. The active catalyst was injected into a 50:50 ratio of the SA:GEP (**1**). The reaction was conducted at 120 °C for 18 h before the polymer was recovered and analysed. The mass yield of the reaction was 91 %, a small loss may be due to the low molecular weight fraction being soluble in the non-solvent used for polymer recovery. It is well documented that solubility behaviour is dependent on the molecular weight of the polymer and not an intrinsic property.[28] The resulting polymer was soluble in water which supports the incorporation of the pyrrolidone group into the product. Homopolymerisation of SA and GEP (**1**) under the same reaction conditions produced no polymer in either case.

The ^{1}H NMR spectrum (Figure 4.5) shows the disappearance of characteristic epoxide peaks for the CH and CH_2 of the three-membered ring at δ = 2.61 – 3.15 ppm indicating that all the epoxide has been consumed. The broad resonances at δ = 2.01 and 2.38 ppm correspond to two proton environments in the pyrolidine pendant group **a** and **b**, respectively. In the ^{1}H-^{1}H COSY NMR spectrum (Figure 4.6), the two environments couple to a resonance in the multiplet at δ = 3.40 – 3.64 ppm are assigned to proton **c**. The multiplet also contains resonances which are attributed to protons **d**, **e** and **f**. At δ = 2.51 ppm there are overlapping resonances corresponding to DMSO and proton environments **i** and **j**. Because of the overlapping nature of these resonances it is not possible to integrate between the two monomer units within the polymer and hence establishing the copolymer composition.

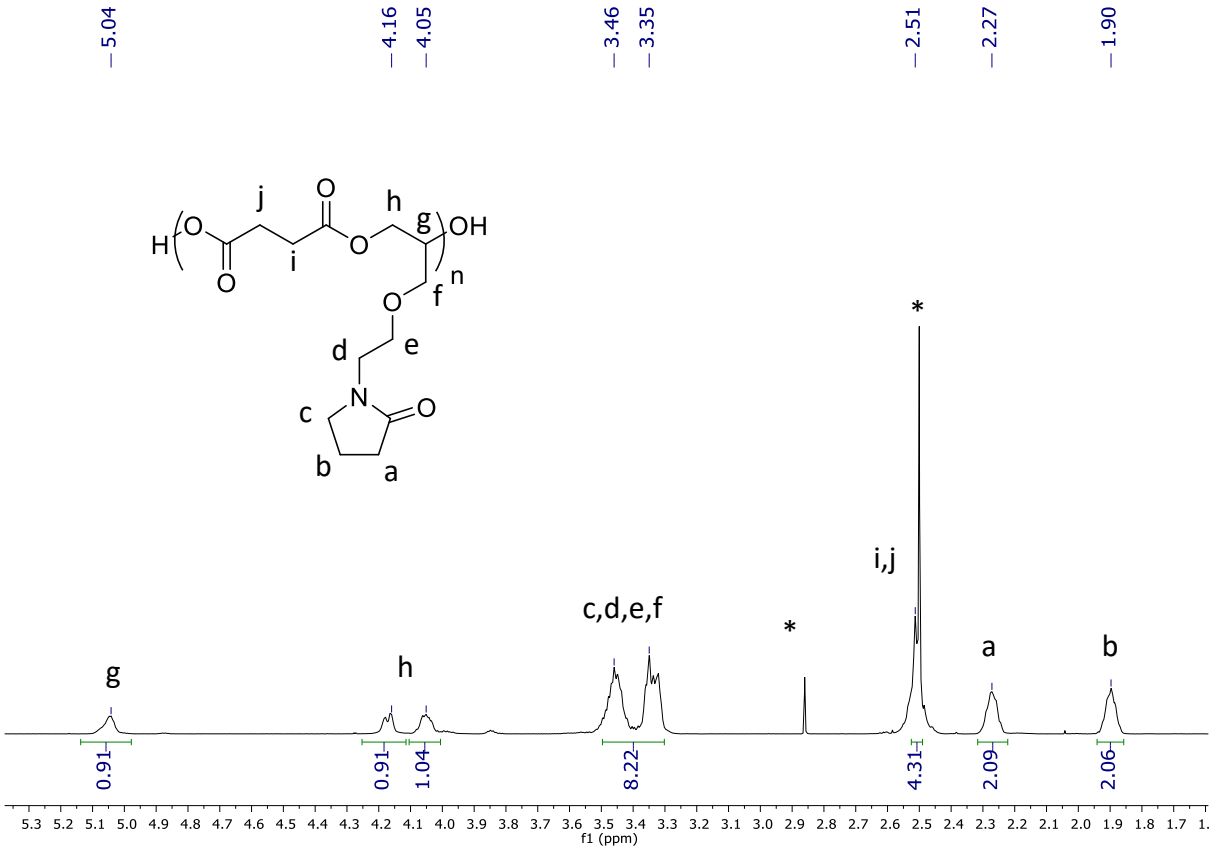

Figure 4.5 – ^{1}H NMR spectrum of polymer 10

The resonance at δ = 5.16 ppm correlates to a broad multiplet at δ = 4.16-4.28 ppm in the ^{1}H-^{1}H COSY NMR spectrum (Figure 4.6). The downfield proton is attributed to proton **g** and the broad multiplet to **h** as seen in the literature.[26]

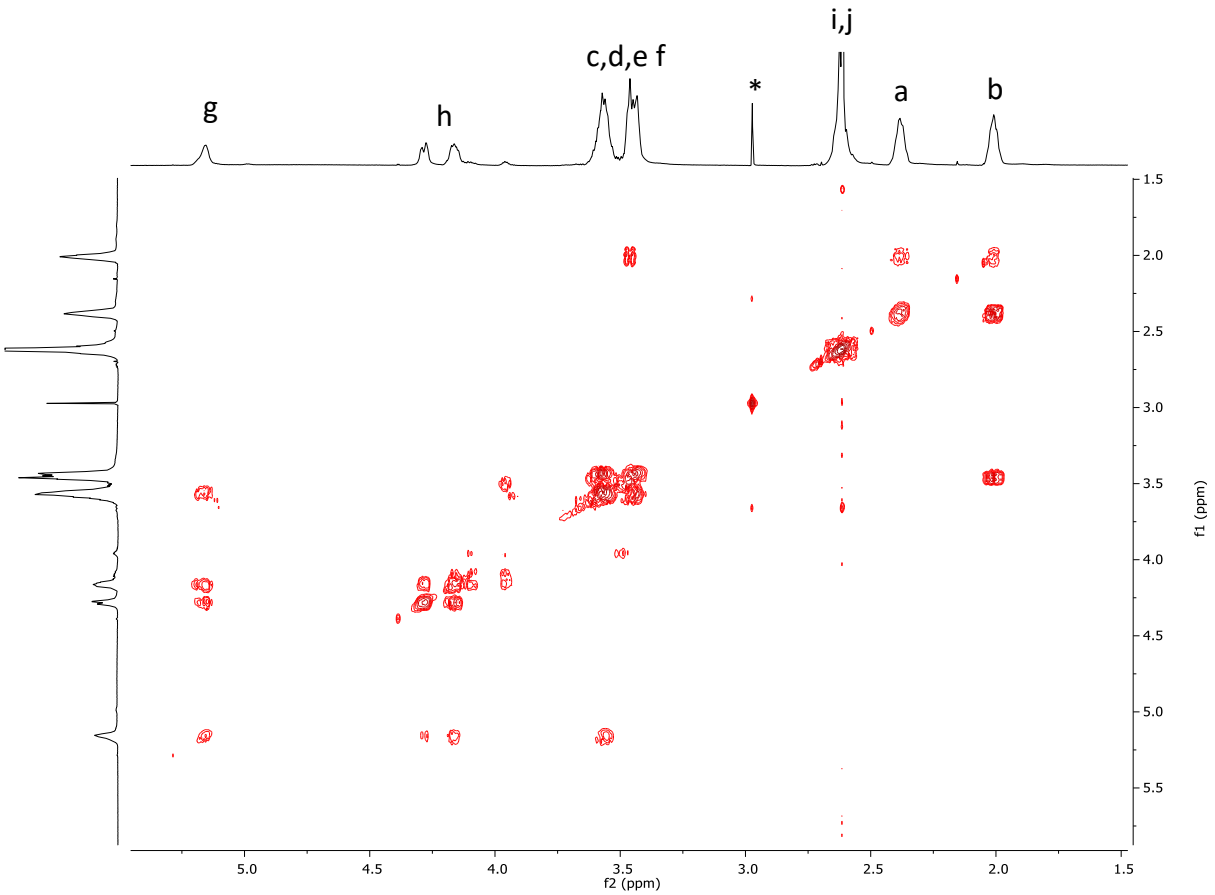

Figure 4.6 – ^{1}H-^{1}H COSY NMR spectrum of polymer 10

The ^{13}C NMR spectrum (Figure 4.7) shows both sharp and broad resonances. There are two broad resonances above δ = 170 ppm, these are attributed to the carbonyl environments in the polymer. The remaining 7 resonances are all below δ = 75 ppm, in order to full assign the ^{13}C NMR spectrum, the ^{1}H-^{13}C HSQC and ^{1}H-^{13}C HMBC must be analysed.

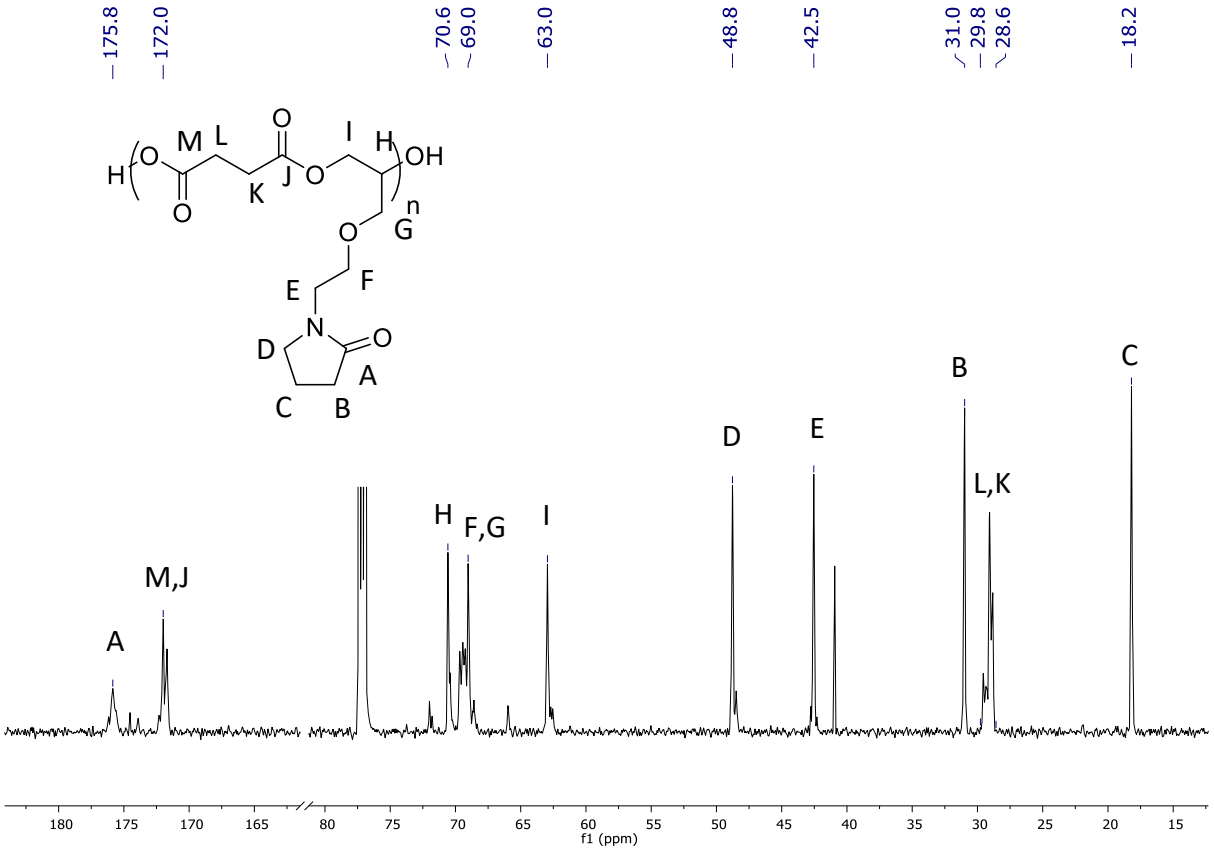

Figure 4.7 – ^{13}C NMR spectrum of polymer 10 with removed section (from δ = 80 – 165 ppm)

The ^{1}H-^{13}C HSQC NMR spectrum (Figure 4.8) allows for corroboration and clarification of the ^{1}H NMR analysis. The 2D NMR technique combines the correlation data with distortion-less enhancement by polarisation transfer (DEPT) information. In Figure 4.8, primary and tertiary environments are red and secondary environments are blue. It is clear that the resonance at δ = 5.16 ppm is due to the only CH group in the polymer, proton **g**. The carbon associated with proton **g** is observed at δ = 70.6 ppm, carbon **H**. The HSQC confirms that the protons for the broad multiplet at δ = 4.16-4.28 ppm which contains two distinct peaks, are attached to one carbon, **I** at δ = 63.0 ppm. Carbons **G** and **F** are observed in a multiplet at δ = 68.6 – 69.7 ppm. The broad multiplet at δ = 3.40 – 3.64 ppm in the ^{1}H NMR spectrum contains two separate resonances, each integrating to 4H. The downfield resonance at δ = 3.57 ppm corresponds to protons **e** and **f**. The upfield resonance at δ = 3.46 ppm is attributed to protons **c** and **d**. The resonances for carbons **D** and **E** are observed at δ = 48.8 and 42.5, respectively. The broad resonance at δ = 28.5 – 29.6 ppm is due to carbons **L** and **K**. Carbons **B** and **C** are observed at δ = 31.0 and 18.2 ppm, respectively.

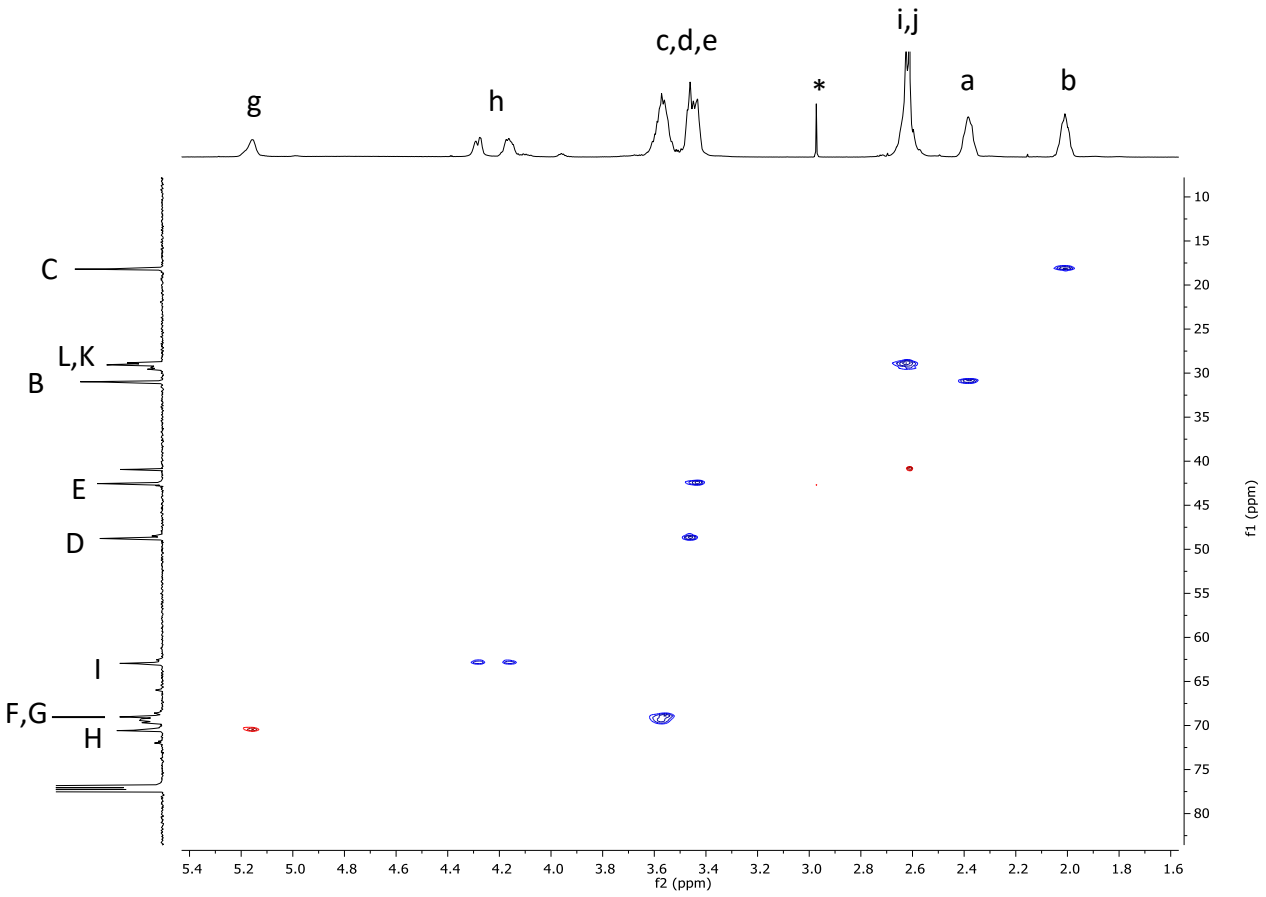

Figure 4.8 – ^{1}H-^{13}C HSQC NMR spectrum of polymer 10

Figure 4.9 shows the ^{1}H-^{13}C HMBC spectrum for polymer **10** and allows the characterisation of the carbonyl carbon environments. The multiplet resonance at δ = 171.3 – 172.4 ppm is attributed to carbonyls **M** and **J** as a correlation can be seen between protons **i**, **j**, **h** and **g**. The broad resonance at 175.7 ppm correlates to protons **c**, **b** and **a**, therefore must correspond to carbonyl **A**.

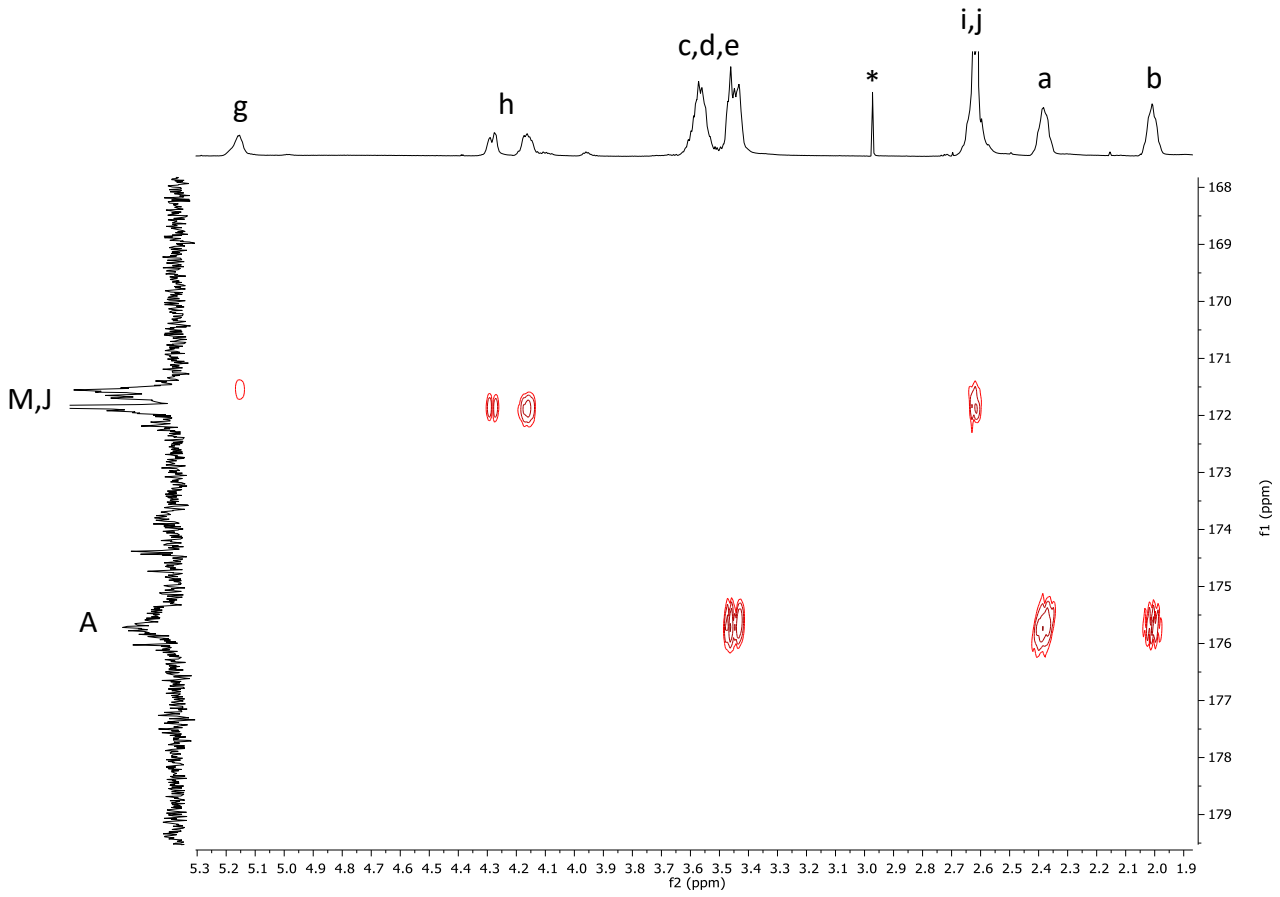

Figure 4.9 – ^{1}H-^{13}C HMBC NMR spectrum of polymer 10, expansion

It was not possible to calculate the molecular weight of the polymer by end group analysis as the OH end groups were not visible in the ^{1}H NMR spectrum.

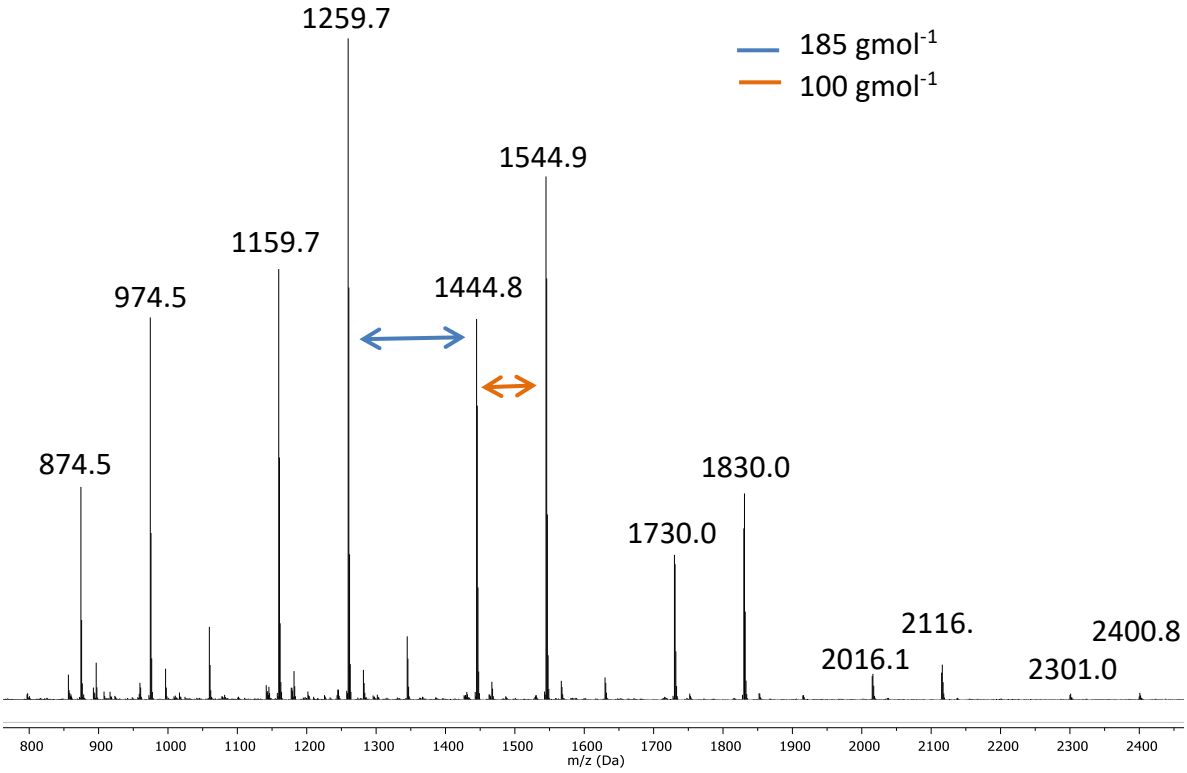

Figure 4.10 – MALDI MS of polymer 10 in DHB matrix

Table 4.1 shows the calculated molecular weights for oligomers containing between 3 – 8 units of GEP (**1**) and 3 – 9 units of SA. The molecular weights correspond to those found in the MALDI (Figure 4.10). The step-wise increase in molecular weight of the polymer suggests that the polymer is alternating. Signals are not observed for polymers containing large quantities of one monomer only.

Table 4.1 – Calculated molecular weight for $[M + H]^+$ for polymer 10

		Number of GEP (**2**) units					
		3	4	5	6	7	8
	3	874.5					
	4	974.6	1159.7				
	5		1259.8	1444.9			
	6			1544.9	1730.1		
	7				1830.1	2015.3	
	8					2115.3	2300.4
	9						2400.5

Figure 4.11 shows the MALDI mass spectrum of polymer **10** with the CHCA matrix where the end groups are both OH and the ions observed are $[M + Na]^+$. It is also possible to see the differences of 185 and 100 $gmol^{-1}$ between the signals corresponding to the pyrrolidone and SA units, respectively. There appears to be two progressions, one starting with an SA unit and the other with GEP (**1**), indicating that GEP has been successfully employed in this copolymerisation.

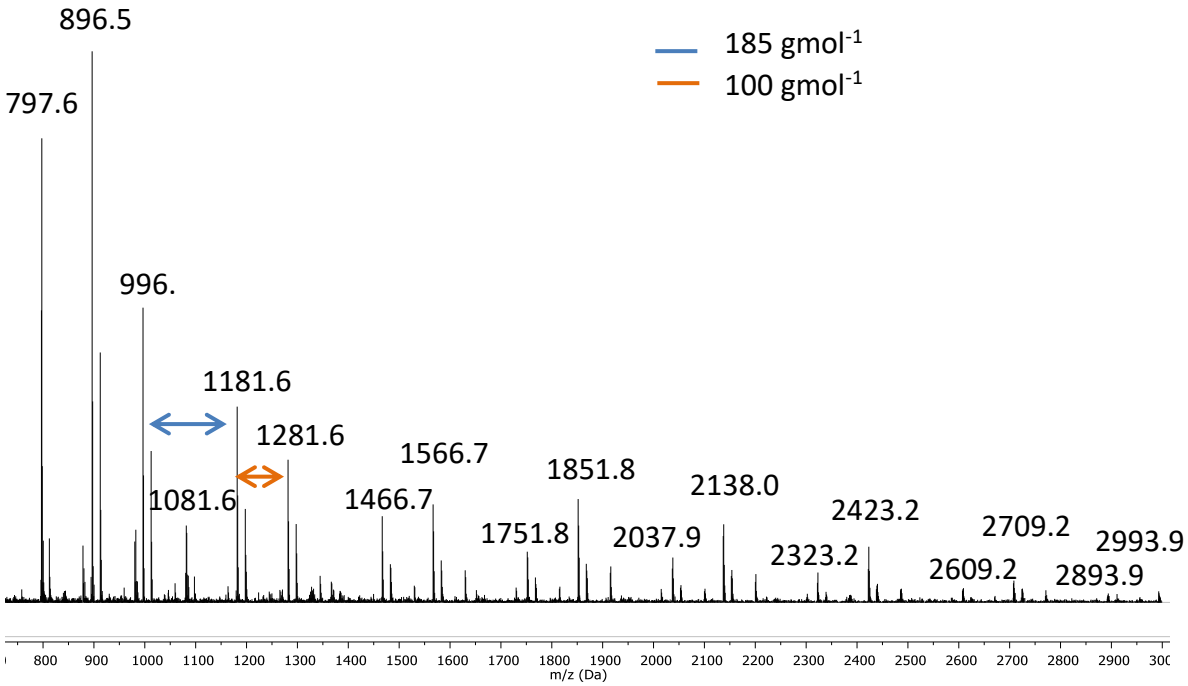

Figure 4.11 – MALDI MS of polymer 10 in CHCA matrix

The calculated values for the molecular weight of $[M + Na]^+$ for polymer **10** are shown in Table 4.2. The values show identified show telomeres containing between two and eleven units of SA units and three and ten GEP (**2**) units. The α-cyano-4-hydroxycinnamic acid (CHCA) matrix allows for larger molecular weight species to be identified when compared to the 2,5-dihydroxybenzoic acid (DHB) matrix. Both matrices show a stepwise trend of alternating addition of each monomer unit. It is interesting to note that the majority of polymer chains identified by MALDI analysis contain equal quantities of GEP:SA or one additional SA unit (compared to GEP), this suggests that mechanism primarily proceeds with the ring opening of SA first.

Table 4.2 – Calculated molecular weight for $[M + Na]^+$ for polymer 10

		Number of GEP (**2**) units							
		3	4	5	6	7	8	9	10
	2	796.5							
	3	896.5	1081.7						
	4	996.6	1181.7						
	5		1281.8	1466.9					
	6			1567.0	1752.1				
	7				1852.1	2037.3			
	8					2137.3	2322.4		
	9						2422.5	2607.6	
	10							2707.7	2892.8
	11								2992.9

The SEC trace (Figure 4.12) showed a bimodal distribution with M_n = 570 $gmol^{-1}$ and Đ = 1.21. The M_p for the low molecular weight peak was observed to be 172 $gmol^{-1}$ and the broad higher molecular weight peak at 650 $gmol^{-1}$. The calculations are based on a Polymethyl methacrylate (PMMA) standard calibration and the analysis was run in DMF solvent. Triple detector calculations were not possible as the sample did not produce a light scattering signal large enough to detect. 570 $gmol^{-1}$ is equal to an oligomer consisting of two GEP and two SA units respectively. However, as conventional SEC analysis provides molecular weight analysis relative to the polymer used for the calibration, the results obtained are imprecise. The peak at 172 $gmol^{-1}$ could be attributed to GEP monomer. As observed in the MALDI mass analysis the polymerisation produced a wide range of molecular weights, this pattern is also observed in the bimodal distribution of the SEC. It is also noted that the peaks are close to that of the solvent introducing more error with the difficulty in setting baseline limits. The SEC data supports the formation of small oligomers.

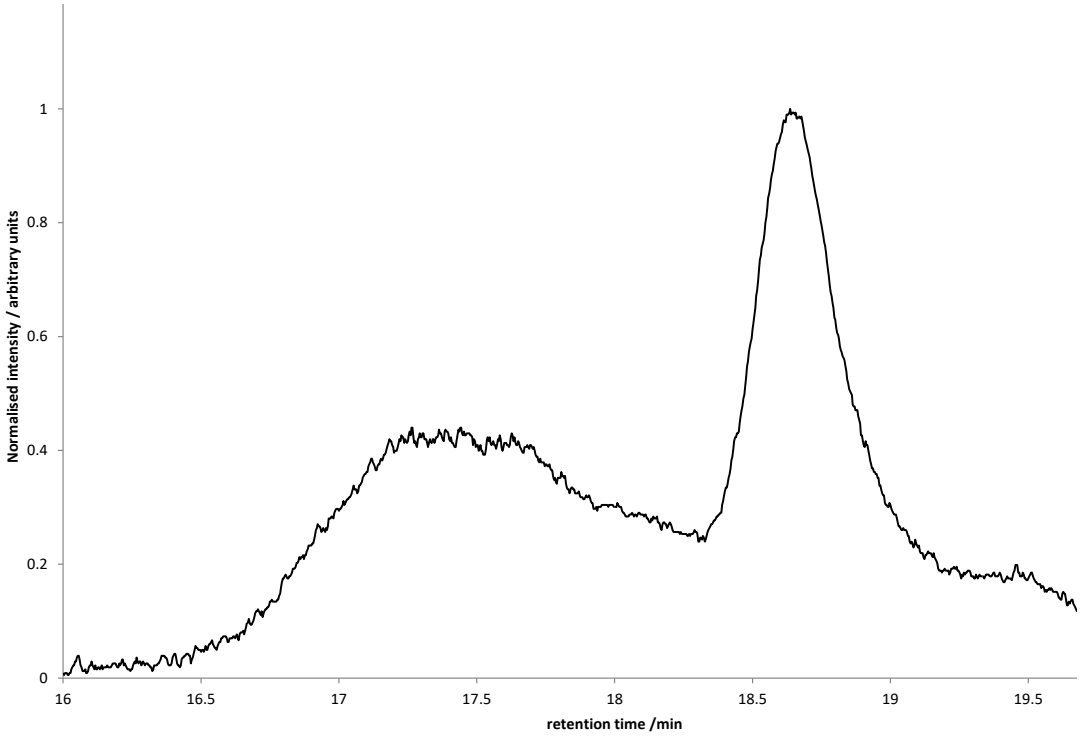

Figure 4.12 – SEC trace of polymer 10

The FTIR spectrum shows two carbonyl bands at 1732 (backbone) and 1678 cm^{-1} (lactam) along with multiple bands between 2850 and 2981 cm^{-1} corresponding to CH_2 stretching. MALDI mass analysis was conducted on the polymer sample in two different matrices, DHB (Figure 4.10) and CHCA (Figure 4.11). In the both matrices, it is possible to see the incremental increases in molecular weight of the polymer, corresponding to the molecular weight of SA (100.1 $gmol^{-1}$) and GEP, **1** (185.1 $gmol^{-1}$). The signals observed in Figure 4.10 correspond to the $[M + H]^+$ ions of polymers varying in molecular weight with two OH end groups.

An aqueous work up was avoided as polyester polymers of this type have been shown to degrade in aqueous solutions.[26] The presence of the OH end groups is contradictory to this. The presence of any water in the reaction vessel would result in the deactivated catalyst aluminium hydroxide. The formation of the desired polymer suggests that little or no water was present during the reaction. It is possible that the water present in the air during the work up along with the hydrochloric acid which is found in chloroform could hydrolyse the ester and terminate the polymer, removing aluminium from the polymer chain end. To test for the presence of aluminium, a filter paper was wetted with a solution of cobalt (II) nitrate

and polymer **10** and the filter paper was dried with a heat gun. If aluminium was present, a blue solid would be observed with the formation of cobalt aluminate. Upon heating, the filter paper became purple in colour (Figure 4.13) which indicated the presence of cobalt hydrate, no blue ash was observed. It is important to erase or reduce metal content in polymers for certain applications such as food production and packaging due to inherent toxicity.

Figure 4.13 – Cobalt (II) nitrate test for aluminium in polymer 10

In order to determine whether the polymer is truly alternating in composition, the reactivity ratios of the monomers could be determined by a series of experiments with varying monomer feed ratios. However, due to time constraints during this project, the reactivity ratios for the monomers under these reaction conditions were not determined.

The polymer was also characterised by DSC and TGA analysis. The degradation temperature was found to have an onset of 351 °C. The DSC curve (Figure 4.14) shows the T_g is determined to be -36 °C. This is consistent with other copolymers of SA and other monomers. The T_g for SA-*co*-EO was shown to be between -18 and -24 °C depending on the SA content of the polymer.[29] The SA-*co*-EO polymers also exhibit crystallisation behaviour where the SA-*co*-GEP (**10**) does not, this could be due to the reduced molar mass of polymer **10**. For ME_mMO-*alt*-SA the glass transition was between -31 and -46 °C depending on the length of the oligomer chain.[26] The flexible pendant pyrrolidone chain will lower the glass transition for SA-*co*-**2** when compared to the SA-*co*-EO polymer.

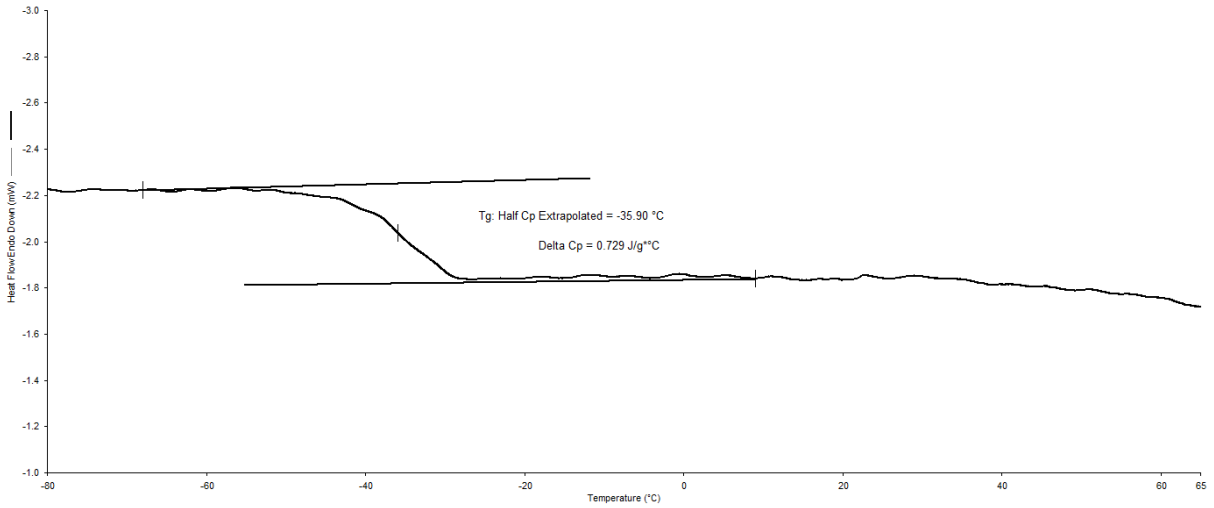

Figure 4.14 – DSC curve for polymer 10

In summary, the copolymerisation of SA and GEP (**1**) was successful by utilising an aluminium isopropoxide initiating system. The resulting polymer was characterised by 1D and 2D NMR, SEC, MALDI, FTIR and DSC. The SEC trace of the polymer was bimodal, the M_p of the high molecular weight peak was found to be 650 $gmol^{-1}$ by SEC. The MALDI mass analysis was carried out in two different matrices (CHCA and DHB) and the molecular weight of the polymer was found to vary from 796.5 to 2992.9 $gmol^{-1}$. The MALDI showed differences of 185.1 and 100.1 $gmol^{-1}$, correlating to the monomer units in the polymerisation. The large mass range indicates the polymerisation is not controlled, this could be due to the presence of a small quantity water. The step-wise increase in the molecular weight suggests that the copolymer could be alternating. A cobalt (II) nitrate test was conducted to identify if any aluminium remained in the polymer sample. The absence of blue ash indicated that cobalt aluminate had not formed, therefore suggesting that no aluminium is present in the polymer sample. Therefore, lending the biodegradable pyrrolidone containing polymer to applications such as food production and packaging where the absence of toxicity is vital. The glass transition temperature of the polymer was found to be -36 °C which is comparable to other copolymers or SA and (substituted) epoxides.

4.3.3 Copolymers of 4-vinylbenzyloxy ethyl pyrrolidone

The copolymerisation of monomer **2** (4-vinylbenzyloxy ethyl pyrrolidone) with styrene (St), *m*-hydroxystyrene (MHS) and *p*-methylstyrene (PMS) has been previously reported (Figure 4.15).[30] The reactions were carried out at 60 °C for 30 - 60 min and the conversion of monomers was kept below 5% to enable the reactivity ratios of the monomers to be easily determined. The reaction conditions were employed in the attempted copolymerisation of 4-vinylbenzyloxy ethyl pyrrolidone with St, *N*-vinyl pyrrolidone (NVP) and hydroxyethyl acrylate (HEA) (Figure 4.16).

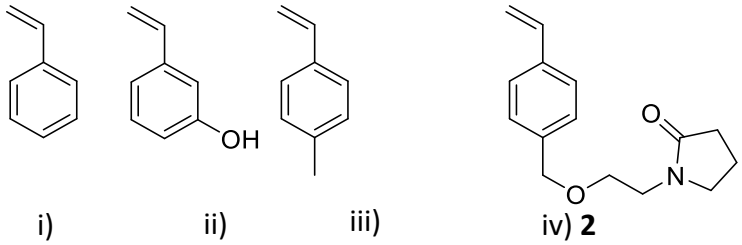

i) ii) iii) iv) **2**

Figure 4.15 – Structures of i) St ii) MHS iii) PMS and iv) monomer 2

The aim of this work was to prove the reproducibility of the literature procedure with the synthesis of **11** and to establish the synthesis of the novel polymers **12** and **13**. The copolymerisation of monomer **2** with St was conducted in bulk. In bulk conditions the reaction had ceased stirring after 30 min due to the formation of solid. The resulting solid was extracted in DCM at 40 °C for 4 h.

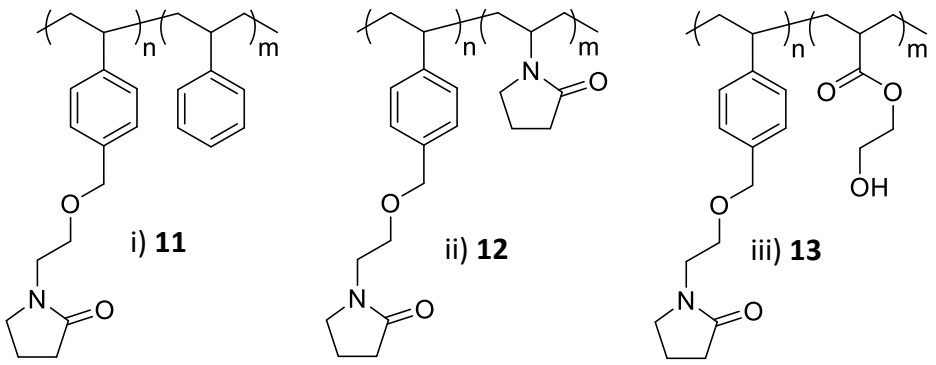

Figure 4.16 – Structure of i) polymer 11 ii) polymer 12 and iii) polymer 13

The solid extracts were analysed by solid state nuclear magnetic resonance (SSNMR) spectroscopy by both direct excitation and cross polarisation experiments. In the cross polarisation spectra (Figure 4.17), only minor differences in the strength of the resonances are observed due to the structural similarities of the rigid parts of the (co-)polymers. The resonances attributed to the aromatic carbon environments are broadened in the spectrum for **11**, this could indicate the increased styrene content in the polymer when compared to the homopolymer **7**. The strength of the pyrrolidone signals are increased in the spectrum of **12**, indicating the presence of structurally restricted pyrrolidone moiety. The greatest deviation is observed in the SSNMR spectrum of copolymer **13** (Figure 4.17) due to the introduction of a new moiety in the hydroxyethyl acrylate co-monomer. The presence of **J'** and **I'** (overlapping with **F'**) as well as the decrease in strength of the aromatic carbon resonances indicate the presence of the desired copolymer **13**.

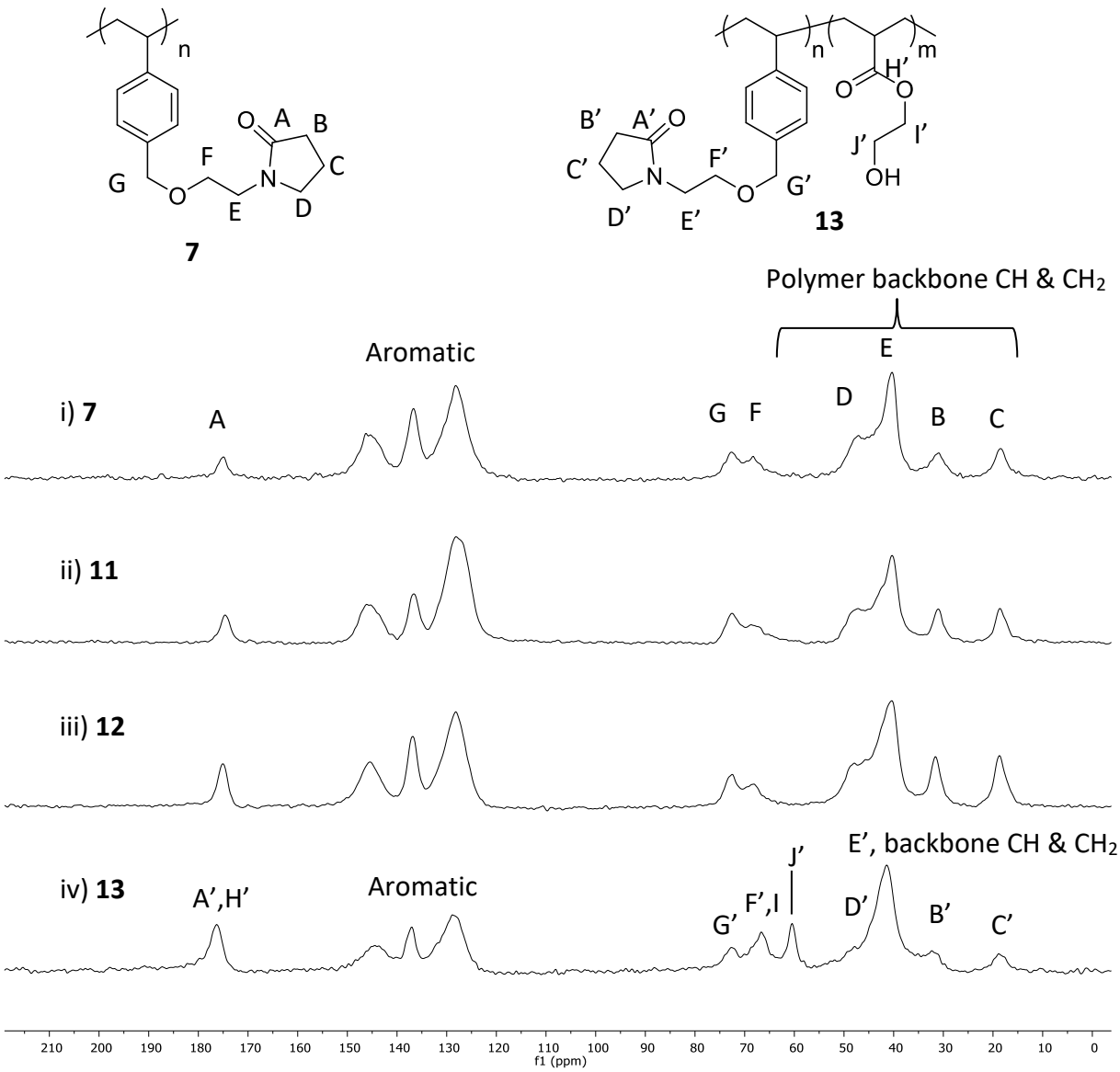

Figure 4.17 – Cross polarisation ^{13}C SSNMR spectrum of i) homopolymer 7 ii) polymer 11 iii) polymer 12 and iv) polymer 13

As the direct excitation experiment has a short relaxation time, only the more flexible sections of the polymer are observed. As observed for the homopolymer (Figure 4.18, i) **7**) and discussed in Chapter 3 (Section 3.3.2) the resonances of the polymer backbone and aromatic carbons are suppressed in the direct excitation due to the structural rigidity of the polymer. There are no discernible differences observed between the spectra of **7**, **11** and **12**. This could be due to the short relaxation time allowing only the most flexible environments of the polymer to be detected. The addition of relatively small co-monomers (St and NVP), could be structurally confined within the polymer chain and therefore not

observed in the direct excitation SSNMR spectrum. The greatest deviation is observed in the SSNMR spectrum of copolymer **11** (Figure 4.17 - iv) due to the introduction of a new moiety in the hydroxyethyl acrylate co-monomer. The resonance assigned to the aromatic carbon environments reduced when compared to the homopolymer **7** which could be due to the strength of the other signals dwarfing styrene based resonance. The appearance of the new resonances attributed to the ethyl protons **J'** and **I'** indicates that the hydroxyethyl acrylate group is incorporated into the polymer as intended.

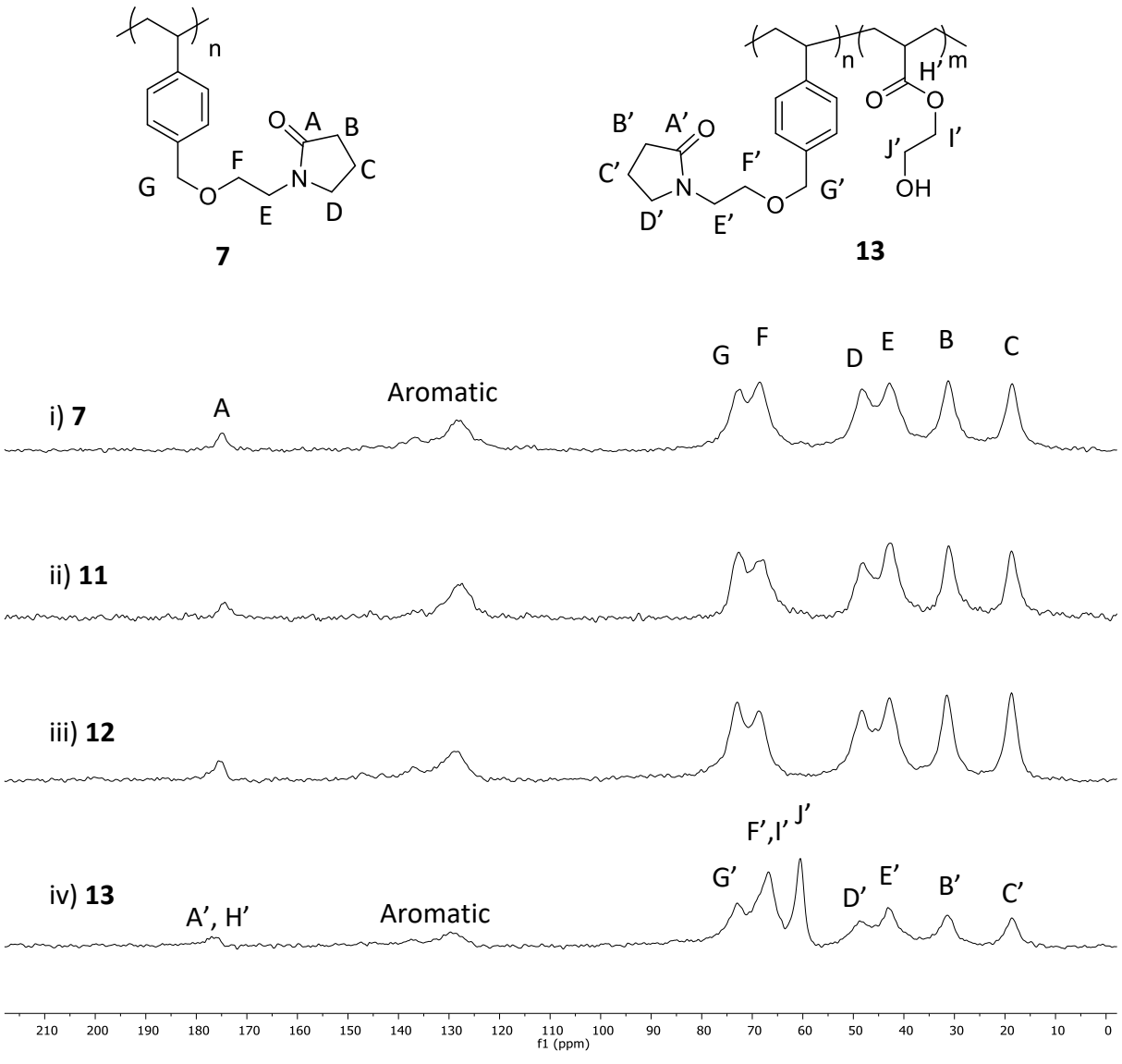

Figure 4.18 – Direct Excitation ^{13}C SSNMR spectrum of i) homopolymer 7 ii) polymer 11 iii) polymer 12 and iv) polymer 13

The polymers were further analysed by TGA and DSC analysis. The TGA showed two thermal events occur during the decomposition of **11**, **12** and **13** as well as for the homopolymer, poly(4-vinylbenzyloxy ethyl pyrrolidone) (**7**) (Table 4.3). Polystyrene homopolymer synthesised by the same method showed only one thermal event with an onset of 391 °C. The two thermal events could be due to the cross-linking caused by chain transfer in the synthesis of **7**, **11**, **12** and **13**.

Table 4.3 – TGA data of Poly(4-vinylbenzyloxy ethyl pyrrolidone) based (co-)polymers and polystyrene (PSt)

	7	**11**	**12**	**13**	**PSt**
First onset (°C)	420	438	432	398	391
Second onset (°C)	445	540	520	475	-

DSC analysis of **7**, **11**, **12** and **13** show no events up to 300 °C, it is possible that this could indicate the samples are fully cross-linked.[31] It is also possible that the change was very slight and therefore not detected by the DSC analysis.

To try and reduce the rate of chain transfer and termination, the reaction was repeated in cyclohexane solvent. After 1 h, the reaction mixture became heterogeneous and the reaction was terminated. NMR characterisation of the liquid phase showed the presence of broad resonances associated with the formation of polystyrene (PSt) homopolymer as well as unreacted monomer, no insoluble solid was produced and all of the 4-vinylbenzyloxy ethyl pyrrolidone was recovered.

FTIR analysis of the **11** shows CH stretching at ν = 2922 and 2857 cm^{-1} as well as a carbonyl stretch at ν = 1677 cm^{-1} and C-O stretching at ν = 1097 cm^{-1}, these bands correlate to the expected stretching frequencies. The FTIR spectrum of **12** contains very broad bands at ν = 2966, 2925, 2858, 1670 and 1088 cm^{-1} which are in line with that for **11**. Due to the structural similarities between **11**, **12** and indeed the homopolymer **7**, little change in the FTIR spectra are expected. The FTIR spectrum for **13** includes the expected bands as observed in **11** and **12** in addition to the presence of new stretching frequencies, as expected with the addition of a dissimilar functionality. A broad band at ν = 3392 is

observed due to OH stretching as well as a second carbonyl stretch at ν = 1728 cm^{-1}, indicating the presence of the HEA unit.

In summary, the attempted synthesis of poly(4-vinylbenzyloxy ethyl pyrrolidone-*co*-styrene) (**11**), poly(4-vinylbenzyloxy ethyl pyrrolidone-*co*-vinyl pyrrolidone) (**12**), poly(4-vinylbenzyloxy ethyl pyrrolidone-*co*-hydroxyethyl acrylate) (**13**) following the method outlined by Endo *et al.*[1] did not produce the desired polymer due to cross-linking. The isolated cross-linked polymers were analysed by SSNMR, FTIR, DSC and TGA analysis. Conduction the reactions under high dilution could reduce the chain transfer and termination reactions.[32] The desired outcome to produce a synthetically simple reaction method was not achieved and work was focussed on other monomers produced.

4.3.4 Poly(5-ethacryloxyethyl-12-ethylpyrrolidyl-N,N'hexane biscarbamate-*co*-vinyl pyrrolidone), (14)

With the successful synthesis of the poly(5-ethacryloxyethyl-12-ethylpyrrolidyl-N,N'hexane biscarbamate) **8** (Ch. 3, 3.3.3) *via* a conventional free radical polymerisation with AIBN initiator, a random copolymer of 5-ethacryloxyethyl-12-ethylpyrrolidyl-N,N'hexane biscarbamate (**3**) and *N*-vinyl pyrrolidone (NVP) was synthesised utilising the same reaction conditions. The polymer was synthesised with the aim of increasing the pyrrolidone content to increase the binding properties to allow the application in drug delivery system (Scheme 4.3).

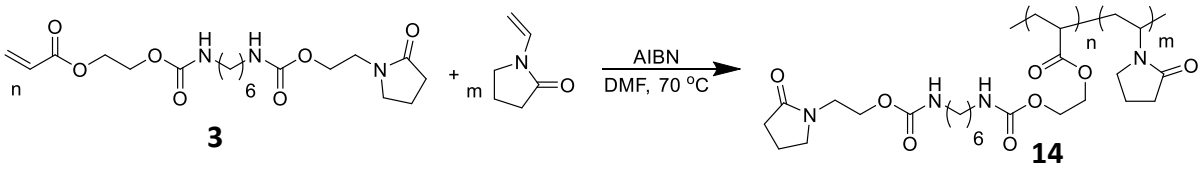

3 **14**

Scheme 4.3 – Synthesis of polymer 14

The ^{1}H NMR spectrum (Figure 4.19) shows the disappearance of the resonances associated with the vinyl protons in the acrylate monomer, indicating that polymerisation has occurred. The peaks associated with the homopolymer **8** (Ch. 3. 3.3.3) are also observed along with

overlapping peaks attributed to the incorporation of the pyrrolidone monomer. The resonance associated with proton **t** is δ = 3.29 ppm and the broad resonances between δ = 1.50 – 2.50 ppm are attributed to protons **u** and **v**. As the resonances are entirely overlapping it is not possible to estimate a percentage composition of the polymer from ^{1}H NMR analysis.

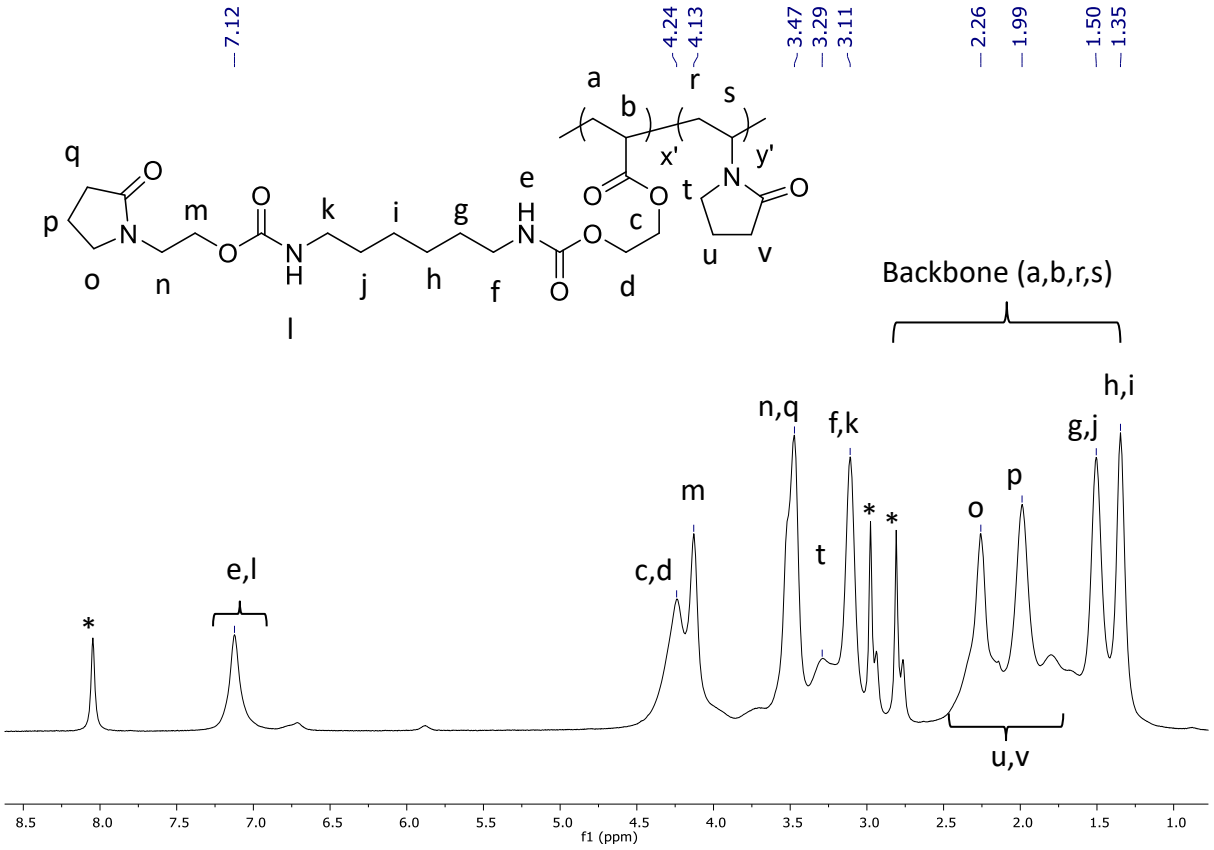

Figure 4.19 – ^{1}H NMR spectrum of polymer 14

The resonances observed in the ^{13}C NMR spectrum (Figure 4.20) are congruent to the resonances observed in the homopolymer **8** (Ch. 3. 3.3.3) plus the resonances associated with the incorporation of the vinyl pyrrolidone moiety. Carbon **Y** is a broad resonance from δ = 164.8 – 176.4 ppm overlapping with **S** at δ = 1753 ppm. The resonance for **W** (δ = 18.9 - 19.4 ppm) is also overlapping with carbon **Q** at δ = 19.0 ppm. The broad resonance at δ 31.8 – 32.6 ppm is attributed to carbon **X** and is adjacent to the corresponding pyrrolidone proton **R** in the 5-ethacryloxyethyl-12-ethylpyrrolidyl-N,N'hexane biscarbamate monomer unit (monomer **3**, Ch.2 2.3.4). It is postulated that the carbon

resonances associated with carbons **A**, **B**, **T**, **U** and **V** are not visible due to signal suppression from the strong solvent signals as well as carbon **F**-**S**. The resonances associated with the vinyl pyrrolidone (**W**, **X** and **Y**) are broad like the resonances for carbons **D** and **E** due to the rigid structure of the polymer close to the backbone.

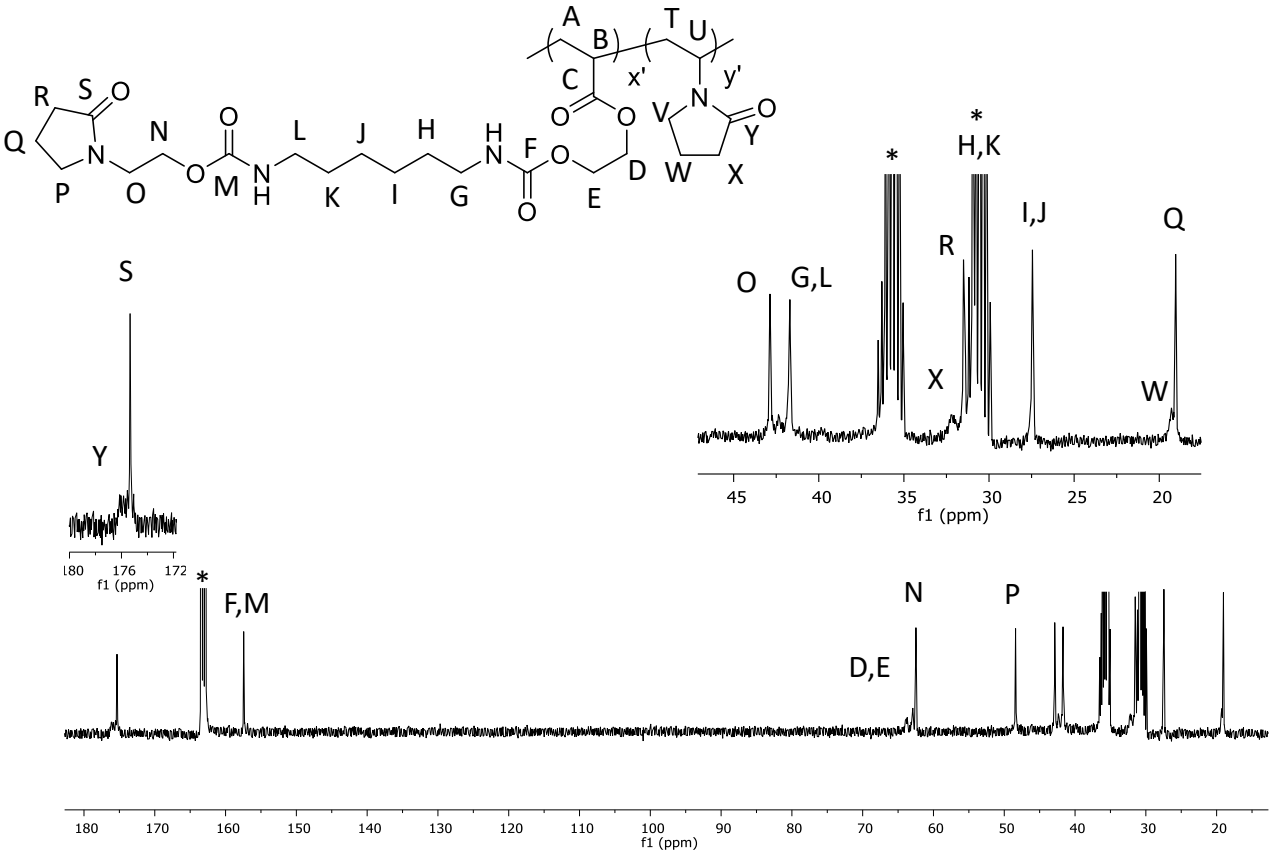

Figure 4.20 – ^{13}C NMR spectrum of polymer 14

FTIR analysis shows the stretching bands associated with the carbonyl of the amide at 1717 cm^{-1} and of the pyrrolidone at 1666 cm^{-1}. As well as the NH stretch at 3319 cm^{-1}, a broad OH stretch is observed at 3537 cm^{-1} indicating that there is hydrogen bonded water within the polymer.

SEC analysis shows a broad distribution with a low molecular weight shoulder (Figure 4.21), the M_n was determined to be $4.2x10^5$ $gmol^{-1}$ with a Đ of 3.54. The SEC was conducted in DMF solvent and a triple detector calibration was used to calculate the molecular weight with a dn/dc value calculated to be 0.076 mLg^{-1}, however, the polymer was not completely soluble in DMF and therefore, the calculated dn/dc value is inaccurate. The SEC analysis

confirms that a polymer was produced with a reasonable Đ and M_n for the free radical polymerisation conducted. The triple detection method of calibration is a more accurate calculation of molecular weight than conventional calibration methods. Conventional calibration methods generate a molecular weight relative to the calibration standard polymer e.g. PSt, PEO, PMMA. When using triple detection methods, the molecular weight of the polymer is determined from the light scattering and the dn/dc value for that polymer sample. It is imperative, therefore, that the dn/dc value be accurate and that the polymer is fully soluble.

MALDI analysis was attempted on **14**, however, no meaningful information was acquired. It is hypothesised that high levels of hydrogen-bonding within the polymer could lead to difficulty maintaining the polymer in the gas phase. In order to analyse more complex polymers, such as **14**, it is essential to develop an optimised MALDI method. Due to the time constraints of this project, this was not achieved.

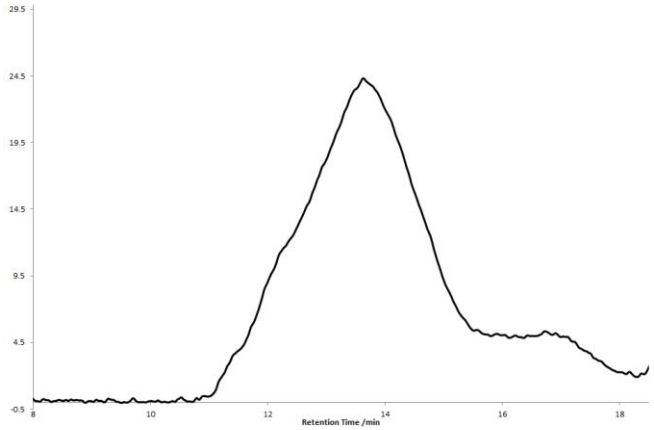

Figure 4.21 – SEC chromatogram of polymer 14

DSC analysis of **14** showed the T_g to be 9 °C, this is much lower than that of the homopolymer **8** at 22 °C. The decrease in T_g is hypothesised to be due to the interruption of hydrogen bonding between the large pendant side groups of the 5-ethacryloxyethyl-12-ethylpyrrolidyl-N,N'hexane biscarbamate with the introduction of the small pyrrolidone monomer. The TGA showed an 8% water loss below 200 °C and three thermal events were observed in the first derivative (blue line), as observed for the homopolymer **8** (Ch 3, Figure

3.19). A comparrison of the onset temperatures (Table 4.4) shows X_1 and X_2 to be very close, indicating that these thermal degredation events are indeed due to the 5-ethacryloxyethyl-12-ethylpyrrolidyl-N,N'hexane biscarbamate moiety as discussed in Ch.3, 3.3.3. X_3 was found to be reduced in the copolymer, showing that the incorporation of the *N*-vinyl pyrrolidone moiety allows formation of the highly cross-linked and cyclised material at a lower temperature. This could be due to the small pyrrolidone monomer allowing the greater flexibility as it interrupts the hydrogen bonding between the long side chains of the 5-ethacryloxyethyl-12-ethylpyrrolidyl-N,N'hexane biscarbamate units.

Table 4.4 – DSC and TGA data of copolymer 14 and homopolymer 8

	T_g /°C	X_1 Onset /°C	X_2 Onset /°C	X_3 Onset /°C
Homopolymer **8**	22	260	341	472
Copolymer **14**	9	261	342	428

In summary, the novel copolymer poly(5-ethacryloxyethyl-12-ethylpyrrolidyl-N,N'hexane biscarbamate-*co*-vinyl pyrrolidone) has been succesfully synthesised. The novel copolymer was characterised by ^{1}H NMR, ^{13}C NMR, TGA, DSC, SEC and FTIR. It was not possible to calculate the molecular weight by ^{1}H NMR analysis (due to overlapping resonances) and only limited information could be attained from SEC analysis due to the partial solubility in DMF. SEC analysis in water would provide more accurate molcular weight data, unfortunately this technique was not available during the project timeframe. It is postulated that the incorporation of NVP led to the interruption of hydrogen bonding and therefore reduced the T_g. The copolymer was found to exhibit three thermal events in the TGA as was observed for the homopolymer. The copolymer was found to exhibit three thermal events in the TGA as was observed for the homopolymer **8**. X_3 was found to be reduced due to the incorporation of the *N*-vinyl pyrrolidome monomer interrupting hydrogen bonding and therefore allowing greater flexibility within the polymer.

4.4 Conclusions

In conclusion, the initiating system of benzyl alcohol/potassium naphthalenide proved unsuccessful for the copolymerisation of EO and GEP (**1**). The homopolymerisation of EO was possible under the same conditions. However, no EO homopolymer was formed in the presence of GEP (**1**). A copolymer of SA and GEP (**1**) was successfully synthesised with an aluminium isopropoxide initiating system proceeding *via* a coordination insertion mechanism. The resulting polymer appeared to be alternating in nature based on MALDI mass analysis. MALDI showed the number of monomer repeat units to vary from 2 to 14 with a molecular weight range of 796.5 – 2992.9 $gmol^{-1}$. The spacing of ester bonds along the polymer backbone will allow for efficient degradation of the polymer under mild conditions.

The attempted synthesis of copolymers poly(4-vinylbenzyloxy ethyl pyrrolidone-*co*-styrene) (**11**), poly(4-vinylbenzyloxy ethyl pyrrolidone-*co*-vinyl pyrrolidone) (**12**) and poly(4-vinylbenzyloxy ethyl pyrrolidone-*co*-hydroxyethyl acrylate) (**13**) following the method outlined by Endo *et al.*[1] produced insoluble cross-linked polymers. Each copolymer exhibited two thermal degradation events which is in-line with the homopolymer (**7**) as discussed in chapter 3.

The novel copolymer poly(5-ethacryloxyethyl-12-ethylpyrrolidyl-N,N'hexane biscarbamate-*co*-vinyl pyrrolidone) (**14**) has been succesfully synthesised and characterised. It is postulated that the incorporation of NVP led to the interruption of hydrogen bonding producing a polymer with greater flexibility. This was deduced from the reduction in T_g and X_3 as observed in the DSC and TGA, respectively.

4.5 References

1 I. Atobe, T. Takata and T. Endo, **1993**, 8, 3004–3008.

2 K. Wlodarski, L. Tajber and W. Sawicki, *Eur. J. Pharm. Biopharm.*, **2016**, 109, 14–23.

3 Y. S. Vygodskii, D. A. Sapozhnikov, B. A. Bayminov, S. L. Semjonov, A. F. Kosolapov and E. A. Plastinin, *Prog. Org. Coatings*, **2016**, 99, 210–215.

4 L. Zhang, Y. Liang, L. Meng and C. Wang, *Polym. Adv. Technol.*, **2009**, 20, 410–415.

5 J. M. Harris, in *Poly(Ethylene Glycol) Chemistry: Biotechnical and Biomedical Applications*, ed. J. M. Harris, Springer US, Boston, MA, **1992**, pp. 1–14.

6 F. E. Bailey and J. V. Koleske, *Alkylene Oxides and Their Polymers*, Marcel Dekker Inc., **1991**.

7 F. E. Bailey, *Poly(ethlyene oxide)*, Academic Press, **1976**.

8 A. Tiwari, M. Ramalingam, H. Kobayashi and A. P. F. Turner, *Biomedical Materials and Diagnostic Devices*, Scrivener Publishing LLC. and John Wiley & Sons, Inc., **2012**.

9 J. Edward Semple, B. Sullivan, T. Vojkovsky and K. N. Sill, *J. Polym. Sci. Part A Polym. Chem.*, **2016**, 54, 2888–2895.

10 T. Loftsson, H. Fririksdóttir and T. K. Gumundsdóttir, *Int. J. Pharm.*, **1996**, 127, 293–296.

11 R. Reisfeld, V. Levchenko, A. Lazarowska, S. Mahlik and M. Grinberg, *Opt. Mater. (Amst).*, **2016**, 59, 3–7.

12 N. Saha, R. Benlikaya, P. Slobodian and P. Saha, *J. Biobased Mater. Bioenergy*, **2015**, 9, 136–144.

13 O. Sarapulova, V. Sherstiuk, V. Shvalagin and A. Kukhta, *Nanoscale Res. Lett.*, **2015**, 10, 1–8.

14 N. Roy, N. Saha, T. Kitano and P. Saha, *Carbohydr. Polym.*, **2012**, 89, 346–353.

15 A. L. Brocas, C. Mantzaridis, D. Tunc and S. Carlotti, *Prog. Polym. Sci.*, **2013**, 38, 845–873.

16 A. Duda and S. Penczek, *Macromolecules*, **1998**, 31, 2114–2122.

17 A. Duda and S. Penczek, *Macromolecules*, **1995**, 28, 5981–5992.

18 Z. Sun, F. Bai, H. Wu, S. K. Schmitt, D. M. Boye and H. Fan, *J. Am. Chem. Soc.*, **2009**, 131, 13594–13595.

19 S. Pargen, C. Willems, H. Keul, A. Pich and M. Möller, *Macromolecules*, **2012**, 45, 1230–1240.

20 R. Hoogenboom and H. Schlaad, *Polym. Chem.*, **2017**, 8, 24–40.

21 J. Kost and R. Langer, *Adv. Drug Deliv. Rev.*, **2012**, 64, 327–341.

22 B. A. Merrill, *e-EROS Encyclopedia of Reagents for Organic Synthesis*, John Wiley & Sons, Inc., **2001**.

23 B. F. Lee, M. Wolffs, K. T. Delaney, J. K. Sprafke, F. A. Leibfarth, C. J. Hawker and N. A. Lynd, *Macromolecules*, **2012**, 45, 3722–3731.

24 S. Han, C. Kim and D. Kwon, *Polymer (Guildf).*, **1997**, 38, 317–323.

25 L. Feng, J. Hao, C. Xiong and X. Deng, *Chem. Commun.*, **2009**, 4411–4413.

26 L. Feng, Y. Liu, J. Hao, X. Li, C. Xiong and X. Deng, *Macromol. Chem. Phys.*, **2011**, 212, 2626–2632.

27 L. Feng, Z. Yang, Y. Liu, J. Hao, C. Xiong and X. Deng, *Iran. Polym. J. (English Ed.*, **2014**, 23, 217–226.

28 W.-F. Su, *Principles of Polymer Design and Synthesis*, Springer US, **2013**.

29 Y. Maeda, A. Nakayama, N. Kawasaki, K. Hayashi, S. Aiba and N. Yamamoto, *Polymer (Guildf).*, **1997**, 38, 4719–4725.

30 T. Takata, I. Atobe and T. Endo, *J. Polym. Sci. Part A Polym. Chem.*, **1992**, 30, 1495–1498.

31 M. Kessler, *Advanced Topics in Characterization of Composites*, Trafford Publishing Ltd., **2006**.

32 I. Atobe, T. Takata and T. Endo, *J. Polym. Sci. Part A Polym. Chem.*, **1993**, 31, 1543–1549.

Chapter 5

Pyrrolidone Functionalisation of Poly(epichlorohydrin), Poly(butadiene) and Poly(vinyl alcohol-*graft*-hyperbranched polyglycerol)

Due to the difficulty in the production of a high molecular weight homopolymer of the epoxide monomer **1**, as discussed in chapter 3, alternative methods to synthesise pyrrolidone containing polymers with moderate to high molecular weights are explored. This chapter describes the post-polymerisation functionalisation of selected polymer motifs utilising the pyrrolidone functional group in the form of hydroxyethyl pyrrolidone or the unexplored 1-(2-(oxiran-2-ylmethoxy) ethyl) pyrrolidone or glycidyl ethylpyrrolidone (GEP, **1**).

5.1 Introduction

Post-polymerisation functionalisation is an extensively employed technique to produce novel modified polymers with varying properties. It is a simple method to adjust the properties of well-defined polymers under mild conditions to increase the scope of possible applications. Addition of the functional group post-polymerisation allows the integration of motifs not compatible with the polymerisation conditions (Scheme 5.1).

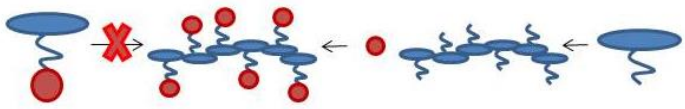

Scheme 5.1 – Demonstrating generic post-polymerisation functionalisation method

Achieving complete conversion of functional groups is desirable but often challenging. Side reactions are common and, where copolymers are employed, differences in reactivity can introduce complications.[1] However, even minor modifications of polymer structure and functional group composition can impart positive changes in the polymer properties.[2] There are many different types of post-polymerisation functionalisation, for example, esterification,[3,4] epoxidation,[5,6] 'click' reactions -thiol-ene[7,8] and azide-alkyne.[9,10] The versatility of these methods is demonstrated by the range of applications and the ability to employ multiple modifications to one system.[11,12]

Polybutadiene is a widely utilised polymer in post-polymerisation functionalisation which attracted interest due to the ease of production[13] and challenges associated with limited functionality.[14] The synthesis and characterisation of polyhydroxylated polybutadiene (PHPB) *via* the hydroboration-oxidation reaction is well known.[15–17] The method takes advantage of the regioselective hydroboration reaction to produce well-defined polymers with primary hydroxyl units which can undergo further reaction (Scheme 5.2).

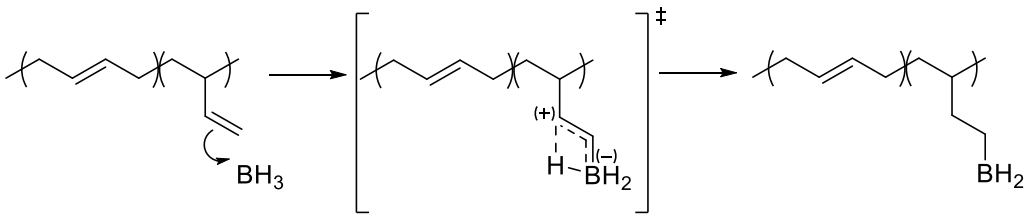

Scheme 5.2 – Mechanism of hydroboration of polybutadiene

It has been shown that the degree of functionalisation can be controlled by the equivalents of borane reagent used in the reaction.[17] In order to maximise conversion, an excess of borane reagent and subsequent hydrogen peroxide is required. An alternative route to

PHPB is *via* the thiol-ene 'click' reaction. The advantage of this method is the high levels of conversion, mild reaction conditions and simple purification. The reaction can be initiated by a radical initiator or UV light and the mechanism involves three steps: initiation, thiyl addition and chain transfer to regenerate the radical (Scheme 5.3).[18] This mechanistic cycle allows for high levels of conversion and regeneration of the thiyl radical.

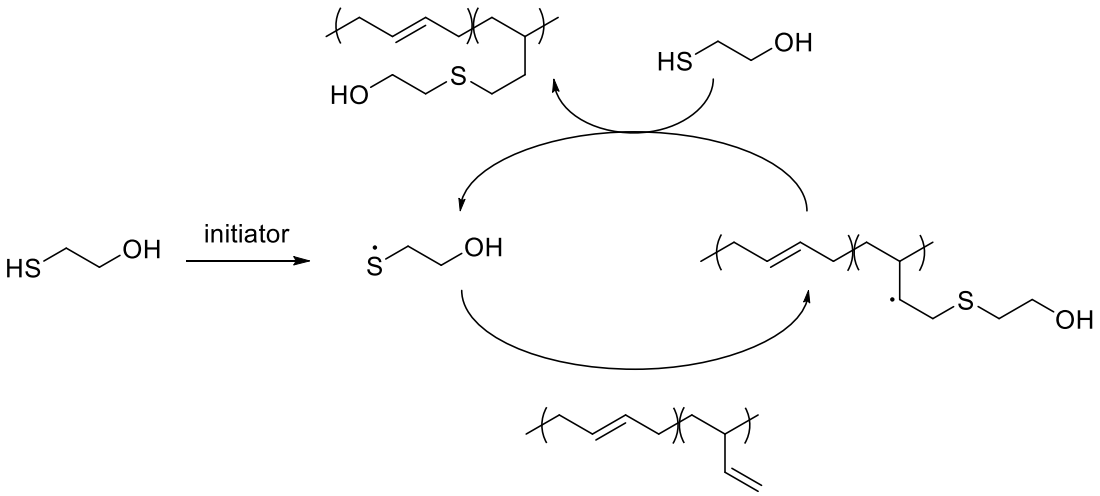

Scheme 5.3 – Pathway of thiol-ene 'click' reaction with polybutadiene

The ring opening polymerisation of glycidyl ethylpyrrolidone (GEP, monomer **2**) was unsucessful, however, the epoxide can be utilised as an end capping agent, to integrate the pyrrolidone functionality into polymers containing a reactive primary hydroxy group. This negates the determination of polymerisation conditions, difficulties with which are discussed in chapter 3 (3.3.1) and allows the complete characterisation of the polymer prior to functionalisation.

5.2 Experimental

5.2.1 Materials

9-Borabicyclo[3.3.1]nonane solution (9-BBN, 0.5 M in THF), Boron trifluoride diethyl etherate (≥46.5% $BF_3{\cdot}Et_2O$), 1,4-butanediol (99%), epichlorohydrin (ECH, ≥99%), polybutadiene (PB, $M_{w(supplied)}$ 2.0x10^4 to 2.2x10^4 gmol^{-1}, $M_{n(SEC)}$ 3.7x10^3 gmol^{-1}), polyepichlorohydrin (PECH, M_w 7.0x10^5 gmol^{-1} by SEC), potassium carbonate (K_2CO_3, 99.995%), potassium hydroxide (KOH), sodium iodide (NaI, 99.999%), sodium hydroxide (NaOH), MeOK (25% in MeOH w/v solution), hydrogen peroxide (H_2O_2, 30 wt.% solution) and 2-butanone (≥99%) were used as supplied from Sigma Aldrich. Azobisisobutyronitrile (AIBN, 98%) was purchased from Sigma Aldrich and recrystallised from MeOH prior to use. Hydroxyethyl pyrrolidone (HEP) was used as supplied from Ashland Inc. Hydrochloric acid (HCl, 37%), diethyl ether, DMSO and DCM analytical grade solvents were purchased from Fisher Scientific and used as received. Dry DMF, THF and Toluene were obtained from the Durham University Chemistry Department solvent purification service (SPS). Monomer **2** was synthesised as described in chapter 2 (2.3.1). Polyvinyl alcohol-*graft*-hyperbranched polyglycerol was synthesised by Dr. Peter King.[19]

5.2.2 Instrumentation

^{1}H and ^{13}C Nuclear Magnetic Resonance (NMR) spectra were recorded on a Bruker Avance 400 operating at 400 MHz or a Varian VNMRS 700 spectrometer operating at 700 MHz (^{1}H) and 176 MHz (^{13}C) with *J* values given in Hz. $CDCl_3$ was used as the deuterated solvent for ^{1}H and ^{13}C NMR analysis and the spectra were referenced to the solvent at 7.26ppm and 77.16 ppm, respectively. The following abbreviations are used in describing NMR spectra: s = singlet, d = doublet, t = triplet, m = multiplet and b = broad, bm = broad multiplet. 2D NMR experiments were also used to fully assign the proton and carbon environments in the products. ^{1}H-^{1}H Correlation Spectroscopy (COSY) demonstrated proton-proton correlations over two or three bonds. ^{1}H-^{13}C Heteronuclear Shift Correlation Spectroscopy (HSQC)

showed the correlation between directly bonded proton and carbon atoms. ^{1}H-^{13}C Heteronuclear Multiple-bond Correlation (HMBC) NMR demonstrated the correlation between proton and carbon atoms through several bonds.

Fourier transform infra-red (FTIR) spectroscopy was conducted using a Perkin Elmer 1600 series spectrometer. MALDI results were collected on the Autoflex II ToF/ToF mass spectrometer (Brucker Daltonik GmBH) with reflection enhanced mass resolution.

SEC analysis was conducted using a Viskotek TDA 302 with 2 x 300 mL PLgel 5µm mixed C columns with THF or DMF eluent with a flow rate of 1 ml mg^{-1} at 35°C and 1 ml mg^{-1} at 70°C, respectively. The detectors were calibrated using narrow molecular weight distribution linear polystyrene or polyethylene oxide as standard. A conventional calculation was used to determine molecular weight.

Differential scanning calorimetry (DSC) was carried out using a TA instrument Q1000 DSC, in N_2 gas, with a flow rate of 30 mL min^{-1} and heating rate of 10 °C min^{-1}. The second heating run was analysed. Thermogravimetric analysis (TGA) was carried out using a Perkin Elmer Pyris 1 TGA connected to a HIDEN HPR20 MS, in N_2 gas, with a heating rate of 10 °C min^{-1}.

5.2.3 Synthesis of Poly(epichlorohydrin-*co*-polyepiiodohydrin), (15)

Polyepichlorohydrin (0.220 g, 2.18 mmol) was dissolved in butanone (5 mL) and stirred at 50 °C until homogenous. NaI (0.70 g, 4.36 mmol) was added and the mixture was stirred for 1 h at 50 °C. HEP (0.66 g, 4.86 mmol) was added slowly and the reaction was stirred for a further 12 h under reflux (85 °C). The polymer was isolated by precipitation into hydrochloric acid (5 M) and dried under reduced pressure at 40 °C to give the white solid, **15** (0.435 g, mass yield 53%). ^{1}H NMR (400 MHz, $CDCl_3$) δ = 3.28-3.53 (5H, b, C**H**,C$\mathbf{H_2}$ and C$\mathbf{H_2}$I of PEIH), 3.56-3.77 (5h, b, C**H**,C$\mathbf{H_2}$ and C$\mathbf{H_2}$Cl of PECH) ppm. ^{13}C NMR (176 MHz, $CDCl_3$) δ = 43.8 (**C**H_2 backbone), 69.5 and 69.8 (**C**H_2X), 79.1 (**C**H backbone) ppm. FTIR ν (cm^{-1}) = 2979, 2914 and 2867 (CH and CH_2), 744 (C-Cl), 570 (C-I). Polymer composition by NMR, PECH = 41%, PEIH = 59%, (Conversion = 59%).

5.2.4 Synthesis of Poly(epichlorhydrin-*co*-epiiodohydrin-*co*-glycidyl ethylpyrrolidone), (16)

Polyepichlorohydrin-*co*-polyepiiodohydrin (**15**) (0.153 g, 1.62 mmol) was dissolved in DCM (5 mL) before K_2CO_3 (0.67 g, 4.86 mmol) was added. The mixture was stirred at room temperature until homogenous. Hydroxyethyl pyrrolidone (0.64 g, 4.86 mmol) was added dropwise and the reaction was stirred for 12 h. The polymer was isolated by precipitation into hydrochloric acid (5 M) and dried under reduced pressure at 40 °C to give a white solid, **16** (0.587 g, mass yield 74%). ^{1}H NMR (400 MHz, $CDCl_3$) δ = 2.06 (m, 2H, $NCH_2C\mathbf{H_2}CH_2CO$), 2.42 (m, $NCH_2CH_2C\mathbf{H_2}CO$), 3.27-3.83 (bm, 21H, C**H** and C$\mathbf{H_2}$ backbone, C$\mathbf{H_2}$X, CHC$\mathbf{H_2}$O, OC$\mathbf{H_2}$C$\mathbf{H_2}$N, NC$\mathbf{H_2}CH_2CH_2CO$) ppm. FTIR ν (cm^{-1}) = 2979, 2914 and 2867 (CH and CH_2), 1708 (C=O), 744 (C-Cl), 570 (C-I). Polymer composition by NMR, PECH = 41%, PEIH = 35%, Py = 24% (Conversion = 41% of PEIH).

5.2.5 Synthesis of Polyhydroxylated Polybutadiene *via* Hydroboration-Oxidation, (17)

Polybutadiene (1.02 g, 5.50 mmol) in THF (5 mL) was dried by freeze-pump-thaw cycles and stirred under nitrogen at 0 °C. 9-Borabicyclo[3.3.1]nonane solution (22 mL) was added dropwise and the mixture was maintained at 0 °C and stirred for 2 h. The reaction was allowed to warm to room temperature and stirred for a further 14 h. The reaction was cooled to 0 °C before $NaOH_{aq}$ (10 mL, 1.25 M solution, 12.1 mmol) was added dropwise followed by H_2O_2 (30% in H_2O, 3.4 mL, 33.0 mmol). The mixture was stirred at 0 °C for 2 h then at 55 °C for 4 h. The reaction was allowed to cool to room temperature before the polymer was isolated by precipitation into $NaOH_{aq}$ (0.5 M) and dried under reduced pressure at 40 °C to obtain **17** (0.51 g, 85 %). ^{1}H NMR (400 MHz, d_6-DMSO) δ = 0.80-1.65 (bm, 7H, C$\mathbf{H_2}$ backbone 1,2-addition, C$\mathbf{H_2}$ backbone hydroxylated, C**H** backbone hydroxylated, C$\mathbf{H_2}CH_2OH$), 1.81-2.22 (bm, 3H, C$\mathbf{H_2}$ backbone 1,4-addition, C**H** backbone 1,2-addition), 3.39 (b, 2H, $CH_2C\mathbf{H_2}OH$), 4.17 (b, 1H, O**H**), 4.92 (b, 2H, C$\mathbf{H_2}$=CH), 5.34 (bm, 2H, CH_2=C**H**, C**H** 1,4-addition). ^{13}C NMR (176 MHz, d_6-DMSO) δ = 29.2-31.3 (**C**H backbone hydroxylated, **C**H_2 1,4-addition), 36.9 (), 38.5-41.4 (overlapping with d_6-DMSO, **C**H_2 backbone 1,2-addition, **C**H_2 backbone hydroxylated, **C**H backbone hydroxylated, **C**H_2 1,4-addition, **C**H_2CH_2OH), 58.8 (CH_2**C**H_2OH),

114.5 (**C**H_2=CH), 123.7-131.9 (**C**H backbone 1,4-addition), 143.2 (CH_2=**C**H). SEC M_n = 2.1x10^4 gmol, Đ = 1.16. FTIR ν (cm^{-1}) = 3345 (OH), 2919 and 2862 (CH, CH_2). TGA Onset = 461 °C. DSC, T_g = 186 °C.

5.2.6 Synthesis of Polypyrrolidonated Polybutadiene, (18)

Polyhydroxylated polybutadiene (0.233 g, 1.28 mmol) and KOH (0.087 g, 1.44 mmol) were stirred in DMF (5 mL) until homogeneous. 1-(2-(oxiran-2-ylmethoxy) ethyl) pyrrolidin-2-one (**1**, 0.271 g, 1.44 mmol) was added and the reaction was stirred at room temperature for 12 h. Excess DMF was removed under reduced pressure before the polymer was dissolved in water, isolated by precipitation into diethyl ether and dried under reduced pressure at 40 °C to give a white solid, **18** (0.431 g, 82%). ^{1}H NMR (400 MHz, d_6-DMSO) = 0.89-1.61 (bm, 7H, C**H$_2$** backbone 1,2-addition, C**H$_2$** backbone hydroxylated, C**H** backbone hydroxylated, CHC**H$_2$**CH_2O), 1.79-2.26 (b, 3H, overlapping other resonances, C**H$_2$** backbone 1,4-addition) 1.89 (b, 2H, NCH_2C**H$_2$**CH_2CO), 2.19 (b, 2H, NCH_2CH_2C**H$_2$**CO), 3.12-3.78 (bm, 13H, overlapping with residual water, $CHCH_2$C**H$_2$**O, C**H$_2$**CH(OH), CH_2C**H**(OH)CH_2, CH_2CH(OH)C**H$_2$**, OC**H$_2$**CH_2N, OCH_2C**H$_2$**N, NC**H$_2$**CH_2CH_2CO), 4.52 (b, 1H, O**H**), 4.94 (b, 2H, C**H$_2$**=CH), 5.33 (bm, 2H, CH_2=C**H**, C**H** 1,4-addition). ^{13}C NMR (176 MHz, d_6-DMSO) δ = 17.8 (NCH_2**C**H_2CH_2CO), 28.8-41.8 (overlapping other resonances, **C**H_2 backbone 1,4-addition, **C**H_2 backbone 1,2-addition, **C**H backbone 1,2-addition, **C**H_2 backbone pyrrolidonated, **C**HCH_2CH_2O, CH**C**H_2CH_2O), 30.6 (NCH_2CH_2**C**H_2CO), 47.4 (N**C**$H_2CH_2CH_2$CO), 58.9 ($CHCH_2$**C**H_2O), 68.4-74.2 (**C**H_2CH(OH)CH_2, CH_2**C**H(OH)CH_2, CH_2CH(OH)C**H$_2$**, O**C**H_2CH_2N, OCH_2**C**H_2N), 114.5 (**C**H_2=CH), 124.0-132.5 (**C**H backbone 1,4-addition), 143.1 (CH_2=**C**H), 174.5 (**C**=O). FTIR ν (cm^{-1}) = 3345 (OH), 2919 and 2862 (CH, CH_2), 1666 (C=O), 1107 (CO). TGA Onset X_1 = 298 °C, X_2 = 457 °C. DSC, T_g = -28 °C

5.2.7 Synthesis of Thioether-Polyhydroxylated Polybutadiene, (19)

Polybutadiene (1.03 g, 5.5 mmol), 2-mercaptoethanol (3.9 mL, 55 mmol) and azobisisobutyronitrile (0.458 g, 2.64 mmol) were stirred at 70 °C for 2 h 30 min. The reaction mixture was cooled to room temperature before precipitation into NaOH (0.5 M) and drying under reduced pressure at 40 °C. The polymer was purified by repeated precipitations by

dissolving in DMSO and precipitating into NaOH (0.5 M) until no 2-mercaptoethanol was observed in the ^{1}H NMR spectrum. The polymer was a white flaky solid, **19** (0.915 g, 64% mass yield). ^{1}H NMR (400 MHz, d_6-DMSO) = 0.61-1.19 (bm, 3H, CH backbone, CH_2 backbone), 2.27 (bm, 2H, SC**H$_2$**CH_2OH), 3.25 (b, 2H, SCH_2C**H$_2$**OH), 4.47 (b, 1H, SCH_2CH_2O**H**). ^{13}C NMR (176 MHz, d_6-DMSO) δ = 15.4, 18.5, 21.9 and 25.6 (CH backbone), 29.3 and 34.4 (CH_2 backbone, S**C**H_2CH_2OH) (CH_2 backbone), 61.4 and 61.7 (SCH_2**C**H_2OH). SEC M_n = 4.3x10^4 gmol^{-1}, Đ = 1.0. FTIR ν (cm^{-1}) = 33456 (OH), 2918 and 2860 (CH and CH_2), 1044 (C-OH). TGA Onset = 319 °C. DSC, T_g = 117 °C

5.2.8 Synthesis of Thioether-Polypyrrolidonated Polybutadiene, (20)

Thioether-polyhydroxylated polybutadiene (0.174 g, 1.28 mmol) and KOH (0.083 g, 1.44 mmol) were stirred in DMF (5 mL) until homogeneous. 1-(2-(oxiran-2-ylmethoxy) ethyl) pyrrolidin-2-one (**1**, 0.275 g, 1.44 mmol) was added and the reaction was stirred at room temperature for 12 h. Excess DMF was removed before the polymer was precipitated into water and dried under reduced pressure at 40 °C to give a white solid, **20** (0.113 g, 28%). ^{1}H NMR (400 MHz, d_6-DMSO) = 0.78-2.09 (bm, 3H, CH and CH_2 backbone), 1.89 (b, 2H, NCH_2C**H$_2$**CH_2CO), 2.18 (b, 2H, NC**H$_2$**CH_2CH_2CO), 2.55 and 2.63 (overlapping with solvent, CH_2S backbone, SC**H$_2$**CH_2O), 3.17-3.67 (bm, NC**H$_2$**CH_2O, NCH_2C**H$_2$**O, C**H$_2$**CH(OH)CH_2, CH_2CH(OH)C**H$_2$**, NCH_2CH_2C**H$_2$**CO, SCH_2C**H$_2$**O), 3.67 (CH_2C**H**(OH)CH_2). ^{13}C NMR (176 MHz, d_6-DMSO) δ = 11.3-34.2 (**C**H, **C**H_2 and **C**H_2S backbone, S**C**H_2CH_2O), 17.4 (NCH_2**C**H_2CH_2CO), 30.7 (N**C**$H_2CH_2CH_2$CO), 41.7 (SCH_2CH_2O**C**H_2), 47.1 (NCH_2CH_2**C**H_2CO), 58.4-74.1 (SCH_2**C**H_2O, NCH_2CH_2O**C**H_2, NC**H$_2$**CH_2O, NCH_2C**H$_2$**O), 68.3 (CH_2**C**H(OH)CH_2), 173.8 ($NCH_2CH_2CH_2$**C**O). FTIR ν (cm^{-1}) = 3323 (OH), 2930 and 2871 (CH and CH_2), 1659 (C=O), 1104 (C-O).

5.2.9 Synthesis of Poly(vinyl alcohol-*graft*-hyperbranched polyglycerol-glycidyl ethylpyrrolidone), (21)

KOMe (25% in MeOH, 3.12 mL, 11.1 mmol) was charged to a reaction flask and excess MeOH was removed leaving KOMe as a white solid. Polyvinyl alcohol-*graft*-hyperbranched polyglycerol (PVA-*g*-hPG) (0.297-0.302 g, 8.5-9.27 mmol) in water (2 mL) and 1-(2-(oxiran-2-

ylmethoxy) ethyl) pyrrolidin-2-one (**1**, 1.90-2.06 g, 10.2-11.1 mmol) in water (2 mL) were added to the stirring flask. The reaction was stirred for 12 h then neutralised with HCl (5M). The polymer was recovered by precipitation into acetone and dried under reduced pressure to obtain **21** (0.492-1.100 g, 24-59% mass yield). ^{1}H NMR (400 MHz, d_6-DMSO) = 1.57-1.93 (C**H$_2$** backbone), 2.12 (NCH$_2$C**H$_2$**CH$_2$CO), 2.50 (NC**H$_2$**CH$_2$CH$_2$CO), 3.47-4.15 (C**H$_2$**CH(OH)CH$_2$, CH$_2$C**H**(OH)CH$_2$, CH$_2$CH(OH)C**H$_2$**, C**H$_2$**CH(OH)CH$_2$O-etPy, CH$_2$CH(OH)C**H$_2$**O-etPy), 3.53 (NC**H$_2$**CH$_2$O), 3.62 (NCH$_2$CH$_2$C**H$_2$**CO), 3.57 (NCH$_2$C**H$_2$**O), 3.84 (C**H** backbone hPG), 4.08 (CH backbone PVA, CH$_2$C**H**(OH)CH$_2$O-etPy). ^{13}C NMR (176 MHz, d_6-DMSO) δ = 17.5 (NCH$_2$**C**H$_2$CH$_2$CO), 31.1 (N**C**H$_2$CH$_2$CH$_2$CO), 41.3 (**C**H$_2$ backbone hPG), 42.2 (N**C**H$_2$CH$_2$O), 44.2 (**C**H$_2$ backbone PVA), 48.5 (NCH$_2$CH$_2$**C**H$_2$CO), 62.7 (**C**H$_2$CH(OH)CH$_2$, CH$_2$CH(OH)**C**H$_2$), 64.8 (**C**H backbone PVA), 66.3 (**C**H backbone PVA), 67.8 (**C**H backbone PVA), 69.1 (CH$_2$**C**H(OH)CH$_2$), 69.8-80.3 (NCH$_2$**C**H$_2$O, **C**H$_2$CH(OR)CH$_2$, CH$_2$CH(OR)**C**H$_2$, CH$_2$**C**H(OR)CH$_2$, **C**H$_2$CH(OH)CH$_2$, CH$_2$**C**H(OH)CH$_2$, CH$_2$CH(OH)**C**H$_2$, NCH$_2$**C**H$_2$O), 74.6 (**C**H backbone hPG), 178.5 (NCH$_2$CH$_2$CH$_2$**C**O). FTIR ν (cm^{-1}) = 3338 (OH), 2940 and 2889 (CH and CH$_2$), 1658 (C=O), 1096 (C-O). TGA Onset X_1 = 176-308°C, X_2 = 244-405 °C. DSC, T_g = 115-118 °C, T_m = 242-243 °C.

5.3 Results & Discussion

5.3.1 Functionalisation of Poly(epichlorohydrin)

The attempted homopolymerisation of 1,2-epoxy-3-oxyethyl pyrrolidone or glycidyl ethylpyrrolidone (GEP) **1** *via* cationic ring opening polymerisation to produce polymer **6** (Scheme 5.4) gave oligomers ranging from 2 to 14 monomer units, as determined by MALDI analysis (Ch. 3, 3.3.1). The oligomers were found to have a variety of end groups. This, along with the low molecular weight calculated by SEC (M_n = 335 gmol^{-1}) and dispersity (Đ) of 1.5 indicate that side reactions such as chain transfer and termination were dominant. The water solubility of the oligomers was encouraging as this is a desirable property for a

wide variety of applications such as drug delivery systems and functions that require biocompatibility.

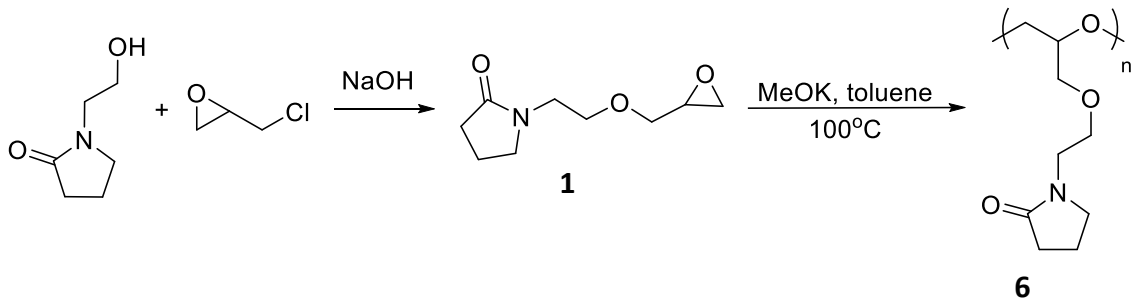

Scheme 5.4 – Synthesis of polymer 6 from monomer 1

Monomer **1** (GEP) was synthesised by the reaction of epichlorohydrin and hydroxyethyl pyrrolidone (Scheme 5.4). As the homopolymerisation of **1** had limited success, an alternative method of synthesis was required. The aim of the synthesis was to produce a high molecular weight polymer containing the desired functionality as in polymer **6**. Inorganic bases, such as K_2CO_3 in aprotic polar solvents are known to promote the formation of an ether bond with alcohol and alkyl halides. This nucleophilic substitution reaction can be slow in some cases and generally the presence of an electron withdrawing group (EWG) adjacent to the alkyl halide or a heavier halide (such as iodide) yield better results (Scheme 5.5).[20]

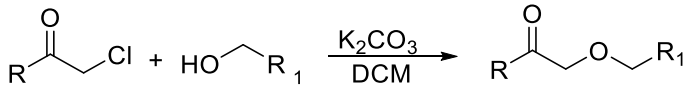

Scheme 5.5 – Ether formation using potassium carbonate in DCM

As there is no EWG adjacent to the alkyl chloride in PECH, a classical Finkelstein reaction was conducted to increase the reactivity of the polymer pendant group towards nucleophilic substitution. Therefore, the post-polymerisation functionalisation of poly(epichlorohydrin) (PECH) was undertaken according to Scheme 5.6.

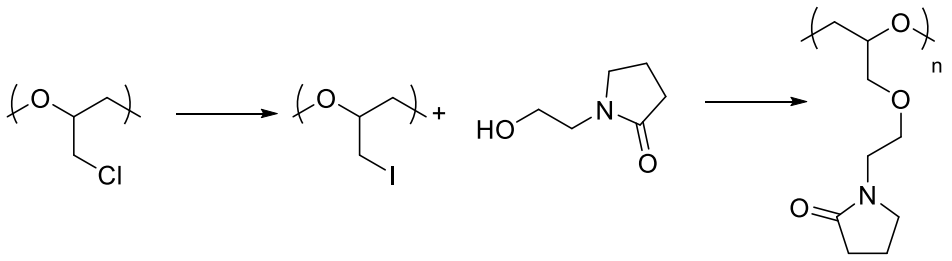

Scheme 5.6 – Functionalisation of poly(epichlorohydrin) *via* Finkelstein followed by reaction with hydroxyethyl pyrrolidone

Challenges associated with post-polymerisation functionalisation include achieving <100% conversion and therefore retaining the functionality of the starting polymer. The attempted reaction of hydroxyethyl pyrrolidone (HEP) with polyepichlorohydrin did not produce any functionalised polymer. Hence, it was necessary to exchange the halogen leaving group to a larger halogen to aid the conversion to the desired pyrrolidone capped polymer. Therefore, the first step is to perform the Finkelstein reaction to produce the polyepiiodohydrin (PEIH), following the literature procedure.[21] The ^{1}H NMR spectrum (Figure 5.1) shows the appearance of the new resonance from δ = 3.30 – 3.50 ppm corresponding to the protons **d'**, **e'** and **f'**. However, the retention of the resonances between δ = 3.57 and 3.77 ppm indicate that there are remaining chlorohydrin moieties present within the product i.e. the reaction did not reach 100% conversion. The literature reported an 88% conversion from chloride to iodide, analysis of the ^{1}H NMR spectrum of the recovered polymer (Figure 5.1) estimates the conversion to be 59%.

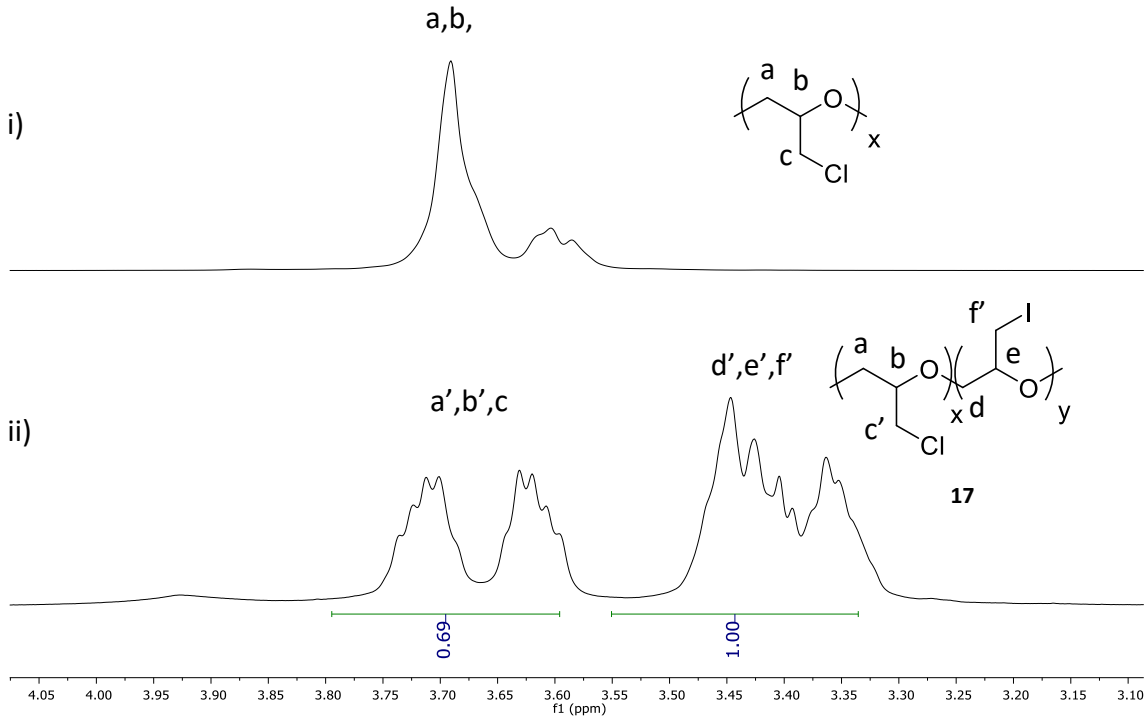

Figure 5.1 – ^{1}H NMR spectrum of i) PECH and ii) polymer 15

The P(ECH-*co*-EIH), **15**, was taken forward in a reaction with HEP to afford the target polymer poly(epichlorohydrin-*co*-epiiodohydrin-*co*-glycidyl ethylpyrrolidone) (P(ECH-*co*-EIH-*co*-GEP) (**16**) based on a literature procedure.[20] ^{1}H NMR spectrum (Figure 5.2) shows the characteristic peaks observed for protons **n''** and **m''** at δ = 2.42 and 2.06 ppm, respectively [as observed for the product of the ring opening polymerisation of 1-(2-(oxiran-2-ylmethoxy) ethyl) pyrrolidin-2-one, (**2**, Ch. 2, 2.3.2)]. The remaining protons **g''** to **l''** are attributed to the broad coalesced resonances between δ = 3.28 and 3.81 ppm, overlapping with the resonances associated with the chloro- (**a''** to **c''**) and iodo- (**d''** to **f''**) moieties of the starting material. If it is assumed that the chlorohydrin moiety did not react and therefore the percentage of chlorohydrin present in the final polymer **16** is the same as the starting polymer **15** at 41%, it is possible to calculate the percentage conversion of the iodohydrin. The average value for 1 proton based on the integrations for **n''** and **m''** is 0.52, therefore the total integration for the 15 protons in the pyrrolidone moiety (**g''**-**n''**) would be 7.76. The total integration for all protons in the system (**a''**-**n''**) is 32.88 (30.81 + 1.00 + 1.07), from this it is possible to calculate the estimated percentage of pyrrolidone functionality, 24%

((7.76÷32.88)*100). 41% of the total polymer is attributed to the chlorohydrin (**a''-c''**), leaving the remaining 35% corresponding to the iodohydrin protons (**d''-f''**)

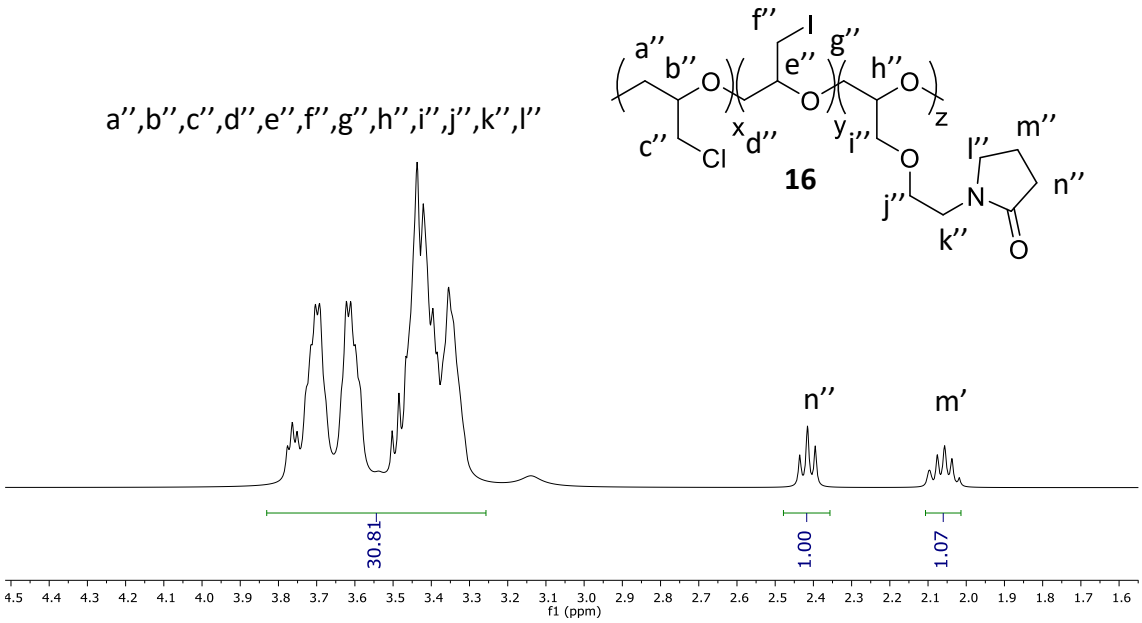

Figure 5.2 – ^{1}H NMR spectrum of polymer 16

The retention of the chloro- and iodo- functionality in the final polymer is undesirable for applications such as drug delivery systems due to associated toxicity. Therefore, the advancement of this synthesis was not pursued.

In summary, the Finkelstein reaction replaced an estimated 59% of the halogen groups from chloro- to iodo- to produce the random copolymer P(ECH-*co*-EIH), **15**. The percentage conversion was calculated based on ^{1}H NMR analysis. The copolymer **15** was then further reacted with HEP with the aim of functionalising the polymer with the pyrrolidone moiety to give P(ECH-*co*-EIH-*co*-GEP) (**16**). The final estimated composition of the polymer based on ^{1}H NMR analysis was 24% pyrrolidone, 35% PEIH and 41% PECH, assuming no chlorohydrin reacted in the second step of the reaction.

5.3.2 Functionalisation of Poly(butadiene)

With the limited success of homo and copolymerisation of 1-(2-(oxiran-2-ylmethoxy) ethyl) pyrrolidin-2-one (**2**) (Ch. 2, 2.3.1) by direct and indirect synthetic strategies, the focus expanded to include polymer modification. Polybutadiene was chosen due to reports of successful polyhydroxylation reactions.[22]

5.3.2.1 Route 1 *via* Polyhydroxylated Polybutadiene, (17)

Polyhydroxylated polybutadiene (PHPB) was synthesised *via* a hydroboration-oxidation reaction as described in the literature (Scheme 5.7). [17] The PHPB was chosen as a the polybutadiene (PB) starting material is comercially available and the synthesis is well established. The polymer produced would contain many terminal hydroxyl groups capable of undergoing further modification.

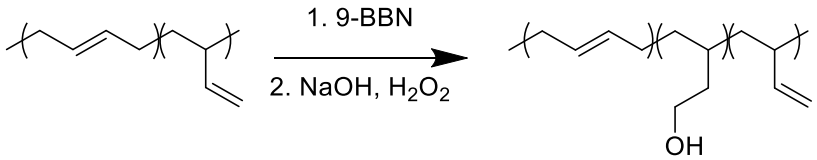

17

Scheme 5.7 – Synthesis of polyhydroxylated polybutadiene (PHPB, 17) *via* hydroboration-oxidation

The molecular weight of the PB starting material was described as 2.0×10^4 to 2.2×10^4 $gmol^{-1}$ from the vendor however, SEC analysis determined the M_n to be 3.7×10^3 $gmol^{-1}$ with a Đ of 1.42. The SEC analysis was conducted in THF solvent using a conventional calibration using polystyrene standards. In addition to this, the product was advertised as approximately 90% 1,2-addition, though the percentage of 1,2-addition determined by ^1H NMR analysis was found to be 72%. The calculation was based on the integration of protons **b** + **e** a broad resonance at δ = 5.27-5.66 ppm and, **f** at δ = 4.97 ppm (Figure 5.3) following Equation 5.1. The integral of **b** was determined to be 0.19, 28% of the total, indicating that 72% of the polymer was 1,2-addition. All calculations were relative to the determined molecular weight and percentage 1,2-addition.

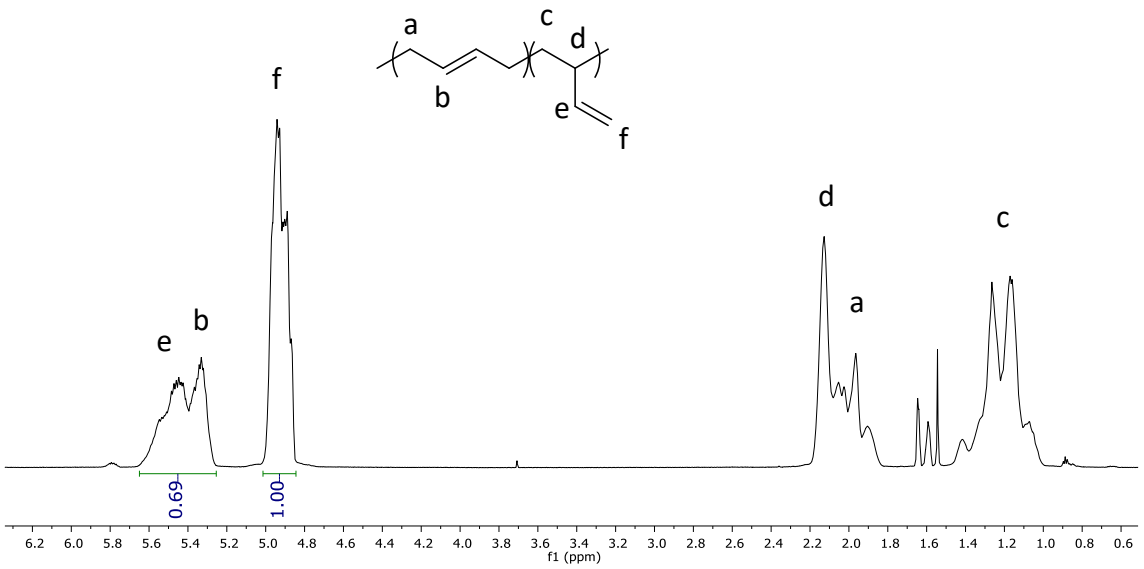

Figure 5.3 – ^{1}H NMR spectrum of polybutadiene

$$\int (e + b) - \left(\frac{\int f}{2}\right) = \int b$$

Equation 5.1 – Calculation to determine relative integral of proton b, where ∫e=(∫f÷2)

The ^{1}H NMR spectrum of **17** (Figure 5.4) contains two new signals when compared to the PB starting material (Figure 5.3). The resonance at δ = 3.38 ppm is attributed to the proton **j** which is in correlation to previously reported literature.[22] The broad resonance at δ = 4.17 ppm corresponds to the OH environment within the polymer. There is a notable decrease in the resonance associated with **f** at δ = 4.29 ppm due to the conversion of pendant vinyl groups. Protons **e** and **b** are observed as a broad resonance at δ = 5.34 ppm with a slight reduction observed for **e**. There is also a decrease observed for **d** around δ = 2.10 ppm. Protons **a** is at δ = 1.94 ppm as found in the starting material. There is a large, broad resonance from δ = 0.80-1.65 ppm which is assigned to the overlapping resonances of the proton environments **c**, **g**, **h** and **i**. Once again, it was possible to determine the conversion by ^{1}H NMR analysis, in the same way as for the PB starting material. Conversion was determined with the integrals for **b** + **e**, **f** and **j** and 74% of the 1.2-addition was found to be converted to the hydroxylated moiety. The composition of **17** was determined to be 28% 1,4-addition, 19%, 1,2-addition and 53% hydroxylated, showing that the hydroboration

reaction occurs only at the 1,2-addition alkene and not the 1,4-addition alkene units, as expected due to the regioselectivity of the hydroboration mechanism.

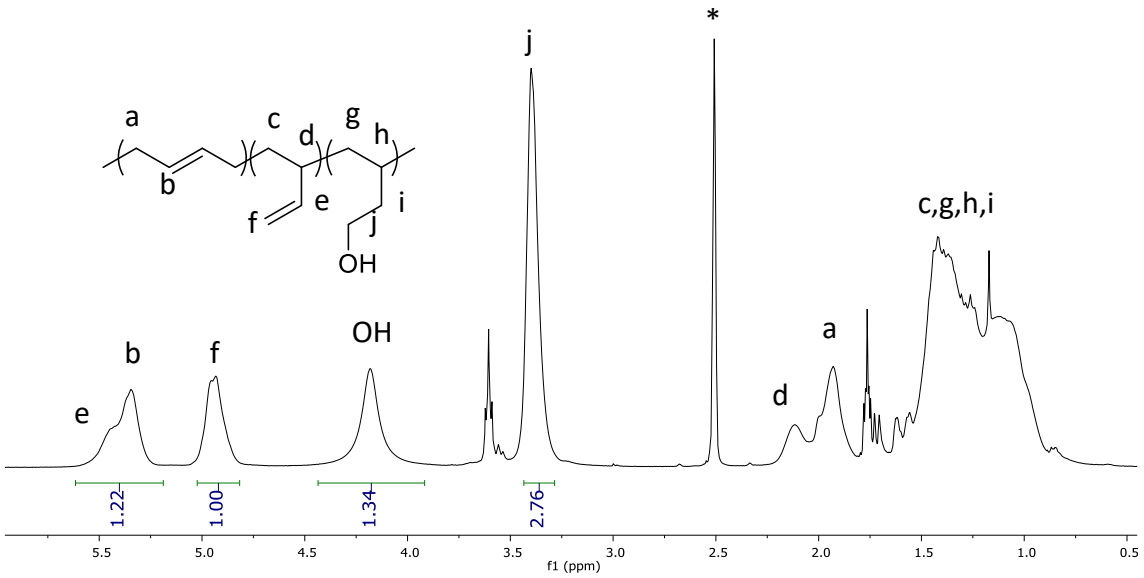

Figure 5.4 – ^{1}H NMR spectrum of polymer 17

The broad resonance at δ = 4.17 ppm was observed in the spectra for every reaction conducted by this method. The resonance shows no correlation in the 2D NMR spectra (COSY, HSQC or HMBC) and a shift can be seen between spectra of the purified polymers (Figure 5.5). The resonance is also observed in the PSYCHE NMR spectrum as a broad resonance, indicating that it is due to the averaging of a large number of resonances and not one single resonance. It is postulated that this resonance is due to the exchangeable proton of the hydroxylated group.

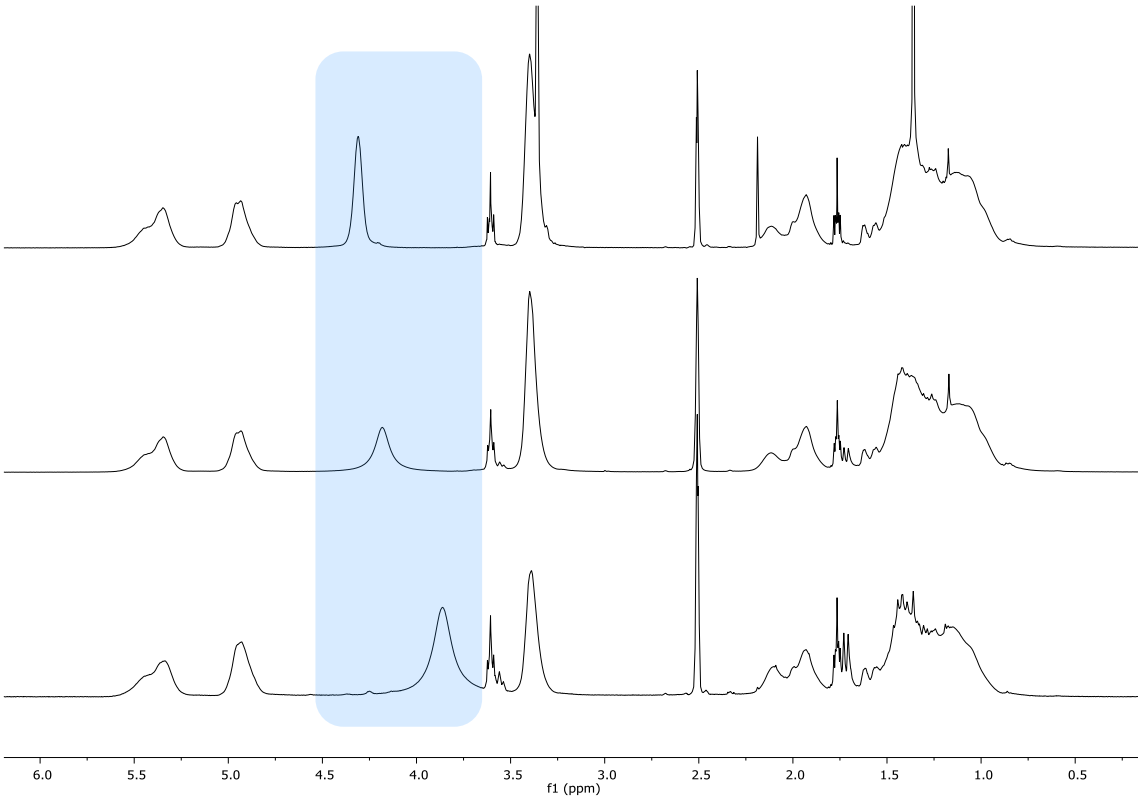

Figure 5.5 – Stacked ^{1}H NMR spectra of polyhydroxylated polybutadiene (PHPB, 17) showing shift of OH resonance

The characterisation was confirmed by ^{13}C, COSY, HSQC and HMBC NMR spectroscopy and the polymer further analysed by TGA, DSC and FTIR spectroscopy. The polymer was taken forward for further modification.

PHPB synthesised by the hydroboration-oxidation of PB (Scheme 5.7) was modified with 1-(2-(oxiran-2-ylmethoxy) ethyl) pyrrolidin-2-one (**1**) to produce the novel polymer polypyrrolidonated polybutadiene (PPPB, **18**) (Scheme 5.8).

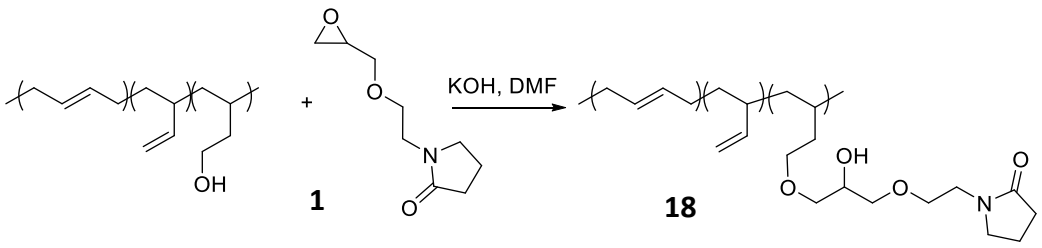

Scheme 5.8 – Synthesis of polypyrrolidonated polybutadiene (PPPB, 18)

The ^{1}H NMR spectrum of **18** (Figure 5.6) shows that the resonance for the terminal OH group (observed in Figure 5.4 and Figure 5.5) has significantly changed under similar pH conditions, indicating that the terminal OH groups have reacted. The intense, broad resonance from δ = 3.12-3.78 ppm is attributed to protons **n**, **o**, **q**, **r**, **s** and **t** which are overlapping with water that is trapped within the polymer. The protons associated with unmodified polybutadiene still present within the polymer (**a**, **b**, **c**, **d**, **e** and **f**) are observed at the shifts expected, as observed in the starting material PB and PHPB **17**. The resonances at δ = 1.89 and 2.19 ppm are associated with **u** and **v**, respectively. Protons **k**, **l** and **m** are ascribed to the broad resonance between δ = 0.89-1.61 ppm.

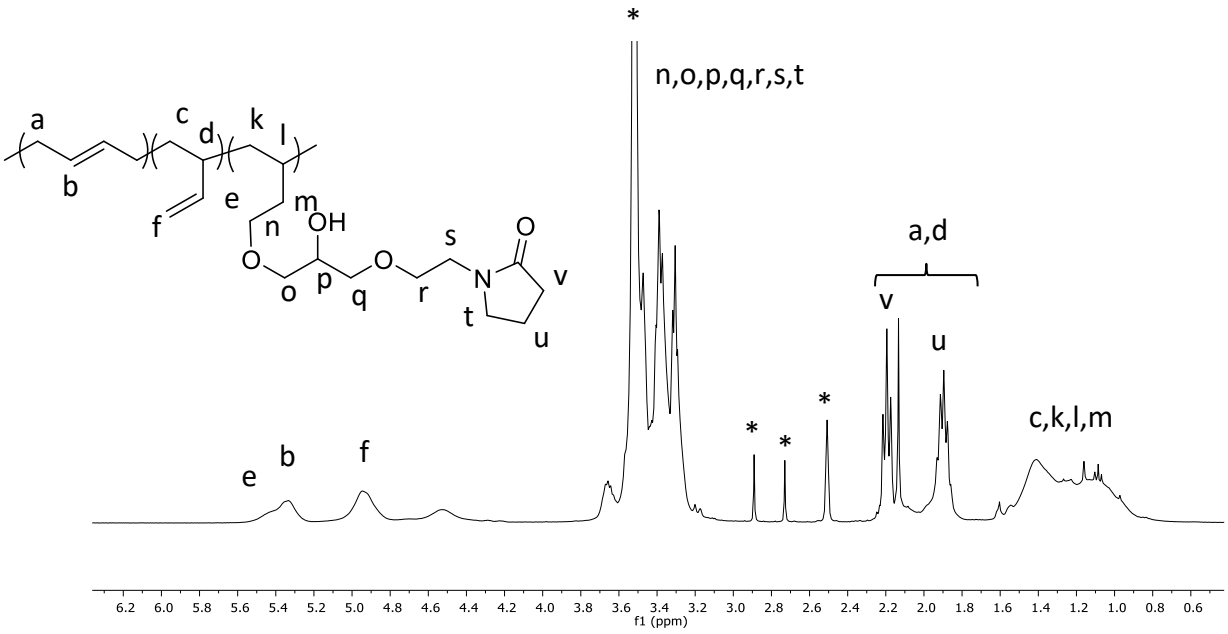

Figure 5.6 – ^{1}H NMR spectrum of polypyrrolidonated polybutadiene (PPPB, 18)

The ^{13}C NMR spectrum (Figure 5.7) shows the broad resonances expected for the remaining 1,4-addition polybutadiene units (**A** - **F**) as well as additional resonances for the incorporated pyrrolidone unit. The characteristic carbonyl of the pyrrolidone group is observed at δ = 174.5 ppm, **W**. Full analysis of the NMR spectra was aided by the HSQC-Total Correlation Spectroscopy (TOCSY) experiment resolved in the carbon dimension (Figure 5.8) in addition to standard ^{1}H-^{13}C HSQC NMR spectroscopy (Figure 5.9).

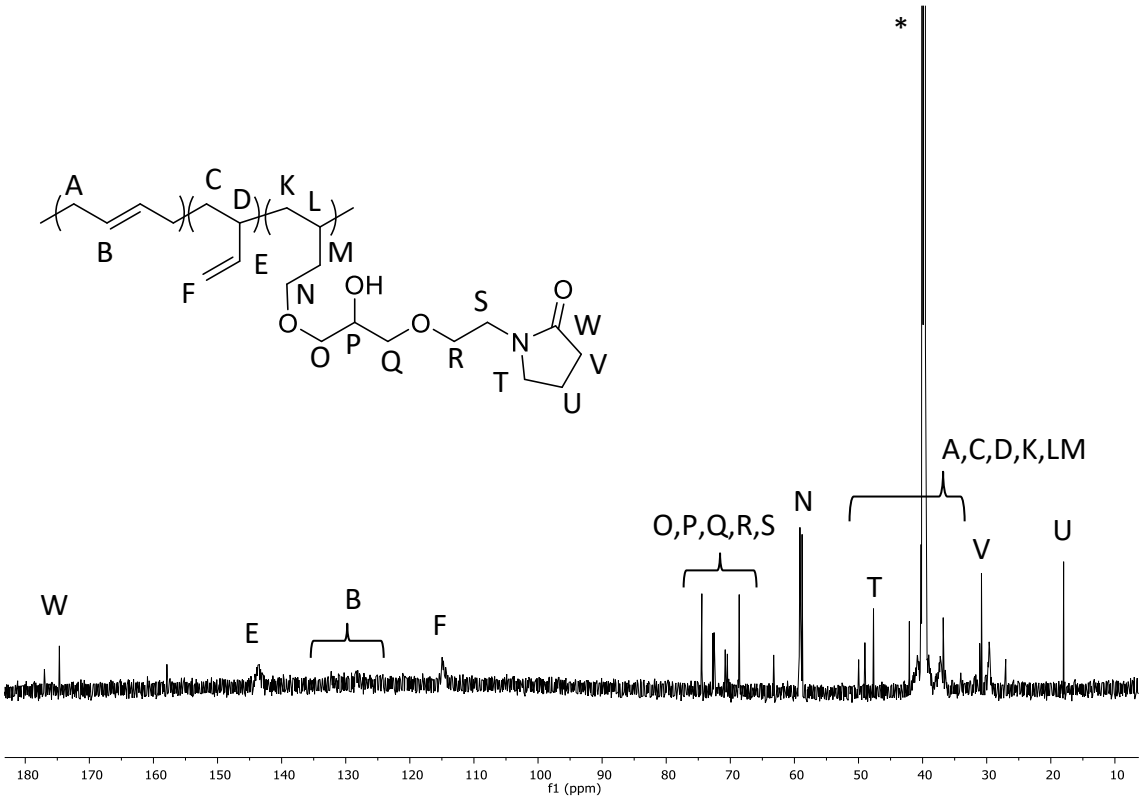

Figure 5.7 – ^{13}C NMR spectrum of polypyrrolidonated polybutadiene (PPPB, 18)

This NMR experiment is an extremely useful analytical method, particularly when resonances in the proton spectrum overlap preventing full elucidation. The HSQC-TOCSY spectrum shows a correlation resonance for protons adjacent to each other allowing simplified characterisation. A correlation is observed in the HSQC-TOCSY spectrum (Figure 5.8) between protons **v**, **u** and one peak in the broad resonance from δ = 3.22 to 3.54 ppm, and, the carbon resonance at δ = 17.8 ppm. The same pattern is observed for the carbon resonances at δ = 30.6 and 47.4 ppm. These three resonances are attributed to the lactam of the pyrrolidone group. From the HSQC spectrum (Figure 5.9) it is possible to discern that the carbon resonance at δ = 17.8 ppm is attributed to **U**, δ = 30.6 ppm to **V** and δ = 47.4 ppm to **T**.

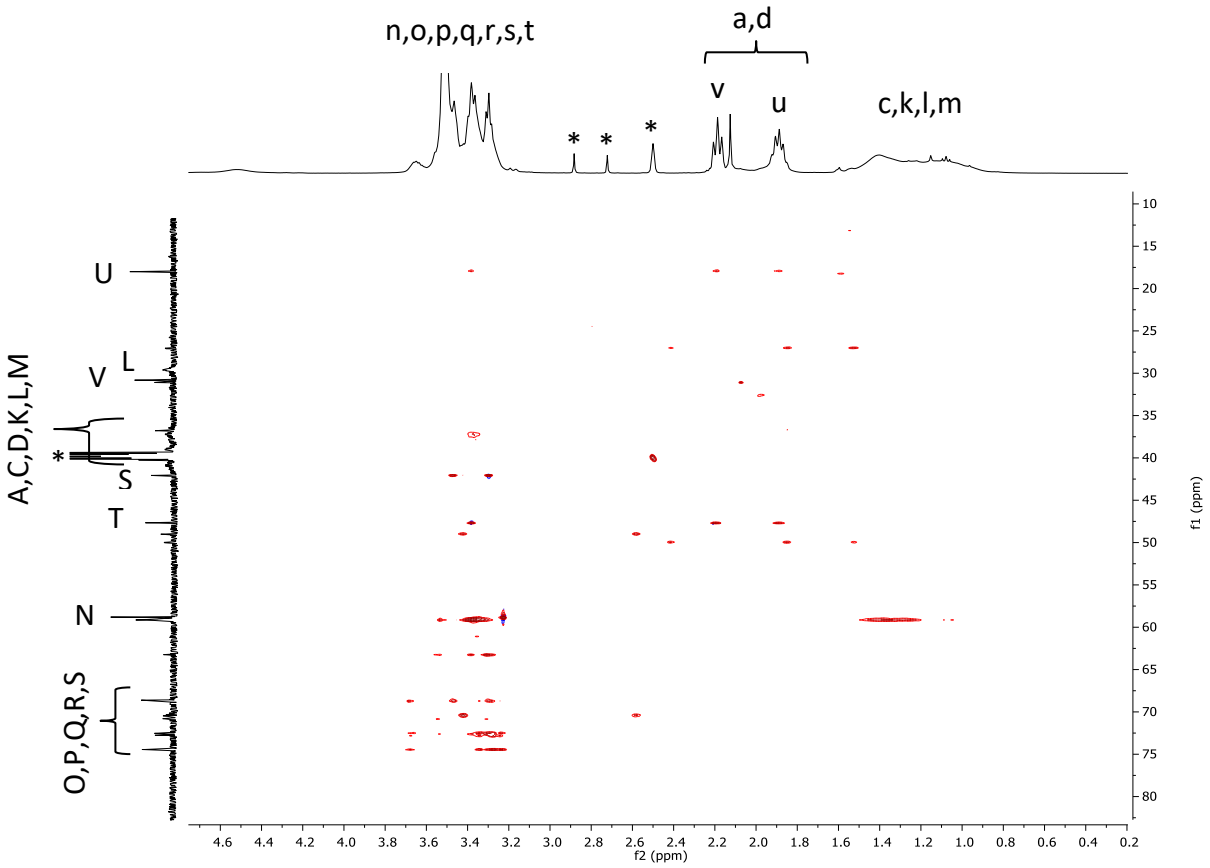

Figure 5.8 – ^{1}H-^{13}C HSQC-TOCSY NMR spectrum of polypyrrolidonated polybutadiene (PPPB, 18)

There are number of broad resonances at δ = 36.6, 39.5 (overlapping with d_6-DMSO) and 40.6 and ppm which show a majority correlation in the same phase at other CH_2 carbon environments in the spectrum (blue), suggesting that these are due to the CH_2 environments in and adjacent to the polymer backbone (**A**, **C**, **K**, and **M**). There are also three correlations observed in the opposite phase (red) indicating that these are attributed to the CH environments of the polymer backbone (**D** and **L**). No correlation is observed in the HSQC-TOCSY spectrum (Figure 5.8) for these environments due to the sensitivity of the technique. A strong correlation is observed (Figure 5.8) for the carbon resonance at δ = 58.9 ppm and the hydrogen environments of the polymer backbone, this resonance is attributed to carbon **N**. It is also evident from the HSQC spectrum (Figure 5.9) that the carbon resonances between δ = 68.4 and 74.2 ppm are ascribed to the pyrrolidone carbon environments **O** to **S**.

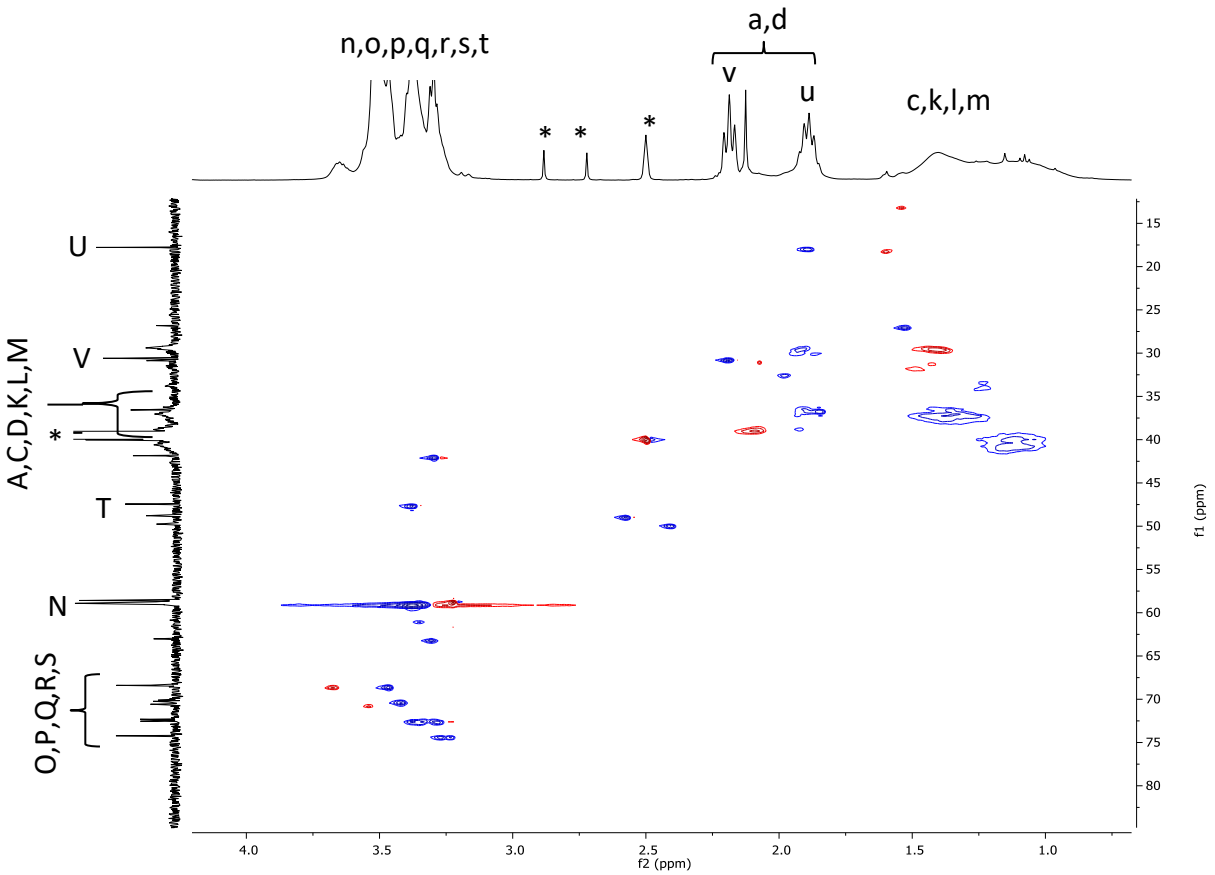

Figure 5.9 – ^{1}H-^{13}C HSQC NMR spectrum of polypyrrolidonated polybutadiene (PPPB, 18)

In addition to 1D and 2D NMR spectra, the polymer was analysed by FTIR, MALDI mass analysis and thermal analysis techniques TGA and DSC. It was not possible to analyse the polymer by SEC as it was not soluble in THF solvent.

The FTIR spectrum showed the expected bands for CH and CH_2 stretches at 2919 and 2862 cm^{-1} as well as the carbonyl stretch at 1666 cm^{-1}. There was also a broad OH stretch observed at 3345 cm^{-1} indicating intramolecularly hydrogen bonded OH[23]. In the fingerprint region a C-O stretch at 1107 cm^{-1} was observed.

The TGA thermogram (Figure 5.10) showed two major thermal degradation events in addition to the loss of water below 200 °C, 10.442% of the sample. The first major thermal decomposition has an onset X_1 = 298 °C with a maximum in the first derivative of 310 °C. The second event has an onset of X_2 = 457 °C with a maximum in the first derivative of 483 °C. The X_1 is reduced for the PPPB when compared to the PHPB, this suggests that the

addition of a longer side chain produces a polymer with greater flexibility and therefore decreased thermal decomposition temperature. It is postulated that X_2 is due to random chain scission of the PB backbone as this is also observed in the PHPB starting material and the TGA of the PB starting material was determined to be 470 °C. DSC analysis showed the T_g to be -28 °C which is similar to the PB starting material (-32 °C).

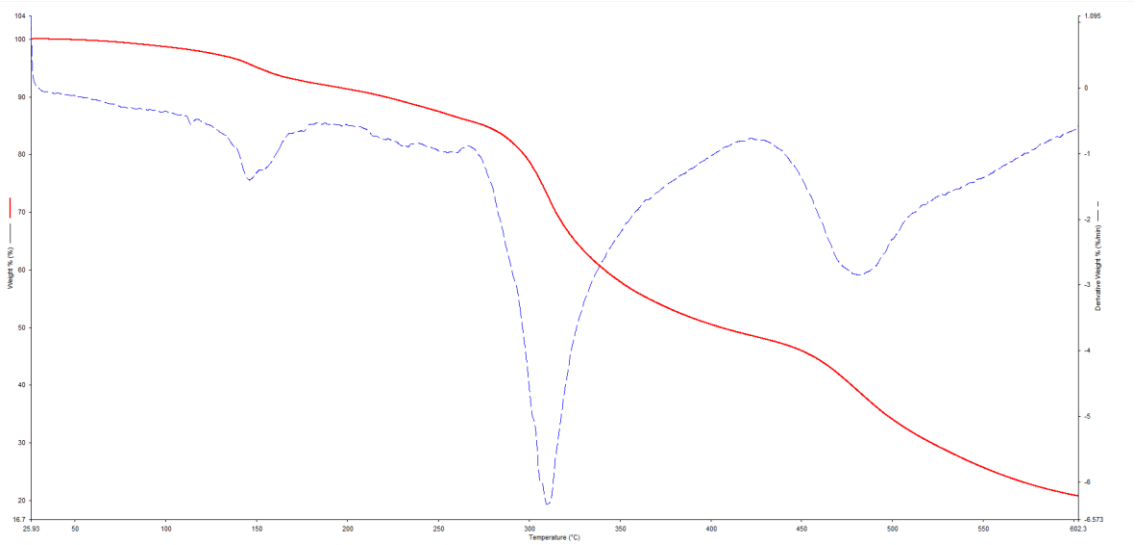

Figure 5.10 – TGA thermogram for polypyrrolidonated polybutadiene (PPPB, 18, red line) and first derivative (blue line)

MALDI analysis was conducted with trans-2-[3-(4-tert-Butylphenyl)-2-methyl-2-propenylidene]malononitrile (DCTB) matrix with both linear and reflectron analysis methods, however, no polymer molecular weight analysis could be deduced from the spectra obtained.

In summary, the polypyrrolidonated polybutadiene (PPPB, **18**) was synthesised *via* the hydroboration-oxidation of polybutadiene (PB) followed by subsequent reaction with 1-(2-(oxiran-2-ylmethoxy) ethyl) pyrrolidin-2-one (**1**). The polymer was characterised 1D and 2D NMR, FTIR, DSC and TGA analysis, MALDI mass analysis did not allow any polymer molecular weight deductions to be made. Due to the remaining alkene units from the polybutadiene, this polymer would have limited applicability as a drug binder, stabiliser and, carrier.

Therefore it was necessary to devise an alternative method to synthesis a fully pyrrolidone functionalised polymer based on polybutadiene.

5.3.2.2 Route 2 *via* Tholether-Polyhydroxylated Polybutadiene, (19)

From the same starting PB discussed above, polyhydroxylated polybutadiene was synthesised *via* a thiol-ene 'click' reaction to produce a thioether-polyhydroxylated polybutadiene (TPHPB), **19** (Scheme 5.9). 'Click' reactions are simple, highly efficient and robust, making them an excellent tool for organic synthesis. The reaction was attempted under photochemical radical conditions, however, no reaction was found after 48h exposure to a UV source. Therefore, the reaction was conducted under thermal radical conditions.

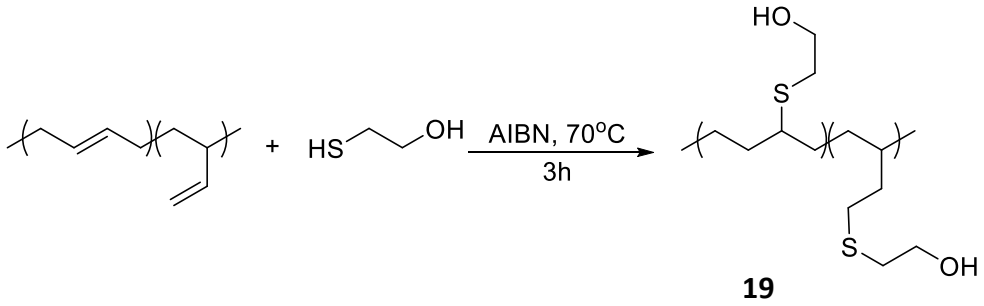

Scheme 5.9 – Synthesis of thiol-ene modified polyhydroxylated polybutadiene (TPHPB, 19)

The polymer was recovered with multiple precipitations to remove any unreacted 2-mercaptoethanol as it was in excess. The ^{1}H NMR spectrum of the isolated polymer (Figure 5.11) shows the resonances associated with this known polymer; the OH protons (**c**,**c'**) are ascribed to the resonance at δ = 4.72 ppm, **b**,**b'** at δ = 3.51 ppm, **a**,**a'** at δ = 2.54 ppm and, the resonances associated with the CH and CH_2 of the polymer backbone were observed between δ = 0.79-2.17 ppm. In addition to ^{13}C and 2D NMR techniques, the polymer was further analysed by FTIR, SEC, DSC and TGA analysis. It was deduced from the analysis that 100% of the alkene bonds had reacted to form the thioether linkage producing a polymer with multiple hydroxyl groups along the whole polymer. No evidence of radical ring closing reactions was found.[24]

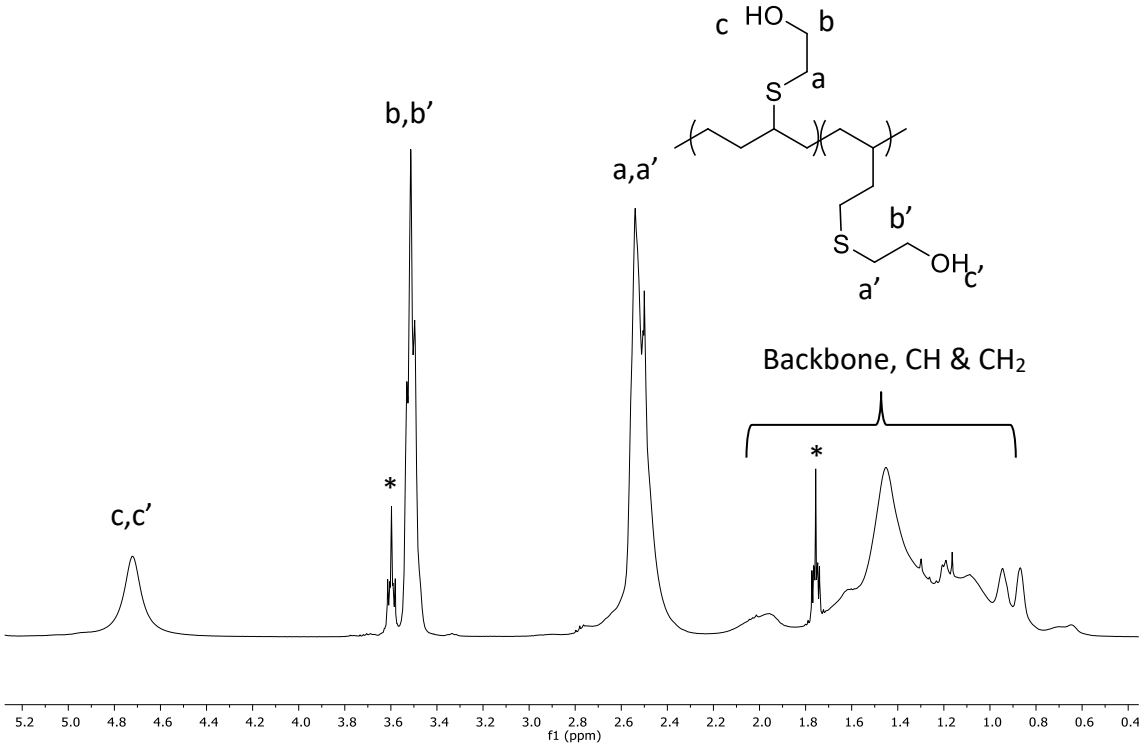

Figure 5.11 – ^{1}H NMR spectrum of thioether-polyhydroxylated polybutadiene (TPHPB, 19)

The TPHPB was further modified by the reaction with 1-(2-(oxiran-2-ylmethoxy) ethyl) pyrrolidin-2-one (**1**) as shown in Scheme 5.10 to produce the thioether-polypyrrolidonated polybutadiene (TPPPB), **20**.

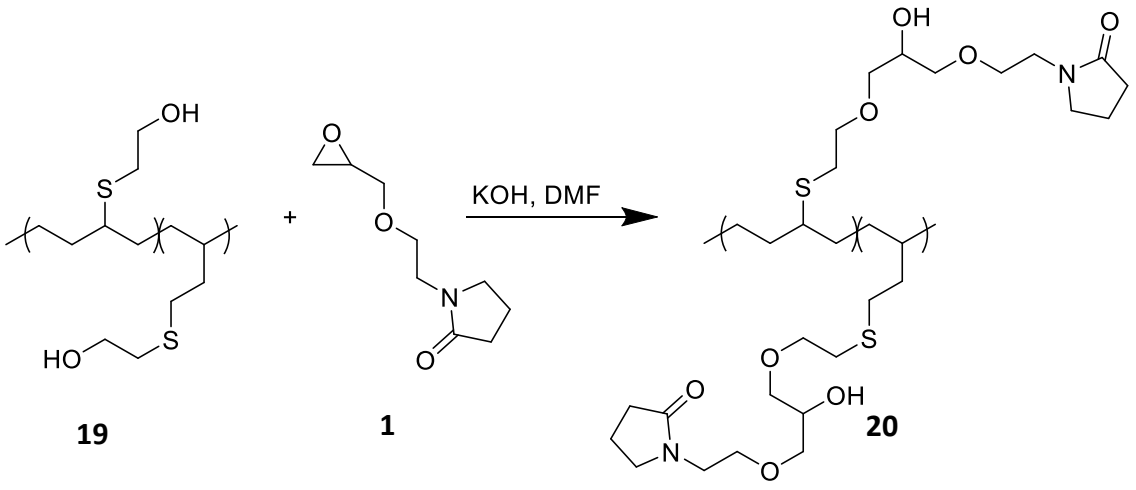

Scheme 5.10 – Synthesis of thioether-polypyrrolidonated polybutadiene (TPPPB, 20)

The polymer was preliminary analysed by ^{1}H and ^{13}C NMR as well as COSY, HSQC and HMBC NMR analysis. The ^{1}H NMR spectrum (Figure 5.12) showed a dramatic decrease in the resonances at δ = 4.72 ppm which correspond to the O**H** of the starting TPHPB (**19**) as described above. However, it is not possible to calculate the percentage conversion due to overlapping resonances in the ^{1}H NMR spectrum (Figure 5.12). Full analysis of the NMR spectra was achieved with ^{13}C and 2D NMR experiments, discussed below. The backbone CH and CH_2 protons are observed in the broad resonance at δ = 0.78-2.09 ppm. The pyrrolidone ring protons **i**, **i'** and **h**, **h'** are attributed to the resonances at δ = 1.89 and 2.18 ppm, respectively. The resonances at δ = 2.55 and 2.63 ppm are assigned to CH_2S protons of the backbone and **a**, **a'** of the pedant group. There are many overlapping resonances between δ = 3.17 and 3.67 ppm, it is not possible to assign protons **e**, **e'**, **f**, **f'**, **g**, **g'** to a specific signal in this region. It is possible to assign **c**, **c'** to the resonance at δ = 3.31, **j**, **j'** δ = 3.39 , **b**, **b'** δ = 3.51 and, **d**, **d'** δ = 3.67 ppm.

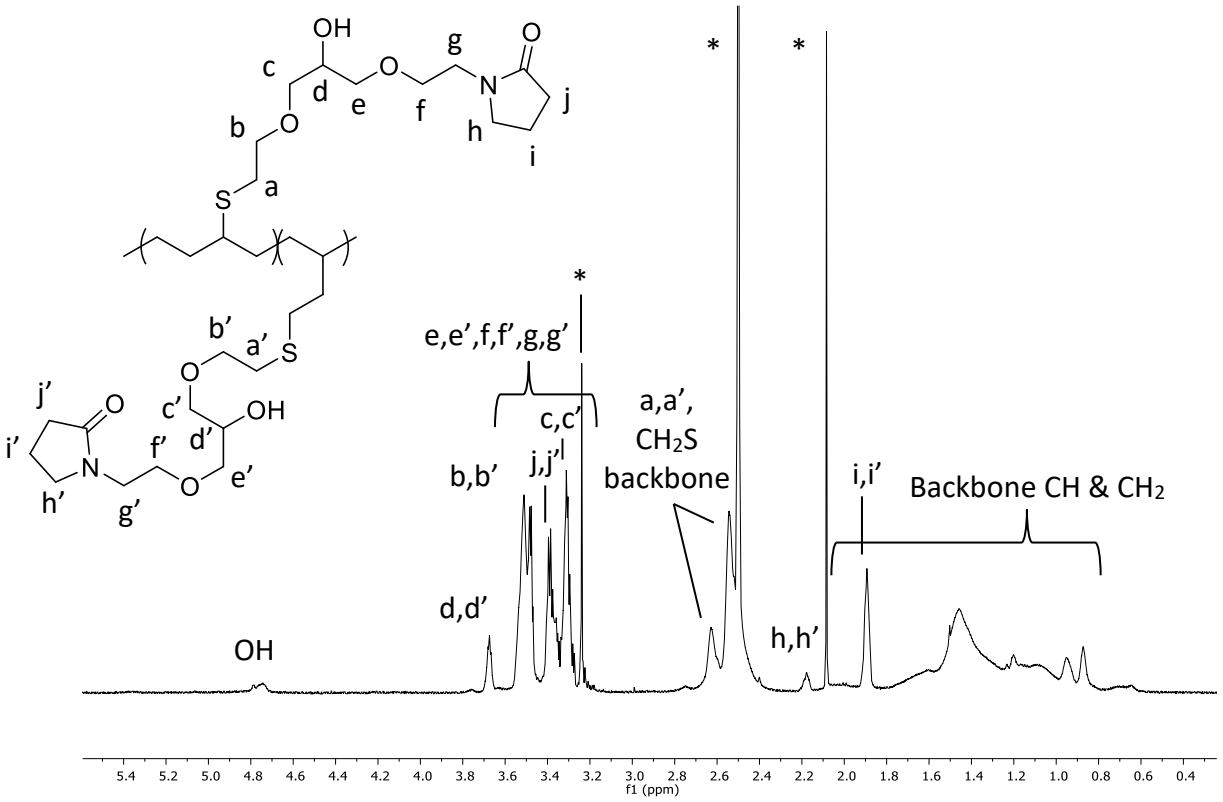

Figure 5.12 – ^{1}H NMR spectrum of thioether-polypyrrolidonated polybutadiene (TPPPB, 20)

It was deduced that the reaction achieved 100% conversion based on the disappearance of the **C**H_2OH resonance observed in the ^{13}C NMR spectrum of the starting material at δ = 61.4 and 61.7 ppm (Figure 5.13). ^{13}C NMR determination was aided by the ^{1}H-^{13}C HSQC spectrum (Figure 5.14). The pyrrolidone carbonyl resonance (**K**, **K'**) was identified at δ = 173.8 ppm.

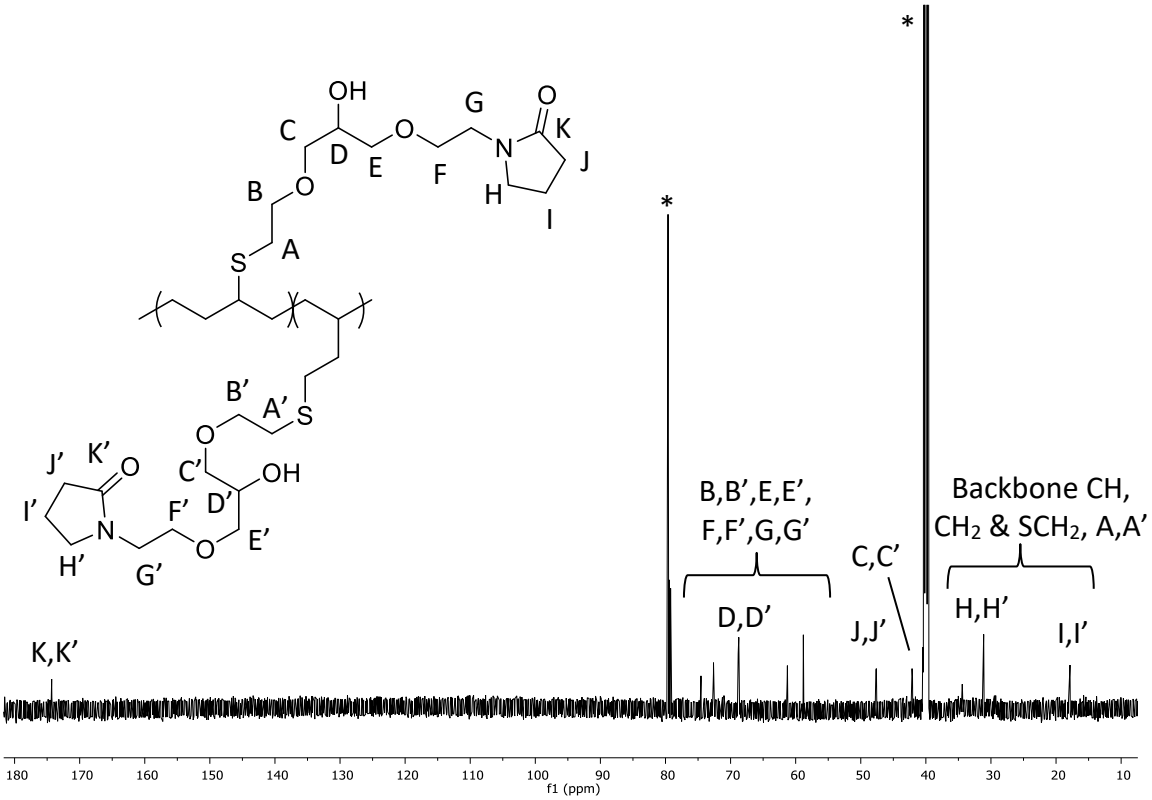

Figure 5.13 – ^{13}C NMR spectrum of thioether-polypyrrolidonated polybutadiene (TPPPB, 20)

The ^{1}H-^{13}C HSQC NMR spectrum (Figure 5.14) shows the correlations for the protons of the CH and CH_2 environments of the polymer backbone to be spread over a large range in the ^{13}C NMR spectrum (from δ = 11.3 to 34.2 ppm). As the resonances are spread over a large range, the backbone carbon resonances are not clearly observed in the ^{13}C NMR spectrum, with only a small broad resonance observed at δ = 34.0 ppm (Figure 5.13). This is due to the sensitivity of the technique and that there are sharp peaks observed for the flexible parts of the polymer chain which allow more tumbling. Carbon environments **D** and **D'** are identified due to the phase of the correlation in the ^{1}H-^{13}C HSQC NMR spectrum (Figure 5.14). Protons

c,**c'** are correlated to the carbon resonance at δ = 41.7 ppm, therefore this is identified at carbon **C**,**C'**. Likewise, carbon **J**,**J'** are observed at δ = 47.1 ppm. Carbon environments **B**,**B'**,**E**,**E'**,**F**,**F'**, and **G**,**G'** are observed between δ = 61.3 and 74.6 ppm.

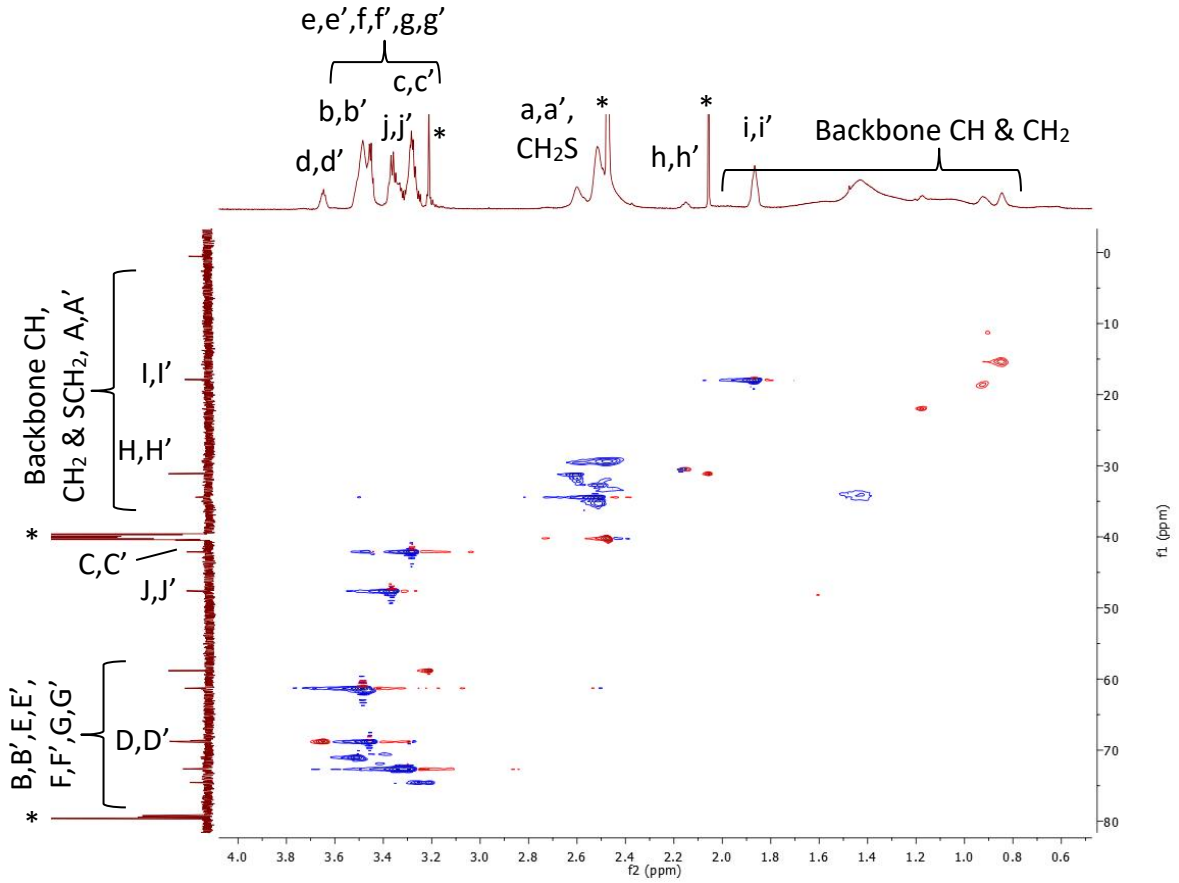

Figure 5.14 – ^{1}H-^{13}C HSQC NMR correlation spectrum of thioether-polypyrrolidonated polybutadiene (TPPPB, 20)

The polymer produced is not soluble in THF solvent, therefore, we were unable to characterise the polymer molecular weight by SEC. Interestingly, the TPPPB is soluble in water where TPHPB is not. FTIR analysis exhibited a broad OH band at 3323 cm^{-1} as well as the pyrrolidone carbonyl stretch at 1659 cm^{-1}, a double band for the CH & CH_2 stretching at 2930 and 2871 cm^{-1} and a C-O stretch at 1104 cm^{-1}. Due to time constraints, further analysis including TGA, DSC and MALDI mass analysis were not achieved for this interesting polymer. The complete conversion of the alkene units in the thiol-ene 'click' reaction led to the

formation of, essentially, a functionalised polyolefin which could lead to wide ranging applications.[2]

In summary, the synthesis of TPPPB **20** *via* the thiol-ene 'click' reaction of 2-mercaptoethanol and PB, followed by further functionalisation with 1-(2-(oxiran-2-ylmethoxy) ethyl) pyrrolidin-2-one (**1**) produced a functionalised polymer containing no alkene units. In addition 1D and 2D NMR techniques, **20** was characterised by FTIR analysis. It was not possible to determine the conversion from PHPB (**19**) to TPPPB (**22**) due to overlapping signals in the ^{1}H NMR spectrum. However ^{13}C NMR analysis showed the disappearance of the resonance associated with **C**H_2OH in **19**, indicating full coversion to the pyrrolidonated polymer. Preliminary anaylsis suggests the TPHPB (**19**) was functionalised with the pyrrolidone moiety as the final polymer (**20**) was soluble in water. This synthetic pathway to an alkene free pyrrolidone functionalised polymer was found to be an improvement upon route 1 *via* the hydroboration-oxidation of PB (discussed above).[19]

5.3.3 Functionalisation of poly(vinyl alcohol-*graft*-hyperbranched polyglycerol), (21)

From the success in utilising 1-(2-(oxiran-2-ylmethoxy) ethyl) pyrrolidone or glycidyl ethylpyrrolidone (GEP, **1**) in the post-polymerisation functionalisation of PB, the objective was applied to poly(vinyl alcohol-*graft*-hyperbranched polyglycerol) (PVA-*g*-hPG). The PVA-*g*-hPG was synthesised by Dr. Peter King by first synthesising the hyperbranched polyglycerol (hPG) then grafting-to the low molecular weight polyvinyl alcohol (PVA), as described in the literature.[19] The subsequent pyrrolidone functionalisation reaction was carried out on PVA-*g*-hPG with a hPG content of 28% and 36% based on ^{1}H NMR calculations of the starting material. The synthesis of polyvinyl alcohol-*graft*-hyperbranched polyglycerol-glycidyl ethylpyrrolidone (PVA-*g*-hPG-GEP, **21**) was conducted under benign reaction conditions to allow for simple industrial application (Scheme 5.11).

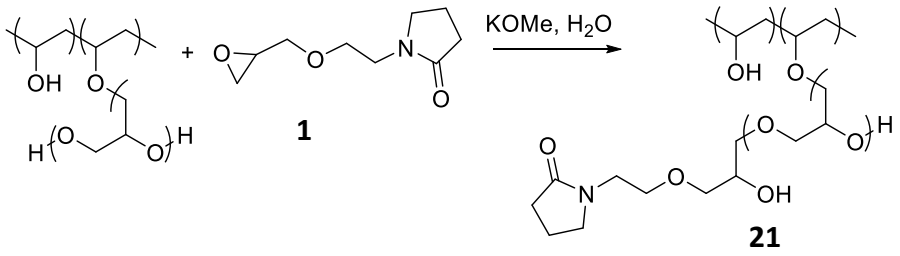

Scheme 5.11 – Synthesis of poly(vinyl alcohol-*graft*-hyperbranched polyglycerol-glycidyl ethylpyrrolidone) (PVA-*g*-hPG-GEP, 21)

The ^{1}H NMR spectrum (Figure 5.15) displays the broad resonances of the starting material and the characteristic resonances associated with the two CH_2 groups in the pyrrolidone ring (**m** and **n**). Full NMR characterisation was possible with ^{13}C and 2D NMR experiments, discussed below.

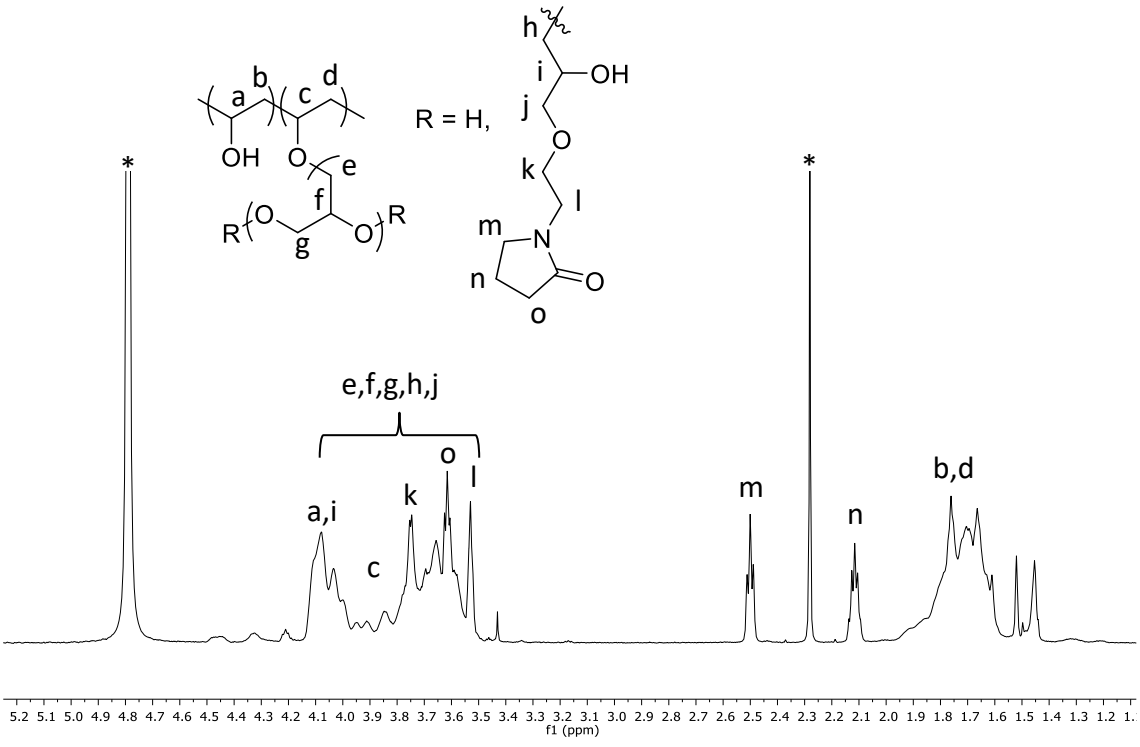

Figure 5.15 – ^{1}H NMR spectrum of poly(vinyl alcohol-*graft*-hyperbranched polyglycerol-glycidyl ethylpyrrolidone) (PVA-*g*-hPG-GEP, 21)

From the ratio of proton **m** to **b**,**d** an estimate of the percentage of the degree of pyrrolidonation (%D(Py)) can be achieved using Equation 5.2. The %D(Py) for PVA-*g*-hPG-GEP with a hPG content of 28 and 36% was determined to be 5% and 10%, respectively. ^{1}H-

^{1}H COSY NMR spectroscopy showed the correlation pattern associated with the ethylpyrrolidone moiety (Figure 5.16).

$$\%D(Py) = \frac{\int m}{(\int b, d + \int m)}$$

Equation 5.2 – Calculation to determine degree of pyrrolidonation (%D(Py))

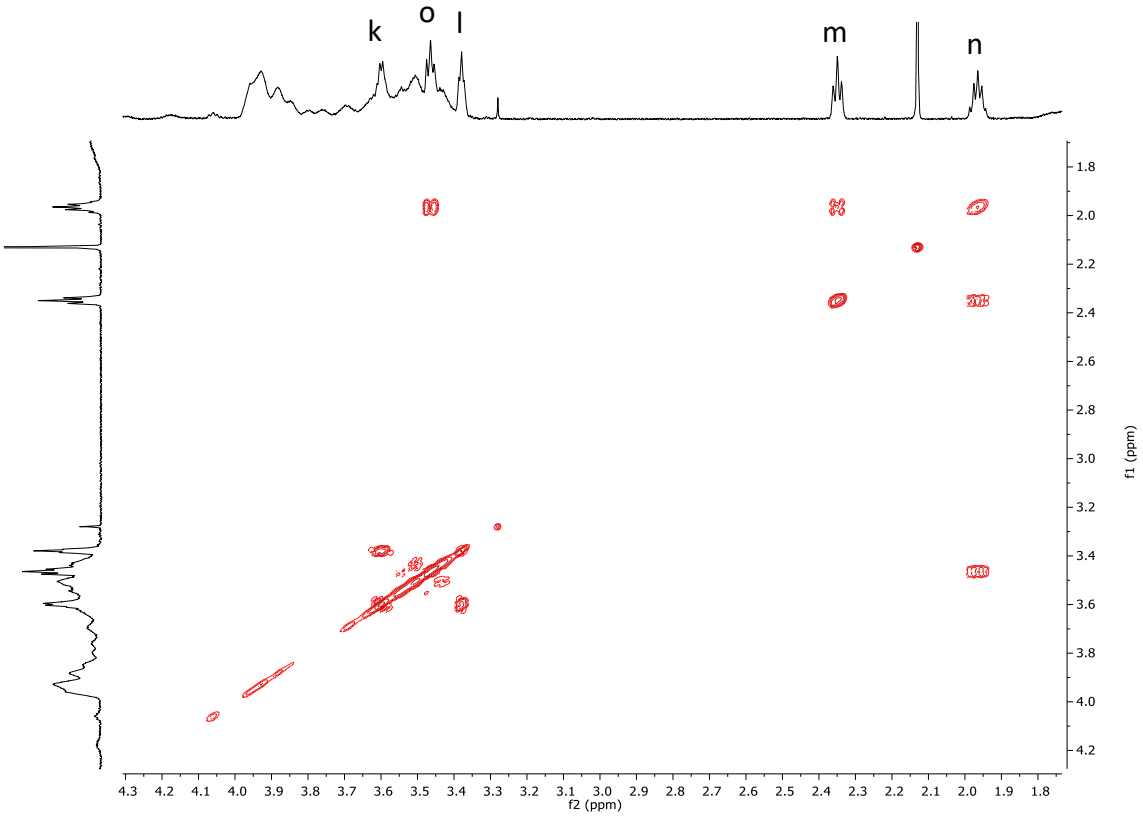

Figure 5.16 – ^{1}H-^{1}H COSY NMR spectrum of poly(vinyl alcohol-*graft*-hyperbranched polyglycerol-glycidyl ethylpyrrolidone) (PVA-*g*-hPG-GEP, 21)

^{13}C NMR analysis revealed more detail about the nature of the GEP addition. The carbonyl of the pyrrolidone is visible at δ = 178.5 ppm (**O** and **C'**), carbons **Z** and **L'** at δ = 31.3 ppm and **A'** and **N'** at δ = 17.5 ppm. The broad resonances associated with the polymer backbone carbons **B** and **D** are observed at δ = 44.2 and 41.3 ppm, respectively. Interestingly the resonances for the resonance for the primary **C**H_2OH (**P**) found at δ = 60.1 ppm in the starting material, is not observed in the ^{13}C NMR spectrum of **21**. Also, the intensity of the resonance at δ = 62.7 ppm is reduced, indicating a change in environment. However, the

secondary **C**HOH environments, **I**, **L** and **O** are evident in the ^{13}C NMR spectrum (Figure 5.17).

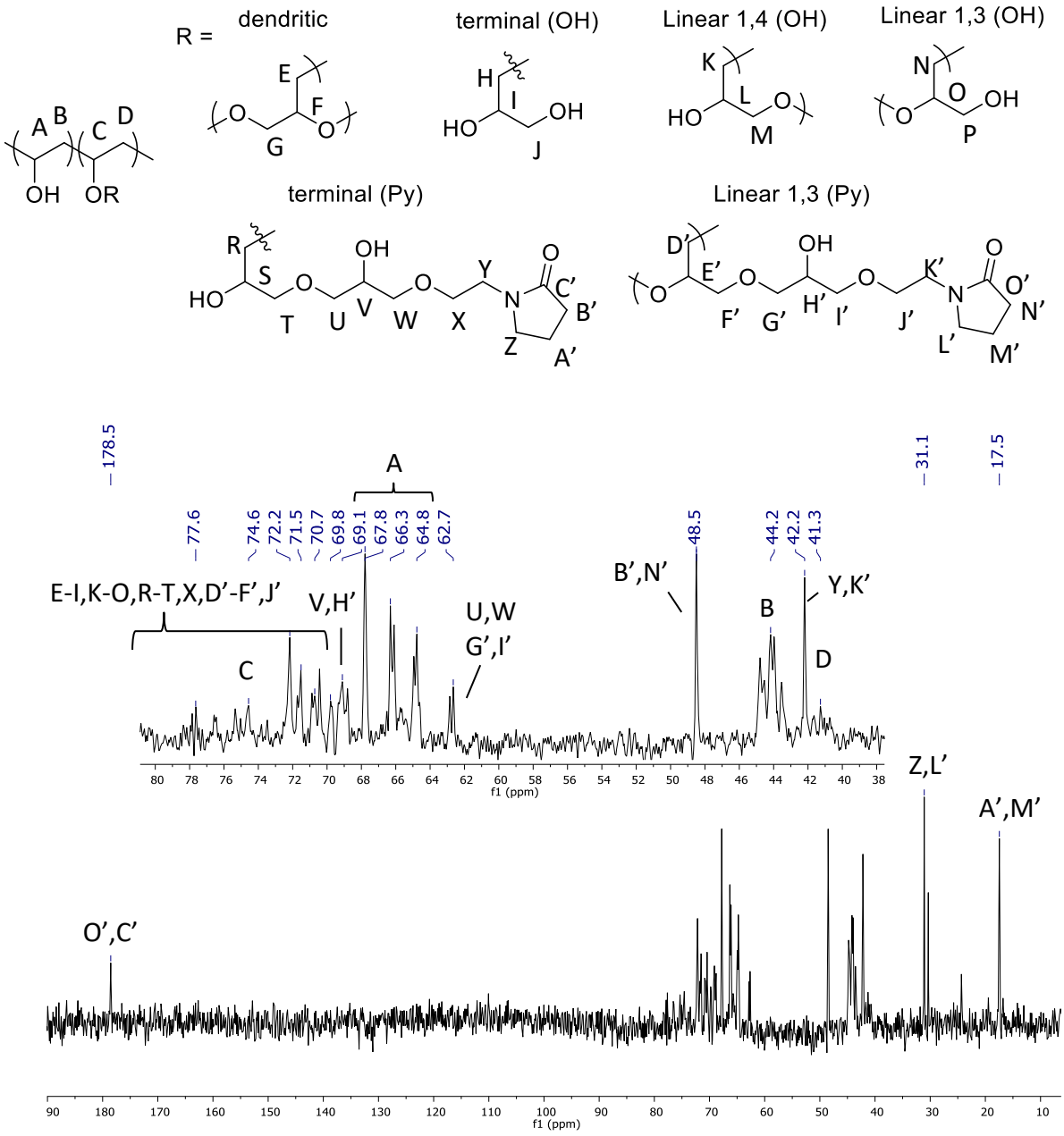

Figure 5.17 – ^{13}C NMR spectrum of poly(vinyl alcohol-*graft*-hyperbranched polyglycerol-glycidyl ethylpyrrolidone) (PVA-*g*-hPG-GEP, 21), with expanded section

To investigate if the secondary OH groups would react with the GEP, the reaction was carried out with PVA starting material under the same reaction conditions (Scheme 5.12).

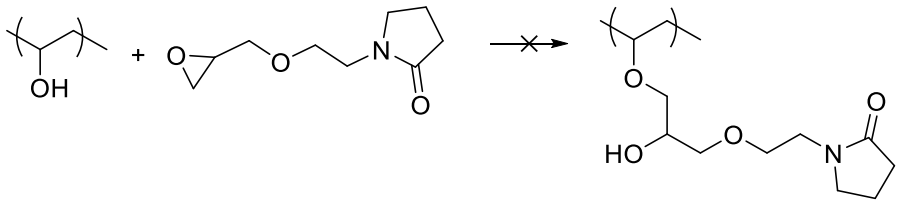

Scheme 5.12 – Attempted reaction of PVA and 1 (GEP)

No functionalised polymer was obtained from the reaction and only PVA and GEP were isolated. Therefore, it was assumed that only primary OH groups reacted with the GEP.

23 was further analysed by FTIR, MALDI, DSC and TGA analysis. The FTIR spectrum exhibited a broad OH stretch at 3338 cm^{-1}, CH and CH_2 stretching bands at 2940 and 2889 cm^{-1} and a carbonyl stretch at 1658 cm^{-1} in the main region. In the fingerprint region, a broad band was observed for the ether linkage (CO) stretch at 1096 cm^{-1}.

The first derivative in the TGA thermogram of 28% hPG content (**21**, Figure 5.18) displayed a two-stage thermal degradation process whereas the starting PVA-*g*-hPG only showed one. The first onset is observed at 176 °C with a maximum in the first derivative at 199 °C. The second onset is at 244 °C with a maximum in the first derivative at 231 °C. Dr. Peter King determined the degradation temperature of the PVA-*g*-hPG starting material to be the same as the PVA it was synthesised from, between 244 to 267 °C.[19] PVA-*g*-hPG-GEP with 36% hPG content also showed two thermal events however, the degradation temperatures were much higher with X_1 = 308 °C and X_2 = 405 °C (Table 5.1). As the degradation of the PVA-*g*-hPG was, on average, the same regardless of hPG content, the cause of the increase must be due to the pyrrolidonation of the primary OH groups.

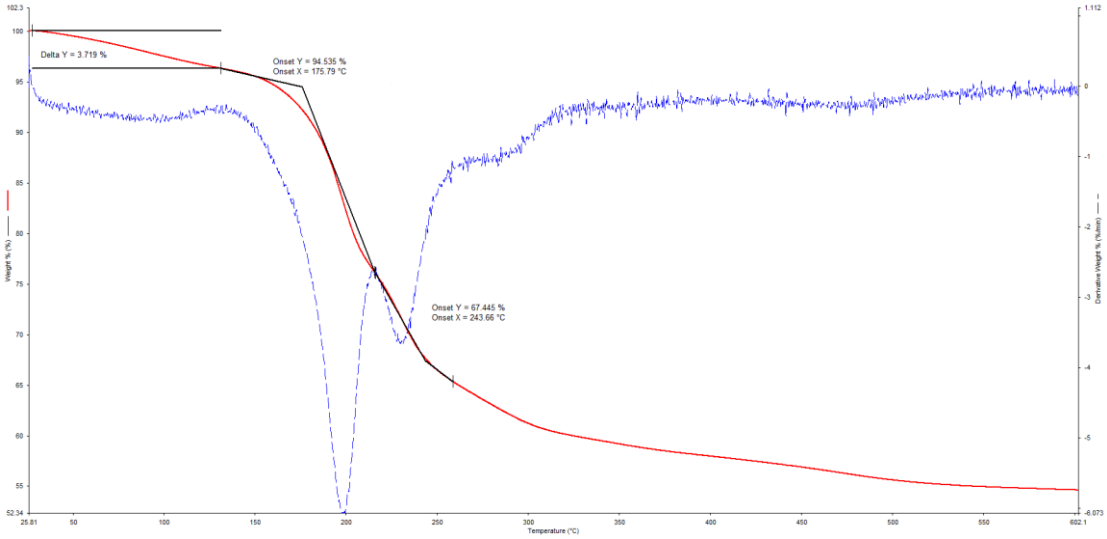

Figure 5.18 – TGA of poly(vinyl alcohol-*graft*-hyperbranched polyglycerol-glycidyl ethylpyrrolidone) (PVA-*g*-hPG-GEP, 26% hPG, 21), red line and, first derivative, blue line

The DSC thermogram of the 36% grafted-hyperbranched polyglycerol (*g*-hPG, Figure 5.19) displays a glass transition (T_g) at 115 °C and a melting temperature (T_m) of 242 °C. Both the T_g and T_m are higher than the PVA-*g*-hPG starting material which displays a T_g of 49 °C and T_m of 209 °C. This could be due to increased intramolecular hydrogen bonding between chains with the incorporation of the pyrrolidone moiety. No crystallisation temperature (T_c) was observed for PVA-*g*-hPG-GEP with 28% or 36% hPG content. It is postulated that the incorporation of the ethylpyrrolidone unit disrupts the crystallinity of the polymer. A reason for the difference in degradation temperatures could be differing GEP content. Unfortunately, it was not possible to explore the pyrrolidone content by ^{13}C NMR analysis within the time project frame.

Table 5.1 – DSC and TGA data for of poly(vinyl alcohol-*graft*-hyperbranched polyglycerol-glycidyl ethylpyrrolidone) (PVA-*g*-hPG-GEP, 21) with 28% and 36% hPG content

% *g*-hPG	%D(Py)	Onset X_1 /°C	Onset X_2 /°C	T_g /°C	T_m /°C
28%	5%	176	244	118	243
36%	10%	308	405	115	242

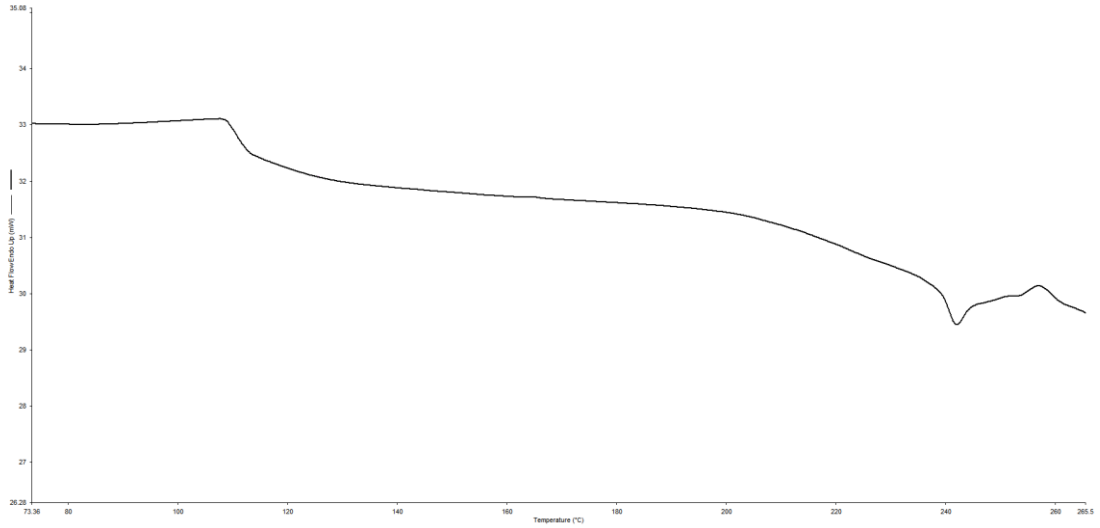

Figure 5.19 – DSC curve of poly(vinyl alcohol-*graft*-hyperbranched polyglycerol-glycidyl ethylpyrrolidone) (PVA-*g*-hPG-GEP, 36% hPG, 23), second scan

In summary, based on the synthetic work described by Dr. King, the hyperbranched polymer polyvinyl alcohol-*graft*-hyperbranched polyglycerol-glycidyl ethylpyrrolidone (PVA-*g*-hPG-GEP) was synthesised and characterised. The reaction was conducted in a benign solvent making the process easily applicable to an industrial plant and maintaining green chemistry standards. The glycidyl ethylpyrrolidone was found to react with the primary OH groups of the hPG side chains. The incorporation of the pyrrolidone moiety was found to increase the T_g and T_m when compared to the corresponding PVA-*g*-hPG starting material.

5.4 Conclusions

In conclusion, to expand the range of pyrrolidone containing polymers discussed in this project, the functionalisation of poly(epichlorohydrin) (PECH), poly(butadiene) (PB) and poly(vinyl alcohol-*graft*-hyperbranched polyglycerol) (PVA-*g*-hPG) was explored. As explained in chapter 2, the attempted homopolymerisation of 1-(2-(oxiran-2-ylmethoxy) ethyl) pyrrolidin-2-one or glycidly ethylpyrrolidone (GEP, **1**) was unsuccessful. The alternative method of postpolymerisation functionalisation of PECH was explored. The Finkelstein reaction was estimated to convert 59% of the halogen groups to the more reaction iodide, producing a random copolymer, P(ECH-*co*-EIH) **15**. The pyrrolidonation of the P(ECH-*co*-EIH) resulted in an estimated 24% pyrrolidone content of the final polymer. The presence of the residual chloro and iodo functional groups would limit the possible applications of this polymer, therefore further investigations into this synthesis were not concluded.

Monomer **1** (GEP) was utilised to functionalise PB *via* two routes. The hydroboration-oxidation of PB produced a polyhydroxylated polybutadiene (**17**) with a composition of 28% 1,4-addition, 19%, 1,2-addition and 53% hydroxylated, indicating that the pendant alkene units were hydrolysed. The conversion of OH to pyrrolidone functionality in **18** was estimated to be 100% based on ^{1}H NMR characterisation. However, the residual alkene functionality of the starting material may impede the application possibilities. Therefore the synthesis of thioether-polyhydroxylated polybutadiene (TPPPB, **19**) *via* a thiol-ene 'click' reaction was explored. The thiol-ene 'click' reaction was found to convert all alkene units to the hydroxyl terminated thioether units. Preliminary anaylsis of the pyrrolidonation product, TPHPB (**20**) suggests that the functionalisation was succesful as the final polymer was soluble in water.

The hyperbranched polymer poly(vinyl alcohol-*graft*-hyperbranched glycerol-glycidyl ethylpyrrolidone) (PVA-*g*-hPG-GEP, **21**) was functionalised with glycidyl ethyl pyrrolidone. The reaction can be considered 'green' due to the benign nature of the solvent and base

used. Based on ^{13}C NMR analysis, it is suggested that the GEP reacted predominantly with primary OH groups of the hPG side chains. The T_g and T_m of the PVA-*g*-hPG-GEP (**21**) were found to be increased with the incorporation of the pyrrolidone group. The degradation temperature was also increased. This could be due to increased hydrogen bonding.

5.5 References

1 K. A. Günay, P. Theato and H. A. Klok, *Funct. Polym. by Post-Polymerization Modif. Concepts, Guidel. Appl.*, **2013**, 1–44.

2 N. K. Boaen and M. Hillmyer, *Chem. Soc. Rev.*, **2005**, 34, 267–275.

3 C. D. Vo, P. D. Iddon and S. P. Armes, *Polymer (Guildf).*, **2007**, 48, 1193–1202.

4 K. A. Y. Koivu, H. Sadeghifar, P. A. Nousiainen, D. S. Argyropoulos and J. Sipilä, *ACS Sustain. Chem. Eng.*, **2016**, 4, 5238–5247.

5 X. Jian and A. S. Hay, *J. Polym. Sci. Part C Polym. Lett.*, **1990**, 28, 285–288.

6 M. M. A. Nikje and H. Hajifatheali, *Polym. Plast. Technol. Eng.*, **2011**, 50, 1071–1076.

7 J. Bai, H. Li, Z. Shi and J. Yin, *Macromolecules*, **2015**, 48, 3539–3546.

8 J. Van Damme, O. van den Berg, J. Brancart, L. Vlaminck, C. Huyck, G. Van Assche, B. Van Mele and F. Du Prez, *Macromolecules*, **2017**, 50, 1930–1938.

9 O. Pop-georgievski, *Macromolecules*, **2017**, 50, 1302–1311.

10 B. A. Laurent and S. M. Grayson, *J. Am. Chem. Soc.*, **2006**, 128, 4238–4239.

11 N. V. Tsarevsky, S. A. Bencherif and K. Matyjaszewski, *Macromolecules*, **2007**, 40, 4439–4445.

12 C. J. Galvin and J. Genzer, *Prog. Polym. Sci.*, **2012**, 37, 871–906.

13 J. A. Kent, *Kent and Riegel's Handbook of Industrial Chemistry and Biotechnology*, Springer Science & Buisness Media LLC., **2010**.

14 C. M. Geiselhart, J. T. Offenloch, H. Mutlu and C. Barner-Kowollik, *ACS Macro Lett.*, **2016**, 5, 1146–1151.

15 H. Yamaguchi, K. Azuma and Y. Minoura, *Polym. J.*, **1972**, 3, 12–20.

16 T. Chung, M. Raate, E. Berluche and D. Schulz, *Am. Chem. Soc.*, **1988**, 1903–1907.

17 R. Tanaka, Y. Kasai, M. Shinzawa, Z. Cai, Y. Nakayama and T. Shiono, *Macromol. Chem. Phys.*, **2014**, 215, 888–892.

18 M. A. Tasdelen, B. Kiskan and Y. Yagci, *Prog. Polym. Sci.*, **2016**, 52, 19–78.

19 P. King, O. M. Musa and E. Khosravi, *J. Polym. Sci. Part A Polym. Chem.*, **2017**, in press.

20 Composition and Methods for the Treatment of Metabolic Syndrome and Diabetes, WO 087307, **2014**.

21 E. Schacht, D. Bailer and O. Vogl, *J. Polym. Sci. Part A Polym. Chem.*, **1978**, 16, 2343–2351.

22 R. Tanaka, Y. Kasai, M. Shinzawa, Z. Cai, Y. Nakayama and T. Shiono, 888–892.

23 D. Williams and I. Fleming, *Spectroscopic Methods in Organic Chemistry*, McGraw-Hill Education Ltd., 6th edn., **2008**.

24 B. Korthals, M. C. Morant-Miñana, M. Schmid and S. Mecking, *Macromolecules*, **2010**, 43, 8071–8078.

Chapter 6

Conclusions

In conclusion, a range of novel pyrrolidone-containing polymers were synthesised, following two approaches and fully characterised. The first approach involved the design, synthesis and characterisation of known and novel pyrrolidone monomers with subsequent homo- and co- polymerisation investigations undertaken. The second route focused on the pyrrolidone functionalisation or pyrrolidonation of well-defined polymers.

Firstly, the known and novel monomers, 1-(2-(oxiran-2-ylmethoxy) ethyl) pyrrolidin-2-one) or glycidyl ethylpyrrolidone (GEP, **1**), 4-vinylbenzyloxy ethyl pyrrolidone (**2**) and 5-ethacryloxyethyl-12-ethylpyrrolidyl-N,N'hexane biscarbamate (**3**) were synthesised and fully characterised. The homopolymerisation of GEP (**1**) was found to produce water soluble oligomers of poly(1-(2-(oxiran-2-ylmethoxy) ethyl) pyrrolidin-2-one) (**6**). The alkoxide initiated homopolymerisation was not controlled. The copolymerisation of GEP with ethylene oxide (EO) with a benzyl alcohol/potassium naphthalenide initiating system to produce poly(1-(2-(oxiran-2-ylmethoxy) ethyl) pyrrolidin-2-one-*co*-ethylene oxide) (**9**) was unsuccessful. Under identical reaction conditions poly(ethylene oxide) (PEO) or poly(ethylene glycol) (PEG) was produced. The aluminium mediated ring opening copolymerisation of GEP and succinic anhydride produced the novel polyester **10,** poly(1-(2-(oxiran-2-ylmethoxy) ethyl) pyrrolidin-2-one-*co*-succinic anhydride). MALDI mass analysis indicated that the polymer was alternating, this should allow degradation pathways *via* ester hydrolysis along the backbone chain.

The homopolymerisation of **2** following the literature procedure was found to produce insoluble solid (poly(4-vinylbenzyloxy ethyl pyrrolidone), (**7**)). It was concluded that chain transfer reactions occurred during the free-radical polymerisation forming a cross-linked polymer network. The same conclusion was deduced for the copolymerisation of **2** with

styrene (**11**), *N*-vinyl pyrrolidone (NVP) (**12**) and hydroxyethyl acrylate (HEA) (**13**). The cross-linked materials produced were characterised by SSNMR, TGA, DSC and FTIR.

The novel monomer **3** was synthesises as a peptide mimic. The synthesis produced two by-products, a di-acrylate (**4**) and a di-pyrrolidone (**5**). The homopolymerisation *via* free-radical polymerisation produced poly(5-ethacryloxyethyl-12-ethylpyrrolidyl-N,N'hexane biscarbamate) (**8**) which is soluble in organic and aqueous media. The copolymerisation with NVP produced poly(5-ethacryloxyethyl-12-ethylpyrrolidyl-N,N'hexane biscarbamate-*co*-vinyl pyrrolidone) (**14**) which exhibited decreased thermal stability due to the interruption of hydrogen bonding between the pendant chains along the polymer backbone.

The Finkelstein reaction of poly(epichlorohydrin) produced a random copolymer, poly(epichlorohydrin-*co*-epiiodohydrin) (PECH-*co*-PEIH) (**15**) with a conversion of 59%. The subsequent pyrrolidonation of the resulted in an estimated 24% pyrrolidone content of the final polymer poly(epichlorohydrin-*co*-epiiodohydrin-glycidyl ethylpyrrolidone) (**16**). However, the residual chloro- and iodo- functionality within the polymer could limit the possible applications.

The pyrrolidonation of poly(butadiene) (PB) was achieved *via* two routes. The first route was the hydroboration-oxidation of PB followed by alkoxide mediated ring opening of GEP (**1**) onto the primary hydroxyl groups. It was found that the hydroboration-oxidation to give polyhydroxylated polybutadiene (PHPB) (**17**) did not successfully convert all the pendant vinyl groups and the product of pyrrolidonation, polypyrrolidonated polybutadiene (PPPB) (**18**), had an estimated composition of 28% 1,4-addition, 19%, 1,2-addition and 53% hydroxylated. The second route utilised thiol-ene "click" chemistry to produce thioether-polyhydroxylated polybutadiene (TPHPB) (**19**) where 100% of the alkene groups were convert into hydroxyl terminated thio-ether moieties. Preliminary analysis of the product of the pyrrolidonation reaction to give thioether-polypyrrolidonated polybutadiene (TPPPB) (**20**) indicated that the pyrrolidone moiety was successfully added to the polymer.

The hyperbranched polymer poly(vinyl alcohol-*graft*-hyperbranched polyglycerol) (PVA-*g*-hPG) was functionalised with GEP (**1**) *via* the alkoxide mediated ring opening reaction in water. GEP (**1**) was found to react with the primary hydroxyl groups of the polyglycidol

hyperbranched chains. However, the conversion could not be calculated due to overlapping ^{1}H NMR resonances. The T_g, T_m and degradation temperature of the poly(vinyl alcohol-*graft*-hyperbranched polyglycerol-glycidyl ethylpyrrolidone) (PVA-*g*-hPG-GEP) (**21**) was found to be increased with the incorporation of the pyrrolidone group. The hypothesis for this is the increased hydrogen bonding due to incorporation of the pyrrolidone functionality.

Chapter 7

Future Perspectives

As this project has shown the ability to synthesise novel pyrrolidone containing polymers with various functional groups in an industrially applicable synthesis, it would be interesting to build on the achievements made here. To this end, the properties of the polymers should be investigated to gain a more complete picture of the applications these polymers could be put to. For example, it would be interesting to look at the film forming properties of the homo- and co-polymers as well as the degradability of polyester **10**.

Looking at controlled polymerisation, such as RAFT, of the pyrrolidone monomers would provide an interesting avenue of research. It would be advantageous to work towards more complex architecture such as blocks, branches or micellar formulations.

Further investigations into the free radical homo- and co-polymerisation of 4-vinylbenzyloxy ethyl pyrrolidone (**2**) are necessary to optimise a proceedure to produce soluble polymer products. It would be interesting to use RAFT polymerisation conditions to form block copolymers of 4-vinylbenzyloxy ethyl pyrrolidone (**2**) with a hydrophilic such as *n*-vinyl pyrroldione (NVP) to see if this produced a soluble polymer.

For the copolymerisation reactions, it would also be interesting to determine the reactivity ratios of the co-monomers, especially for poly(1-(2-(oxiran-2-ylmethoxy) ethyl) pyrrolidin-2-one-*co*-succinic anhydride) (**10**). The ratios would provide more detail about the composition of the polymer produced. Cytotoxicity studies of the peptide mimic poly(5-ethacryloxyethyl-12-ethylpyrrolidyl-N,N'hexane biscarbamate) (**8**) would be extremely interesting to explore. If the results of the cytotoxicity study were ideal and no toxicity was detected, the peptide mimic could go on to be used as an effective drug binding and delivery tool. Monomer **3** (5-ethacryloxyethyl-12-ethylpyrrolidyl-N,N'hexane biscarbamate) could

also be cross-linked with the novel di-acrylate monomer (**4**), the hydrogel produced may have increased binding efficiency due to the pyrrolidone**.**

Having established 1-(2-(oxiran-2-ylmethoxy) ethyl) pyrrolidin-2-one or glycidyl ethylpyrrolidone (GEP) (**1**) as an effective pyrrolidonation agent for hydroxyl-terminated polymers, this could be taken forward onto more polymer motifs to increase solubility and complexation properties. This approach could be applied to any molecule containing a primary hydroxyl group: polymers, such as poly(hydroxyethyl (meth)acrylate), poly(glycerol mono(meth)acrylate) or natural products for example, sugars.

The thiol-ene “click” reaction with polybutadiene (PB) proved extremely successful and full analysis of the thioether-polypyrrolidonated polybutadiene (TPPPB, **20**) should be carried out.

Appendix A: Additional Characterisation data for Chapter 2

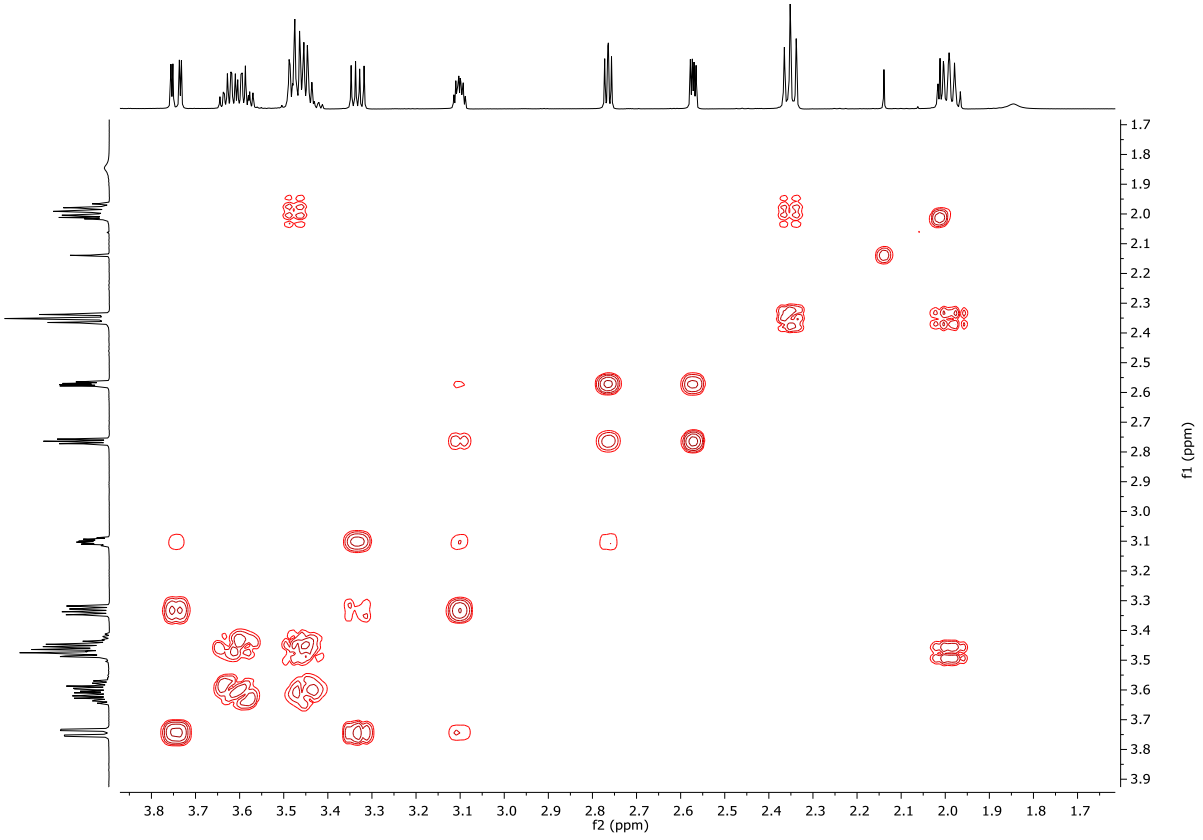

Figure A.1 – ^{1}H-^{1}H COSY NMR spectrum of monomer 1

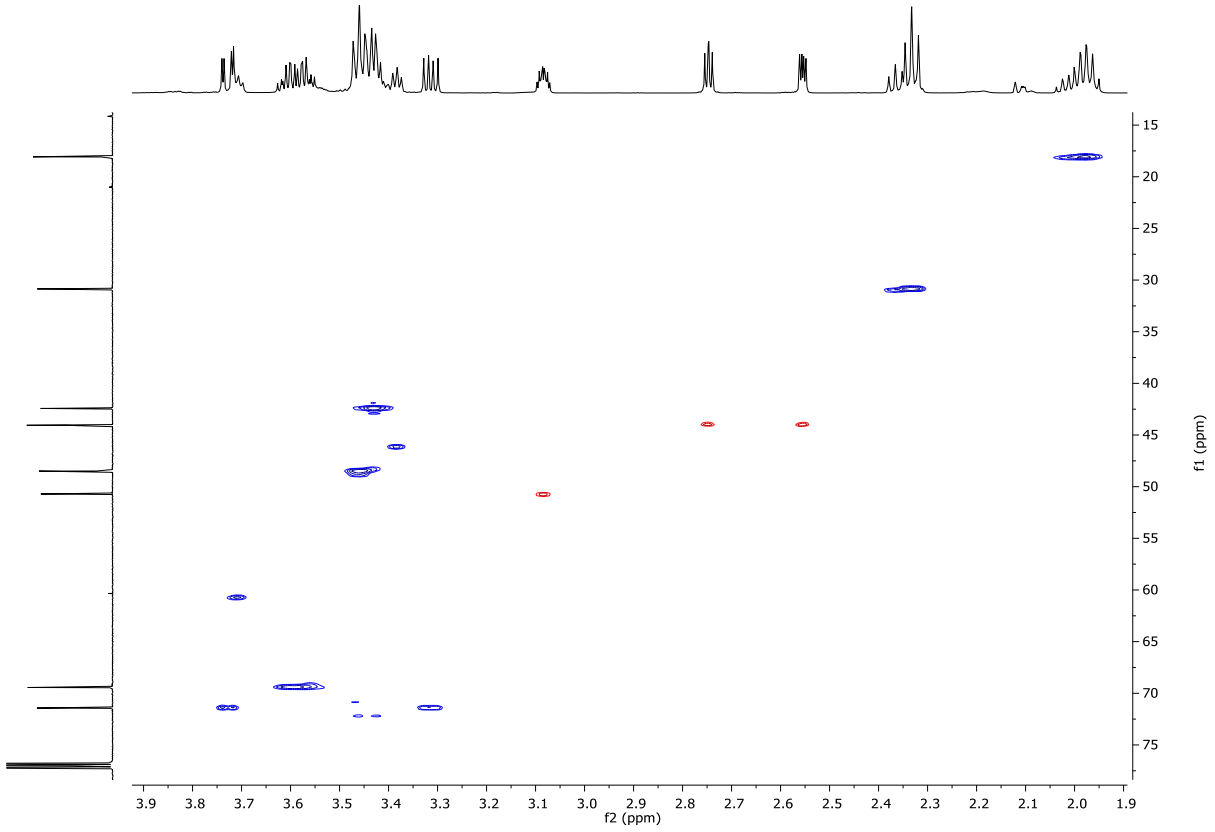

Figure A.2 – ^{1}H-^{13}C HSQC NMR spectrum of monomer 1

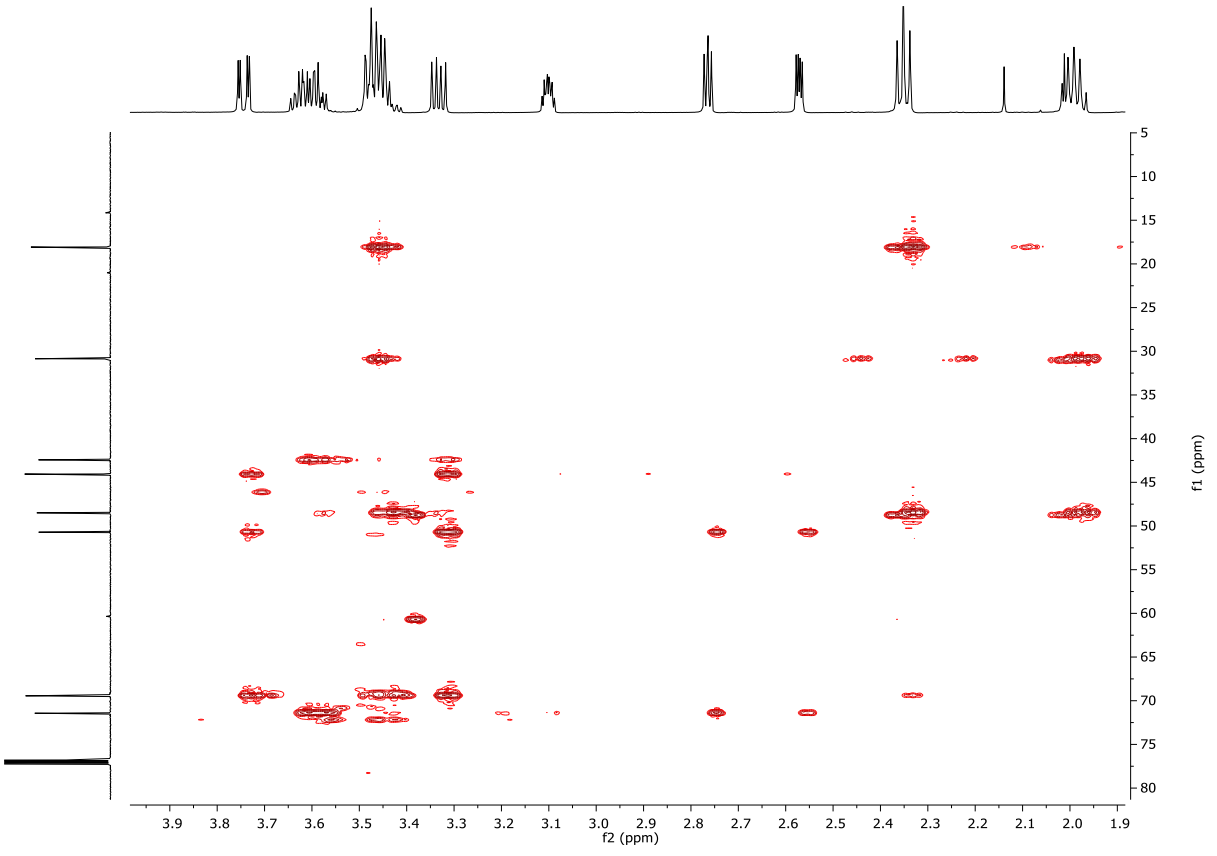

Figure A.3 – ^{1}H-^{13}C HMBC NMR spectrum of monomer 1

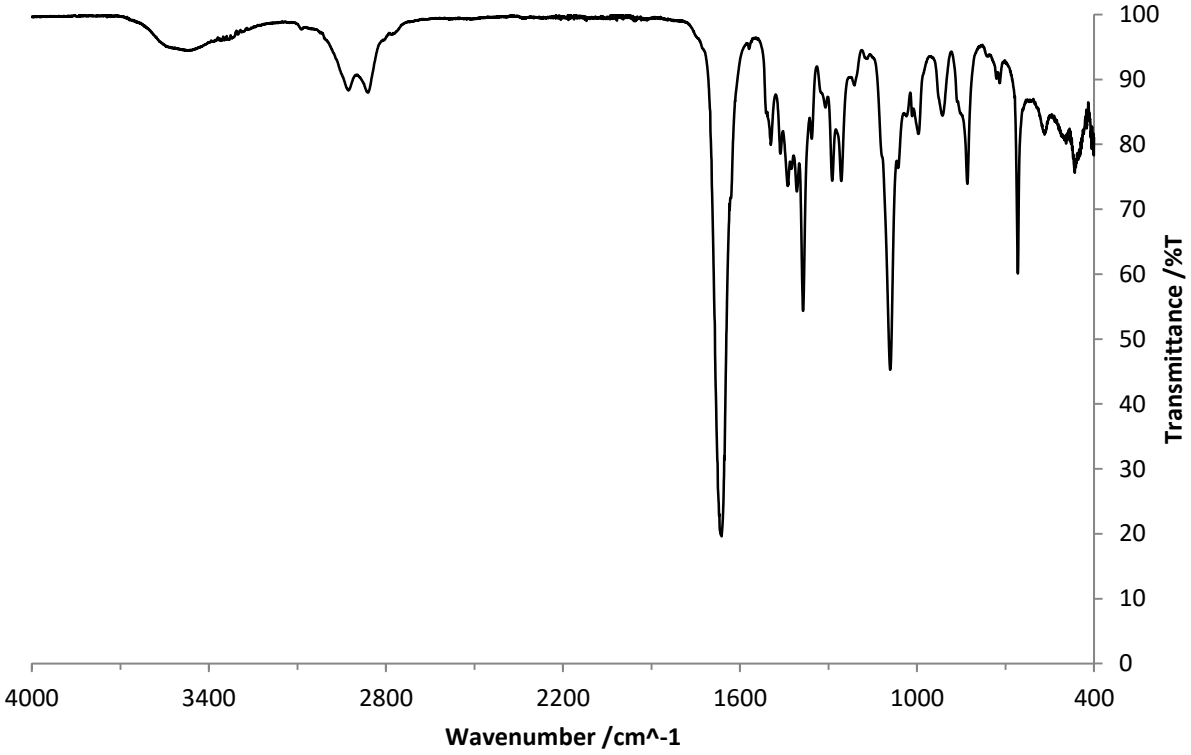

Figure A.4 – FTIR of monomer 1

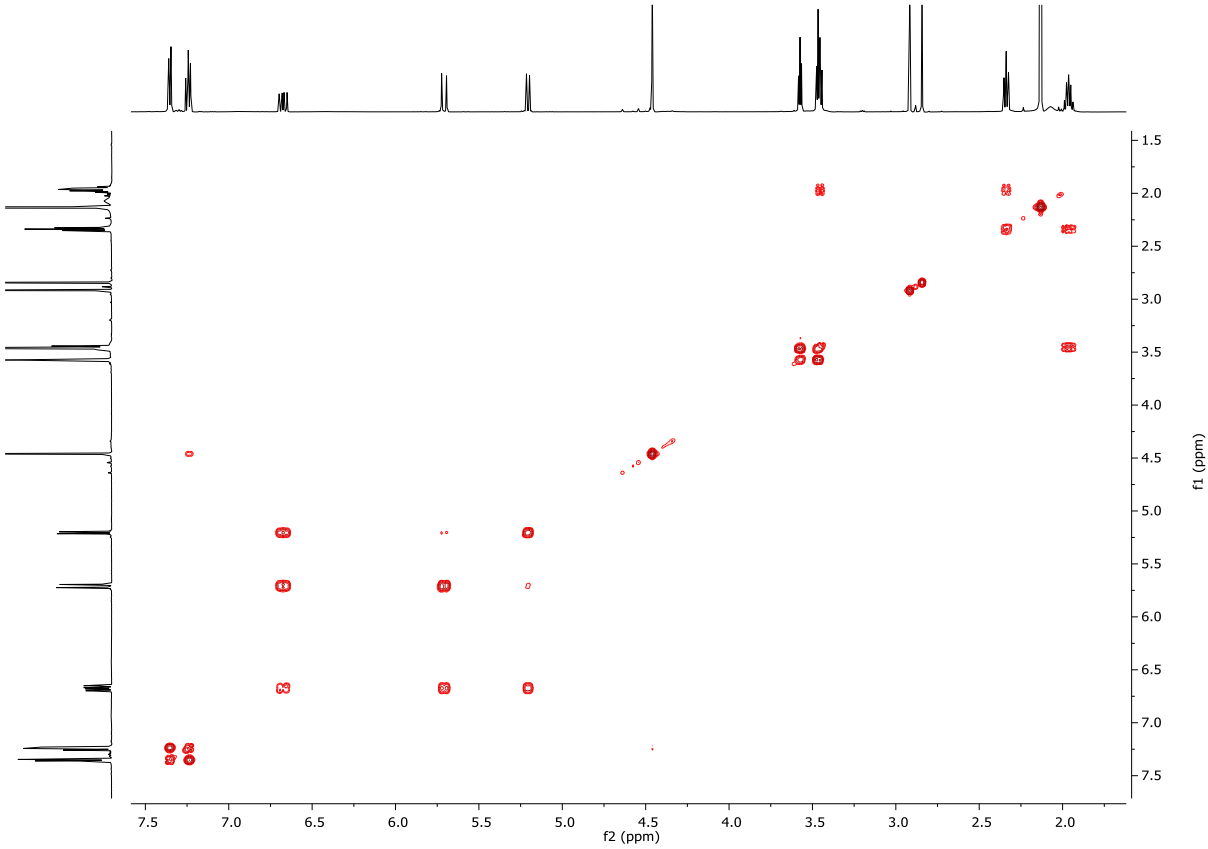

Figure A.5 – ^{1}H-^{1}H COSY NMR spectrum of monomer 2

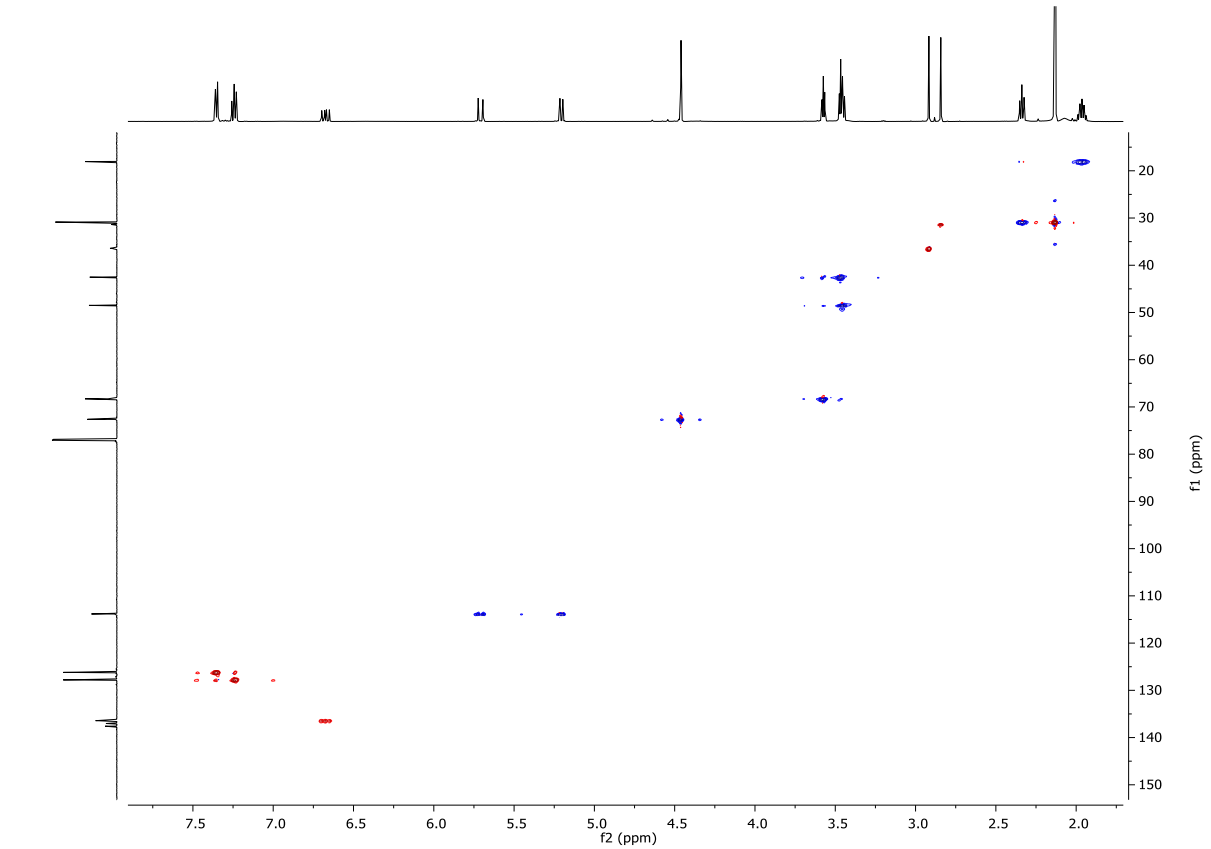

Figure A.6 – ^{1}H-^{13}C HSQC NMR spectrum of monomer 2

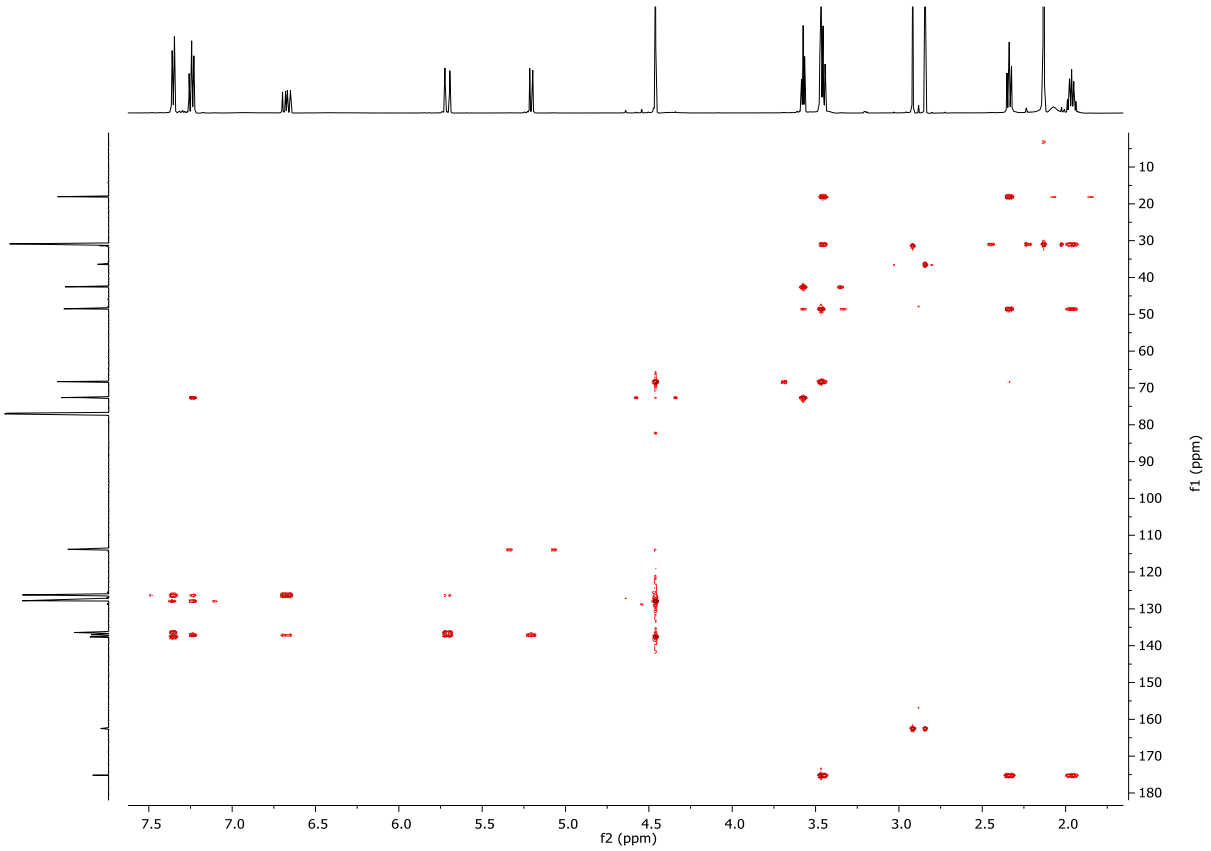

Figure A. 7 – ^{1}H-^{13}C HMBC NMR spectrum of monomer 2

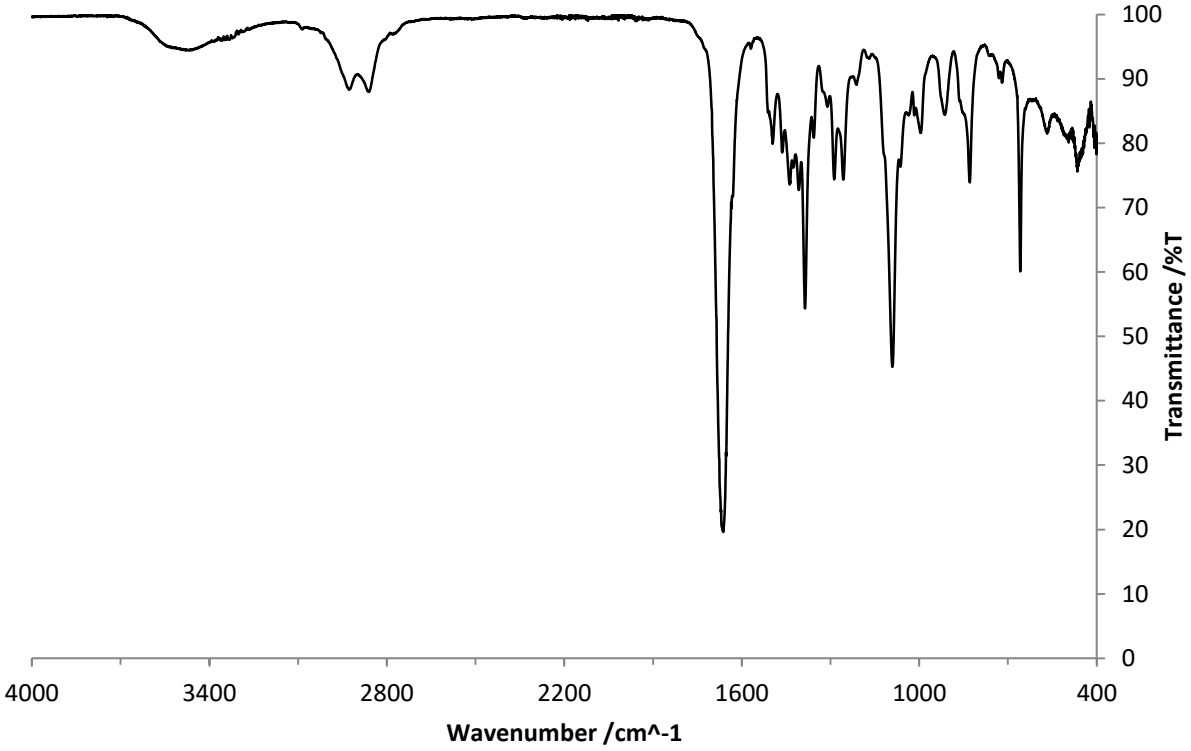

Figure A.8 – FTIR of monomer 2

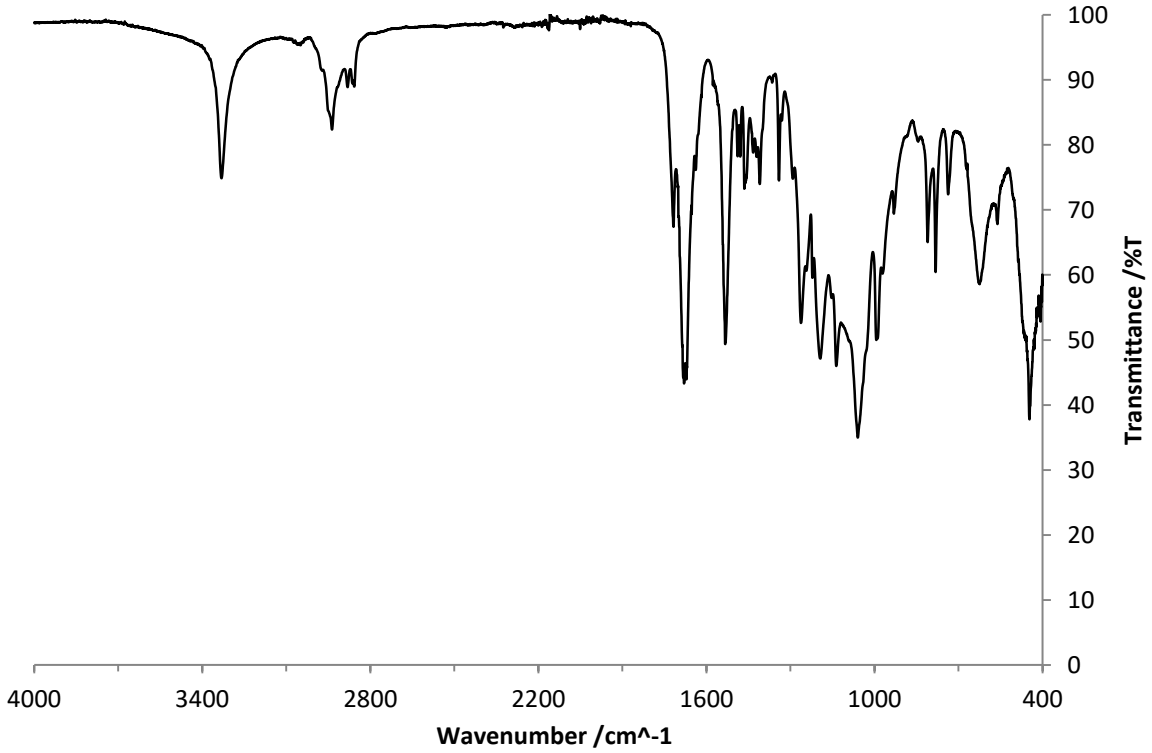

Figure A.9 – FTIR of monomer 3

Appendix B: Additional Characterisation data for Chapter 3

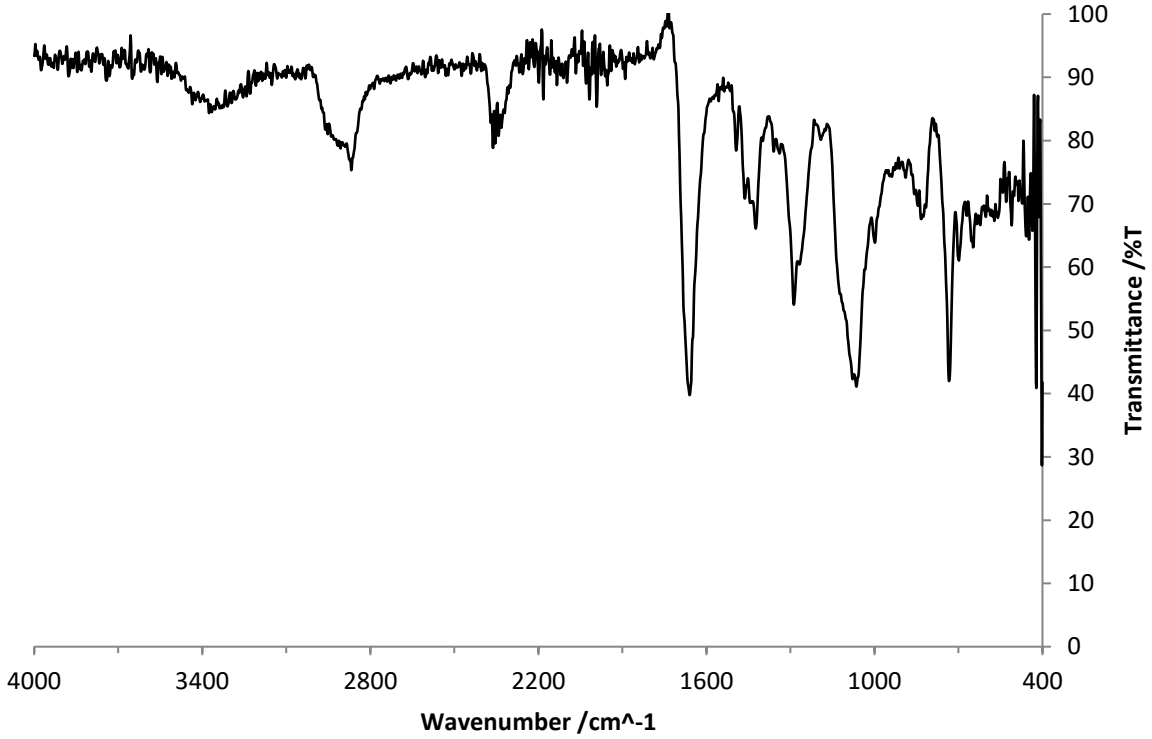

Figure B.1 – FTIR spectrum of polymer 6

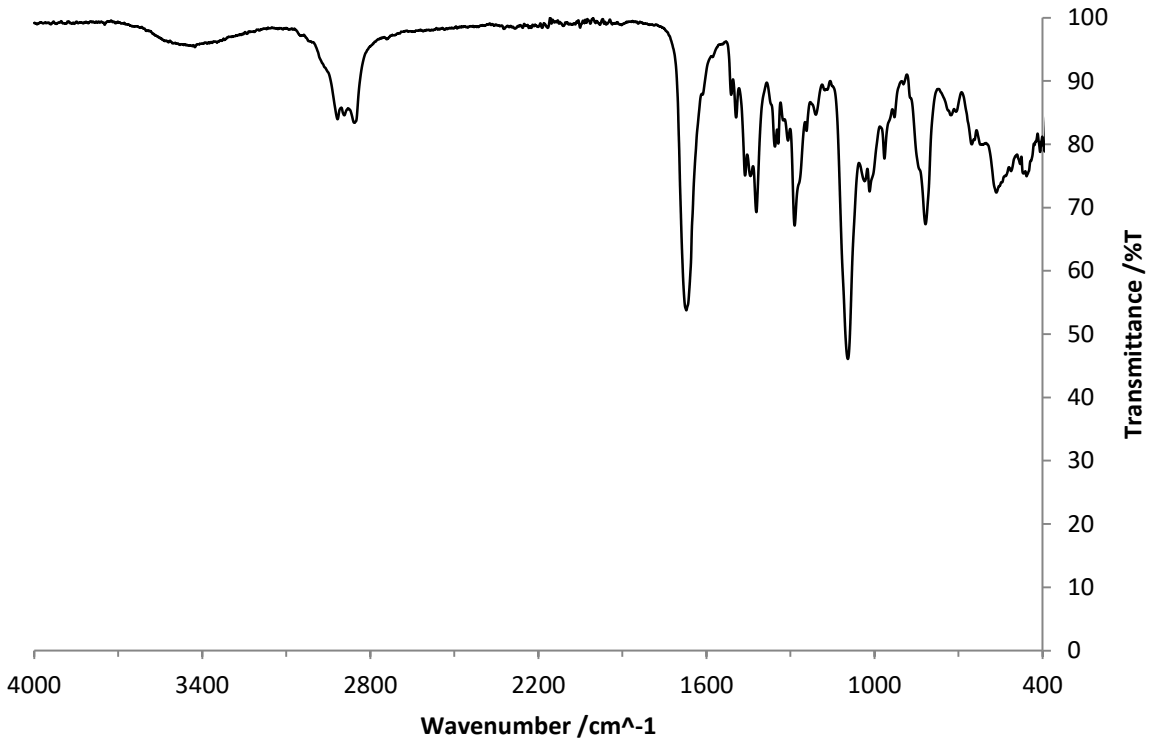

Figure B.2 – FTIR spectrum of polymer 7

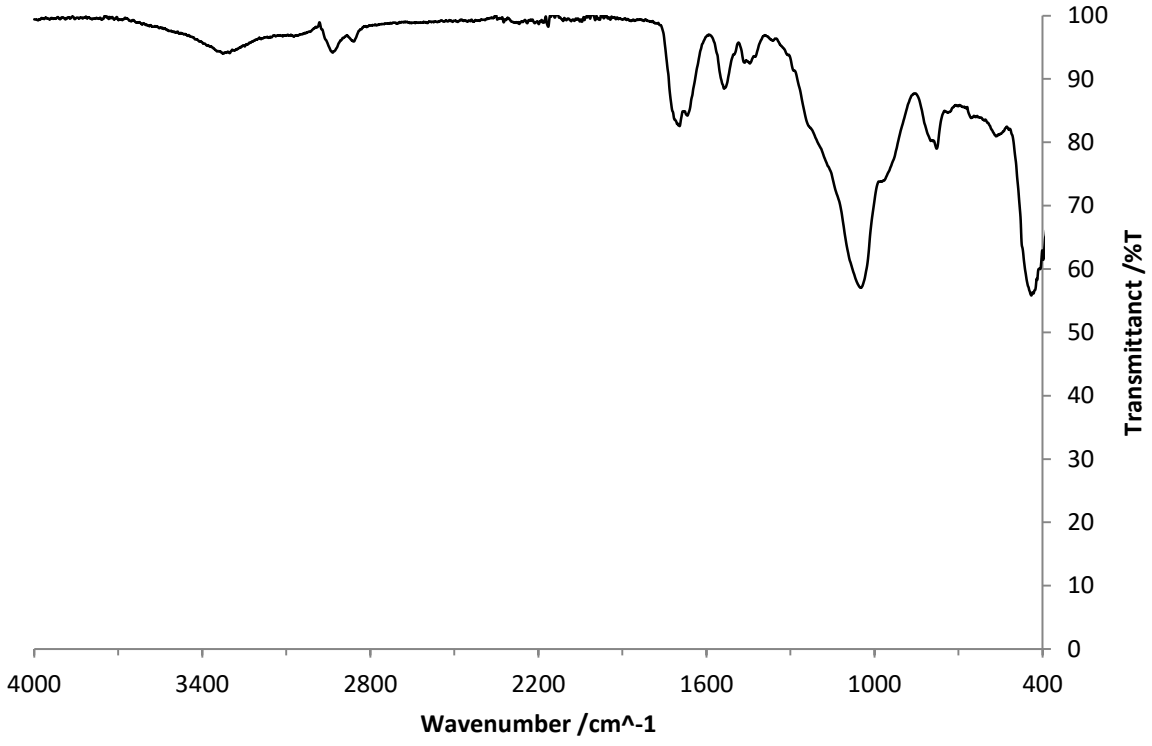

Figure B.3 – FTIR spectrum of polymer 8

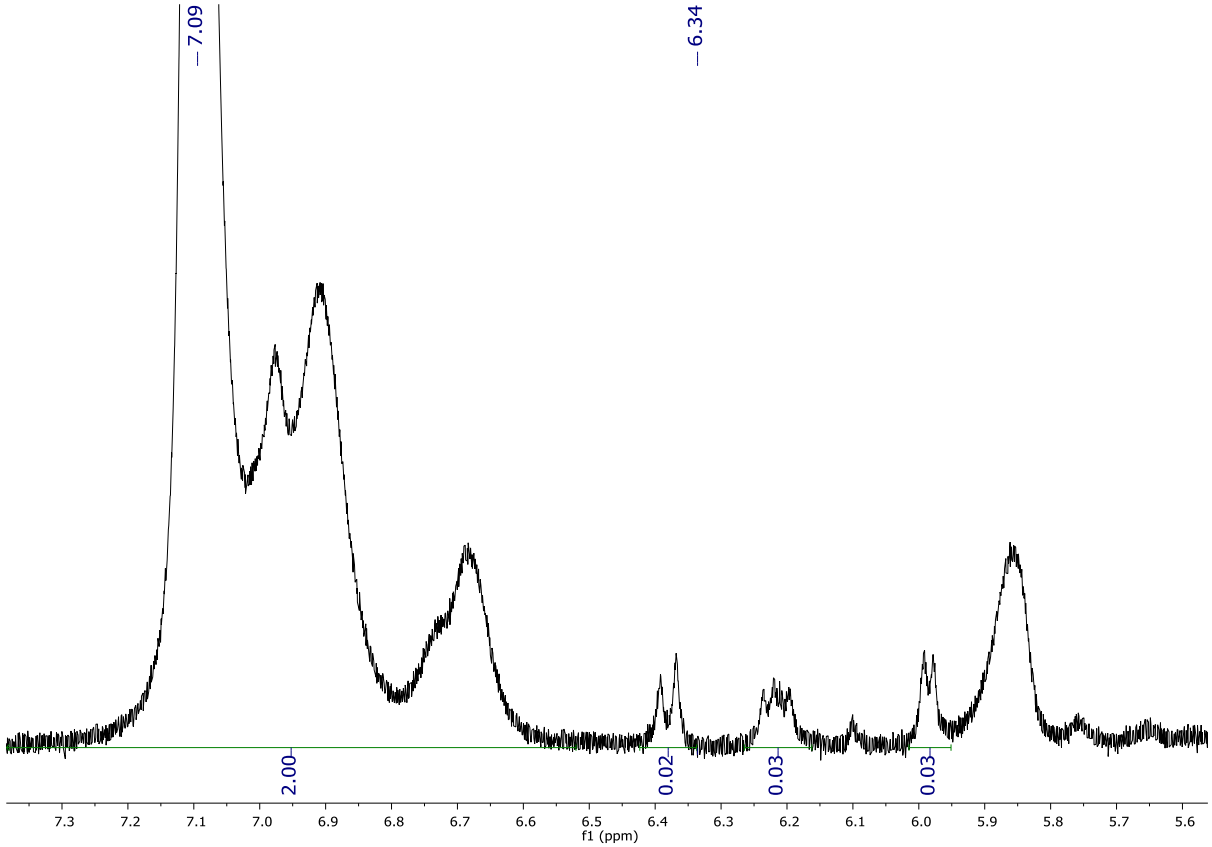

Figure B.4 – ^{1}H NMR spectrum of polymer 8, expanded

Calculation of conversion using integrals of 2.00 and 0.23 (average of 3 vinyl monomer protons)

$$\frac{2.00}{(2.00 + 0.23)} \times 100 = 91\ \%$$

Appendix C: Additional Characterisation data for Chapter 4

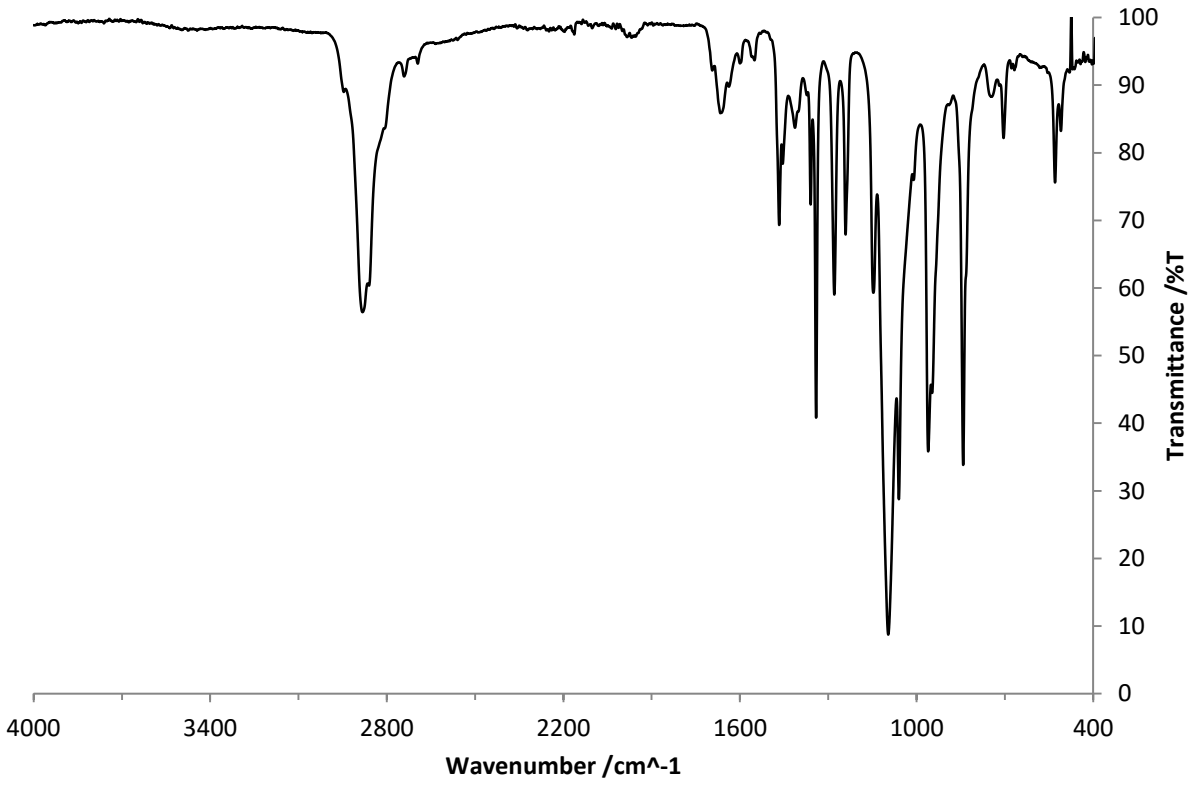

Figure C.1 – FTIR spectrum of PEG

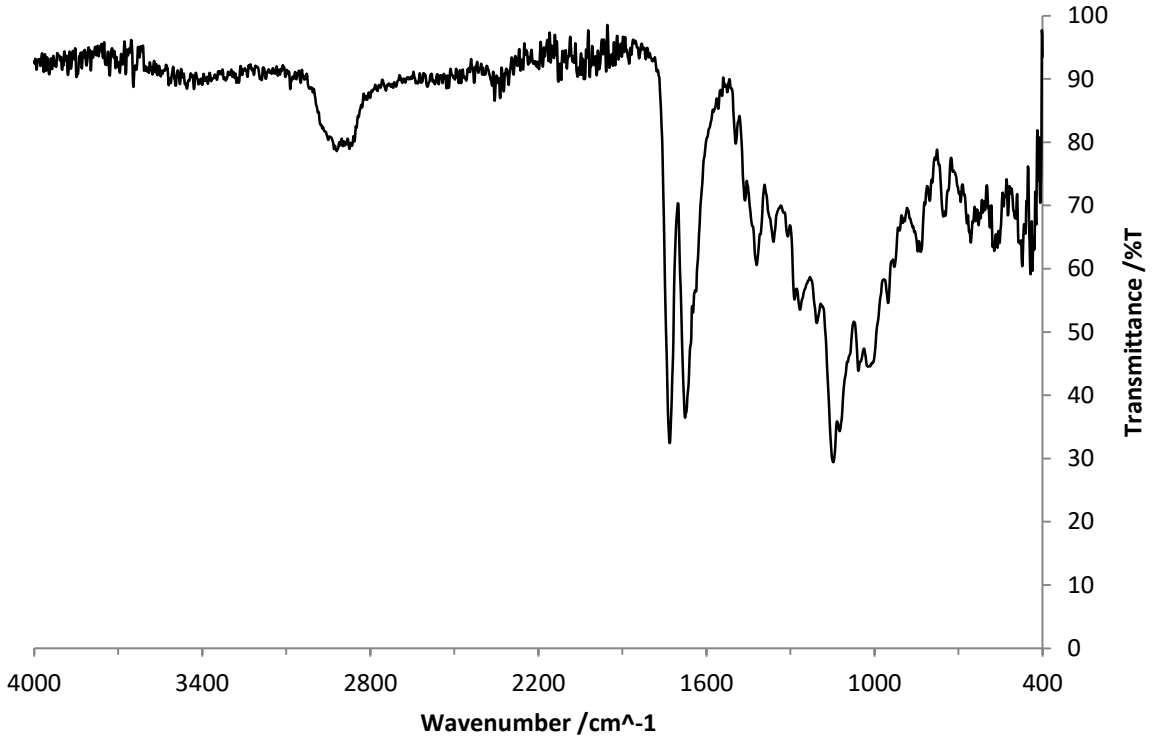

Figure C.2 – FTIR spectrum of polymer 10

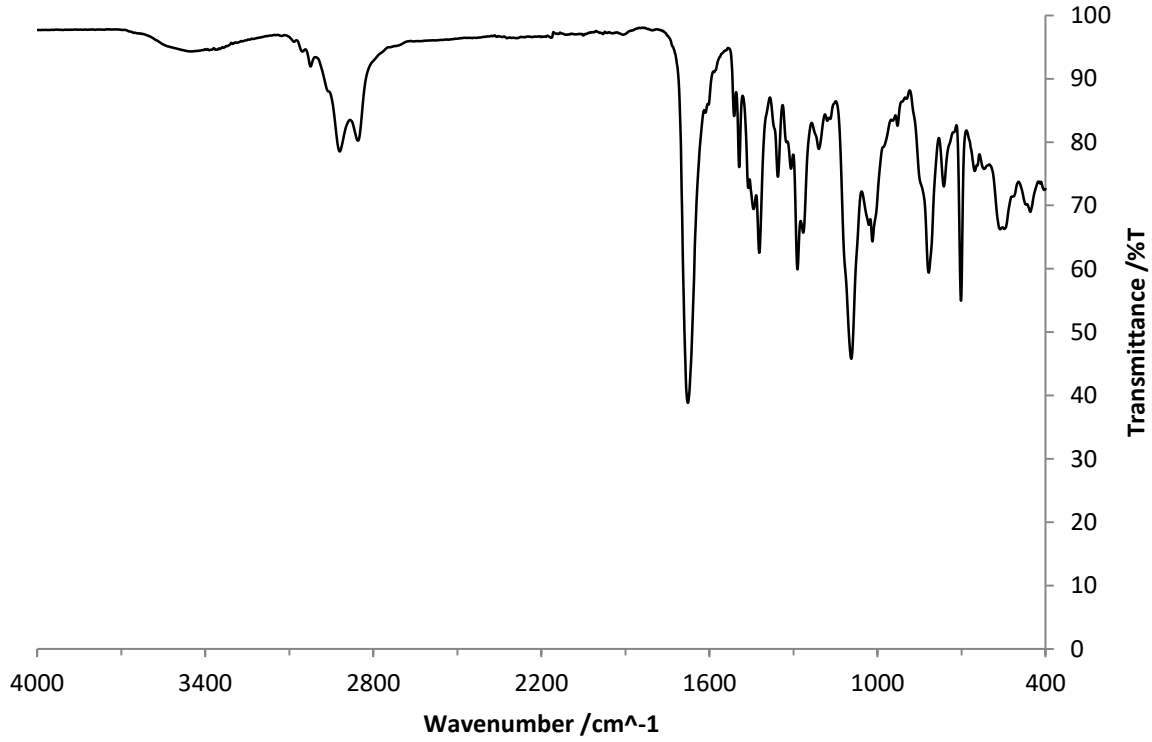

Figure C.3 – FTIR Spectrum of polymer 11

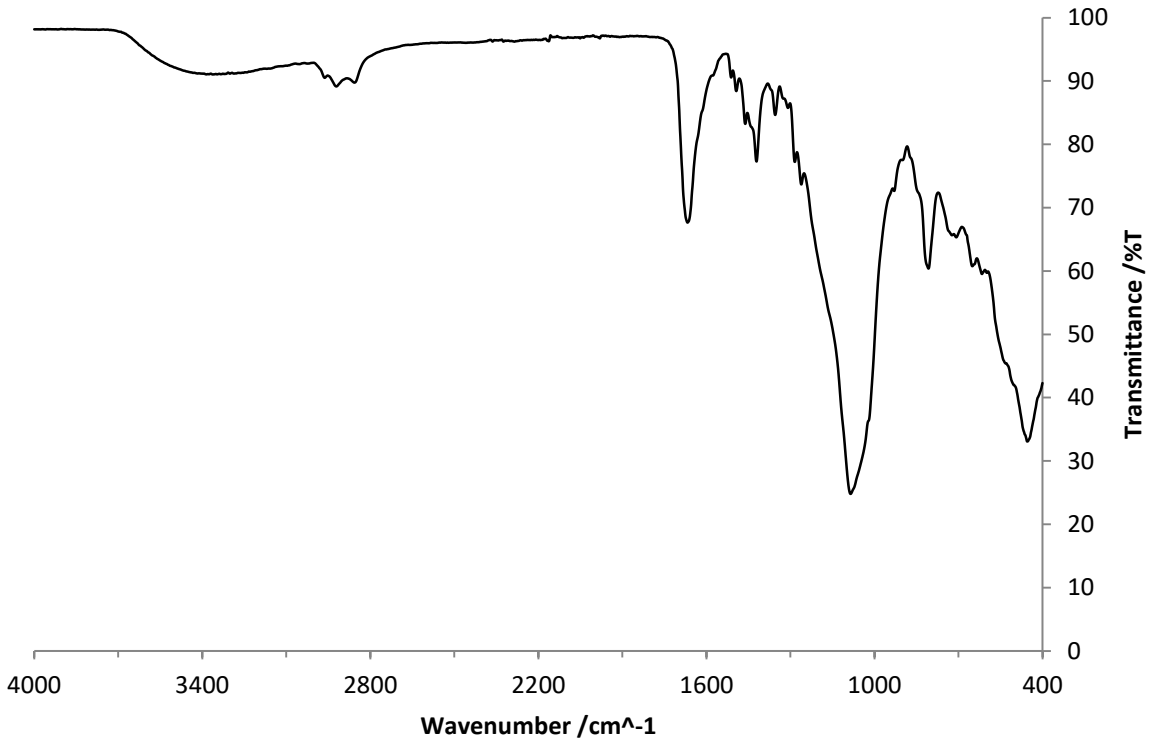

Figure C.4 – FTIR spectrum of polymer 12

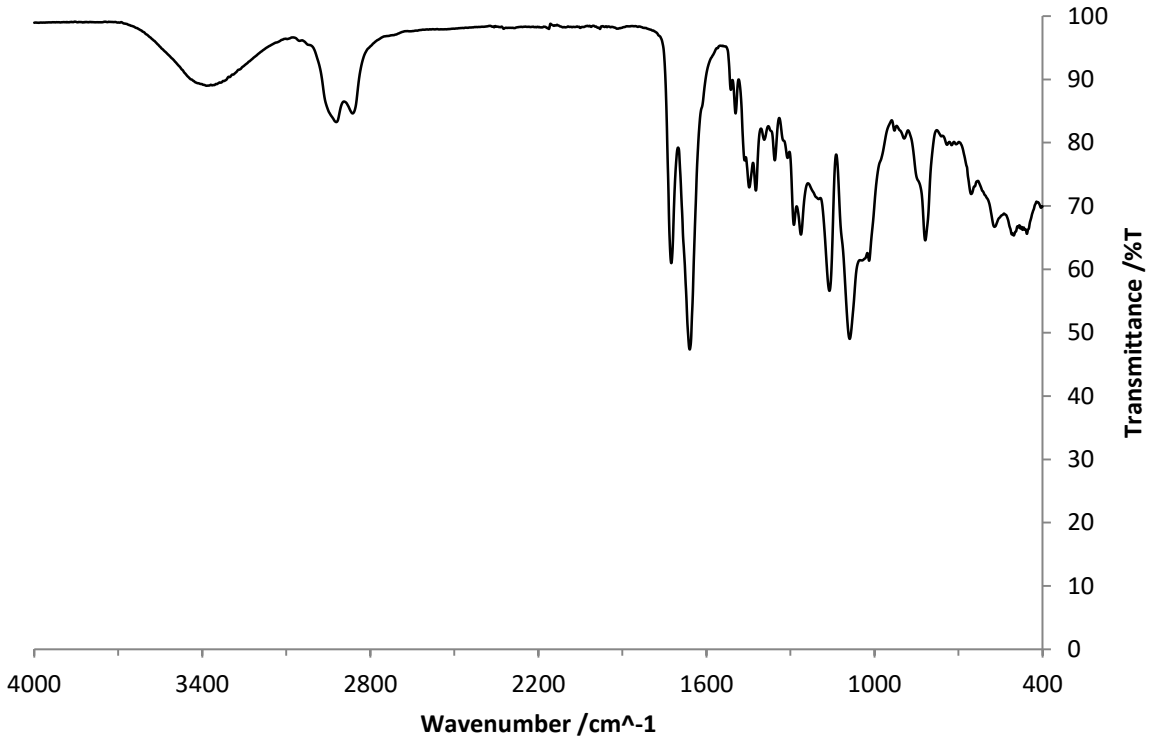

Figure C.5 – FTIR spectrum of polymer 13

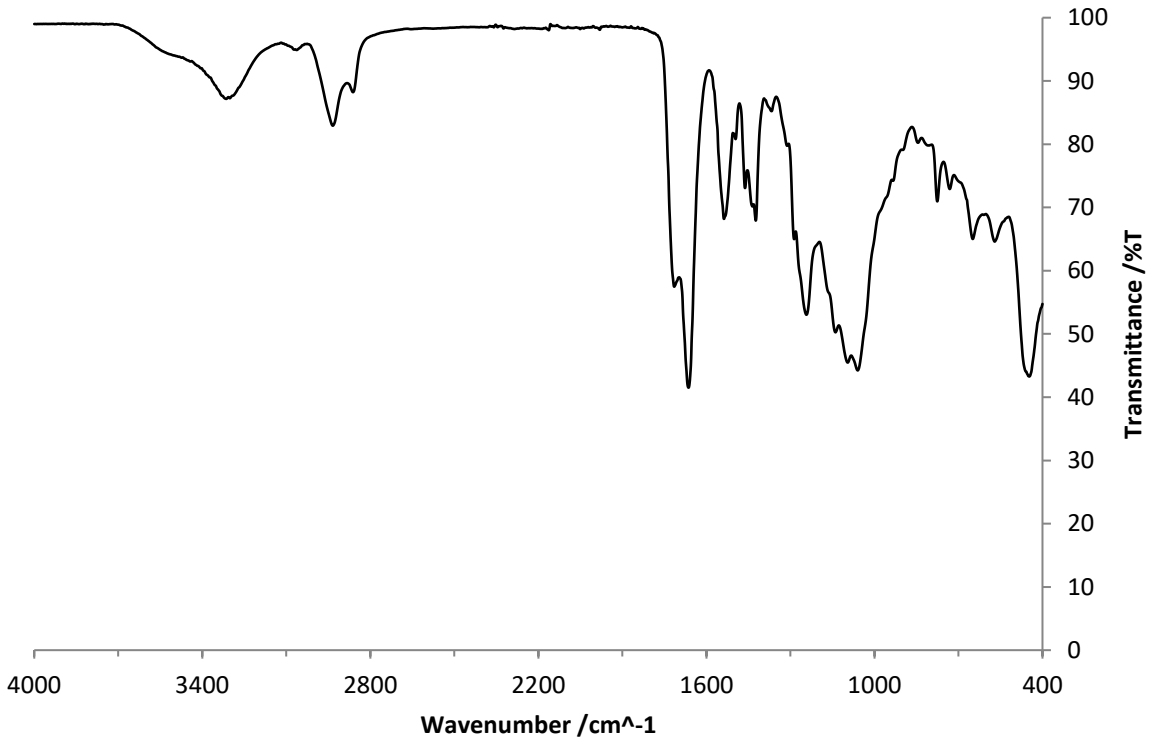

Figure C.6 – FTIR spectrum of polymer 14

Appendix D: Additional Characterisation data for Chapter 5

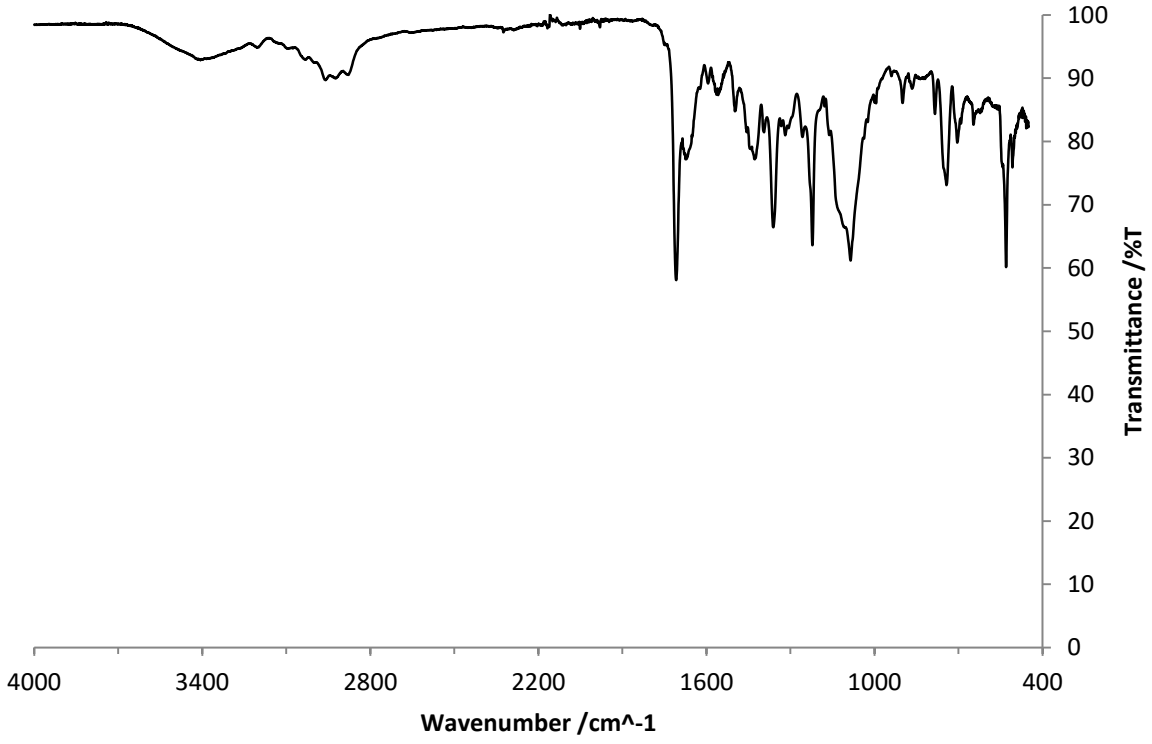

Figure D.1 – FTIR spectrum of polymer 15

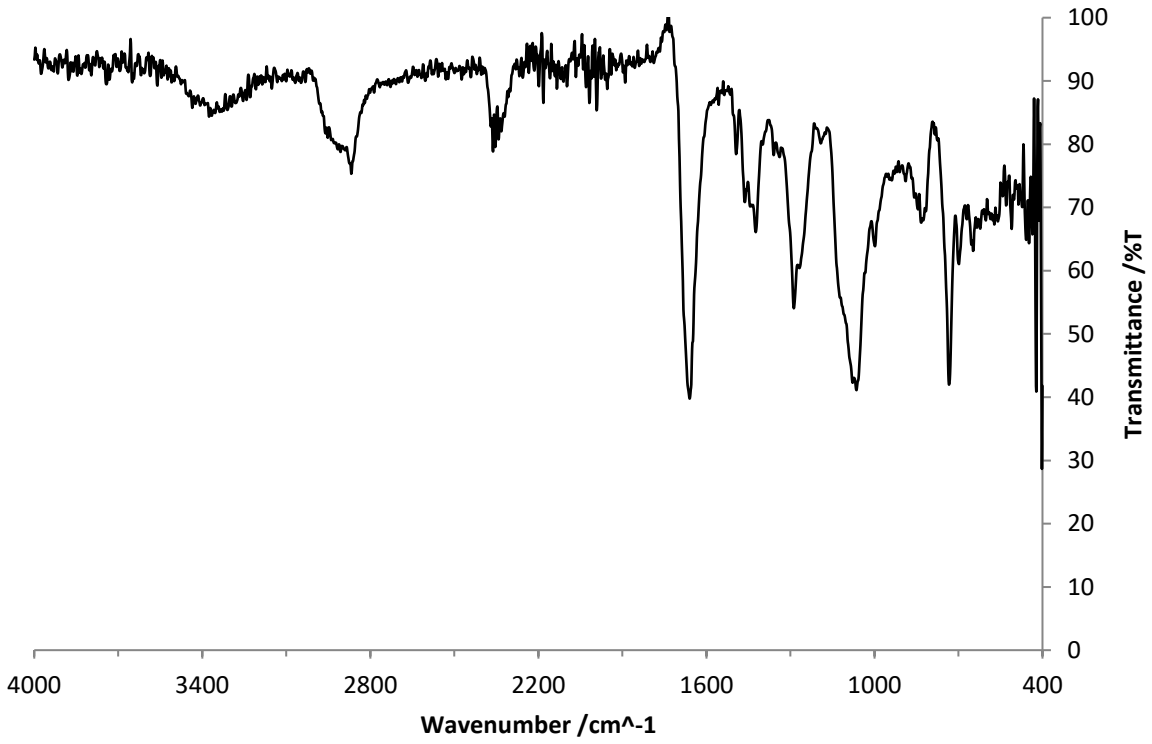

Figure D.2 – FTIR spectrum of polymer 16

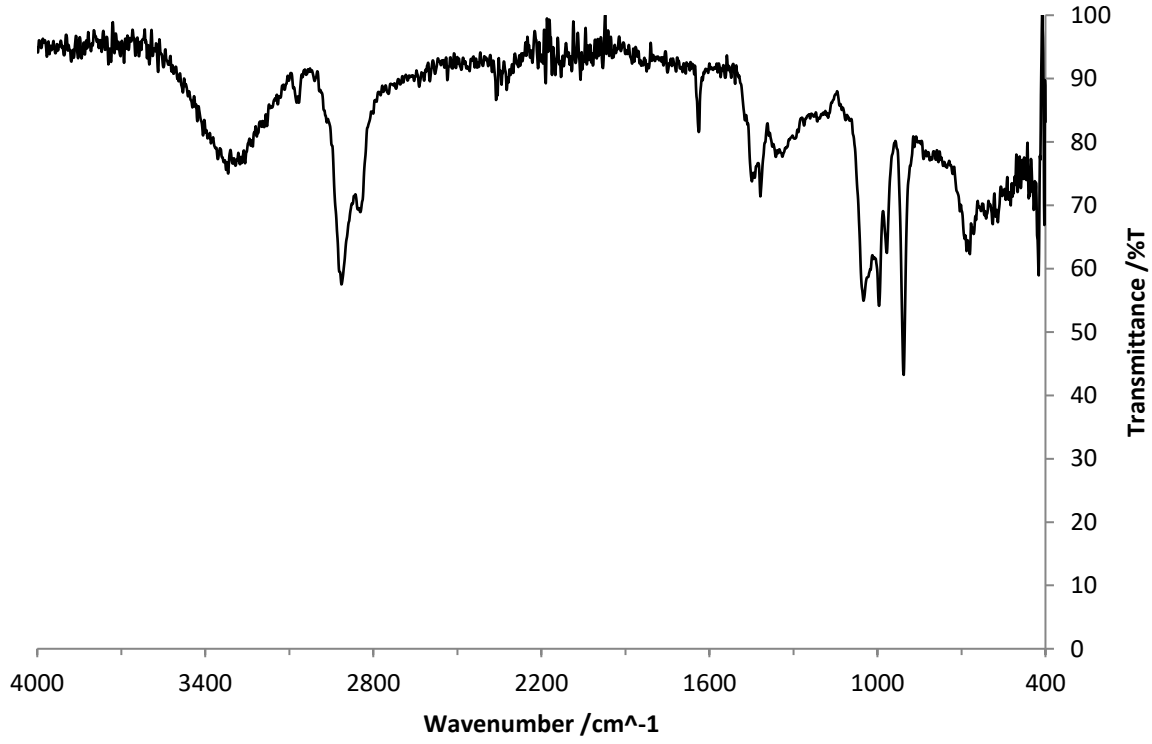

Figure D.3 – FTIR spectrum of polymer 17

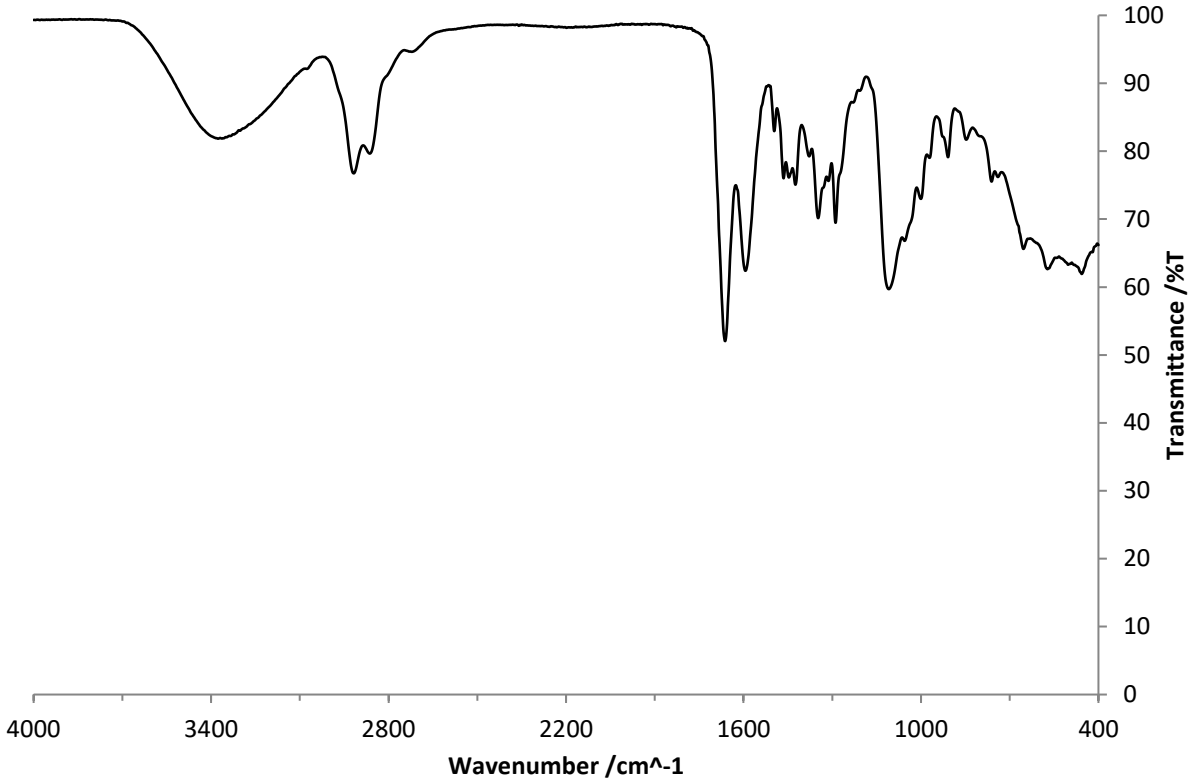

Figure D.4 – FTIR spectrum of polymer 18

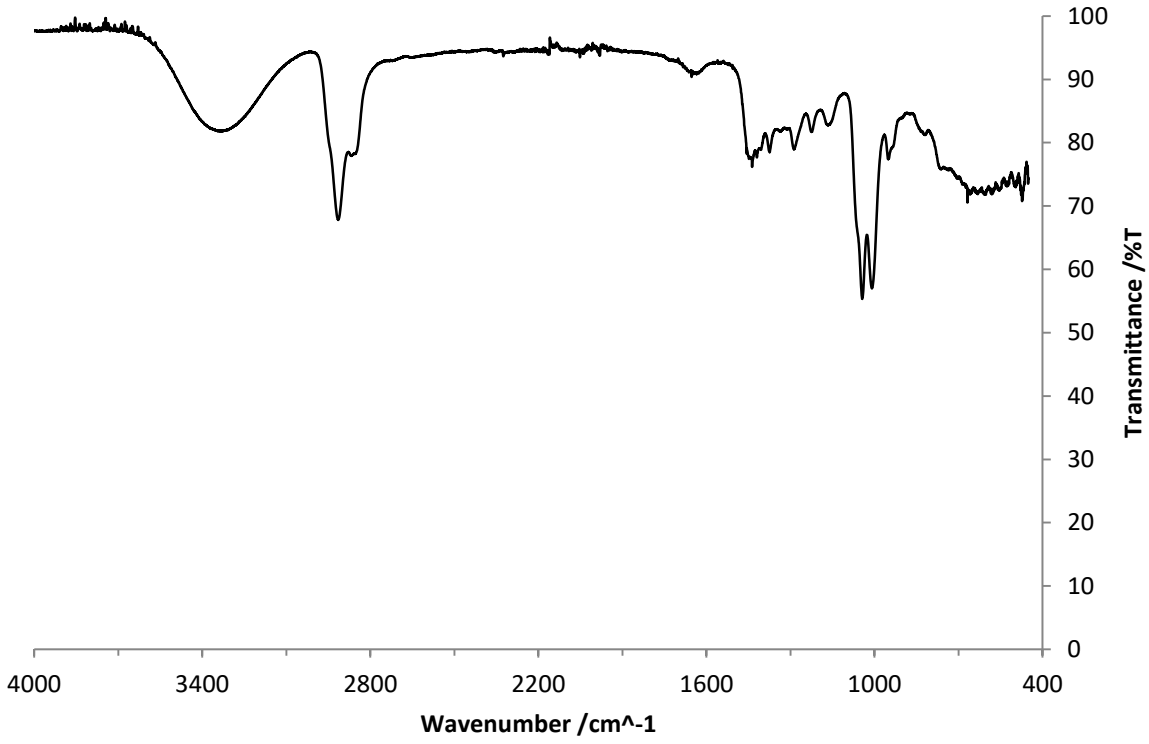

Figure D.5 – FTIR spectrum of polymer 19

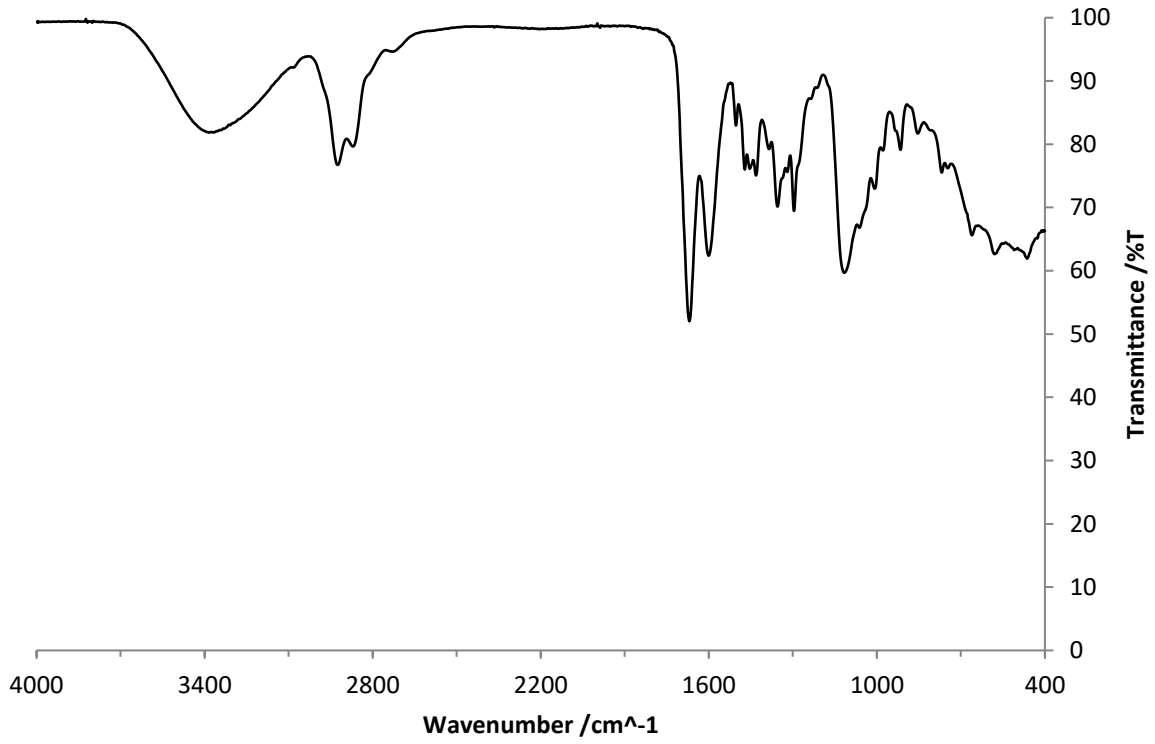

Figure D.6 – FTIR spectrum of polymer 20

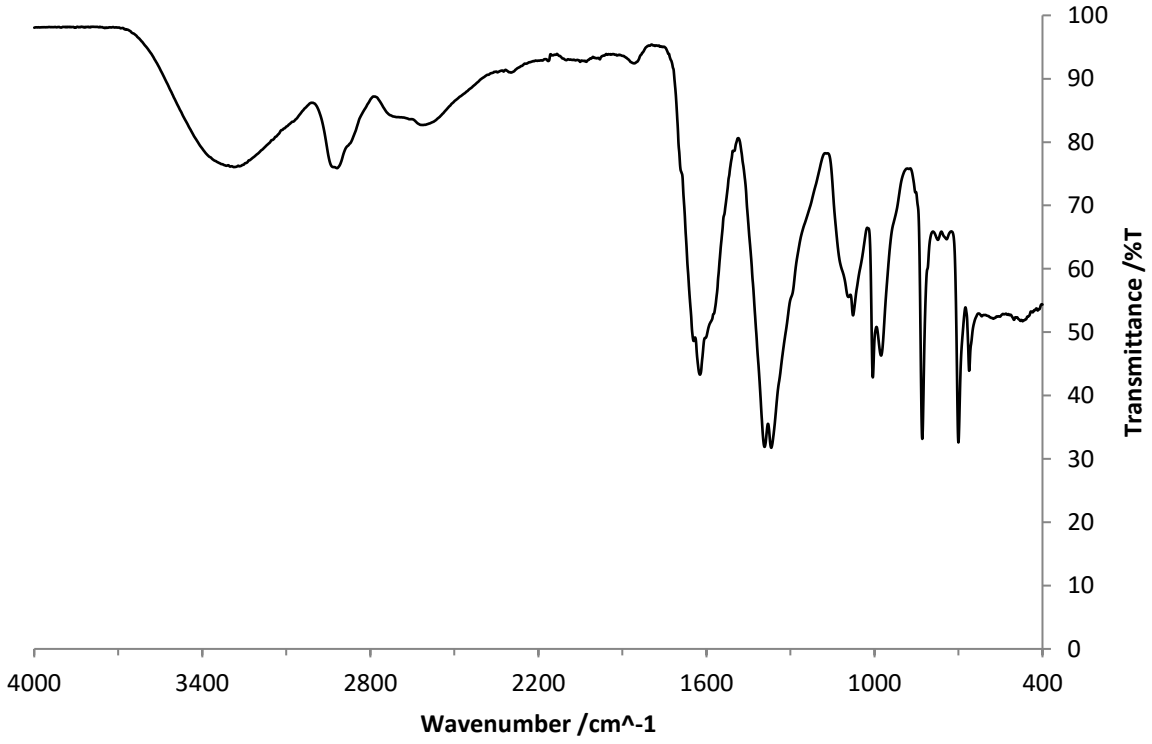

Figure D.7 – FTIR spectrum of polymer 21